MycoKeys 56: 1–11 (2019)
doi: 10.3897/mycokeys.56.35857
http://mycokeys.pensoft.net

RESEARCH ARTICLE

A peer-reviewed open-access journal
MycoKeys
Launched to accelerate biodiversity research

Three new species of *Conlarium* from sugarcane rhizosphere in southern China

Ling Xie[1,2*], Yan-Lu Chen[1,2*], Yan-Yan Long[1], Yan Zhang[1], Shi-Tong Liao[1], Bin Liu[2], Li-Ping Qin[1], Qian Nong[1], Wen-Long Zhang[1]

1 *Microbiology Research Institute, Guangxi Academy of Agricultural Science, Nanning, Guangxi Province 530007, China* **2** *Institute of Applied Microbiology, Agricultural College of Guangxi University, Nanning, Guangxi Province 530005, China*

Corresponding author: *Wen-Long Zhang* (lon1933@163.com)

Academic editor: *Cecile Gueidan* | Received 9 May 2019 | Accepted 20 June 2019 | Published 5 July 2019

Citation: Xie L, Chen Y-L, Long Y-Y, Zhang Y, Liao S-T, Liu B, Qin L-P, Nong Q, Zhang W-L (2019) Three new species of *Conlarium* from sugarcane rhizosphere in southern China. MycoKeys 56: 1–11. https://doi.org/10.3897/mycokeys.56.35857

Abstract

Three new species isolated from sugarcane rhizosphere in China, namely *Conlarium baiseense* **sp. nov.**, *C. nanningense* **sp. nov.**, and *C. sacchari* **sp. nov.**, are described and illustrated. Molecular evidence (phylogenetic analysis of combined LSU, SSU, ITS and RPB2 sequence data) and phenotypical characters support their independent status from related and similar species. The new species, as dark spetate endophytes, inhabit sugarcane rhizosphere and can form a symbiosis with sugarcane.

Keywords

Conlariaceae, conidial fungi, phylogeny, Rhizosphere, taxonomy

Introduction

The genus *Conlarium*, described by Liu et al. (2012), belongs to the Conlariaceae, a family of freshwater ascomycetes (Zhang et al. 2017). This genus includes three species: *C. duplumascospora*, *C. aquaticum*, and *C. thailandense*. In these species, *C. duplumascospora* and *C. aquaticum* were isolated from submerged woody samples in streams (Liu et al. 2012; Zhang et al. 2017) and *C. thailandense* was isolated from dead wood (Phookamsak et al. 2019). During our ongoing survey of dark septate endophytes which inhabit sugarcane rhizosphere in Guangxi province, China, three undescribed

* co-first authorship

species with the morphological characteristics of the genus *Conlarium* were isolated by the baiting method. The specimens were deposited in the Mycological Herbarium, Institute of Microbiology, Chinese Academy of Sciences, Beijing, China (HMAS).

Materials and methods

Fungal isolation and morphological studies

All soil samples were collected from the 5–15 cm deep sugarcane rhizosphere by five sampling methods in Guangxi province, China. Fungal isolations were obtained by using Chinese cabbage as a baiting plant, as described by Narisawa et al. (1998). Cultural characteristics were recorded after two weeks from potato dextrose agar (PDA). Conidiophores, conidiogenous cells, and conidia were examined as slide fungal preparations mounted in PVLG (polyvinyl alcohol, Lactic acid, Glycerin, and MiliQ water). Observations and measurements were made with Olympus BX53 Ci-L light microscope. Scanning electron microscopy (SEM) used a Tescan-vega3 LMU SEM.

Molecular sequencing and phylogenetic analysis

The genomic DNA was extracted from mycelium grown on PDB (potato dextrose broth) at 28 °C for 10 d using the Prepman Ultra Sample Preparation Reagent Protocol (Applied Biosystems, California, USA). The large subunit ribosomal RNA gene (LSU), the small subunit ribosomal RNA gene (SSU), the internal transcribed spacer (ITS) rDNA, and the RNA polymerase II subunit 2 (RPB2) were amplified with fungal specific primers LROR/LR5, NS1/NS4, ITS1/ITS4, and fRPB2-5f/fRPB2-7cR (Vilgalys and Hester 1990; White et al. 1990; Liu et al. 1999). The PCR reaction mixture and conditions followed the modified protocol of 2×*EasyTaq* PCR SuperMix (TransGen Biotech, Beijing, China). Amplification was performed in a 50 μL reaction volume which contained PCR buffer [20 mM KCl, 10 mM $(NH_4)_2SO_4$, 2 mM $MgCl_2$, 20 mM Tris-HCl, pH8.4], 200 μM of each deoxyri-bonucleotide triphosphate, 15 pmols of each primer, 100 ng template DNA, and 2.5 units of Taq DNA polymerase (Biocolor BioScience and Technology, Shanghai, China). The thermal cycling program was as follows: 5 min initial denaturation at 94 °C, followed by 35 cycles of 40 s denaturation at 94 °C, 40 s annealing at 56 °C, 60 s extension at 72 °C, and a final 10 min extension at 72 °C. A negative control using sterilized distilled water instead of template DNA was included in the amplification process. The PCR products were examined by electrophoresis at 75 V for 2 h in 0.8 % (W/V) agarose gel in 1×TAE buffer (0.4 M Tris, 50 mM NaOAc, 10 mM EDTA, pH 7.8) and visualized under ultraviolet light after staining with ethidium bromide (0.5 μg ml^{-1}). The PCR products were purified using PCR Cleanup Filter Plates (MultiScreen ® PCRμ96; Millipore, USA) according to the manufacturer's protocol. Purified PCR products were directly sequenced with primer pairs, as mentioned above, in an ABI 3730-XL DNA sequencer

(Applied Biosystems, USA). The sequences were deposited at GenBank (http://www.ncbi.nlm.nih.gov) and compared in BLAST. Four kinds of rDNA sequences together with reference sequences (Table 1) were respectively aligned by MEGA v. 6.0 based on the neighbor-joining analyses and 1000 bootstrap replications.

Bayesian analyses of the same aligned four kinds of rDNA sequences dataset were conducted with MrBayes v. 3.1.2 (Huelsenbeck and Ronquist 2001) following the protocol of Sun and Guo (2010). The best-fit evolutionary model was determined for each dataset by comparing different evolutionary models via MrModeltest v. 2.3 (Nylander 2008). Four simultaneous chains of Markov Chain Monte Carlo were run starting from random trees and sampling every 100 generations. The analyses were halted at 4,000,000 generations for four kinds of rDNA sequences, when the calculation reached stationarity. At the end of the analysis, 4,000 trees were generated, respectively, and 25 % of them were excluded as the "burn in" when calculating the posterior probabilities. Bayesian posterior probabilities were obtained from the 50% majority rule consensus trees that remained. If more than 95% of the sampled trees contained a given clade, it was considered to be significantly supported by our data.

Results

Taxonomy

Conlarium nanningense **L.Xie, Y.L.Chen & B.Liu, sp. nov.**
MycoBank: MB821416
Figure 1

Etymology. The species is named for Nanning City, the type locality.

Type. CHINA. Guangxi: Nanning City, Datang Town. 22°23'25"N, 108°23'12"E, 144 m alt., in sugarcane rhizosphere, 11 Feb. 2011, L. Xie, M1 (HMAS 247075 holotype) deposited in Microbiology Research Institute, Guangxi Academy of Agricultural Science.

Description. Colony reached 22 mm diameter on PDA medium after 2 weeks, grey-white to grey-brown, nearly circular, flat growth, less aerial hyphae. Hyphae grey-brown, verruculose, septate. Conidiophores 1–15 × 1–5 μm (6 ± 3 × 4 ± 1 μm, n = 54), stubby, unbranched, septate or aseptate, straight or flexuous, hyaline, becoming brown with age. Conidiogenous cells determinate, doliiform, cylindrical, 4–13 × 5–10 μm (6 ± 2 × 7 ± 2 μm, n = 22). Conidia brown, muriform, irregularly globose or subglobose, smooth, constricted at the septa, 0–1 transversely septa, 0–4 longitudinal septa, 11–21 × 9–21 μm (15 ± 3 × 13 ± 3 μm, n = 50). Chlamydospores subglobose or irregular, 4–12 μm (7±2 μm, n = 67). **Sexual morph:** undetermined.

Habitat and distribution. In sugarcane rhizosphere soil of southern China.

Other specimens examined. CHINA. Guangxi: Nanning City, Datang Town. 22°29'54.51"N, 108°24'3.06"E, 102 m alt., in sugarcane rhizosphere, 11 Feb. 2011, L. Xie, M8 **(HMAS 247985).**

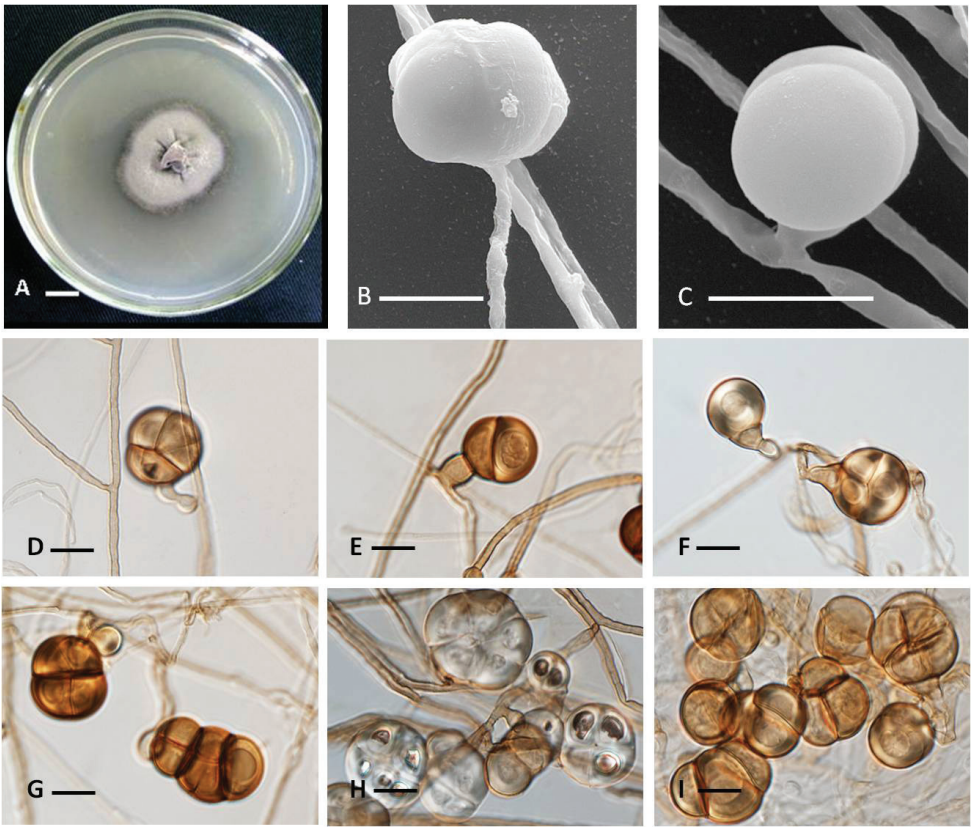

Figure 1. The new species *Conlarium nanningense* (HMAS 247075, holotype). **A** Colony morphology **B, C** Scanning electron microscopy of conidia **D–I** Mature conidia. Scale bars: 10 mm (**A**); 10 μm (**B–E**).

Notes. *Conlarium nanningense* is similar to the asexual morph of *C. aquaticum*, *C. duplumascospora*, and *C. thailandense*. They all have monoblastic, holoblastic conidiogenous cells and mostly irregular, brown, clathrate, muriform conidia (Liu et al. 2012). However, *C. nanningense* can be easily distinguished from *C. aquaticum*, *C. duplumascospora*, and *C. thailandense* by the number of conidial septa (2–4-transversely septate, 1–3-longitudinally septate in *C. duplumascospora*; 6–12-transverse septa, 4–10-longitudinal septa in *C. aquaticum*; 4–8-transverse septa, 4–6-longitudinal septa in *C. thailandense* vs 0–1 transversely septa, 0–4 longitudinal septa in *C. nanningense*) and conidial size (15.5–35 × 11–26.5 μm in *C. duplumascosporum*, 45–70 × 20–57 μm in *C. aquaticum*, 25–45 × 17–33 μm in *C. thailandense* and 11–21 × 9–21 μm in *C. nanningense*) (Liu et al 2012; Zhang et al. 2017; Phookamsak et al. 2019). Phylogenetic reconstructions based on SSU+ITS+LSU+RBP2 sequences show authentic *C. nanningense* is sister to *C. duplumascospora*. A comparison of ITS pairwise indicates that *C. nanningense* differs from *C. aquaticum*, *C. duplumascospora*, and *C. thailandense* in 21 bp, 12 bp, and 18 bp, respectively. Thus, following the guidelines of Jeewon and Hyde (2016), this is a new species.

Conlarium baiseense **L.Xie, Y.L.Chen & B.Liu, sp. nov.**
MycoBank: MB821682
Figure 2

Etymology. The species is named for Baise City, the type locality.

Type. CHINA. Guangxi: Baise City, Tiandong County, Silin Town. 23°30'38"N, 107°20'1"E, 109 m alt., in sugarcane rhizosphere, 11 Sep 2015, Y.L. Chen and L.P. Qin, TD2 (HMAS 247298, holotype) deposited in Microbiology Research Institute, Guangxi Academy of Agricultural Science.

Description. Colony reached 14 mm diameter on medium after 2 weeks at 28 °C, grey-white to grey, circular, flat growth, less aerial hyphae, regular edge of colony. Hyphae light yellow-green to light yellow-brown, septate. Conidiophores yellow-brown, mostly stubby, 0–2-branched, 0–8-septate, straight or flexuous, 3–12 × 2–6 μm (7 ± 2 × 4 ± 1 μm, *n* = 51). Conidiogenous cells determinate, doliiform, yellowbrown to brown, 3–8 × 5–12 μm (6 ± 1 × 7 ± 2 μm, *n* = 51). Muriform conidia yellow-brown to brown, irregularly globose or subglobose, smooth, constricted at the separation, 0–1 transversely septa, 0–4 longitudinal septa, 15–25 × 12–19 μm (18 ± 2 × 15 ± 2 μm, *n* = 26). Columnar conidia, yellow-brown to brown, 2–5 transversely septa, no longitudinal septa, 21–35 × 7–12 μm (28 ± 5 × 10 ± 1 μm, *n* = 23). **Sexual morph:** undetermined.

Habitat and distribution. In sugarcane rhizosphere soil of southern China.

Other specimens examined. CHINA. Guangxi: Baise City, Tiandong County, Silin Town. 23°30'3.68"N, 107°20'1"E, 112.5 m alt., in sugarcane rhizosphere, 11 Sep. 2015, Y.L. Chen and L.P. Qin, TD17 **(HMAS 247986)**.

Notes. *Conlarium baiseense* is similar to the asexual morph of *C. aquaticum*, *C. duplumascospora*, *C. nanningense*, and *C. thailandense*. They all have monoblastic, holoblastic, conidiogenous cells and mostly irregular, brown, clathrate, muriform conidia (Liu et al. 2012). However, *C. baiseense* can be easily distinguished from *C. aquaticum*, *C. duplumascospora*, *C. nanningense*, and *C. thailandense* by its conidial septa number (6–12-transverse septa, 4–10-longitudinal septa in *C. aquaticum*; 2–4-transversely septate, 1–3-longitudinally septate in *C. duplumascospora*; 0–1 transversely septa, 0–4 longitudinal septa in *C. nanningense*; 4–8-transverse septa, 4–6-longitudinal septa in *C. thailandense* vs 0–2 transversely septa, 0–8 longitudinal septa in *C. baiseense*) and conidial size (15.5–35 × 11–26.5 μm in *C. duplumascosporum*, 45–70 × 20–57 μm in *C. aquaticum*, 25–45 × 17–33 μm in *C. thailandense*, 11–21 × 9–21 μm in *C. nanningense* vs 21 × 35–7 ×12 μm in *C. baiseense*) (Liu et al 2012; Zhang et al. 2017; Phookamsak et al. 2019). Phylogenetic reconstructions based on SSU+ITS+LSU+RBP2 sequences shows that authentic *C. baiseense* form independent monophyletic groups, well separated from *C. aquaticum*, *C. duplumascospora*, *C. nanningense*, and *C. thailandense*, respectively. A comparison of ITS sequence shows that *C. baiseense* differs from *C. aquaticum*, *C. duplumascospora*, *C. nanningense*, and *C. thailandense* in 26 bp, 24 bp, 18 bp, and 24 bp, respectively. According to the guidlines in Jeewon and Hyde (2016), we introduce *C. nanningense* as a new species.

Figure 2. The new species *Conlarium baiseense* (HMAS 247298, holotype). **A** Colony morphology **B–I** Conidiophores, conidiogenous cells and conidia. Scale bars: 10 mm (**A**); 10 μm (**B**).

Conlarium sacchari **L.Xie, Y.L.Chen & B.Liu, sp. nov.**
MycoBank: MB821681
Figure 3

Etymology. The epithet "*sacchari*" refers to the habitat where first collected.

Type. CHINA. Guangxi: Chongzuo City, Daxin County, Lanxu Village. 22°44'46"N, 107°15'15"E, 241 m alt., in sugarcane rhizosphere, 8 July 2015, Y.L. Chen and L.P. Qin, DX4 (HMAS 247299, holotype) deposited in Microbiology Research Institute, Guangxi Academy of Agricultural Science.

Description. Colony reached 15 mm diameter on medium after 2 weeks at 28 °C, greywhite to grey, circular, flat growth, less aerial hyphae, regular edge of colony. Hyphae light yellow to yellow-brown, septate. Conidiophores yellow-brown, mostly stubby, 0–2-branched, 0–6-septate, straight or flexuous, 3–30×2–4 μm (10 ± 7 × 3 ± 1 μm, *n* = 43). Conidiogenous cells determinate, doliiform, yellow-brown to brown, 4–12 × 2–7 μm (7 ± 2 × 5 ± 1 μm, *n* = 52). Conidia yellow-brown to brown, muriform, irregularly globose or subglobose, smooth, constricted at the separation, 0–1 transversely septa, 0–4 longitudinal septa, 14–19×13–22 μm (17 ± 3 × 16 ± 2 μm, *n* = 20). **Sexual morph:** undetermined.

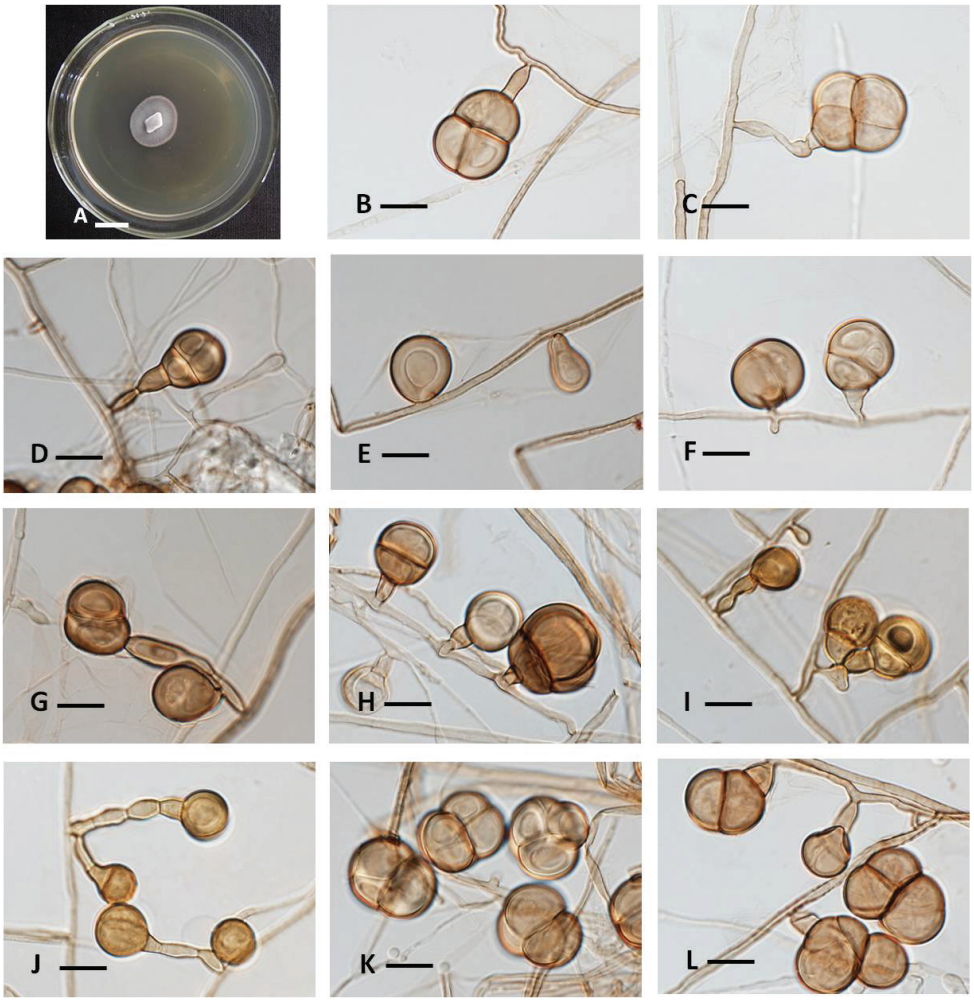

Figure 3. The new species *Conlarium sacchari* (holotype, HMAS 247299). **A** Colony morphology **B–L** Conidiophores, conidiogenous cells and conidia. Scale bars: 10 mm (**A**); 10 μm (**B–L**).

Habitat and distribution. In sugarcane rhizosphere soil of southern China.

Other specimens examined. CHINA. Guangxi: Nanning City, Long'an County, Natong Town. 23°4'48"N, 107°47'31"E, 128 m alt., in sugarcane rhizosphere, 11 Sep. 2015, Y.L. Chen and L.P. Qin, LA3 (HMAS 247300). Nanning City, Suxu town. 23°34'42"N, 108°8'30"E, 325 m alt., in sugarcane rhizosphere, 11 Feb. 2011, L. Xie, NN1 (HMAS 247301).

Notes. *Conlarium sacchari* is similar to the asexual morph of *C. aquaticum*, *C. baiseense*, *C. duplumascospora*, *C. nanningense*, and *C. thailandense*. They all have monoblastic, holoblastic, conidiogenous cells and mostly irregular, brown, clathrate, muriform conidia (Liu et al. 2012). However, *Conlarium sacchari* can be easily distinguished from *C. aquaticum*, *C. duplumascospora*, *C. nanningense*, and *C. thailandense* by its

less number of conidial septa (6–12-transverse septa, 4–10-longitudinal septa in *C. aquaticum*; 2–5 transversely septa, 0–2 longitudinal septa in *C. baiseense*, 2–4-transversely septate, 1–3-longitudinally septate in *C. duplumascospora*; 0–1 transversely septa, 0–4 longitudinal septa in *C. nanningense*; 4–8-transverse septa, 4–6-longitudinal septa in *C. thailandense* vs. 0–1 transversely septa, 0–3 longitudinal septa in *C. sacchari*) (Liu et al 2012; Zhang et al. 2017; Phookamsak et al. 2019). Phylogenetic reconstructions based on SSU+ITS+LSU+RBP2 sequences shows that authentic *C. sacchari* formed independent monophyletic groups which are well separated from *C. aquaticum*, *C. baiseense*, *C. duplumascospora*, *C. nanningense*, and *C. thailandense*, respectively. A comparion of ITS sequence shows that *C. sacchari* differ from *C. aquaticum*, *C. baiseense*, *C. duplumascospora*, *C. nanningense*, and *C. thailandense* in 21 bp, 24 bp, 21 bp, 18 bp, and 16 bp, resectively. Therefore, we introduce *C. sacchari* as a new species, following the guidelines of Jeewon and Hyde (2016).

Phylogenetic analysis

To determine the phylogenetic positions of the three new species, *C. baiseense*, *C. nanningense* and *C. sacchari*, all available SSU, ITS, LSU, and RBP2 sequences of *Conlarium* species and related genera in GenBank were downloaded (Table 1). A combined SSU+ITS+LSU+RBP2 dataset of *C. baiseense*, *C. nanningense*, and *C. sac-*

Table 1. Taxa with GenBank accession numbers for SSU, ITS, LSU and RPB2.

Taxa	Voucher	GenBank no.			
		SSU	ITS	LSU	RPB2
Conlarium nanningense	M1	KX886203	KX886204	KX886202	MK224589
Conlarium baiseense	TD2	MF083159	MF083157	MF083158	MK573000
Conlarium sacchari	NN1	MF083162	MF083160	MF083161	MK224588
Conlarium sacchari	LA3	MF083165	MF083163	MF083164	MK573001
Conlarium sacchari	DX4	MF083168	MF083166	MF083167	MK224587
Conlarium baiseense	TD17	MK164657	MK164653	MK164655	MK572999
Conlarium nanningense	M8	MK164658	MK164654	MK164656	MK572998
Conlarium duplumascospora	CGMCC 14938	JN936987	JN936995	JN936991	NS
Conlarium duplumascospora	CGMCC 14939	JN936988	JN936996	JN936992	NS
Conlarium duplumascospora	CGMCC 14940	JN936989	JN936997	JN936993	NS
Conlarium aquaticum	MFLUCC 15-0992	MF374372	MF374354	MF374363	NS
Conlarium thailandense	MFLUCC 17-2349	MH624128	MH624129	MH624127	NS
Atractospora thailandensis	KUMCC 16-0067	MF374371	MF374353	MF374362	MF370951
Atractospora reticulata	CBS 127884	NS	KT991669	KT991660	KT991649
Atractospora reticulata	CBS 138740	NS	KT991670	KT991661	KT991650
Atractospora decumbens	CBS 139032	KT991640	KT991667	KT991658	KT991647
Atractospora verruculosa	CBS 132040	KT991641	KT991668	KT991659	KT991648
Pseudoproboscispora thailandensis	MFLUCC 15-0989	MF374377	MF374360	MF374369	NS
Rubellisphaeria abscondita	CBS 132078	KT991646	KT991678	KT991666	KT991657
Lentomitella cirrhosa	ICMP 15131	AY761089	KY931780	AY761085	KM492911
Torrentispora biatriispora	A 464-3	NS	KY931803	AY316352	KY931858

Notes: NS No data in GenBank.

chari, six isolates from Atractosporaceae, two taxa from Pseudoproboscisporaceae, and *Lentomitella cirrhosa* as the outgroup, were included in the phylogenetic analysis. In the alignment of the 21 sequences (SSU+ITS+LSU+RBP2), the data matrix comprised 3293 characters. The alignment dataset was performed using the MrBayes program, applied with SYM+I+G model selected by MrModeltest as the best-fit model. The prior probability density is a flat Dirichlet (all values are 278 1.0) for both Revmatpr and Statefreqpr as default settings. A Bayesian tree with posterior probability (BPP) and bootstrap values at branches is shown in Figure 4. In the phylogenetic tree, *C. baiseense* and *C. sacchari* formed a separate clade with 1.00 support of BPP and 100% support of NJ, *C. nanningense* formed a clade with *C. duplumascospora* with 0.96 support of BPP, and three of the new species were clearly separated from other *Conlarium* species.

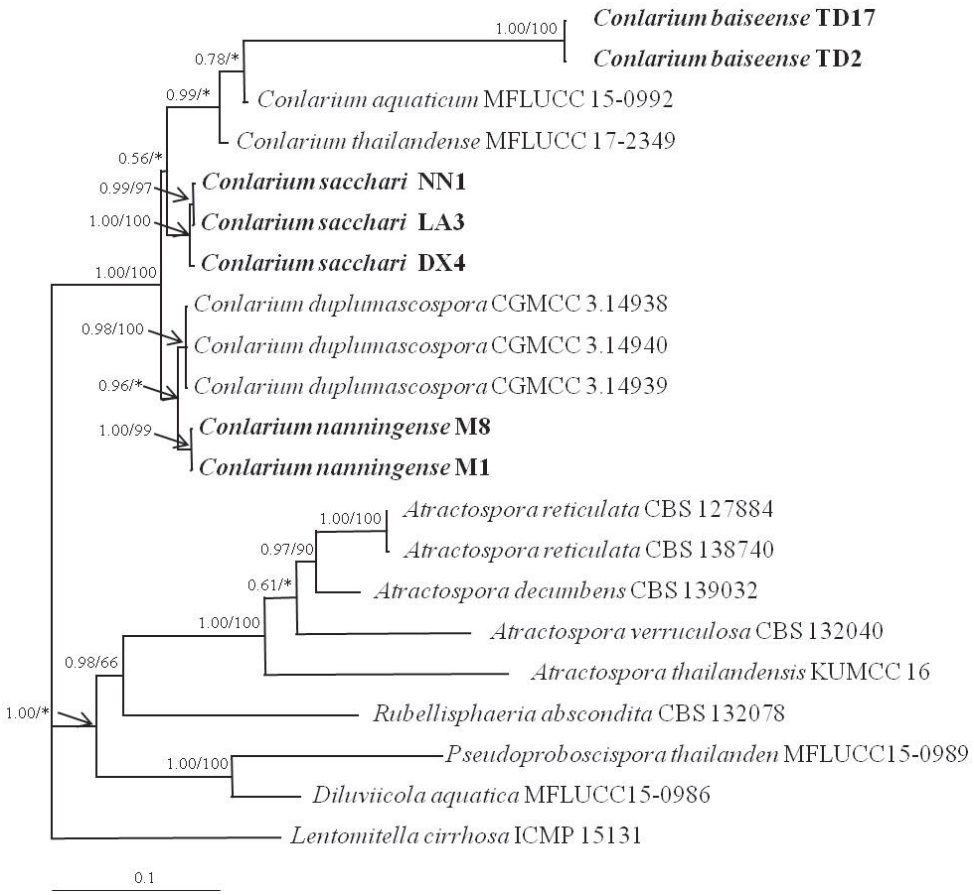

Figure 4. Bayesian tree based on the combined SSU+ITS+LSU+RBP2 sequences of *Conlarium* species and related families. *Lentomitella cirrhosa* was designated as outgroups. The numbers at each branch point represented Bayesian posterior probabilities (left) and percentage bootstrap support calculated from 1,000 replicates (right). *indicates lack of support or support less than 50 % for a particular clade. New species proposed are in bold. Bar 0.1 expected changes per site.

Discussion

The genus *Conlarium* comprises three species, *C. duplumascosporum*, *C. thailandense*, and a hyphomycetous asexualmorph taxon, *C. aquaticum*. They have subglobose or irregular, brown, clathrate, muriform conidia (Zhang et al. 2017). The taxonomy of *Conlarium* is mainly based on the morphological characteristics of gregarious ascomata (Liu et al. 2012). However, the ascomata of *C. aquaticum*, *C. thailandense*, *C. sacchari*, *C. baiseense*, and *C. nanningense* was not observed on the medium. The new species introduced in this paper resemble the asexual morph of *Conlarium* in having muriform conidia. They can be distinguished by the fewer number of septa, as compared with *C. duplumascosporum*, *C. aquaticum*, and *C. thailandense* (Liu et al 2012; Zhang et al. 2017; Phookamsak et al. 2019). *Conlarium baiseense* can be distinguished from other species by its columnar conidia (more transverse and less longitudinal septa) present. *Conlarium sacchari* is characterized by simple conidia (fewer septa) and its longer branched conidiophore. Phylogenetic reconstructions based on SSU+ITS+LSU+RBP2 sequences show that the three new species form independent monophyletic groups and are well separated from *C. duplumascophora*, *C. thailandense*, and *C. aquatcium*; this further supports the erection of these three new species. *Conlarium duplumascophora*, *C. thailandense*, and *C. aquatcium* were from wood samples. Our three new species present as dark spetate endophytes from sugarcane rhizosphere and can be symbiotic with sugarcane. The new species extend the habitat of *Conlarium* from wood to soil.

Acknowledgements

This work was supported by China National Natural Science Foundation (No. 31460016), Guangxi Natural Science Foundation (No. 2015GXNSFBA139083), and Basic Scientific Research Special Project of Guangxi Academy of Agricultural Sciences (No. 2015YT80).

References

Huelsenbeck JP, Ronquist F (2001) MRBAYES: Bayesian inference of phylogeny trees. Bioinformatics 17: 754–755. https://doi.org/10.1093/bioinformatics/17.8.754

Jeewon R, Hyde KD (2016) Establishing species boundaries and new taxa among fungi: recommendations to resolve taxonomic ambiguities. Mycosphere 7 (11):1669–1677. https://doi.org/10.5943/mycosphere/7/11/4

Liu F, Hu DM, Cai L (2012) *Conlarium duplumascospora* gen. et. sp. nov. and *Jobellisia guangdongensis* sp. nov. from freshwater habitats in China. Mycologia 104: 1178–1186. https://doi.org/10.3852/11-379

Liu YJ, Whelen S, Hall BD (1999) Phylogenetic relationships among ascomycetes: evidence from an RNA polymerse II subunit. Molecular Biology and Evolution 16: 1799–1808. https://doi.org/10.1093/oxfordjournals.molbev.a026092

Narisawa K, Tokumasu S, Hashiba T (1998) Suppression of clubroot formation in Chinese cabbage by the root endophytic fungus, *Heteroconium chaetospira*. Plant Pathology 47: 206–210. https://doi.org/10.1046/j.1365-3059.1998.00225.x

Nylander JAA (2008) MrModeltest 2.3 REAME. http://www.abc.se/nylander/mrmodeltest2/mrmodeltest2.html [Accessed 22 May 2008]

Phookamsak R, Hyde KD, Jeewon R, Bhat DJ, Jones EBG, Maharachchikumbura SSN, Raspé O, Karunarathna SC, Wanasinghe DN, Hongsanan S, Doilom M, Tennakoon DS, Machado AR, Firmino AL, Ghosh A, Karunarathna A, Mešić A, Dutta AK, Thongbai B, Devadatha B, Norphanphoun C, Senwanna C, Wei D, Pem D, Ackah FK, Wang GN, Jiang HB, Madrid H, Lee HB, Goonasekara ID, Manawasinghe IS, Kušan I, Cano J, Gené J, Li JF, Das K, Acharya K, Raj KNA, Latha KPD, KWT, He MQ, Dueňas M, Jadan M, Martín MP, Samarakoon MC, Dayarathne MC, Raza M, Park MS, Telleria MT, Chaiwan N, Matoíčec N, de Silva NI, Pereira OL, Singh PN, Manimohan P, Uniyal P, Shang QJ, Bhatt RP, Perera RH, Alvarenga RLM, Nogal-Prata S, Singh SK, Vadthanarat S, Oh SY, Huang SK, Rana S, Konta S, Paloi S, Jayasiri SC, Jeon SJ, Mehmood T, Gibertoni TB, Nguyen TTT, Singh U, Thiyagaraja V, Sarma VV, Dong W, Yu XD, Lu YZ, Lim YW, Chen Y, Tkalčec Z, Zhang ZF, Luo ZL, Daranagama DA, Thambugala KM, Tibpromma S, Camporesi E, Bulgakov TS, Dissanayake AJ, Senanayake IC, Dai DQ, Tang LZ, Khan S, Zhang H, Promputtha I, Cai L, Chomnunti P, Zhao RL, Lumyong S, Boonmee S, Wen TC, Mortimer PE, Xu JC (2019) Fungal diversity notes 929–1035: taxonomic and phylogenetic contributions on genera and species of fungi. Fungal Diversity 95: 1–273. https://doi.org/10.1007/s13225-019-00421-w

Sun X, Guo LD (2010) *Micronematobotrys*, a new genus and its phylogenetic placement based on rDNA sequence analyses. Mycological Progress 9:567–574. https://doi.org/10.1007/s11557-010-0664-7

Vilgalys R, Hester M (1990) Rapid genetic identification and mapping of enzymatically amplified ribosomal DNA from several Cryptococcus species. Journal of Bacteriology 172: 4238–4246. https://doi.org/10.1128/jb.172.8.4238-4246.1990

White TJ, Bruns T, Lee S, Taylor J (1990) Emplification and direct sequencing of fungal ribosomal RNA genes for phylogenetics. In: Innis MA, Gelfand DH, Sninsky JJ, White JT (Eds) PCR Protocols: a Guide to Methods and Applications. Academic Press, San Diego, California, 315–322. https://doi.org/10.1016/B978-0-12-372180-8.50042-1

Zhang H, Dong W, Hyde DK, Maharachchikumbura SSN, Hongsanan S, Bhat DJ, Al-Sadi AM, Zhang D (2017) Towards a natural classification of Annulatascaceae-like taxa: introducing Atractosporales ord. nov. and six new families. Fungal Diversity 85: 75–110. https://doi.org/10.1007/s13225-017-0387-z

MycoKeys 56: 13–32 (2019)
doi: 10.3897/mycokeys.56.35204
http://mycokeys.pensoft.net

RESEARCH ARTICLE

A peer-reviewed open-access journal
MycoKeys
Launched to accelerate biodiversity research

Updated taxonomy of *Lactifluus* section *Luteoli*: *L. russulisporus* from Australia and *L. caliendrifer* from Thailand

Glen Dierickx[1], Marie Froyen[1], Roy Halling[2], Komsit Wisitrassameewong[3], Lynn Delgat[1], Eske De Crop[1], Annemieke Verbeken[1]

1 *Research Group Mycology, Department of Biology, Ghent University, Ghent, Belgium* **2** *Institute of Systematic Botany, The New York Botanical Garden, Bronx, NY, USA* **3** *National Center for Genetic Engineering and Biotechnology (BIOTEC), Chang Wat Pathum Thani, Thailand*

Corresponding author: *Glen Dierickx* (glen.dierickx@ugent.be)

Academic editor: *Olivier Raspé* | Received 10 April 2019 | Accepted 23 May 2019 | Published 10 July 2019

Citation: Dierickx G, Froyen M, Halling R, Wisitrassameewong K, Delgat L, De Crop E, Verbeken A (2019) Updated taxonomy of *Lactifluus* section *Luteoli*: *L. russulisporus* from Australia and *L. caliendrifer* from Thailand. MycoKeys 56: 13–32. https://doi.org/10.3897/mycokeys.56.35204

Abstract

Lactifluus russulisporus Dierickx & De Crop and *Lactifluus caliendrifer* Froyen & De Crop are described from eucalypt forests in Queensland, Australia and different forest types in Thailand, respectively. Both species have recently been published on Index Fungorum and fit morphologically and molecularly in *L.* sect. *Luteoli*, a section within *L.* subg. *Gymnocarpi* that encompasses species with alboochraceous basidiomes, white latex that stains brown and typical capitate elements in the pileipellis and/or marginal cells.

Keywords

Ectomycorrhizal fungi, *Russulaceae*, milkcaps, taxonomy, phylogeny, *Leptocystidia*, sterile elements, paracystidia

Introduction

Since the division of *Lactarius* into *Lactarius* sensu novo and *Lactifluus* (Buyck et al. 2008), our understanding of both genera has increased significantly. Although *Lactifluus* is the smaller of the two genera, it is characterised by a higher genetic diversity with subgroups in very different and genetically distant clades (De Crop et al. 2017). Recently, efforts in *Lactifluus* culminated in a new infrageneric classification based on

a multi-gene phylogeny (De Crop et al. 2017). Herein, the genus *Lactifluus* is subdivided into four subgenera: *L.* subg. *Lactariopsis*, *L.* subg. *Lactifluus*, *L.* subg. *Pseudogymnocarpi* and *L.* subg. *Gymnocarpi*. The latter contains four sections, apart from five isolated species and one unnamed clade: *L.* sect. *Gymnocarpi* and *L.* sect. *Phlebonemi* with exclusively African representatives, *L.* sect. *Tomentosi* with representatives from Oceania and *L.* sect. *Luteoli* with seven species spanning all continents, except South America. De Crop et al. (2017) illustrates the existence of two new sister species, one from Thailand and one from Australia, within the latter section. These two sister species were recently published on Index Fungorum (Dierickx et al. 2019) with a short description, but are fully described in this paper: *L. caliendrifer* from Thailand and *L. russulisporus* from Australia. While in De Crop et al. (2017) four loci (ITS, LSU, *RPB1* and *RPB2*) were used to construct the phylogeny, here only ITS is used.

The Thai collections were found in different habitats: KW 378 was found in montane forest with Fagaceae trees (*Lithocarpus*, *Castanopsis* and *Quercus*) and some bamboo tree species; KW 392 was growing in disturbed Dipterocarp forest, with *Dipterocarpus* spp. The first Australian collection, RH 9398, was growing on sand in wet sclerophyll forest, in the presence of various Myrtaceae (*Leptospermum*, *Syncarpia*, *Eucalyptus pilularis* and *E. microcorys*). It is a closed canopy forest but receives less rainfall than 'true' rainforest. The second collection, RH 9674, was found in subtropical rainforest; nearby vegetation includes *Eucalyptus* spp. and *Lophostemon* spp. (Myrtaceae).

Methods

Sampling

The two collections of *Lactifluus caliendrifer* were made during fieldwork by Komsit Wissitrassameewong in 2012 and are deposited in Herbarium Universitatis Gandavensis, Belgium (GENT) and the herbarium of Mae Fah Luang University, Chiang, Thailand (MFLU). For *L. russulisporus*, fieldwork in 2010 and 2012 by Roy Halling and collaborators resulted in two collections of the species, which are deposited in The William and Lynda Steere Herbarium of the New York Botanical Garden (NY) and the Queensland Herbarium (BRI). We know from earlier research (De Crop et al. 2017; De Crop et al. 2016) that Halling 9398 and Wisitrassameewong 378 belong to *L.* subg. *Gymnocarpi* sect. *Luteoli.* Our dataset contains the ITS sequences used for *L.* subg. *Gymnocarpi* in De Crop et al. (2017), supplemented with newly generated sequences. Five species of *L.* subg. *Lactifluus* were used as outgroup.

Morphology

Macroscopic characters are all based on fresh material. Microscopic features were studied from dried material in Congo red in SDS. Possible excretory products were

checked for in Cotton blue in lactic acid and Cresyl blue (Clémençon 1997; 2009) Spore ornamentation is described and illustrated as observed in Melzer's reagent. A total of 40 spores (20 per collection) were measured for each of the two new species. For details on terminology we refer to Verbeken (1998) and Verbeken and Walleyn (2010). Line-drawings were made with the aid of a drawing tube (Zeiss camera lucida on a Zeiss Axioskop 2 microscope equipped with a magnification changer of 2.5× for spores and an Olympus U-DA on an Olympus CX21 microscope for individual elements and pileipellis structures) at original magnifications: 6000× for spores, 1500× for individual elements and sections. Basidia length excludes sterigmata length. Spores were measured in side view, excluding the ornamentation, and measurements are given as (MINa) [AVa-2*SD]–AVa–AVb–[AVb+2*SD] (MAXb), with AVa = lowest mean value for the measured collections and AVb = greatest mean value for the measured collections, SD = standard deviation, MINa = lowest extreme value of collection "a" and MAXb = greatest extreme value of collection "b". The Q-value (quotient length/width) is given as (MIN Qa) Qa–Qb (MAX Qb), with Qa = lowest mean ratio for the measured collections and Qb = greatest mean ratio for the measured collections, MIN Qa = lowest extreme ratio of collection "a" and MAX Qb = greatest extreme ratio of collection "b". Other measurements are given as MIN–MAX values. Colour codes refer to Kornerup and Wanscher (1978). Microscopic photographs were taken using a Nikon eclipse NI-U–microscope equipped with a DX-Fi1c camera and Nikon NIS-Elements software including EDF module.

Molecular work

DNA from dried collections was extracted using the protocol described by Nuytinck and Verbeken (2003) with modifications described in Van de Putte et al. (2010), and from fresh material using the CTAB extraction method described in Nuytinck and Verbeken (2003). Protocols for PCR amplification follow Le et al. (2007). The internal transcribed spacer (ITS) was sequenced for a second collection for each new species using the primers ITS1-F and ITS4 (Gardes and Bruns 1993; White et al. 1990). PCR products were sequenced using an automated ABI 3730 XL capillary sequencer (Life Technology) at Macrogen. Forward and reverse sequences were assembled into contigs and edited where needed with SequencherTM v5.0 software (Gene Codes Corporation, Ann Arbor, MI, USA).

Phylogenetic analysis

Sequences were aligned online using the E-INS-I strategy of the multiple sequence alignment program MAFFT v7 (Katoh and Standley 2013). Trailing ends were trimmed, and where necessary, the alignment was manually edited in MEGA 7 (Kumar et al. 2016). The alignment can be obtained from the first author and TreeBASE

(Submission ID S23999). The best partition scheme was selected with PARTITIONFINDER 2 (Lanfear et al. 2016) using standard settings. Aligned sequences were partitioned into 18S (1–56), ITS1 (57–334), 5.8S (335–482), ITS2 (483–820) and 28S (821–868). Maximum likelihood (ML) analyses were conducted with RAxML v8.2.10 (Stamatakis 2014), where a ML analysis was combined with the Rapid Bootstrapping algorithm with 1000 replicates under the GTRCAT option (Stamatakis et al. 2008). All analyses were performed on the CIPRES Science Gateway (Miller et al. 2015).

Results

In congruence with De Crop et al. (2017), our molecular results show that the collections from Australia as well as those from Thailand belong to *Lactifluus.* subg. *Gymnocarpi* sect. *Luteoli* (Fig. 2). The newly generated sequences for Halling 9674 and Wisitrassameewong 392 belong to the same species as Halling 9398 and Wisitrassameewong 378 respectively. These two species are supported by morphological and geographical differences (see discussion) and are fully described below as *L. russulisporus* and *L. caliendrifer*.

Taxonomy

Lactifluus russulisporus **Dierickx & De Crop**
MycoBank: MB 829913
Index Fungorum 392: IF 829913
Figs 1, 3–4

Original diagnosis. Basidiocarps small (up to 4 cm cap diam.). Cap and stipe dry, matt, yellowish white to pale brown. Context with unpleasant, fishy smell. Latex copious, watery white, staining tissues brown. Basidiospores broadly ellipsoid 7.0–*7.8*–*7.9*–8.7 × 5.7–*6.4*–*6.5*–7 µm (n=40, Q = 1.14–*1.23*–1.40); ornamented with irregular and isolated warts which are up to 1.3 µm high. True pleurocystidia absent, but with few to abundant sterile elements in the hymenium. Pileipellis a lampropalisade. *L. russulisporus* differs from its sister species, *L. caliendrifer*, by its longer basidia, slightly bigger spores with a somewhat heavier and more irregular ornamentation and the absence of abundant thick-walled marginal cells.

Basidiomes rather small. **Pileus** 20–40 mm diam., convex to plano-convex and depressed on disc to uplifted and slightly depressed, yellowish white (4A2) to pale brown, dry, matted, subtomentose to finely subvelutinous and somewhat subrugulose to subcorrugate; margin inrolled. **Stipe** 10–30 × 5–10 mm cylindrical, dry, matt, yellowish white, sometimes paler brownish towards the base, with white mycelium at the base. **Lamellae** adnexed to subdecurrent, rather close, pale greyish white to yellowish

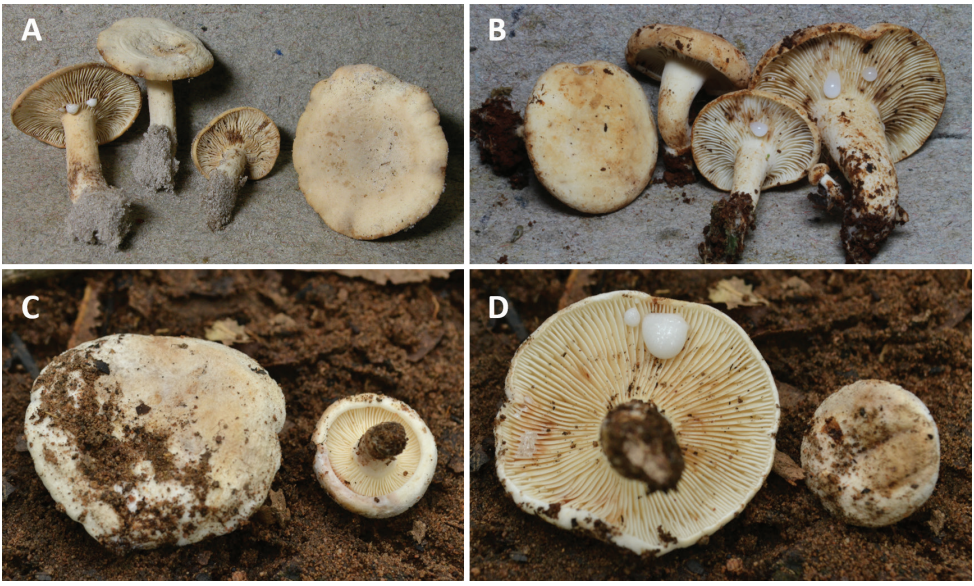

Figure 1.A–B *Lactifluus russulisporus* basidiomes **C–D** *L. caliendrifer* basidiomes **A** holotype, RH 9398 **B** RH 9674 **C** holotype, KW 378 **D** KW 392.

white, turning darker to near pale brown with age. **Context** white, solid to somewhat pithy in the stipe; smell unpleasant, fishy; taste mild. **Latex** copious, watery white, staining tissues brown.

Basidiospores broadly ellipsoid 7.0–*7.8–7,9*–8.7 × 5.7–*6.4–6,5*–7 µm (n=40, Q = 1.14–*1.23*–1.40); ornamentation amyloid, prominent, composed of irregular and isolated warts which are up to 1.3 µm high, never forming a reticulum; plage distinct and inamyloid. **Basidia** 43–71 × 8–14 µm, subcylindrical to subclavate, thin-walled, mostly 4-spored. **Pleurolamprocystidia** absent. **Sterile elements** inconspicuous to abundant, cylindrical, sometimes a bit irregular, 17–64 × 3–7 µm, thin-walled and up to 3-septate, sometimes emerging, with terminal cells 9–39 × 2.5–6.5 µm. **Pleuropseudocystidia** generally abundant, sometimes emerging, 3–8 µm diam., irregularly cylindrical; apex obtuse to subcapitate; content oil-like to granular. **Lamellae edge** sterile, marginal cells 23–74 × 2–7.5 µm, thin-walled, cylindrical to subfusiform or slightly subclavate, often branched, not septate or with up to 3 septae, with terminal cells 7–49 × 2–7.5; apex obtuse to subcapitate; some marginal cells may be slightly thick-walled, but these are scarce. **Hymenophoral trama** cellular, with lactifers. **Pileipellis** a lampropalisade; elements of the suprapellis 35–180 × 2.5–6 µm, cylindrical, thick-walled and often septate; apex obtuse to capitate; subpellis cellular, composed of isodiametric, sometimes slightly thick-walled cells, which are 7–30 µm diam. **Stipitipellis** a trichoderm to lamprotrichoderm; ascending hyphae 35–80 × 4–6 µm, up to 3 septate, slightly thick-walled to thick-walled especially basal cells, apex obtuse to capitate. **Clamp connections** absent.

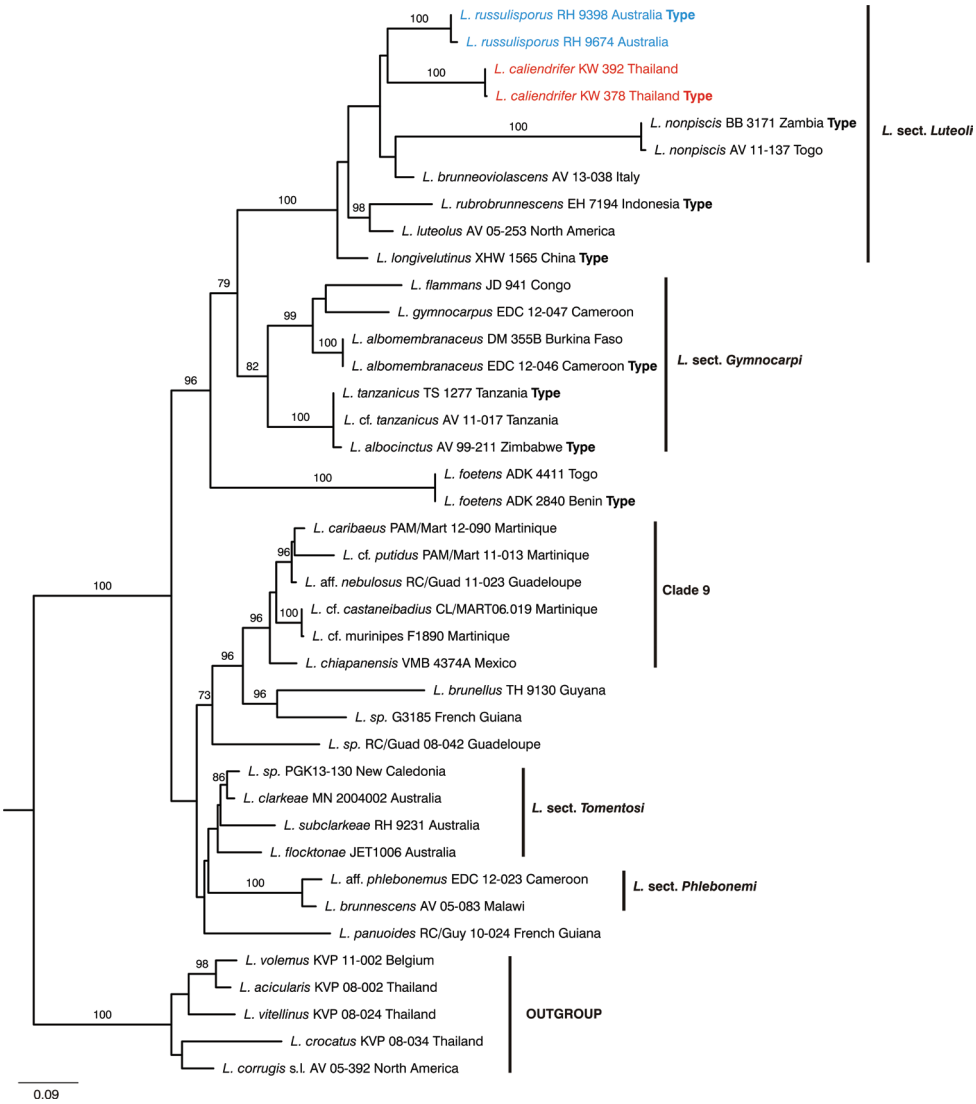

Figure 2. Overview Maximum Likelihood tree of *Lactifluus* subg. *Gymnocarpi*, based on ITS sequence data. Maximum Likelihood bootstrap values >70 are shown.

Distribution. Known from Eastern Australia.

Ecology. East-Australian wet sclerophyll and subtropical rainforest, scattered to gregarious on soil under *Leptospermum*, *Syncarpia*, and *Eucalyptus* spp.

Etymology. Named after the spores which are reminiscent of the spore ornamentation and shape of many *Russula* species.

Conservation status. Unknown.

Specimens examined. Australia. Queensland West of Brisbane, D'Aguilar National Park, Maiala Area walking tracks, alt. 680 m, 27°20'0.3"S, 152°45'48.3"E, rain-

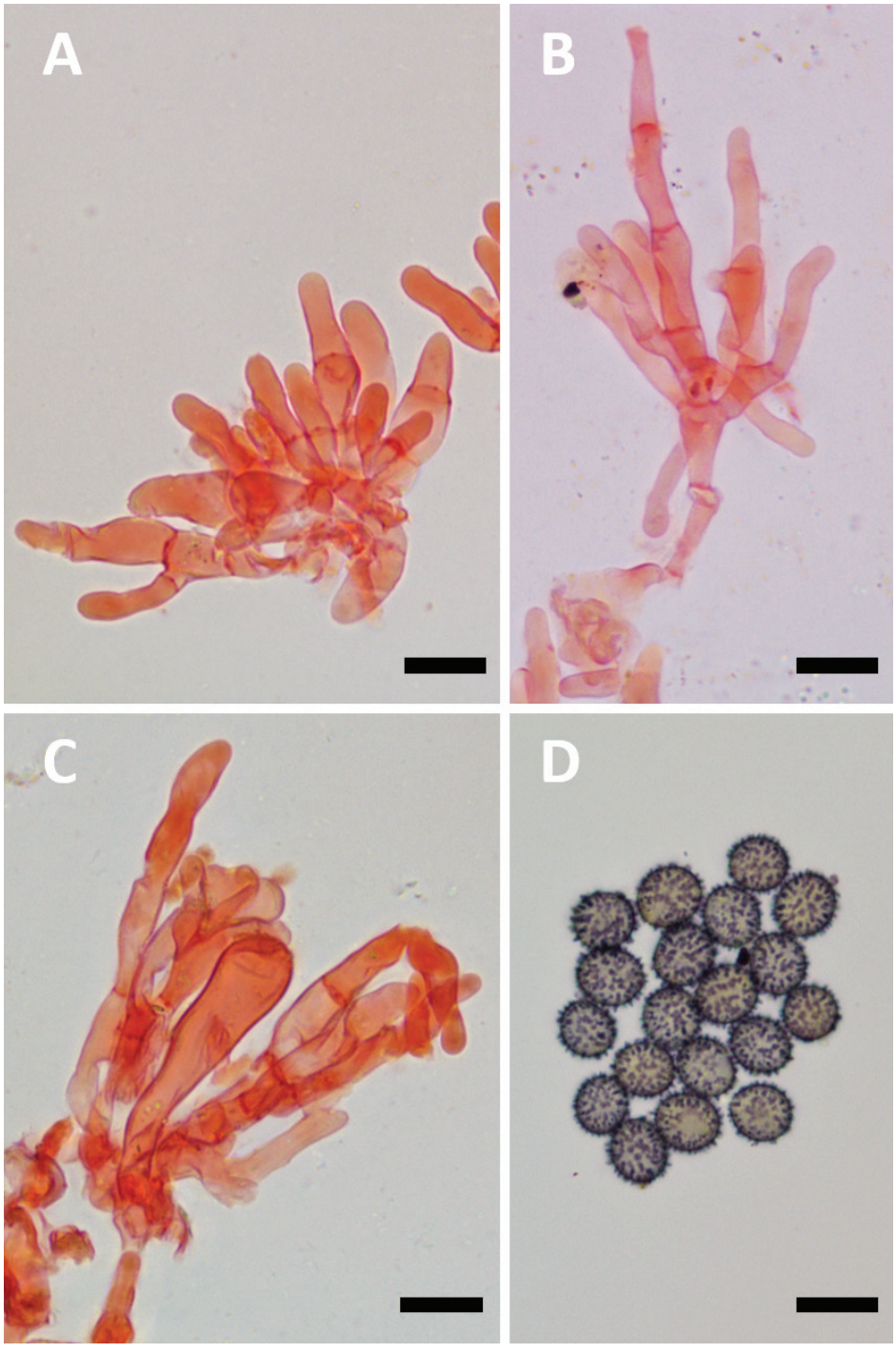

Figure 3.A–D Microscopic characters of *Lactifluus russulisporus* **A** marginal cells, RH 9764 **B** marginal cells, holotype, RH 9398 **C** basidiole and sterile elements, holotype, RH 9398 **D** spores, holotype, RH 9398. Scale bar: 10 µm.

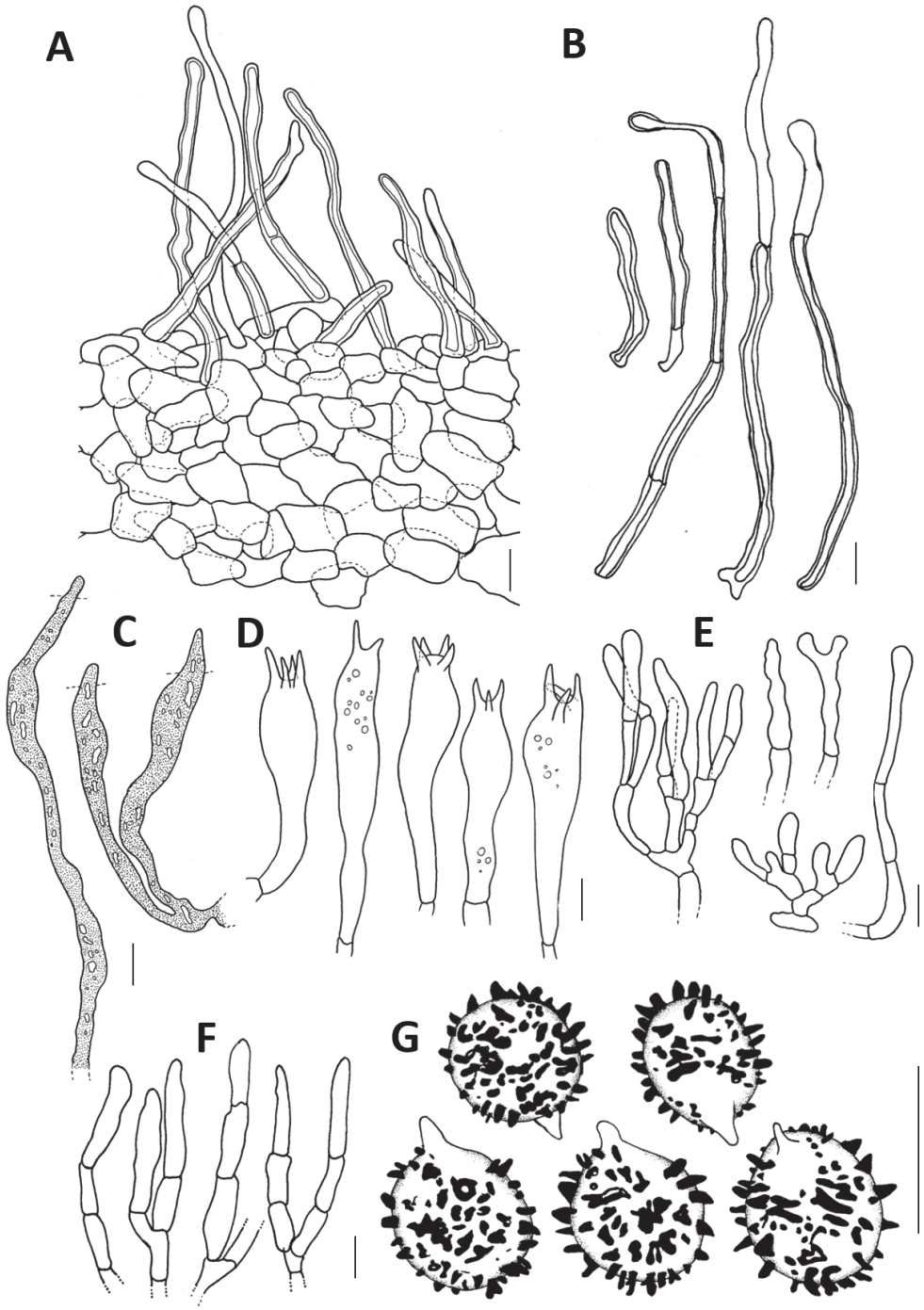

Figure 4. Microscopic features of *Lactifluus russulisporus* **A** section through the pileipellis **B** pileipellis hairs **C** pseudocystidia **D** basidia **E** marginal cells **F** sterile elements from the hymenium **G** basidiospores. Illustrations by G. Dierickx and A. Verbeken. Scale bars: 10 µm.

forest, scattered on the soil near *Eucalyptus* sp. and *Lophostemon* sp., 8 March 2012, R. E. Halling and N. Fechner, R.E.H. 9674 (BRI, NY); Queensland: Fraser Island, Wanggoolba Creek Road, West of Central Station, alt. 90m, 25°28'S, 153°2'E, gregarious on sand with *Leptospermum*, *Syncarpia*, *Eucalyptus pilularis* and *Eucalyptus microcorys*, 27 May 2010, leg.: R. E. Halling, N. Fechner and M. Castellano, R.E.H. 9398 (holotypus BRI, isotypus NY).

Remarks. *Lactifluus russulisporus* differs from its sister species, *L. caliendrifer*, by its longer basidia, slightly bigger spores with a somewhat heavier and more irregular ornamentation and the absence of abundant thick-walled marginal cells.

Lactifluus caliendrifer **Froyen & De Crop**
MycoBank: MB 829914
Index Fungorum 392: IF 829914
Figs 1, 5, 6

Original diagnosis. Basidiocarps small (up to 3.5 cm cap diam.) and turning brown when bruised. Cap very velvety to tomentose, white to cream-coloured. Stipe smooth to velvety, white. Context with smell fruity, strong. Latex copious, watery white to white, sticky, turning dark yellow to mustard brown; taste acrid and a bit bitter. Basidiospores broadly ellipsoid, (5.8) 5.9–*7.0–7.1*–7.9 × (4.5) 4.7–*5.6–5.7*–6.2 µm (n=40, Q = 1.12–*1.24*–1.41); ornamented with irregular and isolated warts which are up to 1 µm high. True pleurocystidia absent, but with sterile elements in the hymenium. Pileipellis a palisade to lampropalisade. *L. caliendrifer* differs from its sister species, *L. russulisporus*, by the abundant thick-walled marginal cells, very long pileipellis hairs and slightly smaller basidia and spores with more regular and lower warts.

Basidiomes rather small. **Pileus** 19–34 mm diam., planoconvex, sometimes centrally depressed; surface very velvety, dull, pruinose, tomentose, covered with hairs in tufts, white to cream-coloured, becoming brown after bruising; margin inflexed. **Stipe** 11–17 × 4–7 mm, cylindrical, centrally attached; surface smooth to velvety, white, turning brownish when bruised. **Lamellae** adnate to decurrent, narrow and thin, 0.5–1.5 mm broad, crowded, with 3 to 4 lamellulae of different lengths between 2 lamellae, whitish, concolorous with pileus and becoming brownish when bruised; edge entire, concolorous. **Context** white, changing to pale pinkish near pileipellis after a while, turning brown when broken (6E8) or sometimes paler caramel (6C6), or camel (6D4); smell fruity, strong; taste unknown. **Latex** copious, watery white to white, sticky, turning dark yellow (4C8) after a few minutes, later mustard brown (5E6) after 15 minutes; taste acrid and a bit bitter.

Basidiospores broadly ellipsoid, (5.8) 5.9–*7.0–7.1*–7.9 × (4.5) 4.7–*5.6–5.7*–6.2 µm (n=40, Q = 1.12–*1.24*–1.41); ornamentation amyloid, composed of irregular or isolated warts which are up to 1 µm high, sometimes connected by low ridges, but not forming a reticulum; plage inamyloid. **Basidia** 27–55 × 8–12 µm, subcylindrical to subclavate, thin-walled, mostly 4-spored; content oil-like to granular.

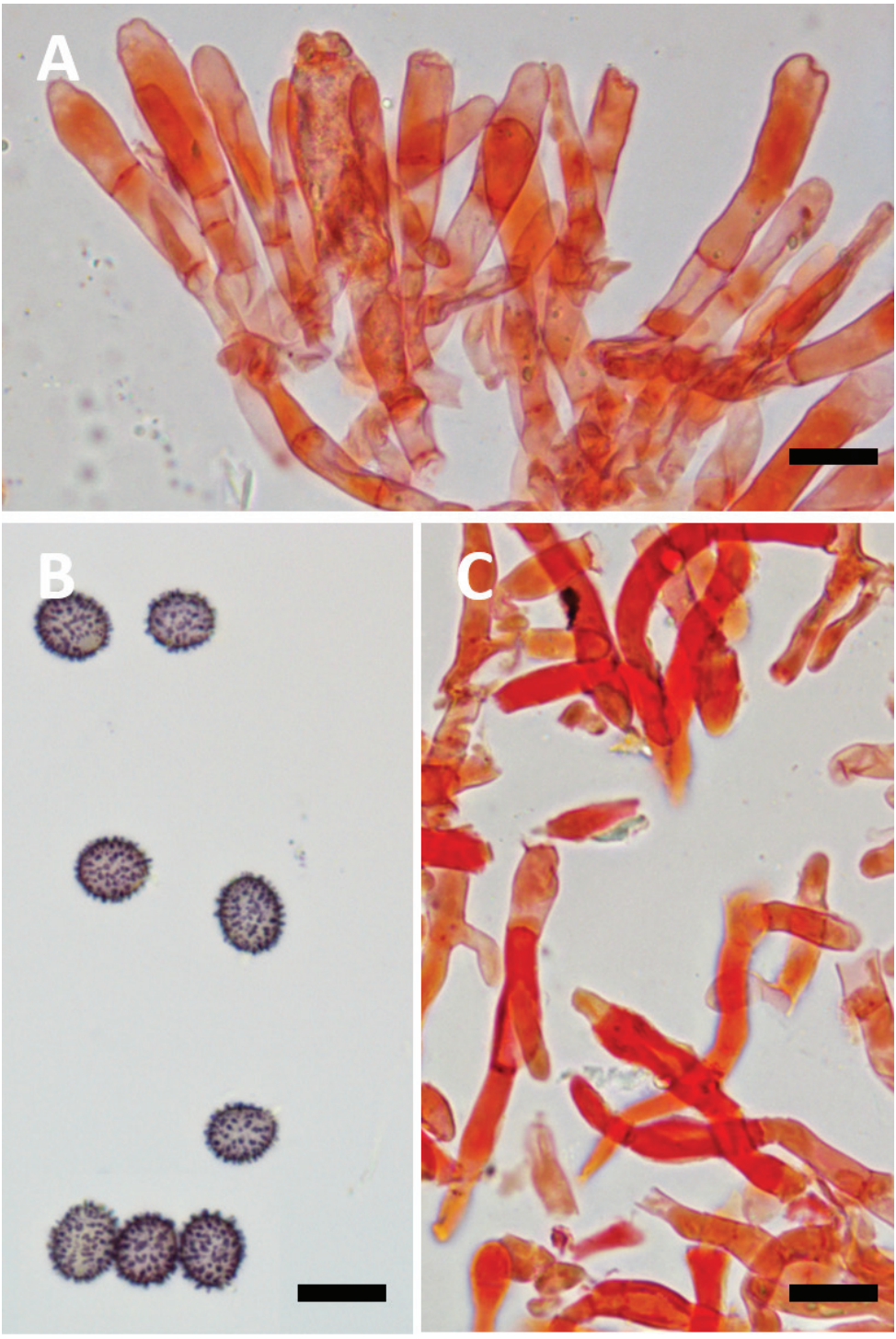

Figure 5.A–C Microscopic characters of *Lactifluus caliendrifer* **A** basidiole and sterile elements, KW 392 **B** spores, holotype, KW 378 **C** marginal cells, holotype, KW 378. Scale bar: 10 µm.

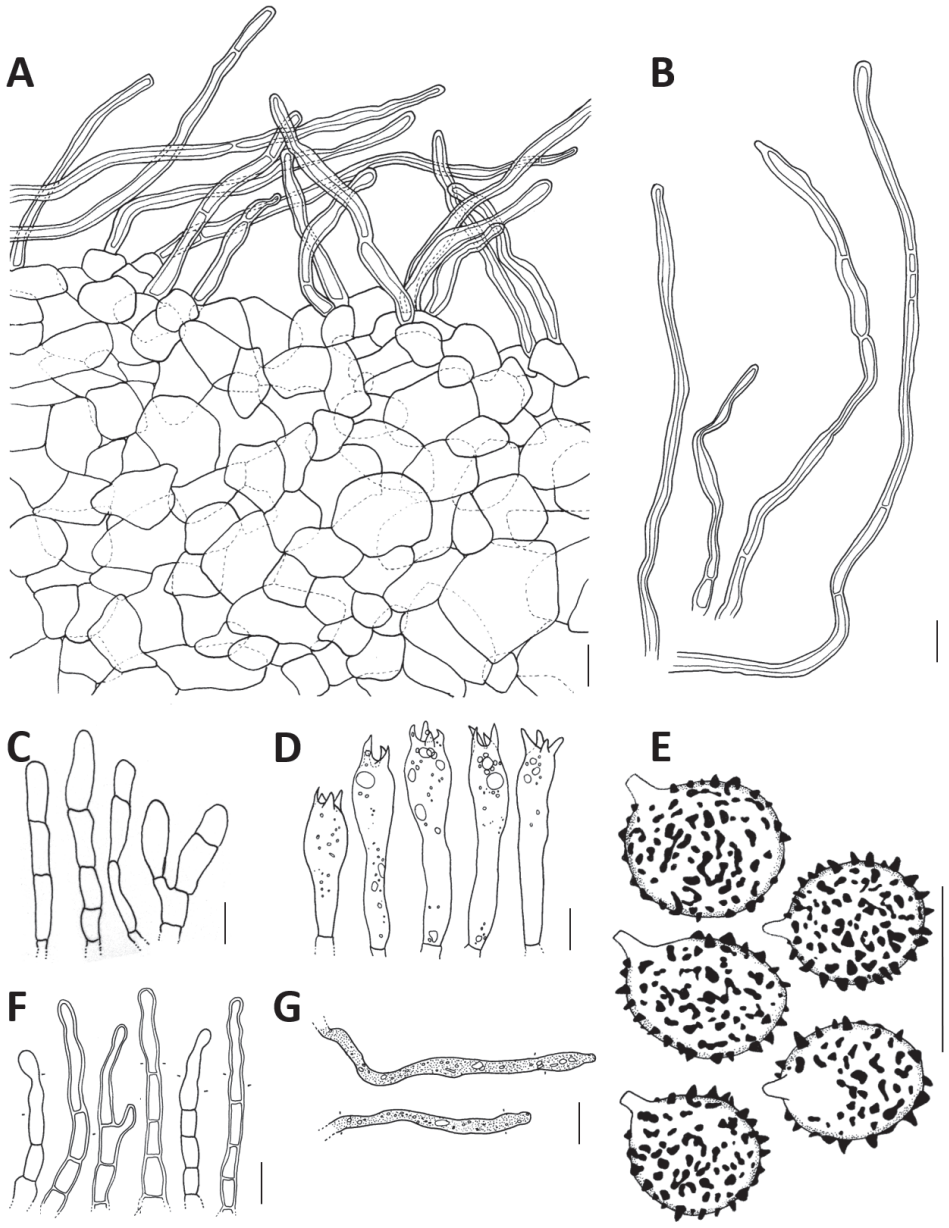

Figure 6. Microscopic features of *Lactifluus caliendrifer*. **A** section through the pileipellis **B** pileipellis hairs **C** sterile elements from the hymenium **D** basidia **E** basidiospores **F** marginal cells **G** pseudocystidia. Illustrations by M. Froyen, G. Dierickx and A. Verbeken. Scale bar: 10 µm.

Pleurolamprocystidia absent. **Sterile elements** cylindrical, 28–52 × 4–8 µm, thin-walled and up to 3-septate, slightly emerging, with terminal cells 6–28 × 4–7.5 µm. **Pleuropseudocystidia** rare to abundant, 4–10 µm diam., emerging, irregularly cylindrical; apex obtuse to subcapitate; content oil-like to granular. **Lamellae edge**

sterile. **Marginal cells** 28–61 × 3–6 µm, often septate: with 1 to 5 septae, with terminal cells up to 47 µm long, thick-walled, occasionally branched; apex obtuse to subcapitate. **Hymenophoral trama** cellular, with lactifers. **Pileipellis** a palisade to lampropalisade, elements of the suprapellis 60–440 × 2.5–5 µm; cylindrical, septate, sometimes capitate, slightly thick-walled; subpellis composed of isodiametric, mostly thin-walled cells. **Stipitipellis** a trichoderm to lamprotrichoderm; ascending hyphae 10–75 × 3–6 µm, up to 2 septate, often thick-walled, apex obtuse to capitate. **Clamp connections** absent.

Distribution. Known from Thailand.

Ecology. Thai montane and dipterocarp forest, growing under *Dipterocarpus*, *Lithocarpus*, *Castanopsis* and *Quercus*.

Etymology. Means 'wearing a wig', referring to the long hairs in the pileipellis.

Conservation status. Unknown.

Additional material examined. Thailand. Thoeng district, Chiang Rai, alt. 420 m, 19°36'45"N, 100°04'00"E, Forest roadside, dry dipterocarp forest (Longan plantation), 20 August 2012, K. Jatuwong, Wisitrassameewong 392 (GENT, MFLU); Doi Pui, Chiang Rai, alt. 650 m, 19°49'26"N, 99°52'19"E, bamboo forest, 3 July 2012, leg.: Wisitrassameewong 378 (holotypus, GENT, isotypus MFLU).

Remarks. *Lactifluus caliendrifer* differs from its sister species, *L. russulisporus*, by the abundant thick-walled marginal cells, very long pileipellis hairs and slightly smaller basidia and spores with more regular and lower warts.

Discussion

The morphological distinction between *Lactarius* and *Lactifluus* is not always straightforward in the field and can only be based on some general trends. For example, the genus *Lactifluus* is generally characterised by the complete absence of zonate and viscose to glutinose caps, and it contains many species with veiled and velvety caps (Buyck et al. 2008; De Crop et al. 2017; Verbeken and Nuytinck 2013). A cellular hymenophoral trama and a lampropalisade as pileipellis structure are both characters which are more often observed in *Lactifluus* than in *Lactarius.*

The newly described species can macroscopically be recognised as members of genus *Lactifluus* by the tomentose to velvety appearance of their caps and the exuded milk that changes to brownish (which is more common in *Lactifluus* and very rare in *Lactarius*). Microscopically the presence of a lampropalisade and a cellular trama indicate the affinity with *Lactifluus*.

Lactifluus russulisporus and *L. caliendrifer* belong to *L.* subg. *Gymnocarpi*, which is supported by molecular (Fig. 2) (De Crop et al. 2017) and morphological data (e.g. brown discolouration of the latex and the absence of true pleurolamprocystidia). Both new species are placed in *L.* sect. *Luteoli*, which consists of seven species from all continents except South America and Antarctica, and are characterised by capitate elements in the pileipellis and/or the presence of differentiated marginal cells.

The sister species *Lactifluus russulisporus* and *L. caliendrifer* are clearly delimited molecularly, which is reflected in both geographical and morphological characters. Geographically, *L. russulisporus* is only known from Eastern Australia (Queensland), while *L. caliendrifer* is only known from Southeast Asia (Thailand). In the field, both species can be recognised by their cream to yellowish white basidiomes, dry and finely velvety to pruinose pilei, rather crowded white to concolorous lamellae and copious watery latex that stains brown. These features are common to most species in *L.* sect. *Luteoli*.

Lactifluus caliendrifer can be distinguished macroscopically by its velvety pileus, whiter basidiomes and its strong and fruity smell. *Lactifluus russulisporus* differs from its sister species by having a more yellowish-brown shade and an unpleasant, fishy smell.

Microscopically, the two species can be differentiated by several characters. First, the pileipellis elements are (35) 85–125 (180) µm long in *Lactifluus russulisporus*, while they can exceed 400 µm in *L. caliendrifer*. Second, *L. russulisporus* has larger spores: on average 7,8–7.9 × 6.3–6.4 µm (*L. russulisporus*) versus 7.0–7.1 × 5.6–5.7 µm (*L. caliendrifer*), which is reflected in basidia size: 43–71 × 8–14 µm vs. 27–55 × 8–12 µm for *L. russulisporus* and *L. caliendrifer* respectively. Third, *L. caliendrifer* is characterised by the presence of numerous thick-walled marginal cells, while these are scarce and therefore difficult to find in *L. russulisporus*. Lastly, the ascending hyphae of the stipitipellis are often shorter in *L. caliendrifer*: 10–75 µm versus 35–80 µm long for *L. caliendrifer* and *L. russulisporus* respectively.

Five other species occur in *Lactifluus* sect. *Luteoli*. *Lactifluus longivelutinus* is known from China and differs from both new species by its often eccentrical to almost lateral stipe, marginal cells with globose apex containing brownish content, and long, thick-walled terminal cells of the stipitipellis (80–150 (200) µm) (Wang and Verbeken 2006). Comparable to *L. caliendrifer*, it possesses long pileipellis elements (300–400 × 3.5–5 (6.0) µm).

Lactifluus rubrobrunnescens is known to occur in Java (Indonesia) and can easily be recognised by a hollow stipe, latex that stains reddish brown, more globose spores (average Q = 1.16) and distinctly capitate elements in the pilei- and stipitipellis, and marginal cells (Verbeken et al. 2001).

Lactifluus nonpiscis has an African distribution and is well characterised by the purplish brown staining basidiomes with a strongly wrinkled to rugulose pileus. In addition, *L. nonpiscis* can be discerned by the shorter elements of the suprapellis (40–80 (100) µm) and the slightly larger and more ellipsoid spores (8–*8.7*–*9.2*–10.0 × 6.1–*6.6*–*6.7*–7.3 µm, Q = 1.21–*1.31*–*1.36*–1.49) (Verbeken and Walleyn 2010). *Lactifluus brunneoviolascens* and *L. luteolus* are two look-a-likes, the first one in Europe, the second one in North America. They differ from the other representatives by their larger basidiome size (pileus 50–80 mm, stipe 40–70 × 10–12 mm). *Lactifluus luteolus* further differs from the two species described here by its more ellipsoid spores (7–8.5 × 5.5–6 µm) that bear slightly lower ornamentation (up to 0.8 µm) and shorter pileipellis hairs (34–70 × 3–5 µm). *Lactifluus brunneoviolascens* is characterised by abundant capitate, slender and sometimes thick-walled marginal cells.

Notes on terminology

When it comes to terminology used in the genera *Lactarius* and *Lactifluus*, most authors tend to follow Verbeken and Walleyn (2010) and Verbeken (1998). Unfortunately, some confusion seems to exist concerning hymenophoral cells that can be termed either leptocystidia or sterile elements. Even though this type of cell is frequently present in *Lactifluus* (pers. observations), these cells are only rarely reported in species descriptions (De Crop et al. 2019; Delgat et al. 2017), probably often being dismissed as basidioles and/or of limited taxonomic value. This problem presented itself during the description of the two new species and a consensus between the authors of this paper was pursued.

The term leptocystidium is composed of the Greek leptós, meaning "smooth, thin-walled" and cystidium, meaning "a sterile body, frequently of distinctive shape, occurring at any surface of a basidiome, particularly the hymenium from which it frequently projects"(Ainsworth 2008). In Clémençon (1997), leptocystidia are described in a similar manner, with the addition that they often have an excretory function. For the latter, we could not find evidence in our collections. According to Verbeken and Walleyn (2010), leptocystidia can be regarded as "thin-walled cystidia without remarkable content and thus only deviating by their shape. They are tapering at the top and often have a rostrate apex, which makes them easy to confuse with monosterigmatic basidia. One can consider them to be cystidia if they are regularly observed and if they never bear a spore or spore primordium". In the two new species, and by extension in most *Lactifluus* species, thin-walled sterile cells with no remarkable content occur in the hymenium. Furthermore, they do not exhibit a deviating shape, being cylindrical and usually ending blunt. If shape deviation is seen as a vital component for being a cystidium, these cells cannot be named as such. In addition, we dismiss the idea that these cells represent basidioles. Firstly, no intermediate forms between these cells and basidioles were observed. Secondly, in *L. russulisporus* these cells display a different morphology in both collections. In RH 9674, and by extension in general, they do not protrude from the hymenium and do not exhibit a deviant form, leaving open the possibility that they constitute basidioles or protobasidia (Fig. 7C). However, in RH 9398, they grow out strikingly, protruding clearly from the hymenium (Fig. 7A, B). The same behaviour is seen in the pseudocystidia and marginal cells in this collection. According to Moore (2005), principle nine of fungal developmental biology states that "meiocytes appear to be the only hyphal cells that become committed to their developmental fate. Other highly differentiated cells retain totipotency–the ability to generate vegetative hyphal tips that grow out of the differentiated cell to re-establish a vegetative mycelium." A possible hypothesis is that some stimulus, perhaps environmental, caused the totipotent cells in the hymenium to grow out, giving rise to the protruding sterile elements, pseudocystidia and marginal cells in RH 9398. This explanation adds to the idea that these cells are not precursor cells of meiocytes (basidia).

As these sterile elements are argued not to be cystidia or basidioles, the question remains as to what they are. Several terms might have been used to indicate the same kind of cells. For example, haplohyphidia refers to unmodified, unbranched or little

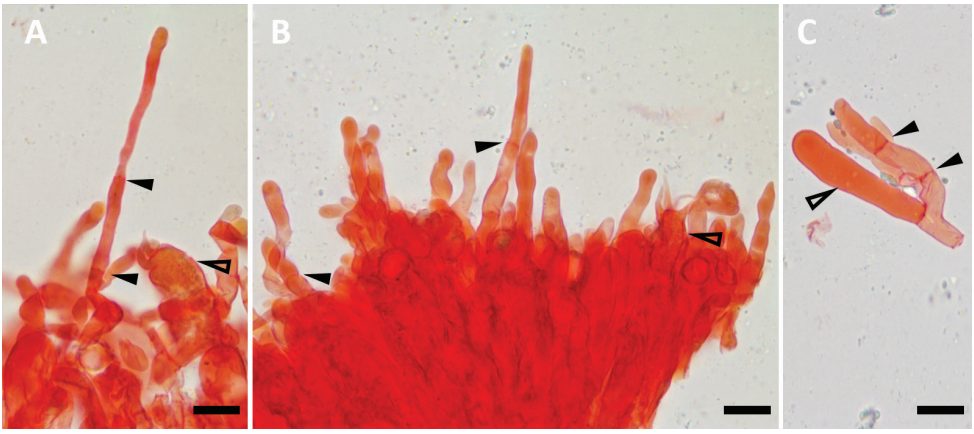

Figure 7. A–C Sterile elements of *Lactifluus russulisporus*, full arrows indicate septa of sterile elements, hollow arrows indicate a basidiole or basidium. **A–B** Protruding sterile cells, holotype, RH 9398 **C** not-protruding sterile element, RH 9674. Scale bar: 10 μm.

branched terminal hyphae in the hymenium of (mostly) Aphyllophorales. An intriguing term, paraphyses, is used in the works on the developmental biology of the hymenium done in *Coprinopsis cinerea* (Horner and Moore 1987; Rosin and Moore 1985a). These cells originate as branches of sub-basidial cells and insert into the basidial layer, later inflating so that they become the main structural component as a pavement from which basidia and cystidia protrude (Horner and Moore 1987; Moore 1985; Rosin and Moore 1985a; b). This description fits well with the sterile elements observed in *Lactifluus* (Figs 7, 8F). Nevertheless, paraphyses is a term strongly associated with Ascomycota, used for more hair-like (filiform) cells. It cannot be stated with certainty that Ascomycete paraphyses are homologous to the cells we find in *Lactifluus.*

Given the lack of a distinctive deviating shape in most cases, the improbability of being basidioles and the neutrality of the term, we recommend the use of the term 'sterile elements' over the terms 'leptocystidia' and 'paraphyses' to refer to these cells.

Thereto can be added that marginal cells often bear a striking resemblance to sterile elements (Fig. 8). Furthermore, in *Inocybe*, little differentiated cystidia are referred to as paracystidia, which also show similar morphology to marginal cells and might constitute the same type of cell (Jacobsson and Larsson 2012; Kuyper 1986). Presently it is difficult to argue whether this is due to homology or homoplasy. Marginal cells are sterile elements on a sterile edge that differ from pleurocystidia and are, in fact, 'hairs' sensu Romagnesi (Verbeken and Walleyn 2010). In species where the edge is fertile, sterile elements are also present on the edge. It is possible that, when no differentiated marginal cells are present on an infertile edge, sterile elements are present and consequently reported as being marginal cells. We suggest paying more attention to these sterile elements which occur predominantly in *Lactifluus*. Given the variation that we observe within *L. russulisporus*, it is likely that the taxonomic value of this character is rather low, but this needs more observations.

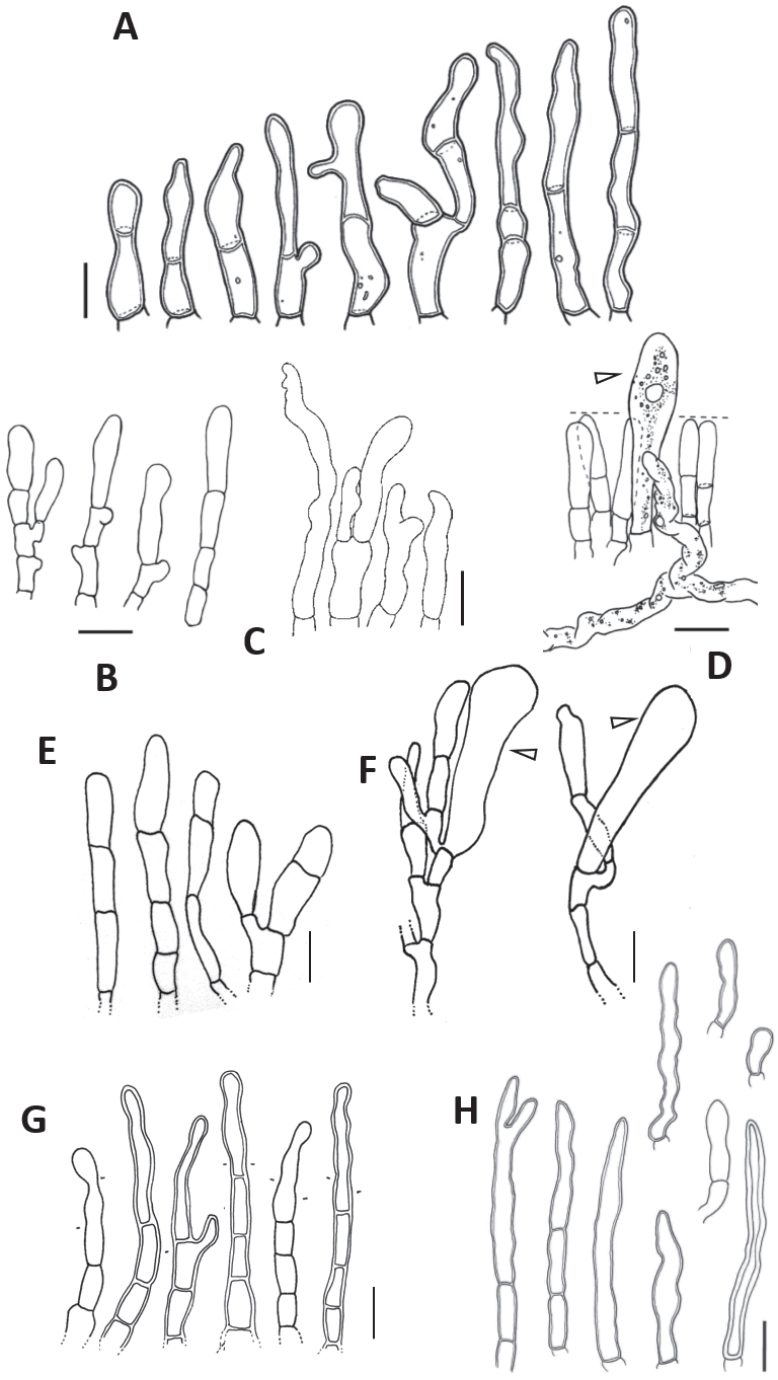

Figure 8. A–F Sterile cells in *Lactifluus* **G, H** marginal cells in *Lactifluus* with striking resemblance to different sterile cells **A** *L. persicinus* from Delgat et al. (2017) **B, D** *L. bicapillus* from De Crop et al. (2019) **C** 'leptocystidia' from (Verbeken and Walleyn 2010) **E** *L. caliendrifer* **F** *L. russulisporus* **G** *L. caliendrifer* **H** *L. albomembranaceus* from (De Crop et al. 2016). Scale bar: 10 µm, arrows indicate basidioles.

Table 1. Specimens and GenBank accession numbers of DNA sequences used in molecular analyses.

Species	Voucher collection (herbarium)	Country	ITS accession no.	Reference
Lactifluus* subg. *Gymnocarpi				
Lactifluus albocinctus **Type**	AV 99-211 (GENT)	Zimbabwe	KR364117	De Crop et al. (2017)
Lactifluus albomembranaceus **Type**	EDC 12-046 (GENT)	Cameroon	KR364064	De Crop et al. (2017)
Lactifluus albomembranaceus	DM 355B	Burkina Faso	LN651269	Maba et al. (2015)
Lactifluus brunellus	TH 9130 (BRG, DUKE)	Guyana	JN168728	Smith et al. (2011)
Lactifluus brunneoviolascens	AV 13-038 (GENT)	Italy	KR364123	De Crop et al. (2017)
Lactifluus brunnescens	AV 05-083 (GENT)	Malawi	KR364019	De Crop et al. (2017)
Lactifluus caribaeus	PAM/Mart 12-090 (LIP)	Martinique	KP691415	De Crop et al. (2017)
Lactifluus cf. *castaneibadius*	CL/MART06.019 (LIP)	Martinique	KP691417	De Crop et al. (2017)
Lactifluus chiapanensis	VMB 4374A (GENT)	Mexico	GU258297	Stubbe et al. (2010)
Lactifluus clarkeae	MN 2004002 (L)	Australia	KR364011	De Crop et al. (2017)
Lactifluus flammans	JD 941 (BR)	Congo	KR364078	De Crop et al. (2017)
Lactifluus flocktonae	JET1006 (MEL)	Australia	JX266621	Lebel et al. (2013)
Lactifluus foetens **Type**	ADK 2840 (BR)	Benin	KR364023	De Crop et al. (2017)
Lactifluus foetens	ADK 4411 (BR)	Togo	KX306937	De Crop et al. (2016)
Lactifluus gymnocarpus	EDC 12-047 (GENT)	Cameroon	KR364065	De Crop et al. (2017)
Lactifluus longivelutinus **Type**	XHW 1565 (GENT)	China	KR364114	De Crop et al. (2017)
Lactifluus luteolus	AV 05-253 (GENT)	North America	KR364016	De Crop et al. (2017)
Lactifluus cf. *murinipes*	F.1890 (LIP)	Martinique	KP691418	De Crop et al. (2017)
Lactifluus aff. n*ebulosus*	RC/Guad 11-023 (LIP)	Guadeloupe	KP691412	De Crop et al. (2017)
Lactifluus nonpiscis **Type**	BB 3171 (GENT)	Zambia	KR364030	De Crop et al. (2017)
Lactifluus nonpiscis	AV 11-137 (GENT)	Togo	KR364058	De Crop et al. (2017)
Lactifluus panuoides	RC/Guy 10-024 (LIP)	French Guiana	KJ786647	De Crop et al. (2017)
Lactifluus aff. p*hlebonemus*	EDC 12-023 (GENT)	Cameroon	KR364062	De Crop et al. (2017)
Lactifluus cf. *putidus*	PAM/Mart 11-013 (LIP)	Martinique	KP691413	De Crop et al. (2017)
Lactifluus rubrobrunnescens **Type**	EH 7194 (GENT)	Indonesia	KR364115	De Crop et al. (2017)
Lactifluus sp.	RC/Guad 08-042 (LIP)	Guadeloupe	KP691414	De Crop et al. (2017)
Lactifluus sp.	G3185	French Guiana	KJ786694	De Crop et al. (2017)
Lactifluus caliendrifer **Type**	KW 378 (GENT)	Thailand	MK517655	This study
*Lactifluus caliendrife*r	KW 392 (GENT)	Thailand	KR364091	De Crop et al. (2017)
Lactifluus russilisporus	RH 9674 (BRI, NY)	Australia	MK517654	This study
Lactifluus russilisporus **Type**	RH 9398 (BRI, NY)	Australia	KR364097	De Crop et al. (2017)
Lactifluus sp.	PGK13-130	New Caledonia	KP691436	De Crop et al. (2017)
Lactifluus subclarkeae	RH 9231 (NY)	Australia	KR364095	De Crop et al. (2017)
Lactifluus cf. *tanzanicus*	AV 11-017 (GENT)	Tanzania	KR364053	De Crop et al. (2017)
Lactifluus tanzanicus **Type**	TS 1277 (GENT)	Tanzania	KR364037	De Crop et al. (2017)
Outgroup *Lactifluus*				
Lactifluus acicularis	KVP 08-002 (GENT)	Thailand	HQ318226	Van de Putte et al. (2010)
Lactifluus corrugis s.l.	AV 05-392 (GENT)	USA	JQ753822	Van de Putte et al. (2016)
Lactifluus crocatus	KVP 08-034 (GENT)	Thailand	HQ318243	Van de Putte et al. (2010)
Lactifluus vitellinus	KVP 08-024 (GENT)	Thailand	HQ318236	Van de Putte et al. (2010)
Lactifluus volemus	KVP 11-002 (GENT)	Belgium	JQ753948	Van de Putte et al. (2016)

Acknowledgements

E. De Crop (grants B/13485/01 and BOF-PDO-2017-001201) and L. Delgat (grant BOFDOC2015007001) are funded by the "Bijzonder Onderzoeksfonds Ghent University" (BOF). K. Wisitrassameewong is thankful to the joint doctorate programme

of the 'Bijzonder Onderzoeksfonds Gent University' (BOF) Gent University and the Thailand Research Fund (BRG5580009) under the research grant entitled 'Taxonomy, Phylogeny, and Biochemistry of Thai Basidiomycetes". Roy Halling was partially supported by National Science Foundation (USA) funds from grant DEB 1020421. The National Geographic Society Committee for Research and Exploration provided funding via grant 8457-08. The Queensland Herbarium (BRI) collaborated generously with assistance and support for herbarium and field studies in Australia. We would like to thank Viki Vandomme for conducting lab work.

References

Ainsworth GC (2008) Ainsworth & Bisby's dictionary of the fungi. Cabi.

Buyck B, Hofstetter V, Eberhardt U, Verbeken A, Kauff F (2008) Walking the thin line between *Russula* and *Lactarius*: the dilemma of *Russula* subsect. *Ochricompactae*. Fungal Diversity 28: 15–40.

Clémençon H (1997) Anatomie der Hymenomyceten.(Anatomy of the Hymenomycetes). F. Flück-Wirth.

Clémençon H (2009) Methods for working with macrofungi: laboratory cultivation and preparation of larger fungi for light microscopy. IHW-Verlag.

De Crop E, Lescroart J, Njouonkou A-L, De Lange R, Van de Putte K, Verbeken A (2019) *Lactifluus bicapillus* (Russulales, Russulaceae), a new species from the Guineo-Congolian rainforest. Mycokeys 45: 25. https://doi.org/10.3897/mycokeys.45.29964

De Crop E, Nuytinck J, Van de Putte K, Wisitrassameewong K, Hackel J, Stubbe D, Hyde KD, Roy M, Halling RE, Moreau P-A (2017) A multi-gene phylogeny of *Lactifluus* (Basidiomycota, Russulales) translated into a new infrageneric classification of the genus. Persoonia: Molecular Phylogeny and Evolution of Fungi 38: 58. https://doi.org/10.3767/003158517X693255

De Crop E, Van de Putte K, De Wilde S, Njouonkou A-L, De Kesel A, Verbeken A (2016) *Lactifluus foetens* and *Lf. albomembranaceus* sp. nov. (Russulaceae): look-alike milkcaps from gallery forests in tropical Africa. Phytotaxa 277: 159–170. https://doi.org/10.11646/phytotaxa.277.2.3

Delgat L, De Crop E, Njouonkou A-L, Verbeken A (2017) *Lactifluus persicinus* sp. nov. from the gallery forests of West Cameroon. Mycotaxon 132: 471–483. https://doi.org/10.5248/132.471

Dierickx G, Froyen M, Halling R, Wisitrassameewong K, Delgat L, De Crop E, Verbeken A (2019) Nomenclatural Novelties. Index Fungorum 392: 1.

Gardes M, Bruns TD (1993) ITS primers with enhanced specificity for basidiomycetes-application to the identification of mycorrhizae and rusts. Molecular Ecology 2: 113–118. https://doi.org/10.1111/j.1365-294X.1993.tb00005.x

Horner J, Moore D (1987) Cystidial morphogenetic field in the hymenium of *Coprinus cinereus*. Transactions of the British Mycological Society 88: 479–488. https://doi.org/10.1016/S0007-1536(87)80031-1

Jacobsson S, Larsson E (2012) Inocybe (Fr.) Fr. Funga Nordica 2: 981–1021.

Katoh K, Standley DM (2013) MAFFT Multiple Sequence Alignment Software Version 7: Improvements in Performance and Usability. Mol Biol Evol 30: 772–780. https://doi.org/10.1093/molbev/mst010

Kornerup A, Wanscher J (1978) Methuen handbook of colour, 3rd edn Methuen. London, England:

Kumar S, Stecher G, Tamura K (2016) MEGA7: Molecular Evolutionary Genetics Analysis Version 7.0 for Bigger Datasets. Mol Biol Evol 33: 1870–1874. https://doi.org/10.1093/molbev/msw054

Kuyper TW (1986) A revision of the genus *Inocybe* in Europe. I. Subgenus *Inosperma* and the smooth-spored species of subgenus *Inocybe*. Persoonia-Supplement 3: 1–247.

Lanfear R, Frandsen PB, Wright AM, Senfeld T, Calcott B (2016) PartitionFinder 2: new methods for selecting partitioned models of evolution for molecular and morphological phylogenetic analyses. Molecular biology and evolution 34: 772–773. https://doi.org/10.1093/molbev/msw260

Le HT, Nuytinck J, Verbeken A, Lumyong S, Desjardin DE (2007) *Lactarius* in Northern Thailand: 1. *Lactarius* subgenus *Piperites*. Fungal Diversity 24: 173–224.

Lebel T, Dunk CW, May TW (2013) Rediscovery of *Multifurca stenophylla* (Berk.) T. Lebel, CW Dunk & TW May comb. nov.(Russulaceae) from Australia. Mycological Progress 12: 497–504. https://doi.org/10.1007/s11557-012-0856-4

Maba DL, Guelly AK, Yorou NS, Verbeken A, Agerer R (2015) Phylogenetic and microscopic studies in the genus *Lactifluus* (Basidiomycota, Russulales) in West Africa, including the description of four new species. IMA fungus 6: 13–24. https://doi.org/10.5598/imafungus.2015.06.01.02

Miller MA, Schwartz T, Pickett BE, He S, Klem EB, Scheuermann RH, Passarotti M, Kaufman S, O'Leary MA (2015) A RESTful API for Access to Phylogenetic Tools via the CIPRES Science Gateway. Evol Bioinform Online 11: 43–48. https://doi.org/10.4137/EBO.S21501

Moore D (1985) Developmental Biology of Higher Fungi: Symposium of the British Mycological Society Held at the University of Manchester April 1984. Cambridge University Press.

Moore D (2005) Principles of mushroom developmental biology. International Journal of Medicinal Mushrooms 7: 79–101. https://doi.org/10.1615/IntJMedMushr.v7.i12.90

Nuytinck J, Verbeken A (2003) *Lactarius sanguifluus* versus *Lactarius vinosus* – molecular and morphological analyses. Mycological Progress 2: 227–234. https://doi.org/10.1007/s11557-006-0060-5

Rosin IV, Moore D (1985a) Differentiation of the hymenium in *Coprinus cinereus*. Transactions of the British Mycological Society 84: 621–628. https://doi.org/10.1016/S0007-1536(85)80116-9

Rosin IV, Moore D (1985b) Origin of the hymenophore and establishment of major tissue domains during fruit body development in *Coprinus cinereus*. Transactions of the British Mycological Society 84: 609–619. https://doi.org/10.1016/S0007-1536(85)80115-7

Smith ME, Henkel TW, Aime MC, Fremier AK, Vilgalys R (2011) Ectomycorrhizal fungal diversity and community structure on three co-occurring leguminous canopy tree species in a Neotropical rainforest. New Phytologist 192: 699–712. https://doi.org/10.1111/j.1469-8137.2011.03844.x

Stamatakis A (2014) RAxML version 8: a tool for phylogenetic analysis and post-analysis of large phylogenies. Bioinformatics 30: 1312–1313. https://doi.org/10.1093/bioinformatics/btu033

Stamatakis A, Hoover P, Rougemont J (2008) A rapid bootstrap algorithm for the RAxML web servers. Systematic biology 57: 758–771. https://doi.org/10.1080/10635150802429642

Stubbe D, Nuytinck J, Verbeken A (2010) Critical assessment of the *Lactarius gerardii* species complex (Russulales). Fungal biology 114: 271–283. https://doi.org/10.1016/j.funbio.2010.01.008

Van de Putte K, Nuytinck J, De Crop E, Verbeken A (2016) *Lactifluus volemus* in Europe: three species in one-revealed by a multilocus genealogical approach, Bayesian species delimitation and morphology. Fungal biology 120: 1–25. https://doi.org/10.1016/j.funbio.2015.08.015

Van de Putte K, Nuytinck J, Stubbe D, Le HT, Verbeken A (2010) *Lactarius volemus* sensu lato (Russulales) from northern Thailand: morphological and phylogenetic species concepts explored. Fungal Diversity 45: 99–130. https://doi.org/10.1007/s13225-010-0070-0

Verbeken A (1998) Studies in tropical African *Lactarius* species, 5: a synopsis of the subgenus *Lactifluus* (Burl.) Hesler & AH Sm. emend. Mycotaxon 66: 363–386.

Verbeken A, Horak E, Desjardin D (2001) Agaricales of Indonesia. 3. New records of the genus *Lactarius* (Basidiomycota, Russulales) from Java. Sydowia 53: 261–289.

Verbeken A, Nuytinck J (2013) Not every milkcap is a *Lactarius*. Scripta Botanica Belgica 51: 162–168.

Verbeken A, Walleyn R (2010) Fungus Flora of Tropical Africa: Monograph of "*Lactarius*" in Tropical Africa. National Botanic Garden of Belgium.

Wang X-H, Verbeken A (2006) Three new species of *Lactarius* subgenus *Lactiflui* (Russulaceae, Russulales) in southwestern China. Nova Hedwigia 83: 167–176. https://doi.org/10.1127/0029-5035/2006/0083-0167

White TJ, Bruns T, Lee S, Taylor J (1990) Amplification and direct sequencing of fungal ribosomal RNA genes for phylogenetics. PCR Protocols: a Guide to Methods and Applications 18: 315–322. https://doi.org/10.1016/B978-0-12-372180-8.50042-1

MycoKeys 56: 33–47 (2019)
doi: 10.3897/mycokeys.56.30280
http://mycokeys.pensoft.net

RESEARCH ARTICLE

A peer-reviewed open-access journal
MycoKeys
Launched to accelerate biodiversity research

Two new species of *Hygrophorus* from temperate Himalayan Oak forests of Pakistan

Arooj Naseer[1], Abdul Nasir Khalid[2], Rosanne Healy[3], Matthew E. Smith[3]

1 *Centre for Undergraduate Studies, University of the Punjab, Lahore, 54590, Pakistan* **2** *Department of Botany, University of the Punjab, Lahore, 54590, Pakistan* **3** *Department of Plant Pathology, University of Florida, Gainesville, FL, USA*

Corresponding author: *Arooj Naseer* (arooj.hons@pu.edu.pk)

Academic editor: *Zai-Wei Ge* | Received 22 October 2018 | Accepted 25 January 2019 | Published 10 July 2019

Citation: Naseer A, Khalid AN, Healy R, Smith ME (2019) Two new species of *Hygrophorus* from temperate Himalayan Oak forests of Pakistan. MycoKeys 56: 33–47. https://doi.org/10.3897/mycokeys.56.30280

Abstract

The genus *Hygrophorus* is poorly studied from Asia. From Pakistan, only one species has been reported so far. Two new species in the genus have been collected from Himalayan oak forests of Pakistan. *Hygrophorus alboflavescens* (section *Pudorini*, subgenus *Colorati*) is characterised by its pure white, centrally depressed pileus, occurrence of white stipe with yellow patches at lower half and broader (4.98 µm) basidiospores. *Hygrophorus scabrellus* (section *Hygrophorus*, subgenus *Hygrophorus*) is characterised by its yellowish-green stipe with white apex that has fine scales on the entire stipe, an off-white pileus with dark green and greyish fibrils, ovoid to ellipsoid basidiospores and clavate 4-spored basidia. Macro- and micromorphological descriptions have revealed that both these taxa are not yet described. Phylogenetic estimation based on DNA sequences from the internal transcribed spacer (ITS) region and large subunit (LSU) of the nuclear ribosomal DNA (rDNA) genes, is congruent with the morphological characters that help to delimit these as new species of *Hygrophorus*. Allied taxa are also compared.

Keywords

Biodiversity, Community structure, Dir, ECM, Shawar Valley

Introduction

The genus *Hygrophorus* Fr. (Hygrophoraceae, Agaricales) is one of the ectomycorrhizal (ECM) genera in Agaricales. The genus name *Hygrophorus* Fr. (Hygrophoraceae, Agaricales) comes from *hygro* meaning moisture and *phorus* meaning bearer. This may refer to the glutinous to viscid pileus character that many of these fungi have due to a layer of gel that makes them sticky to touch when moist. The genus is characterised by diverse basidiomata colours, basidiomata which are tricholomatoid, collybioid, clitocyboid or omphalinoid, lamellae that are subdecurrent, spores that are smooth and hyaline and a hymenium without cystidia. Basidiomata in this group vary from small to large; thin to fleshy; dry to very glutinous or viscid pileus; with a dry to glutinous, glabrous or fibrillose, generally pruinose or granulose stipe (Singer 1986; Bas et al. 1990; Boertmann 1995; Young 2005; Kovalenko 2012). Colour of the pileus is a characteristic feature in the classification of *Hygrophorus* especially at the level of subsection (Hesler and Smith 1963). Sect. *Hygrophorus* has white to cream basidiomata while taxa with colourful basidiomata are in different sections and subsections (Fries 1874; Singer 1943; Candusso 1997).

The family Hygrophoraceae Lotsy was revised by Lodge et al. (2014) on the basis of integrated molecular phylogeny, morphological analyses, pigment chemistry and ecology. They classified the family with three new subfamilies, eight tribes, eight subgenera, 26 sections and 14 subsections. Subgenus *Colorati* of genus *Hygrophorus* contain coloured mushrooms. In the new classification, the subg. *Colorati* (Bataille) E. Larss. has been divided into three sections: *Olivaceoumbrini* (Bataille) Konrad & Maubl., *Pudorini* (Bataille) Konrad & Maubl. and *Aurei* (Bataille) E. Larss. In addition, the section *Pudorini* is divided into two subsections: *Clitocyboides* and *Pudorini*. The subgenus *Hygrophorus* is divided into two sections: *Hygrophorus* and *Fulventes.*

Hygrophorus species are globally distributed and mostly occur in woodlands and forests with pines or with ectomycorrhizal (ECM) angiosperms (Bas et al. 1990). *Hygrophorus* are essential components of ECM communities of temperate regions in the Northern Hemisphere (Tedersoo et al. 2010). Recently, a new edible species, *H. parvirussula* has been described from south-western China (Huang et al. 2018) and it belongs to *Hygrophorus* section *Pudorini.* A few studies on the genus have been performed in Pakistan. Only one species, *Hygrophorus chrysodon,* was reported as a new record by Razaq et al. (2014), from the western Himalayan forests of Pakistan. Here we present two new species of *Hygrophorus* based on both morphology and molecular phylogeny.

Materials and methods

Morpho-anatomical analyses

Collections were made during field investigations for ECM communities associated with the oaks of Swat and Dir districts, Khyber Pakhtunkhwa province, Pakistan dur-

ing 2014–2016. Basidiomata were found in a pure *Quercus* forest from Shawar Valley, Swat that is representative of the western Himalayan Province (Naseer et al. 2017b) and from Toa, Alpurai forests (Naseer et al. 2017), Swat, KP, Pakistan. The ECM roots were collected from the same forests as well as Biar, Upper Dir, KP, Pakistan. Biar is located in moist parts of dry temperate zones and it has *Q. baloot* as the leading species (89.44%) with *Q. dilatata* (10.46%). Basidiomata were collected following Lodge et al. (2014) and photographed in their natural habitats using a Nikon D70S camera. Morphological characters were recorded from fresh specimens. Colours were designated with reference to mColorMeter application (Yanmei He, Mac App Store). Specimens were deposited in the Herbarium, Department of Botany, University of the Punjab, Lahore, Pakistan (LAH) and the University of Florida Fungal Herbarium, Gainesville FL, USA (FLAS).

Microscopic characters are based on freehand sections from fresh and dried specimens mounted in 5% (w/v) aqueous potassium hydroxide (KOH) solution. Tissues from lamellae, pileipellis and stipitipellis were mounted in phloxine (1%) for better contrast and examined using a Meiji Techno MX4300H compound microscope.

A total of thirty basidiospores, basidia, cystidia and hyphae were measured from each collection. For basidiospores, the abbreviation "*n/m/p*" indicates *n* basidiospores measured from *m* fruit bodies of *p* collections. Dimensions for basidiospores are given using length × width (L × W) and extreme values are given in parentheses. The range contains a minimum of 90% of the values. Measurements include arithmetic mean of spore length and width for all spores measured, Q means spore length divided by spore width and avQ indicates average Q of all spores ± standard deviation.

Molecular analyses

Genomic DNA was extracted from basidioma gills following a modified CTAB extraction method (Bruns 1995) and from ectomycorrhizal roots by Extract-N-AmpTM Kit (Sigma- Aldrich, St Louis, MO, USA). ITS and LSU regions of nuclear rDNA were amplified using the pairs of primers ITS1F-ITS4B and LR0R-LR5 (Vilgalys and Hester 1990, White et al. 1990, Gardes and Bruns 1993). Polymerase chain reactions (PCR) were performed in 25 µl volume reactions. Visualisation of PCR products were accomplished using SYBR Green and 1.5% agarose gels with TAE buffer for gel electrophoresis. Successful amplicons were purified by enzymatic purification using Exonuclease I and Shrimp Alkaline Phosphatase enzymes (Werle et al. 1994). Purified products were sequenced by the University of Florida's Interdisciplinary Center for Biotechnology Research (http://www.biotech.ufl.edu/). Sequence chromatograms were trimmed, edited and assembled using Sequencher 4.1 (GeneCodes, Ann Arbor, MI). Once sequences were assembled and edited, they were deposited in GenBank (http://www.ncbi.nlm.nih.gov).

Consensus sequences for ITS and LSU were used to query GenBank and the UNITE database using BLAST searches. Representative sequences from across the genus *Hygro-*

phorus were downloaded and imported into an alignment in Bioedit (Hall 1999). Sequences from ECM roots were also included in the ITS alignment. *Cantharocybe gruberi* (JN006422, DQ200927) sequences were chosen to root the phylogenetic trees following Razaq et al. (2014). Sequences were aligned with the programme MUSCLE (Edgar 2004). Maximum likelihood analyses for individual gene regions were performed via CIPRES Science Gateway (Miller et al. 2010) employing RAxML-HPC v.8. Rapid bootstrap analysis for the best-scoring ML tree was configured for each dataset. For the bootstrapping phase, the GTRCAT model was selected. One thousand rapid bootstrap replicates were run. A bootstrap proportion of ≥ 70% was considered significant.

Results

Molecular phylogenetic analyses

Consensus sequences for the ITS region of *H. alboflavescens* were 601–638 bp after trimming. BLAST searches in NCBI and UNITE revealed 91% similarity to *Hygrophorus penarioides* Jacobsson & Larss. (EF395370, EF395371, EF395372 & UDBO1556) from Sweden (99% query cover, 0.0 E value). The two ITS sequences from ECM root tips of *Q. incana* from same forest (Shawar Valley) matched with *Hygrophorus alboflavescens* fruiting body sequences and these are depicted in the phylogenetic tree (Fig. 5).

The consensus sequence for the LSU region of *H. alboflavescens* was 780 bp after trimming. Initial BLAST analysis revealed it as 94% similar to *H. sordidus* Peck. (AF042562) from the USA and *H. russula* (Schaeff. ex Fr.) Kauffman, (AY586663) from Sweden (100% query, 0.0E value).

The ITS analysis revealed that sequences from *Hygrophorus alboflavescens* clustered with *H. penarioides* and *H. sordidus* with moderate bootstrap support within section *Pudorini* of subgenus *Colorati*. The LSU based phylogram showed that *H. alboflavescens* clustered with *H. sordidus* (Fig. 5). LSU sequences for *H. penarioides* were not available.

The consensus sequences for the ITS region of *Hygrophorus scabrellus* nom. prov. were 603–604 bp. BLAST results revealed that these sequences were 89% similar to *Hygrophorus eburneus* (Bull.) Fr. (AY463485, AY463484 & AY242855) with 100% query coverage. The consensus sequences also showed 87% similarity to *H. cossus* (Sowerby) Fr. as *H. quercetorum* P.D. Orton, which has been synonymised with *H. cossus* (Larsson and Jacobsson 2004) (AY463489) and *H. cossus* (AY242852) from Sweden with 100% query coverage and 0.0 E value.

The consensus sequence for the LSU region of *Hygrophorus scabrellus* was 763 bp. BLAST results revealed that these sequences were 96% similar to *Hygrophorus cossus* (AY548963 & KF381555) with 100% query coverage.

The *H. scabrellus* LSU sequences clustered with high bootstrap support with similar taxa in the section *Hygrophorus* of subgenus *Hygrophorus* (Fig. 6). In both our LSU and ITS analyses, *H. scabrellus* formed a sister lineage to *H. cossus* from Sweden with strong bootstrap support (Figs 5, 6).

Hygrophorus alboflavescens basidiomata were collected from Shawar Valley. Its ECM roots were collected from the same valley. The species falls into *Hygrophorus,* subgenus *Colorati,* section *Pudorini* and subsection *Clitocyboides*. *Hygrophorus scabrellus* clusters within subsect. *Hygrophorus*, section *Hygrophorus* of subgenus *Hygrophorus*. Some of the ECM root sequences clustered with *H. pudorinus* sequences (FJ845408) from Canada and *H. pudorinus* (KT875016) from Mexico in the phylogenetic tree (Fig. 5). *H. pudorinus* belongs to Subgenus *Colorati,* section *Pudorinii* 2, subsection *Pudorini.* The collection of this ECM is the first report of this species from Pakistan.

Taxonomy

***Hygrophorus alboflavescens* A. Naseer & A.N. Khalid, sp. nov.**
MycoBank MB828146
Figures 1, 2

Diagnosis. *Hygrophorus alboflavescens* can be distinguished from related species by its white, centrally depressed pileus having yellow dots, with straight, even margins; occurrence of white stipe with yellow patches at lower half and broader (4.98 µm) basidiospores.

Typification. PAKISTAN. Khyber Pakhtunkhwa Province, Swat, Shawar Valley, 2100 m alt., solitary or in pairs, on soil under *Quercus incana*, 14 July 2014, Arooj Naseer & Abdul Nasir Khalid, ASSW36 (holotype: LAH35243).

Etymology. The species epithet refers to the white pileus with yellow dots and white stipe with yellow patches.

Basidiomata medium to large sized. ***Pileus*** 7–10.5 cm in diameter, butter white (0.1B 8.8/0.3) with yellow (5.2Y 4.3/4) dots, plane, centrally depressed, context moderately thick, margin, even, smooth, straight, sometime incurved. ***Lamellae*** white (5.1GY 7.9/1.9) with yellow (6.1 Y 6.8/5.5) and pink (2.8Y 6.9/3.9) colouration, decurrent, thick, distant, L = 30–41, even, entire. ***Lamellulae*** irregular, of variable length, alternating with lamellae. ***Stipe*** 1.5–2.5 cm thick at apex, 0.5–1.5 cm at base, 8 –12.5 cm long, white (0.1B 8.8/0.3) with yellow (5.4Y 5.3/4) patches at lower half, cylindrical, slightly tapering at base, central, hollow.

Basidiospores [60/3/2] (5.52–) 5.6–7.9 (–8.1) × (3.84–) 3.9–6.5 (–6.7), avL × avW = 6.64 × 4.98, Q = (1.20–) 1.21 × 1.40 (–1.43), avQ = 1.34, light green to hyaline in 5% KOH, ellipsoid, oblong, thick-walled. ***Basidia*** 31.6–48.8 × 5.8–6.7 µm, hyaline in 5% KOH, four-spored, clavate with long sterigmata (up to 3.0–4.2 µm), densely guttulated. ***Hymenophoral Trama*** 4–5.2 µm in diameter, thin-walled, branched, septate, oil contents, clamp connection present. ***Pileipellis*** an ixocutis of wide, thick hyphae, 3.0–5.5 µm in diameter. ***Stipitipellis*** a cutis of parallel and erect hyphae, 3.1–5.3 µm in diameter, light yellow in 5% KOH, septate. ***Clamp Connections*** present in all tissues.

Habit and distribution. Solitary and in pairs on soil under *Quercus incana*, at 2100 m a.s.l., in thick moist temperate forest of the western Himalaya.

Figure 1. Morphology of *Hygrophorus alboflavescens* (Holotype). **A–D** Basidiomata **A, B** LAH35244; FLAS-F-59457 **C, D** LAH35243. Scale bar: 1.5 cm.

Additional material examined. PAKISTAN, Khyber Pakhtunkhwa province, Swat, Shawar Valley, 2100 m a.s.l., solitary or in a pair, on soil under *Quercus incana*, 14 July 2014, Arooj Naseer & Abdul Nasir Khalid, ASSW81 (LAH35244; FLAS-F-59457).

Notes. *Hygrophorus alboflavescens* nom. prov. can be distinguished from closely related species by the following combination of characters: a white, plane, centrally depressed pileus having straight margins; stipe that is white above and yellow below; and broadly ellipsoid spores. The closely related species *Hygrophorus penarioides* is

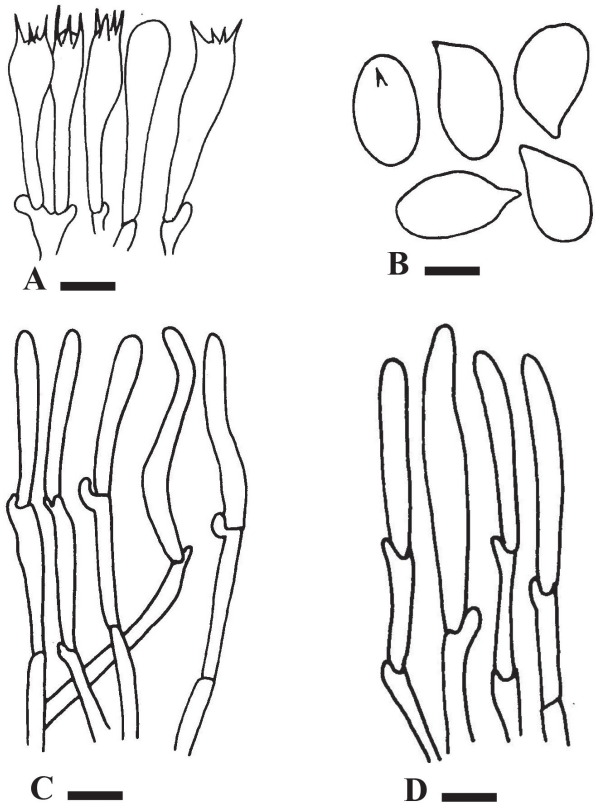

Figure 2. Anatomy of *Hygrophorus alboflavescens*. **A–D** LAH35243 (holotype) **A** Basida **B** Basidiospores **C** Pileipellis **D** Stipitipellis. Scale bars: 2.0 μm (**A**); 4.5 μm (**B**); 13.7 μm (**C**); 7.8 μm (**D**).

also an oak-specific species (Table 1). However, they differ morphologically. *Hygrophorus penarioides* can easily be distinguished by its convex pileus with broad umbo and its involute margins (Jacobsson and Larsson 2007), whereas *H. alboflavescens* has centrally depressed pileus (without umbo) and straight margins. *Hygrophorus penarioides* has a pure white pileus and stipe which become cream or slightly pinkish with age, whereas *H. alboflavescens* has a white stipe and pileus with yellow colouration on both. *Hygrophorus alboflavescens* has a longer stipe (8–12.5 cm) and broader spores (3.9–6.7 μm) as compared to *H. penarioides*. *Hygrophorus alboflavescens* is further differentiated from closely related taxa, *H. sordidus*, which has a convex, expanded to plane pileus that is larger (8–20 cm broad) compared with the smaller (7–10.5 cm broad), centrally depressed pileus of *H. alboflavescens. Hygrophorus alboflavescens* has even, smooth and straight margins that differ from involute and subnoccose margins of *H. sordidus*. Molecular analyses based on ITS and LSU regions also support *H. alboflavescens* as a distinct taxon and demonstrate its ECM relationship with oak in Pakistan.

Hygrophorus scabrellus **A. Naseer & A.N. Khalid, sp. nov.**
MycoBank MB828147
Figures 3, 4

Diagnosis. *Hygrophorus scabrellus* is characterised by off-white, plano-convex pileus with greyish, dark green fibrils; yellowish-green, longer (2.1–2.4 cm) stipe with white apex and fine scales along the whole stipe; ovoid to ellipsoid, smooth and smaller (6.5 × 3.8 µm) basidiospores.

Typification. PAKISTAN. Khyber Pakhtunkhwa Province, Swat, Toa, 2800 m a.s.l., on soil under *Quercus incana,* 15 July 2015, Arooj Naseer & Abdul Nasir Khalid, AST51 (holotype: LAH35245).

Etymology. The species epithet refers to the fine scales on the stipe.

Basidiomata medium sized. ***Pileus*** 2.4–2.8 cm, creamy, off-white (7.9GY 6/1) with dark green, greyish fibrils (2.9GY 2.4/2), plano-convex, context moderately thick,

Table 1. Comparsion of *Hygrophorus* spp. from Pakistan with morphologically similar species.

Characters/ Species	*H. alboflavescens* sp. nov.	*H. penarioides* Jacobsson & E. Larss.	*H. sordidus* Peck	*H.scabrellus* sp. nov.	*H. eburneus* (Bull.) Fr.	*H. cossus* (Sowerby) Fr.
Pileus						
Shape	Centrally depressed	Convex	Convex, expand to plane	Plano convex	Obtuse to convex	Broadly convex to nearly plane
Colour	Pure white with yellow dots	Pure white with creamy centre	Pure white or rarely tinged yellowish buff	Off-white with dark green	White	Pale orchraceous grey
Size	7–10.5 cm	9–15 cm	8–20 cm	2.4–2.8 cm	2–7(10) cm	3–7 cm
Umbo	No umbo	Broad umbo	No umbo	No Umbo	Umbonate	Obtuse nearly plane
Margins	Even, smooth, straight, sometime incurved	Strongly involute	Involute and subnoccose	Even, smooth, incurved	Even, involute and floccose-pubescent	Incurved
Stipe						
Surface	Dry, yellow patches on lower half	Finely floccose in uppermost part	Dry, glabrous, upper portion obscurely noccose	Scales on whole stipe	Fine scales at apex only and rest of stipe is smooth	Fibrillose-punctate to scabrous at apex, lower two-thirds covered by gelatinous sheath
Shape	Cylindrical	Strongly attenuated towards base	Equal, sometimes attenuated towards base	Cylindrical, finely scaled	Equal/tapered downward/ with a greatly attenuated vermiform base,	Equal, tapered at base
Colour	White with yellow patches at lower half	White, in lower part creamy	White	Yellowish-green with white apex	White stipe	Salmon-buff to cinnamon
Size	1.5–2.5 cm thick 8–12.5 cm long	15–35 mm thick 60–100 mm long	1.5–3.0 cm thick 6–10 cm long	0.3–0.5 cm thick 2.1–2.4 cm long	2–8(15) mm thick 4.5–15(18) cm long	(3)8–12 mm thick 4–9 cm long
Basidiospores						
Size	6.64 × 4.98 µm	1.13–1.6 µm	6–8 × (3.5) 4–5.5 µm	6.5 × 3.84 µm	6–8(9) × 3.5–5 µm	7–9 × 4–4.5 µm
Shape	Ellipsoid, oblong	Broadly ellipsoid to ovoid	Ellipsoid, smooth	Ovoid to ellipsoid	Ellipsoid, smooth	Ellipsoid
Habitat	Oak specific	Oak specific	Oak-hickory woods	Oak specific	*Fagus* specific	Oak specific

Figure 3. Morphology of *Hygrophorus scabrellus*. **A, B** Basidiomata. LAH35245 (holotype). Scale bars: 0.88 cm (**A**); 0.48 cm (**B**).

margin even, smooth, incurved. ***Lamellae*** off-white to beige (4GY 6.8/2.4), subdecurrent to decurrent, thick, spaced to moderately close, L= 41–49, even, entire, undulate at margins. ***Lamellulae*** short, in two tiers, 1/3 of length of lamellae. ***Stipe*** 2.1–2.4 cm

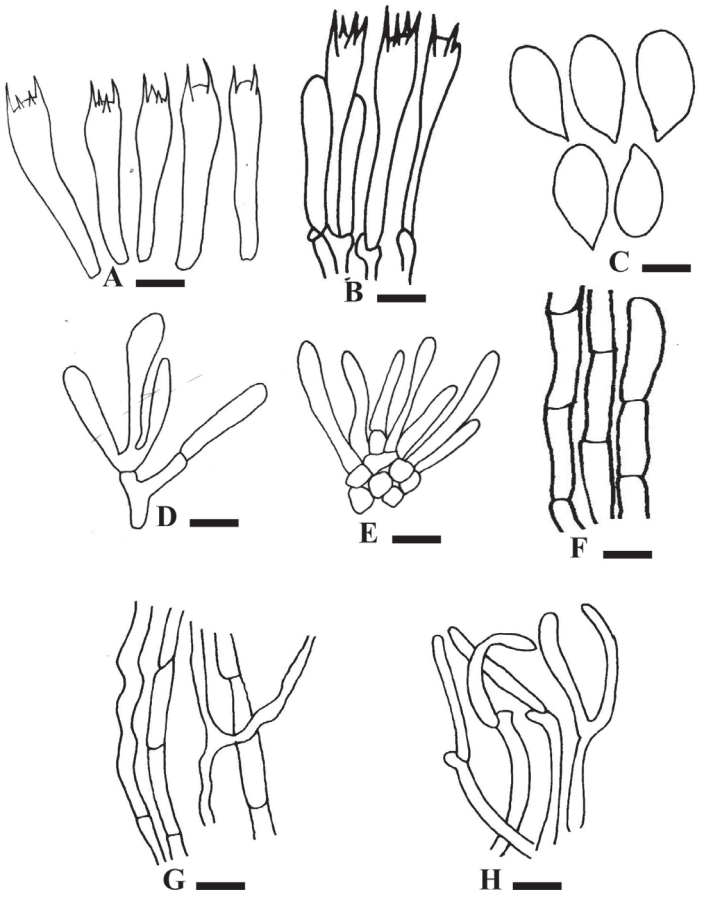

Figure 4. Anatomy of *Hygrophorus scabrellus*. **A–H** LAH35245 (holotype) **A** Basidia **B** Basidia with basidioles **C** Basidiospores **D** Cheilocystidia **E** Pleurocystidia **F** Stipitipellis **G** Tramal Hyphae **H** Pileipellis. Scale bars: 5.83 µm (**A, B, D, E**); 3.55 µm (**C**); 0.12 µm (**F–H**).

long, 0.3–0.5 cm in diameter, yellowish-green (9.3Y 4.4/2.4) with white (6.9GY 7/1) apex, finely scaled, cylindrical, slightly tapering at base, hollow.

Basidiospores [30/1/1] (4.56–) 4.72–8.1 (–8.76) × (2.5–) 2.8–5.1 (–5.2) µm, avL × avW = 6.5 × 3.84 µm, Q = (1.5–) 1.57 × 1.89 (–1.86), avQ = 1.70, white to light yellow in 5% KOH, ovoid to ellipsoid, smooth, inamyloid. ***Basidia*** 30.2–42.3 × 6.8–9.3 µm, hyaline to light green in 5% KOH, narrowly clavate, four-spored, sterigmata long (6.2–7.2 µm), medium thick-walled, densely guttulate. ***Hymenophoral Trama*** 3.7–8.2 µm in diameter, bilateral, divergent hyphae, thin-walled, branched, septate. ***Pileipellis*** 3–3.7 µm in diameter, an ixotrichoderm, composed of branched septate hyphae. ***Stipitipellis*** 3.2–7.0 µm, a thin ixocutis to ixotrichoderm, composed of compact erect hyphae. ***Clamp Connections*** present in all tissues.

Habitat and distribution. Solitary on soil under *Q. incana*, at 2800 m a.s.l., in moist temperate forest of Hindu Kush Himalayan range.

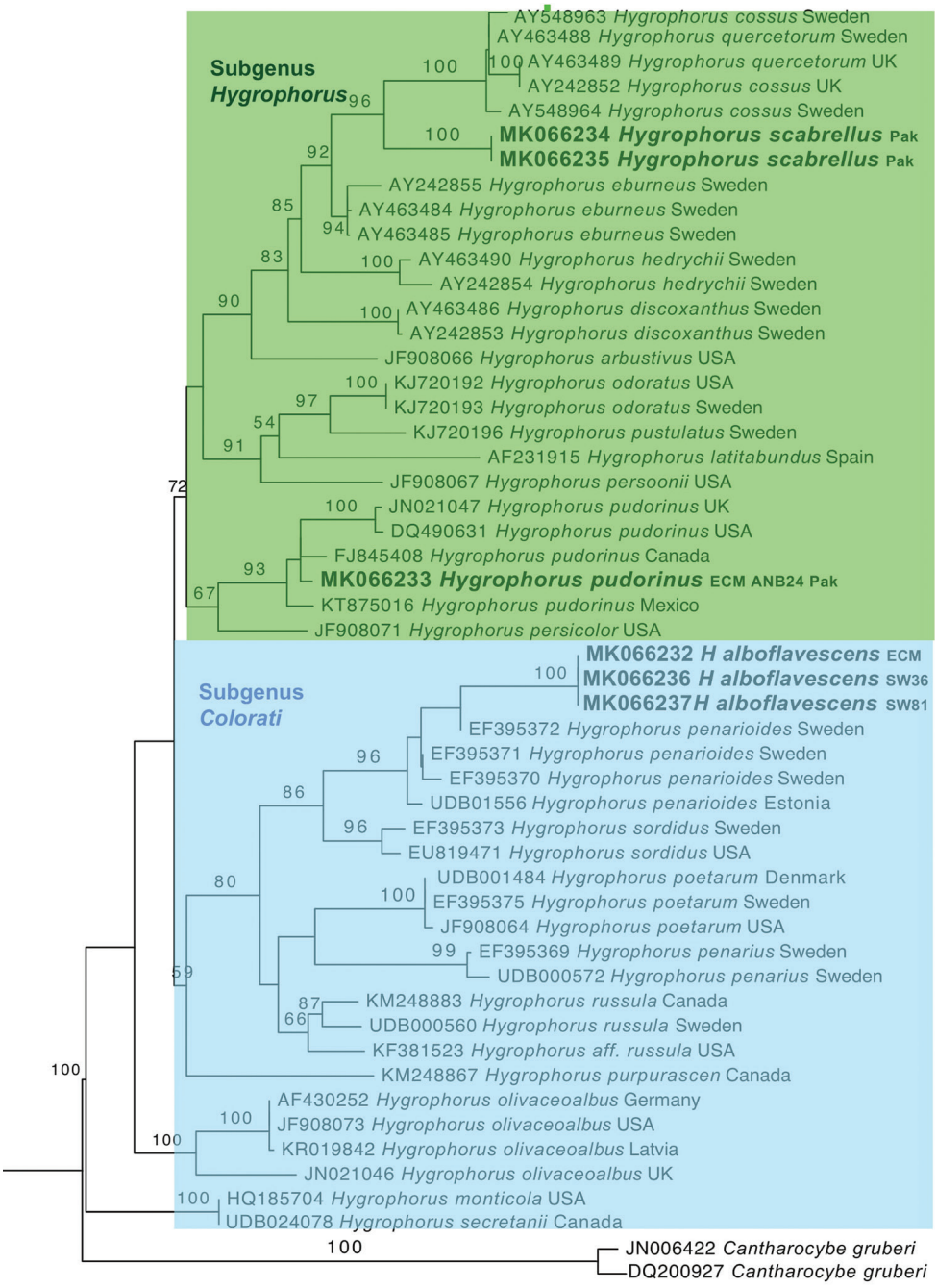

Figure 5. Phylogenetic relationship of *Hygrophorus* spp. and its ECM roots from Pakistan and their allied *Hygrophorus* species based on nrDNA ITS sequences using the Maximum Likelihood method. Sequences generated during this study are in bold letters. Sequences from root tips were labelled as ECM.

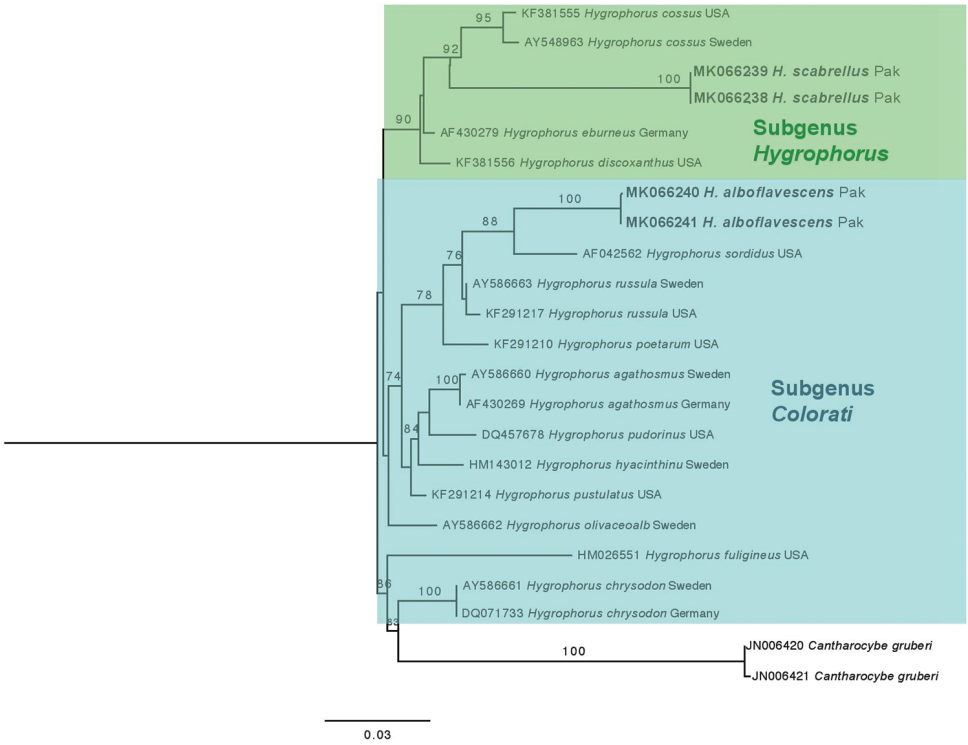

Figure 6. Molecular phylogenetic analysis of *Hygrophorus* spp. based on LSU sequences. Maximum likelihood phylogram of *Hygrophorus* based on nrDNA LSU as generated with RAxML with 1000 bootstrap iterations. Bolded lettering refers to sequences generated in this study.

Comments

Hygrophorus scabrellus is characterised by a yellowish-green stipe with a white apex that has fine scales on the entire stipe, planoconvex pileus which is off-white with dark green and greyish fibrils.

Hygrophorus scabrellus differs morphologically from the phylogenetically related species *H. eburneus*. *Hygrophorus eburneus* has fine scales only at the stipe apex (Table 1), whereas *H. scabrellus* has scales along the entire length of the stipe. *Hygrophorus eburneus* has a white stipe (yellowish-green stipe with a white apex in *H. scabrellus*). *Hygrophorus eburneus* also differs in having a pure white cap. Our new species *H. scabrellus* is similar to *Hygrophorus cossus* (Sow. ex Berk.) Fr. commonly known as Goat Moth Wax Cap, as both share plano-convex pileus. However, *H. cossus* has greyish white, broader pileus (3–9 cm) and smaller stipe (0.6–2 cm long) (Larsson and Jacobsson 2004) as compared to *H. scabrellus* that is distinguished by off-white pileus with dark green and greyish fibrils (2.4–2.8 cm) having longer stipe (2.1–2.4 cm). Anatomically, *H. cossus* has larger basidiospores (7–9 × 4–5 µm) (Larsson and Jacobsson 2004). Molecular phylogenetic analyses based on ITS and LSU sequences also support *Hygrophorus scabrellus* as a distinct species with strong bootstrap support.

Discussion

In this paper, two new species of *Hygrophorus* were studied morphologically and sequences of two DNA regions were analysed for each species. These studies revealed that *H. alboflavescens* falls into section *Pudorini* of subgenus *Colorati* and differs from other species in the section by having yellow dots or patches rather than having entirely white basdiomata. We also confirmed, based on ITS sequences from roots, that this new species forms ECM associations with *Q. incana*. *Hygrophorus scabrellus* clusters within section *Hygrophorus* of subgenus *Hygrophorus* and differs in colour and stipe scaliness from others in that subgenus. These two new species provide evidence that further research is needed to collect and identify the fungal diversity of Asia, which appears to be a global hotspot of fungal diversity.

References

Bas C, Kuyper ThW, Noordeloos ME, Vellinga EC (1990) Flora Agaricina Neerlandica, Vol. 2. Rotterdam Balkema, 137 pp.

Boertmann D (1995) The genus *Hygrocybe*. Fungi of Northern Europe Vol. I (1st edn). Danish Mycological Society, Greve.

Bruns TD (1995) Thoughts on the processes that maintain local species diversity of ectomycorrhizal fungi. Plant and Soil 170: 63–73. https://doi.org/10.1007/BF02183055

Candusso M (1997) *Hygrophorus* s.l. Fungi Europaei 6. Libreria Basso, Alassio.

Edgar RC (2004) MUSCLE: multiple sequence alignment with high accuracy and high throughput. Nucleic Acids Research 32: 1792–1797. https://doi.org/10.1093/nar/gkh340

Fries EM (1874) Hymenomycetes europaei sive Epicriseos systematis mycologici. 755 pp.

Gardes M, Bruns TD (1993) ITS primers with enhanced specificity for basidiomycetes – application to the identification of mycorrhizae and rusts. Molecular Ecology 2: 113–118. https://doi.org/10.1111/j.1365-294X.1993.tb00005.x

Hall TA (1999) BioEdit: a user-friendly biological sequence alignment editor and analysis program for Windows 95/98/NT/7. Nucleic Acids Symposium Series 41: 95–98. https://doi.org/10.4172/2167-0412.1000264

Hesler LR, Smith AH (1963) North American species of *Hygrophorus*. University of Tennessee Press, Knoxville. https://doi.org/10.5962/bhl.title.61976

Huang HY, Yang SD, Zeng NK, Zhang GL, Hu Y, Tang LP (2018) *Hygrophorus parvirussula* sp. nov., a new edible mushroom from southwestern China. Phytotaxa 373(2): 139–146. https://doi.org/10.11646/phytotaxa.373.2.4

Jacobsson S, Larsson E (2007) *Hygrophorus penarioides*, a new species identified using morphology and ITS sequence data. Mycotaxon 99: 337–343.

Kovalenko A (2012) In: Knudsen H, Vesterholt J (Eds) Funga Nordica. Agaricoid, boletoid cyphelloid and gasteroid genera. Nordsvamp, Copenhagen, 282–293.

Larsson E, Jacobsson S (2004) Controversy over *Hygrophorus cossus* settled using ITS sequence data from 200 year-old type material. Mycological Research 108: 781–786. https://doi.org/10.1017/S0953756204000310

Lodge DJ, Padamsee M, Matheny PB, Aime MC, Cantrell SA, Boertmann D, Kovalenko A, Vizzini A, Dentinger B, Kirk P, Ainsworth M, Moncalvo JM, Vilgalys R, Larsson E, Lücking R, Griffith G, Smith M, Norvell LL, Desjardin DE, Redhead SA, Ovrebo CL, Lickey E, Ercole E, Hughes KW, Courtecuisse R, Young A, Binder M, Minnis A, Lindner DL, Ortiz-Sanatan B, Haight J, Læssøe T, Baroni TJ, Geml J, Hattori T (2014) Molecular phylogeny, morphology, pigment chemistry and ecology in Hygrophoraceae (Agaricales). Fungal Diversity 64: 1–99. https://doi.org/10.1007/s13225-013-0259-0

Miller MA, Pfeiffer W, Schwartz T (2010) Creating the CIPRES Science Gateway for inference of large phylogenetic trees. Proceedings of the Gateway Computing Environments Workshop (GCE), New Orleans, Louisiana, 1–8. https://doi.org/10.1109/GCE.2010.5676129

Razaq A, Ilyas S, Khalid AN (2014) Taxonomic and phylogenetic affinities of *Hygrophorus chrysodon* from western Himalayan forests. Austrian Journal of Mycology 23: 21–29.

Singer R (1943) Das System der Agaricales. III. Ann Mycologici 41: 1–189.

Singer R (1986) Agaricales in modern taxonomy, 4th edn. Koeltz Scientific Books, Koenigstein.

Tedersoo L, May TW, Smith ME (2010) Ectomycorrhizal lifestyle in fungi: global diversity, distribution, and evolution of phylogenetic lineages. Mycorrhiza 20: 217–263. https://doi.org/10.1007/s00572-009-0274-x

Vilgalys R, Hester M (1990) Rapid genetic identification and mapping of enzymatically amplified ribosomal DNA from several *Cryptococcus* species. Journal of Bacteriology 172: 4238–4246. https://doi.org/10.1128/jb.172.8.4238-4246.1990

Werle E, Schneider C, Renner M, Völker M, Fiehn W (1994) Convenient single-step, one tube purification of PCR products for direct sequencing. Nucleic Acids Research 22: 4354–4355. https://doi.org/10.1093/nar/22.20.4354

White TJ, Bruns T, Lee SJWT, Taylor JW (1990) Amplification and direct sequencing of fungal ribosomal RNA genes for phylogenetics. PCR protocols: a guide to methods and applications 18 (1): 315–322. https://doi.org/10.1016/B978-0-12-372180-8.50042-1

Young AM (2005) Fungi of Australia: Hygrophoraceae. CSIRO Publishing, Australian Biological Resources Study, Canberra.

Supplementary material 1

Microscopic features of *Hygrophorus alboflavescens*

Authors: Arooj Naseer, Abdul Nasir Khalid, Rosanne Healy, Matthew E. Smith

Data type: media

Explanation note: **A–E** LAH35243 (holotype). **A** Pleurocystidia; **B** Basidaia with Cheilocystidia **C, D** Basidiopsores; **E** Pileipellis.

Link: https://doi.org/10.3897/mycokeys.56.30280.suppl1

Supplementary material 2

Microscopic features of *Hygrophorus scabrellus*

Authors: Arooj Naseer, Abdul Nasir Khalid, Rosanne Healy, Matthew E. Smith

Data type: media

Explanation note: **A–D** LAH35245 (holotype). **A** Basidiospores; **B** Hyphal Trama; **C** Basidiospores; **D** Pileipellis.

Link: https://doi.org/10.3897/mycokeys.56.30280.suppl2

MycoKeys 56: 49–66 (2019)
doi: 10.3897/mycokeys.56.36079
http://mycokeys.pensoft.net

RESEARCH ARTICLE

A peer-reviewed open-access journal
MycoKeys
Launched to accelerate biodiversity research

Nectria-related fungi causing dieback and canker diseases in China, with *Neothyronectria citri* sp. nov. described

Qin Yang[1], Wen-Yan Chen[1], Ning Jiang[1], Cheng-Ming Tian[1]

1 *The Key Laboratory for Silviculture and Conservation of the Ministry of Education, Beijing Forestry University, Beijing 100083, China*

Corresponding author: *Cheng-Ming Tian* (chengmt@bjfu.edu.cn)

Academic editor: *R. Phookamsak* | Received 10 May 2019 | Accepted 28 June 2019 | Published 10 July 2019

Citation: Yang Q, Chen W-Y, Jiang N, Tian C-M (2019) *Nectria*-related fungi causing dieback and canker diseases in China, with *Neothyronectria citri* sp. nov. described. MycoKeys 56: 49–66. https://doi.org/10.3897/mycokeys.56.36079

Abstract

To clarify phylogenetic relationships amongst *Nectria*, *Neothyronectria* and *Thyronectria* in *Nectriaceae*, we examined detailed morphological characters and performed phylogenetic analyses of a concatenated dataset, based on the ITS, LSU, *tef1* and *tub2* DNA sequences of fungal specimens in China. Four species of nectria-related fungi were identified, i.e. *Nectria dematiosa*, *N. pseudotrichia*, *Neothyronectria citri* and *Thyronectria pinicola*. The newly described species, *Neothyronectria citri*, is characterised by its ascomatal wall with bright yellow scurf, unitunicate asci, each with 4-spored and ascospores allantoid to short-cylindrical, uniseriate, muriform, hyaline to slightly yellowish-brown. This species has affinities with other one known species of *Neothyronectria* and can be distinguished by molecular data.

Keywords

DNA phylogeny, *Nectriaceae*, Systematic, Taxonomy

Introduction

Nectriaceae Tul. & C. Tul., typified by the genus *Nectria* (Fr.) Fr., was established by Tulasne and Tulasne (1865) to include nectria-related fungi having brightly pigmented ascomata with fusiform to allantoid ascospores and globose to fusiform phialidic conidia (Rossman et al. 1999, 2013, Rossman 2000, Lombard et al. 2015, Maharachchikumbura et al. 2015, Huang et al. 2018, Yang et al. 2018). Members of the family are unified

by phenotypic characters such as uniloculate ascomata that are yellow, orange-red to purple and phialidic asexual morphs. Lombard et al. (2015) defined the generic concepts in *Nectriaceae*, based on a multi-gene phylogenetic analysis and resolved 47 genera supported by morphological observations. Since then, *Neothyronectria* was proposed as a new genus to accommodate the species, *Neothyronectria sophorae*, which is known only from the pycnidial asexual morph (Crous et al. 2016) and *Cosmosporella* was proposed as a new genus (Huang et al. 2018), thus 49 genera are now accepted in the *Nectriaceae*.

Nectria, typified by *N. cinnabarina* (Tode: Fr.) Fr., was initially established by Fries (1849). Some species of *Nectria* are weak parasites of woody plants (Samuels et al. 2009, Hirooka et al. 2011). Hirooka et al. (2012) reviewed the genus, based on the type and additional herbarium specimens, and accepted 29 species. They also monographed the genus *Thyronectria* as *Pleonectria* but because *Thyronectria* (1875) is older, it has priority over *Pleonectria* (1876) as explained by Jaklitsch and Voglmayr (2014). Many members of *Nectria* and *Thyronectria* occur on dead corticated twigs or branches of woody plants worldwide mainly in temperate and subtropical regions (Hirooka et al. 2012, Jaklitsch and Voglmayr 2014, Zeng and Zhuang 2016). To date, 42 species of *Thyronectria* have been accepted (Jaklitsch and Voglmayr 2014, Voglmayr et al. 2016, Zeng and Zhuang 2016, Lechat et al. 2018).

During trips to collect forest pathogens in China, several nectria-related fungi associated with canker or dieback diseases were collected. Based on a multi-locus phylogeny (ITS, LSU, *tef1* and *tub2*), we identified four nectria-related species in three genera of *Nectriaceae* and propose one new species in *Neothyronectria*.

Materials and methods

Isolates

Fresh specimens were collected from infected branches or twigs of diverse hosts from Beijing, Heilongjiang, Jiangxi, Shaanxi and Xinjiang provinces, China. Strains were isolated from fresh diseased branches and grown from ascospores or conidia by spreading the suspension on the surface of 1.8% potato dextrose agar (PDA), incubated at 25 °C for up to 24 h. Single germinating conidia were removed and transferred to fresh potato dextrose agar (PDA) plate. Specimens and isolates of the new species have been deposited in the Museum of Beijing Forestry University (BJFC). Axenic cultures are maintained in the China Forestry Culture Collection Center (CFCC).

Morphological analysis

Morphological observations of the sexual and asexual morph in the natural environment were based on features of the fruiting bodies produced on infected plant tissues and micromorphology, supplemented by cultural characteristics. Gross morphology of fruiting bodies was recorded using a Leica stereomicroscope (M205 FA). Perithecia,

pycnidia, synnemata and stromata were observed and described. To test ascomatal wall reactions, 3% KOH and 100% lactic acid (LA) were used. The micromorphological characteristics were examined by mounting fungal structures in clear lactic acid and 30 measurements at 1000× magnification were determined for each isolate using a Leica compound microscope (DM 2500) with differential interference contrast (DIC) optics. Colony characters and pigment production on PDA were noted after 10 d. Colony colours were described according to Rayner (1970). Longitudinal descriptions, nomenclature and illustrations of taxonomic novelties are deposited in MycoBank (http://www.MycoBank.org; Crous et al. 2004).

DNA extraction, PCR amplification and sequencing

Genomic DNA was extracted from colonies grown on cellophane-covered PDA, using a modified CTAB [cetyltrimethylammonium bromide] method (Doyle and Doyle 1990, Zhang et al. 2010). For PCR amplifications of phylogenetic markers, four different primer pairs were used (Table 1). PCR amplification products were assayed via electrophoresis in 2% agarose gels. DNA sequencing was performed using an ABI PRISM 3730XL DNA Analyzer with a BigDye Terminater Kit v.3.1 (Invitrogen, USA) at the Shanghai Invitrogen Biological Technology Company Limited (Beijing, China).

Phylogenetic analyses

The quality of our amplified nucleotide sequences was checked and combined by SeqMan v.7.1.0 and reference sequences were retrieved from the National Center for Biotechnology Information (NCBI), according to recent publications of the family *Nectriaceae* (Jaklitsch and Voglmayr 2014, Lombard et al. 2015, Crous et al. 2016, Yang et al. 2018). Sequences were aligned using MAFFT v. 7.310 (http://mafft.cbrc.jp/alignment/server/index.html) (Katoh and Standley 2016) and manually corrected using Bioedit 7.0.9.0 (Hall 1999).

Phylogenetic analyses of the combined gene regions were performed using Maximum Parsimony (MP), Maximum-Likelihood (ML) and Bayesian Inference (BI) methods. The data were edited in AliView version: 1.19-beta1k and the evolutionary model obtained using MrModeltest v. 2.3 (Nylander et al. 2008) under the Akaike

Table 1. Genes used in this study with PCR primers, process and references.

Gene	PCR primers (forward/reverse)	PCR: thermal cycles: (Annealing temp. in bold)	References of primers used
ITS	ITS1/ITS4	(95 °C: 30 s, **51 °C**: 30 s, 72 °C: 1 min) × 35 cycles	White et al. 1990
LSU	LROR/ LR5	(95 °C: 45 s, **55 °C**: 45 s, 72 °C: 1 min) × 35 cycles	Vilgalys and Hester 1990, Rehner and Samuels 1994
tef1	EF1-728F and EF-1567R	(95 °C: 15 s, **55 °C**: 20 s, 72 °C: 1 min) × 35 cycles	Carbone and Kohn 1999, Rehner 2001
tub2	T1/T2	(95 °C: 30 s, **55 °C**: 30 s, 72 °C: 1 min) × 35 cycles	O'Donnell and Cigelnik 1997

Information Criterion (AIC) performed in PAUP v. 4.0b10. The MP analysis was performed by a heuristic search option of 1000 random-addition sequences with a tree bisection and reconnection (TBR) algorithm. Maxtrees were set to 5000, branches of zero length were collapsed and all equally parsimonious trees were saved. Other calculated parsimony scores were tree length (TL), consistency index (CI), retention index (RI) and rescaled consistency (RC). ML was performed using RAxML-HPC v.8 on XSEDE in CIPRES Science Gateway (Miller et al. 2010, 2015, Stamatakis 2014) with 1000 rapid bootstrap replicates using the GTR+I+G model of nucleotide substitution. BI was implemented by MrBayes v. 3.0b4 (Ronquist and Huelsenbeck 2003) with GTR+I+G as the best-fit model. Posterior Probabilities (PP) were estimated by Markov Chain Monte Carlo sampling (MCMC) in MrBayes v. 3.0b4 (Huelsenbeck and Ronquist 2001). Two MCMC chains, started from random trees for 1,000,000 generations and trees, were sampled every 100th generation, resulting in a total of 10,000 trees. The first 25% of trees were discarded as the burn-in phase of each analysis. Branches with significant Bayesian Posterior Probabilities (BPP) were estimated in the remaining 7500 trees. Phylogenetic trees were viewed with FigTree v.1.3.1 (Rambaut and Drummond 2010) and processed by Adobe Illustrator CS5. Alignment and trees were deposited in TreeBASE (submission ID: 24366). The nucleotide sequence data of the new taxon have been deposited in GenBank (Table 1).

Results

Phylogenetic analyses

To reveal the phylogenetic position amongst *Nectria*, *Neothyronectria* and *Thyronectria* in *Nectriaceae*, a phylogenetic analysis was performed with combined ITS, LSU, *tef1* and *tub2* sequence data. Sequences of representative species were selected from NCBI (Jaklitsch and Voglmayr 2014, Crous et al. 2016, Yang et al. 2018). The ITS, LSU, *tef1*, *tub2* and combined data matrices contained 545, 781, 1033, 643 and 3010 characters with gaps, respectively. The alignment comprised 59 strains and *Emericellopsis glabra* (CBS 125295), *Hydropisphaera fungicola* (CSB 122304), *Nectriopsis exigua* (CBS 126110) and *Verrucostoma freycinetiae* (MAFF 240100) were selected as the outgroups.

The concatenated sequence alignment contained 932 parsimony-informative characters, 259 were variable and parsimony uninformative and 1819 were constant. The parsimony analysis yielded the maximum of 10 equally most parsimonious trees (TL = 5493 steps; CI = 0.386; RI = 0.685; RC = 0.264; HI = 0.614).

The phylogeny, resulting from the MP analysis of combined gene sequence data, is shown in Fig. 1. Overall, the topologies obtained from the different phylogenetic analyses were mostly similar and the best scoring MP tree is illustrated here. The MP and ML bootstrap support values above 50% are shown at the first and second position, respectively. Branches with significant BPP (≥ 0.95) in Bayesian analyses were thickened in the phylogenetic tree.

Table 2. Strains and GenBank accession numbers of the isolates used in this study.

Species	Isolate No.	Substrate/Host	Country	GenBank Accession No.			
				ITS	LSU	*tef1*	*tub2*
Allantonectria miltina	CBS 121121	*Agave americana*	Italy	HM484547	HM484572	HM484524	HM484609
Emericellopsis glabra	CBS 125295	Soil	Mexico	HM484860	GQ505993	HM484843	HM484879
Hydropisphaera fungicola	CBS 122304	Decaying leaves on *Populus trichocarpa*	USA	HM484863	GQ505995	HM484845	HM484877
N. antarctica	CBS 115033	*Berberis aquifolium*	USA	HM484556	HM484560	HM484516	HM484601
N. asiatica	MAFF 241439	Bark of dead wood	Japan	HM484701	HM484563	–	HM484604
N. aurantiaca	CBS 308.34	*Ulmus* sp.	UK	JF832628	JF832682	JF832519	JF832886
N. balansae	CBS 123351	*Coronilla* sp.	France	HM484552	GQ505996	HM484525	HM484607
N. balansae	CBS 129349	Twigs	China	JF832653	JF832711	JF832522	JF832908
N. berberidicola	CBS 128669	*Berberis vulgaris*	France	JF832662	JF832712	JF832538	JF832887
N. cinnabarina	CBS 125165	Dead twigs of *Aesculus* sp.	France	HM484548	HM484562	HM484527	HM484606
N. dematiosa Subclade A	CBS 126570	Bark	USA	HM484557	HM484561	HM484534	HM484603
***N. dematiosa* Subclade A**	**CFCC 53585**	***Tilia mandshurica***	**China**	**MK861084**	**MK861075**	**MK902792**	**MK902801**
***N. dematiosa* Subclade A**	**CFCC 53586**	***Betula platyphylla***	**China**	**MK861085**	**MK861076**	**MK902793**	**MK902802**
N. dematiosa Subclade B	CBS 125125	Dead twigs of *Acer macrophyllum*	Canada	HM484676	HM484717	HM484645	HM484797
N. eustromatica	CBS 121896	–	–	HM534896	HM534896	HM534875	–
N. eustromatica	CBS 125578	–	–	HM534897	HM534897	HM534876	–
N. magnispora	CBS 129362	–	Japan	JF832663	JF832683	JF832539	JF832896
N. magnispora	CBS 129361	Twigs	Japan	JF832664	JF832685	JF832540	JF832897
N. mariae	CBS 125294	*Buxus sempervirens*	France	JF832629	JF832684	JF832542	JF832899
N. nigrescens	CBS 125148	Dead twigs of dicotyledonous tree	USA	HM484707	HM484720	HM484672	HM484806
N. nigrescens	CBS 128988	*Elaeagnus angustifolia*	USA	JF832630	JF832687	–	JF832888
N. nigrescens	CBS 129808	*Ulmus pumila*	USA	JF832632	JF832690	–	JF832894
N. polythalama	CBS 128672	Twigs	New Zealand	JF832638	JF832695	JF832523	JF832900
N. pseudocinnabarina	CBS 129366	Dead wood	Venezuela	JF832642	JF832697	JF832533	–
N. pseudotrichia	CBS 551.84	Bark	Japan	HM484554	GQ506000	HM484532	HM484602
N. pseudotrichia	MAFF 241452	Bark	Japan	JF832649	JF832706	JF832531	JF832903
N. pseudotrichia	G.J.S. 09-1329	Dead wood	Venezuela	JF832647	JF832702	JF832530	JF832902
N. pseudotrichia	**CFCC 53587**	***Robinia* sp.**	**China**	**MK861086**	**MK861077**	**MK902794**	**MK902803**
N. pseudotrichia	**CFCC 53588**	***Cinnamomum porrectum***	**China**	**MK861087**	**MK861078**	**MK902795**	**MK902804**
N. pseudotrichia	**CFCC 53589**	***Rubus corchorifolius***	**China**	**MK861088**	**MK861079**	**MK902796**	**MK902805**
N. sordida	CBS 125119	Living woody vine	French Guiana	HM484857	HM484868	HM484848	HM484874
N. triseptata	HAMS 252485	On rotten twig	China	KM026503	KM026504	KM026506	KM026501
N. ulmicola	CFCC 52117	*Ulmus davidiana* var. *japonica*	China	MG231959	MG231980	MG232022	MG232043
N. ulmicola	CFCC 52118	*Ulmus davidiana* var. *japonica*	China	MG231960	MG231981	MG232023	MG232044
Nectriopsis exigua	CBS 126110	*Myxomycete*	Puerto Rico	HM484865	GQ506014	HM484852	HM484883
Neothyronectria citri	**CFCC 53590**	***Citrus maxima* cv. *Shatian***	**China**	**MK861080**	**MK861071**	**MK902788**	**MK902797**
N. citri	**CFCC 53591**	***Citrus maxima* cv. *Shatian***	**China**	**MK861081**	**MK861072**	**MK902788**	**MK902798**
N. sophorae	CBS 142094	*Sophora microphylla*	Zew Zealand	KY173470	KY173559	–	KY173619
Thyronectria aquifolii	CBS 307.34	*Ilex aquifolium*	UK	JF832597	JF832718	JF832548	JF832842

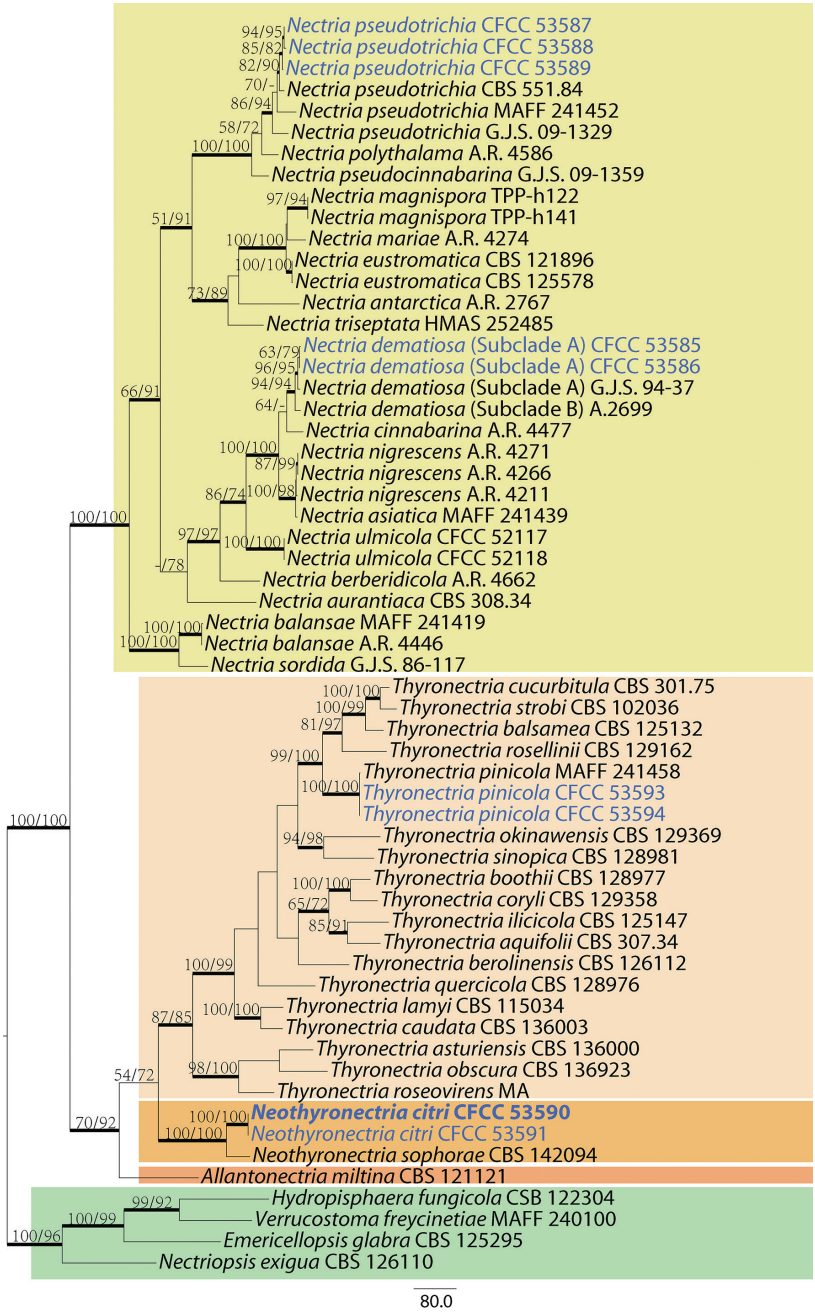

Figure 1. Maximum parsimony phylogenetic tree generated from analysis of a combined ITS, LSU, *tef1* and *tub2* sequence dataset for 59 taxa of *Allantonectria*, *Nectria*, *Neothyronectria* and *Thyronectria*. *Emericellopsis glabra* (CBS 125295), *Hydropisphaera fungicola* (CSB 122304), *Nectriopsis exigua* (CBS 126110) and *Verrucostoma freycinetiae* (MAFF 240100) as outgroup taxa. Values above the branches indicate maximum parsimony and maximum likelihood bootstrap (left, MP BP ≥ 50%; right, ML BP ≥ 50%). The branches with significant BIPP values (≥ 0.95) in the BI analysis are thickened. Scale bar = 80 nucleotide substitutions. Strains in current study are in blue. Ex-type strains are indicated in bold.

Taxonomy

***Nectria* (Fr.) Fr., Summa veg. Scand., Sectio Post. (Stockholm): 387, 1849**

Type species. *Nectria cinnabarina* (Tode) Fr., Summa veg. Scand., Sectio Post. (Stockholm): 388, 1849.

Note. Members of *Nectria* are typically weak parasites of woody plants and occur on hardwood trees and shrubs throughout the temperate zone of the northern hemisphere (Samuels et al. 2009, Hirooka et al. 2011). The genus *Nectria* is characterised by well-developed stromata, subglobose to globose, red to dark red, fleshy, soft-textured, uniloculate, warted perithecia that become cupulate when dry and are associated with coelomycetous asexual morphs. Asci are unitunicate and clavate to cylindrical in shape. Ascospores are variable and usually broadly ellipsoid to long-fusiform, hyaline to yellow brown, smooth to striate and non- to multi-septate or muriform (Rossman et al. 1999, Hirooka et al. 2009, Maharachchikumbura et al. 2015).

***Nectria dematiosa* (Schwein.) Berk., Grevillea 4: 16, 1875**
Fig. 2

Description. See Yang et al. (2018)

Additional specimens examined. CHINA. Heilongjiang Province, Liangshui Nature Reserve, 47°10'50.64"N, 128°53'41.03"E, on twigs or branches of *Tilia mandshurica* Rmpr.et Maxim., 29 July 2016, Q. Yang (BJFC-S1400, living culture CFCC 53585); Xinjiang, 45°13'07.97"N, 81°46'24.71"E, on twigs or branches of *Betula platyphylla* Suk., 18 July 2017, C.M. Tian (BJFC-S1767, living culture CFCC 53586).

Note. *Nectria dematiosa* has a broad host range and is widely distributed in China, occurring as the most commonly *Nectria* species (Yang et al. 2018). This study is the first report of *N. dematiosa* from *Betula platyphylla* and *Tilia mandshurica*.

***Nectria pseudotrichia* Berk. & M.A. Curtis, J. Acad. Nat. Sci. Philadelphia 2, 2: 289. 1853**
Fig. 3

Description. See Yang et al. (2018)

Additional specimens examined. CHINA. Shaanxi Province, Ankang City, 32°40'32.85"N, 109°18'57.38"E, on twigs or branches of *Robinia* sp., 29 July 2016, N. Jiang (BJFC-S1403, living culture CFCC 53587); Jiangxi Province, Ganzhou City, 24°40'51.80"N, 115°31'49.99"E, on twigs or branches of *Cinnamomum porrectum* (Roxb.) Kosterm., 12 May 2018, Q. Yang (BJFC-S1768, living culture CFCC 53588); Jiangxi Province, Ganzhou City, 24°59'44.81"N, 115°30'58.85"E, on twigs or branches of *Rubus corchorifolius* Linn. f., 12 May 2018, Q. Yang (BJFC-S1769, living culture CFCC 53589).

Note. *Nectria pseudotrichia* is one of the common tropical fungi in the genus *Nectria* and is distinguished in the genus by having muriform ascospores and a synnematous asexual morph.

Neothyronectria Crous & Thangavel, Persoonia 37: 329, 2016.

Type species. *Neothyronectria sophorae* Crous & Thangavel, Persoonia 37: 329, 2016.

Note. The genus *Neothyronectria* was described by Crous & Thangavel (2016) based on the only species, *N. sophorae*, which is known from a pycnidial asexual morph. *Neothyronectria* is characterised by pycnidial conidiomata that exude a creamy mucoid conidial mass and hyaline, ampulliform to subcylindrical conidia. In this study, we collected and illustrated here one additional taxon in *Neothyronectria*.

Neothyronectria citri C.M. Tian & Q. Yang, sp. nov.

MycoBank: MB830779
Figure 4

Diagnosis. *Neothyronectria citri* differs from its closest phylogenetic neighbour *Neothyronectria sophorae* in ITS, LSU and *tub2* loci, based on the alignments deposited in TreeBASE.

Holotype. CHINA. Jiangxi Province: Ganzhou city, 25°51'27.87"N, 114°58'18.95"E, on symptomatic branches of *Citrus maxima* (Burm.) Merr. cv. *Shatian* Yu, 11 May 2018, Q. Yang, Y.M. Liang & Y. Liu (holotype BJFC-S1770 designated here, ex-type culture CFCC 53590).

Etymology. Named after the host genus on which it was collected, *Citrus*.

Description. *Mycelium* not visible around ascomata or on the host. *Stromata* erumpent through epidermis, up to 0.6 mm high and 1 mm diam., pseudoparenchymatous, cells forming *textura angularis* to *t. globulosa*, intergrading with ascomatal wall. *Ascomata* superficial on well-developed stromata, scattered to aggregated in groups of 3–10, subglobose to globose, 200–270 µm diam., rarely slightly cupulate upon drying, sometimes with only a depressed apical region, yellowish-brown to grey, apical region slightly darker, no colour change in KOH or LA, sometimes surface scurfy or scaly, bright yellow to greenish-yellow. *Ascomatal surface cells* forming *textura globulosa* or *t. angularis*, sometimes including bright yellow scurf, 9–15 µm diam., walls pigmented, uniformly about 1.5 µm thick. *Ascomatal wall* 27–46 µm thick, of two regions: outer region 22–35 µm thick, intergrading with stroma, cells forming *textura globulosa* or *t. angularis*, walls pigmented, about 1.5 µm thick; inner region 9–15 µm thick, of elongate, thin-walled, hyaline cells, forming *textura prismatica*. *Asci* clavate, unitunicate, 53.5–65 × 8.5–11 µm, with inconspicuous ring at apex, 4-spored. *Ascospores* allantoid to short-cylindrical, uniseriate, rounded at both

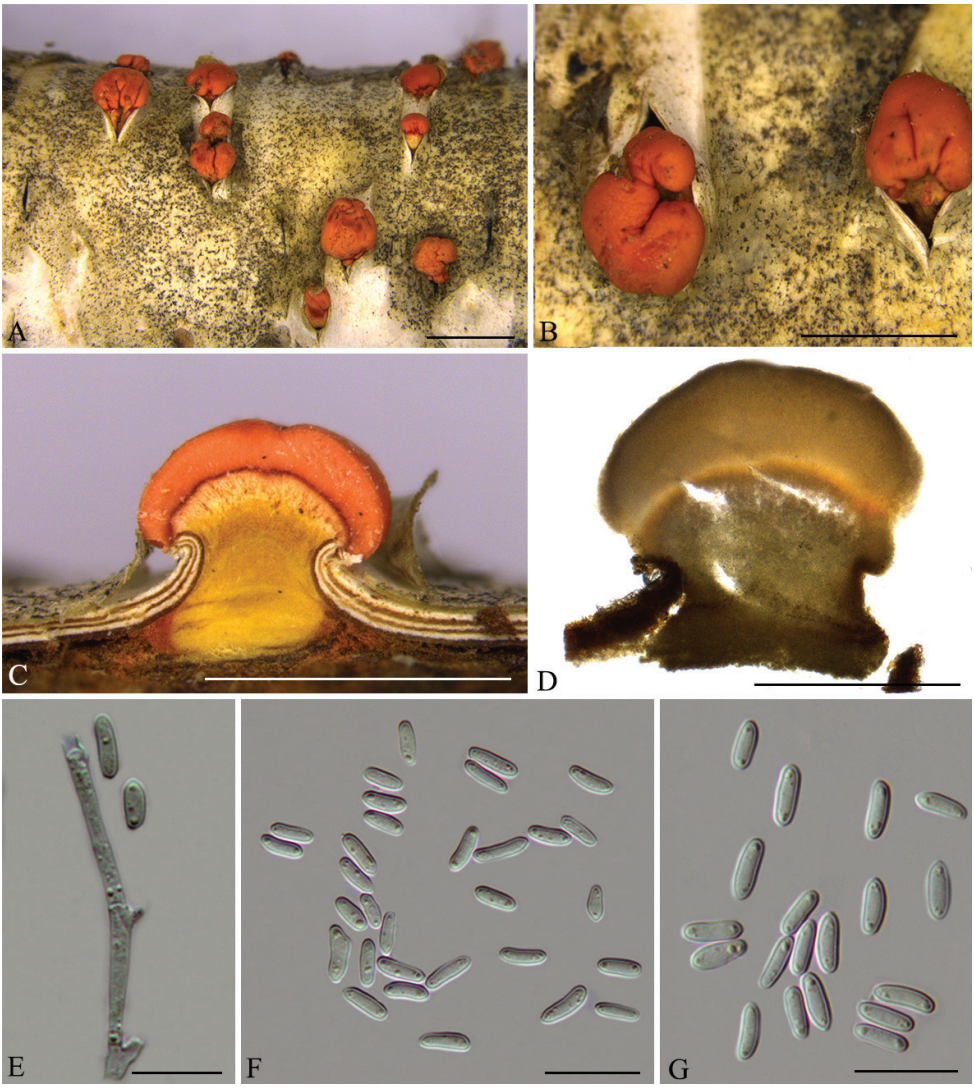

Figure 2. *Nectria dematiosa* (CFCC 53585) **A–B** habit of conidiomata on branches **C** transverse section of conidioma **D** longitudinal section of conidioma **E** conidiophores **F–G** conidia. Scale bars: 1 mm (**A–C**); 500 μm (**D**); 10 μm (**E–G**).

ends, (17–)18–21(–23.5) × 8–9(–10) μm (n = 20), muriform, hyaline to slightly yellowish-brown.

Culture characters. Cultures incubated on PDA at 25 °C in darkness. Colony originally flat with white aerial mycelium, becoming pale yellowish due to pigment formation, conidiomata absent.

Additional specimen examined. CHINA. Jiangxi Province: Ganzhou City, 25°51'27.87"N, 114°58'18.95"E, on symptomatic branches of *Citrus maxima* (Burm.)

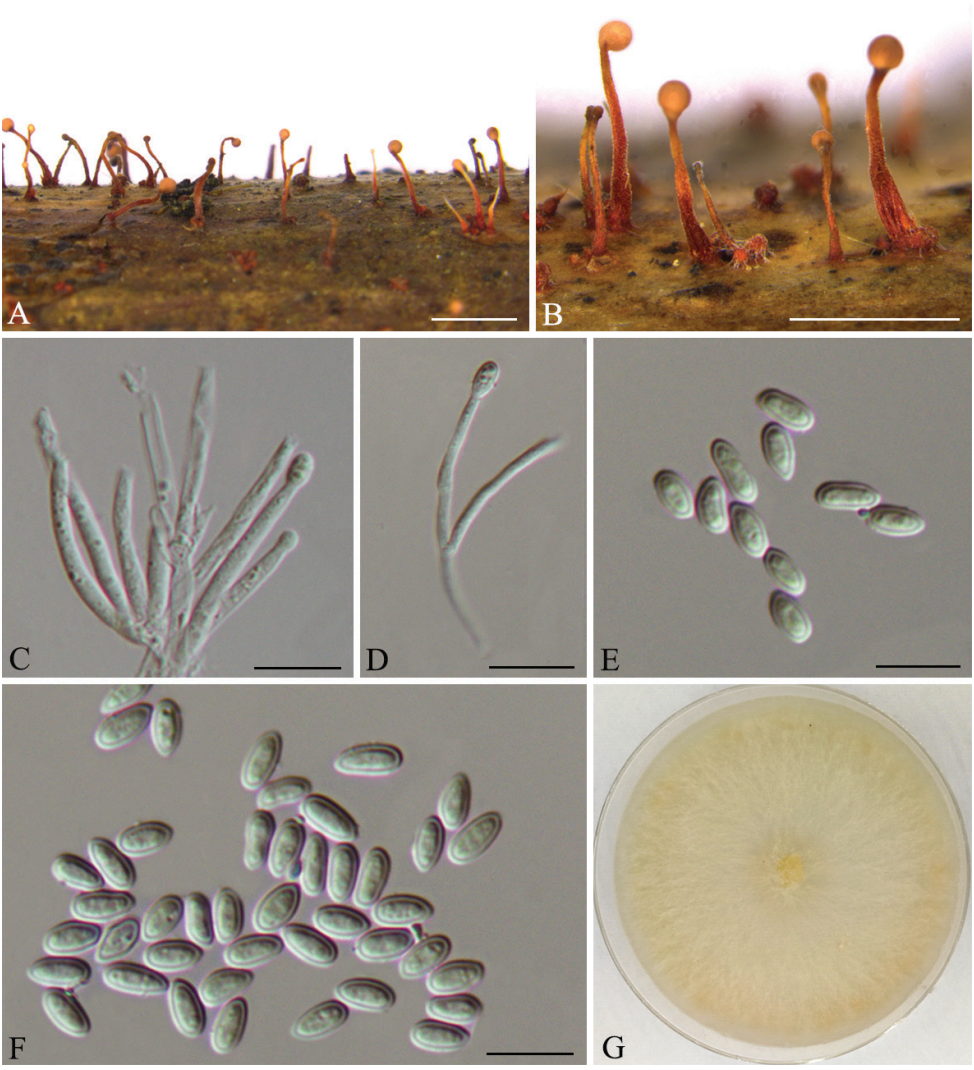

Figure 3. *Nectria pseudotrichia* (CFCC 53587) **A–B** habit of conidiomata on branches **C–D** conidiophores **E–F** conidia. Scale bars: 1 mm (**A–B**); 10 μm (**C–F**).

Merr. cv. *Shatian* Yu, 11 May 2018, Q. Yang, Y.M. Liang & Y. Liu (BJFC-S1771, living culture CFCC 53591).

Note. *Neothyronectria citri*, as described here, is known from an ascomatal sexual morph phylogenetically allied to species of *Allantonectria* and *Thyronectria* (Fig. 1). In this study, two strains representing *Neothyronectria citri* cluster in a well-supported clade and appear most closely related to *Neothyronectria sophorae*, which was isolated from *Sophora microphylla* in New Zealand (Crous et al. 2016). *Neothyronectria citri* can be distinguished, based on ITS, LSU and *tub2* loci from *Neothyronectria sophorae* (16/464 in ITS, 9/772 in LSU and 60/494 in *tub2*).

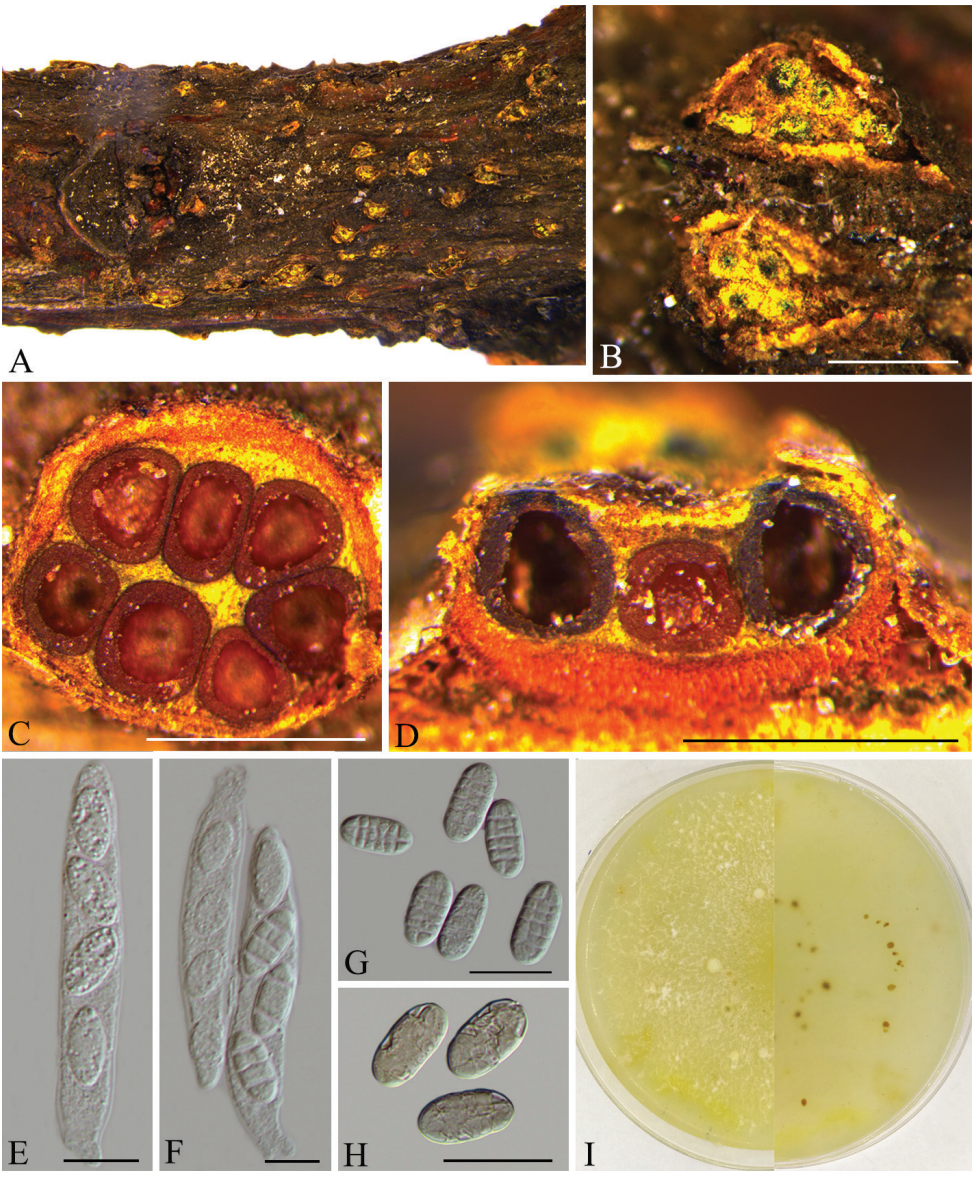

Figure 4. *Neothyronectria citri* (CFCC 53590) **A–B** habit of conidiomata on branches **C** transverse section of conidioma **D** longitudinal section of conidioma **E–F** asci **G–H** ascospores. Scale bars: 500 μm (**B–D**); 10 μm (**E–H**).

Thyronectria Sacc., Grevillea 4: 21, 1875.

Type species. *Thyronectria rhodochlora* (Mont.) Seeler, J. Arnold Arbor. 21: 455, 1940.

Note. *Thyronectria* Sacc. was established by Saccardo (1875) to include nectria-like fungi with immersed ascomata and muriform ascospores and characterised by well-

developed erumpent stromata which are often covered with yellow-green amorphous scurf and ascospores that sometimes bud in the ascus to produce ascoconidia (Jaklitsch and Voglmayr 2014, Lombard et al. 2015). Members of the genus occur on dead corticated twigs or branches of woody plants worldwide mainly in temperate and subtropical regions (Hirooka et al. 2012, Jaklitsch and Voglmayr 2014).

Thyronectria pinicola **(Kirschst.) Jaklitsch & Voglmayr, Persoonia 33: 203, 2014.**
Figure 5

Basionym. *Pleonectria pinicola* Kirschst., Abh. Bot. Ver. Prov. Brandenburg 48: 59, 1906.

Description. *Stromata* erumpent through epidermis, orange to red. *Pycnidia* solitary or aggregated in groups of 3–6, superficial on stroma or rarely immersed at base, subglobose, smooth to slightly roughened, cerebriformis or slightly cupulate upon drying, 225–400 µm high, 240–440 µm diam., red to bay, KOH+ slightly darker, LA+ slightly yellow. *Pycnidial wall* 16–40 µm thick, of two regions: outer region 11–15 µm thick, intergrading with stroma, cells forming *textura globulosa* or *t. angularis*, walls pigmented, about 1.5 µm thick; inner region 10–24 µm thick, of elongate, thin-walled, hyaline cells, forming *textura prismatica*. *Conidiophores* densely branched, generally with 1–3 branches, 8.5–24 µm long, 1.3–1.5 µm wide. *Conidiogenous cells* cylindrical monophialides on aerial, submerged or repent hyphae. *Conidia* formed abundantly on slimy heads, ellipsoidal to oblong, hyaline, straight, rounded at both ends, non-septate, (2–)3–3.5 × 0.7–1.0 µm (n = 20), smooth-walled.

Culture characters. Cultures incubated on PDA at 25 °C in darkness. Colony surface cottony with aerial mycelium, becoming yellowish-brown due to pigment formation, small reddish-brown sporodochial conidial masses produced after 3–4 wk.

Specimens examined. CHINA. Beijing: Chaoyang District, 40°00'35.31"N, 116°47'55.32"E, on symptomatic branches of *Pinus sylvestris* Linn. var. *mongolica* Litv., 11 June 2018, Q. Yang & N. Jiang (BJFC-S1773, living culture CFCC 53593 and CFCC 53594).

Note. The hosts of *Thyronectria pinicola*, synonymised with *Pleonectria pinicola,* are restricted to *Pinus*. Members of the genus distributed in Asia (China, Japan, Pakistan), Australia, Europe (Germany, Russia), North America (USA) and South America (Chile) (Jaklitsch and Voglmayr 2014). The asexual morph of *T. pinicola* in the natural environment has long, sterile hyphae extending from the hymenium and abundant conidiophores (Figs 4E–G). In the present study, two isolates from twigs of *Pinus sylvestris* var. *mongolica* were congruent with *T. pinicola*, based on morphology and DNA sequences data (Fig. 1). We therefore describe *T. pinicola* as a known species for this clade.

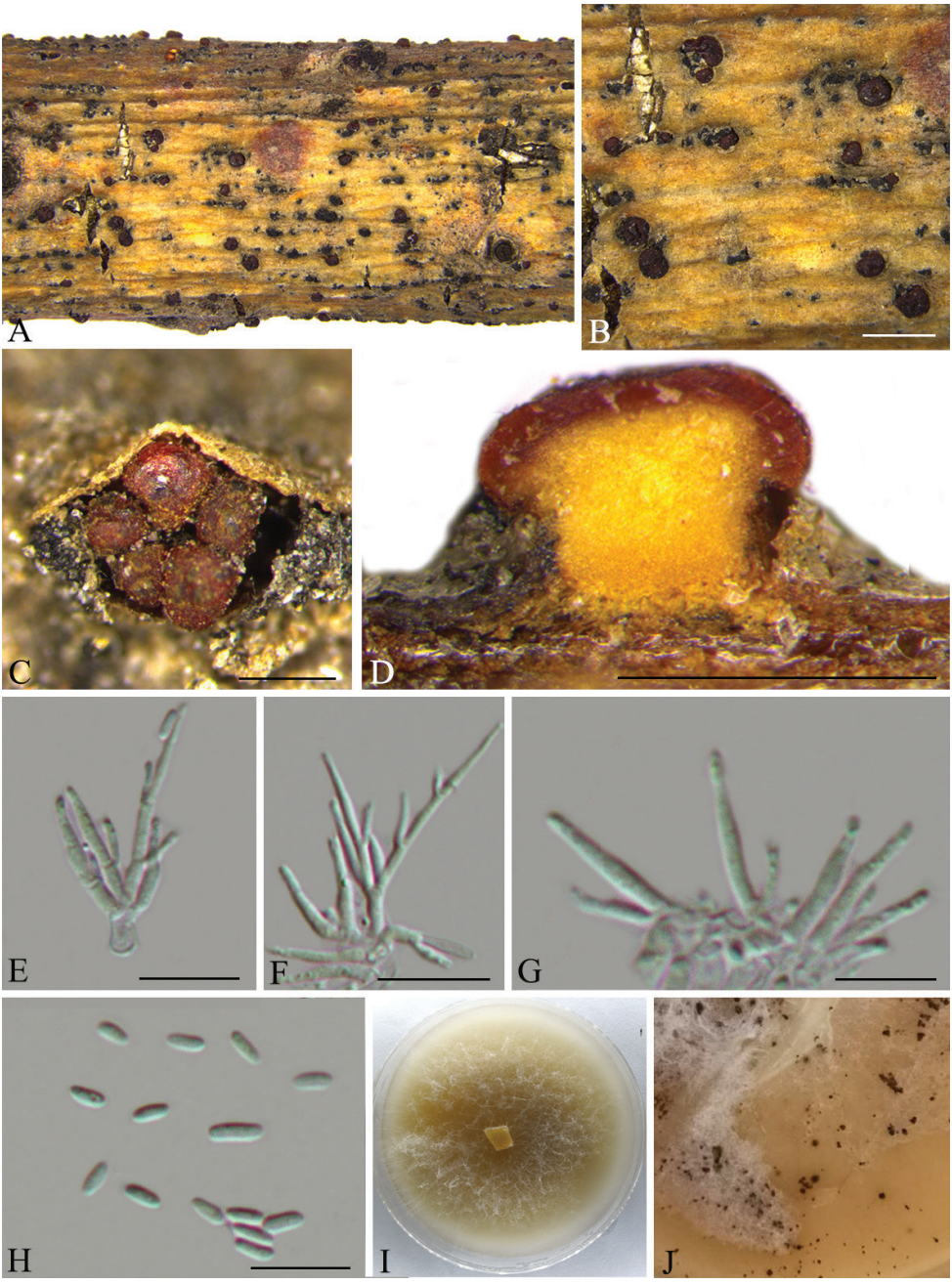

Figure 5. *Thyronectria pinicola* (CFCC 53593) **A–C** habit of conidiomata on branches **D** longitudinal section of conidioma **E–G** conidiogenous cells with conidia **H** conidia **I–J** culture on PDA and conidiomata. Scale bars: 1 mm (**B**); 500 μm (**C–D**); 10 μm (**E–H**).

Discussion

In this investigation of nectria-related fungi in China, we identified four species in three genera (*Nectria*, *Neothyronectria* and *Thyronectria*) of *Nectriaceae*, based on four combined loci (ITS, LSU, *tef1* and *tub2*), as well as morphological characters. It includes *Nectria dematiosa*, *N. pseudotrichia*, and *Thyronectria pinicola* as well as one new species named *Neothyronectria citri*. The new species is characterised by well-developed erumpent stromata that are often covered with yellow-green amorphous scurf; asci unitunicate, clavate, with inconspicuous ring at apex, each with 4-spored; ascospores allantoid to short-cylindrical, uniseriate, muriform, hyaline to slightly yellowish.

Species revised by Rossman et al. (1999) in *Nectria* were monographed by Hirooka et al. (2012), who recognised three genera, i.e. *Allantonectria*, *Nectria* and *Pleonectria*. *Allantonectria*, based on *Allantonectria miltina*, was recognised as a monotypic genus with small, aseptate ascospores, trichoderma-like conidiophores and occurring on monocotyledonous plants. The genus *Thyronectria* (as *Pleonectria*) is characterised by having ascomata with bright yellow scurf, ascospores that often bud to produce ascoconidia inside or outside of the asci and/or a pycnidial anamorph (Hirooka et al. 2012). Based on the lack of bright yellowish scurf on the ascomata, the genus *Nectria* is easily distinguished from *Allantonectria* and *Thyronectria*. In this study, *Neothyronectria citri* was identified as a new species in *Neothyronectria*, which was typified by *Neothyronectria sophorae* having ampulliform to subcylindrical conidia (Crous et al. 2016). Unlike species of *Thyronectria*, *Neothyronectria* did not produce ascoconidia but they have bright yellow scurf on the ascomatal wall.

In the taxonomy of hypocrealean fungi, the reaction of the perithecial wall to KOH is considered as an important character (Rossman et al. 1999, Zeng and Zhuang 2016). Most species of *Allantonectria* and *Thyronectria* have perithecial colour turning darker to blood-red or purple in KOH. However, some species in *Thyronectria* display a weak or negative reaction to KOH, which might be influenced by the presence of scurf covering the perithecia or their dark-coloured ascomata (Hirooka et al. 2012, Jaklitsch and Voglmayr 2014, Zeng and Zhuang 2016). In our study, the dark perithecial walls of *Neothyronectria citri* do not change colour in KOH but the major features, such well-developed stromata and ascomata with bright yellow scurf, as well as the molecular data, also provide strong evidence that it belongs to *Neothyronectria*.

Acknowledgements

This study is financed by National Natural Science Foundation of China (Project No.: 31670647). We are grateful to Chungen Piao, Minwei Guo (China Forestry Culture Collection Center (CFCC), Chinese Academy of Forestry, Beijing.

References

Carbone I, Kohn LM (1999) A method for designing primer sets for speciation studies in filamentous ascomycetes. Mycologia 3: 553–556. https://doi.org/10.2307/3761358

Crous PW, Gams W, Stalpers JA, Robert V, Stegehuis G (2004) MycoBank: an online initiative to launch mycology into the 21st century. Studies in Mycology 50: 19–22.

Crous PW, Wingfield MJ, Burgess TI, Hardy GESJ, Crane C, Barrett S, Cano-Lira JF, Le Roux JJ, Thangavel R, Guarro J, Stchigel AM, Martín MP, Alfredo DS, Barber PA, Barreto RW, Baseia IG, Cano-Canals J, Cheewangkoon R, Ferreira RJ, Gené J, Lechat C, Moreno G, Roets F, Shivas RG, Sousa JO, Tan YP, Wiederhold NP, Abell SE, Accioly T, Albizu JL, Alves JL, Antoniolli ZI, Aplin N, Araújo J, Arzanlou M, Bezerra JDP, Bouchara JP, Carlavilla JR, Castillo A, Castroagudín VL, Ceresini PC, Claridge GF, Coelho G, Coimbra VRM, Costa LA, da Cunha KC, da Silva SS, Daniel R, de Beer ZW, Dueñas M, Edwards J, Enwistle P, Fiuza PO, Fournier J, García D, Gibertoni TB, Giraud S, Guevara-Suarez M, Gusmão LFP, Haituk S, Heykoop M, Hirooka Y, Hofmann TA, Houbraken J, Hughes DP, Kautmanová I, Koppel O, Koukol O, Larsson E, Latha KPD, Lee DH, Lisboa DO, Lisboa WS, López-Villalba Á, Maciel JLN, Manimohan P, Manjón JL, Marincowitz S, Marney TS, Meijer M, Miller AN, Olariaga I, Paiva LM, Piepenbring M, Poveda-Molero JC, Raj KNA, Raja HA, Rougeron A, Salcedo I, Samadi R, Santos Tab, Scarlett K, Seifert KA, Shuttleworth LA, Silva GA, Silva M, Siqueira JPZ, Souza-Motta CM, Stephenson SL, Sutton DA, Tamakeaw N, Telleria MT, Valenzuela-Lopez N, Viljoen A, Visagie CM, Vizzini A, Wartchow F, Wingfield BD, Yurchenko E, Zamora JC, Groenewald JZ (2016) Fungal Planet description sheets: 469–557. Persoonia 37: 218–403. https://doi.org/10.3767/003158516X694499

Desjardins P, Hansen JB, Allen M (2009) Microvolume protein concentration determination using the NanoDrop 2000c spectrophotometer. Journal of visualized experiments: JoVE 33: 1–3. https://doi.org/10.3791/1610

Doyle JJ, Doyle JL (1990) Isolation of plant DNA from fresh tissue. Focus 12: 13–15. https://doi.org/10.2307/2419362

Fries EM (1849) Summa vegetabilium Scandinaviae, Sectio posterior: 259–572.

Hall T (1999) BioEdit: a user-friendly biological sequence alignment editor and analysis program for Windows 95/98/NT. Nucleic Acids Symposium Series 41: 95–98.

Hirooka Y, Rossman AY, Chaverri P (2009) Systematics of the genus *Nectria* based on six-gene phylogeny. Inoculum 60: 22.

Hirooka Y, Rossman AY, Chaverri P (2011) A morphological and phylogenetic revision of the *Nectria cinnabarina* species complex. Studies in Mycology 68: 35–56. https://doi.org/10.3114/sim.2011.68.02

Hirooka Y, Rossman AY, Samuels GJ, Lechat C, Chaverri P (2012) A monograph of *Allantonectria*, *Nectria*, and *Pleonectria* (Nectriaceae, Hypocreales, Ascomycota) and their pycnidial, sporodochial, and synnematous anamorphs. Studies in Mycology 71: 1–210. https://doi.org/10.3114/sim0001

Huang SK, Jeewon R, Hyde KD, Jayarama Bhat D, Wen TC (2018) Novel Taxa within Nectriaceae: *Cosmosporella* gen. nov. and *Aquanectria* sp. nov. from Freshwater Habitats in China. Cryptogamie, Mycologie 39(2): 169–192. https://doi.org/10.7872/crym/v39.iss2.2018.169

Huelsenbeck JP, Ronquist F (2001) MRBAYES: Bayesian inference of phylogenetic trees. Bioinformatics 17: 754–755. https://doi.org/10.1093/bioinformatics/17.8.754

Jaklitsch WM, Voglmayr H (2014) Persistent hamathecial threads in the Nectriaceae, Hypocreales: *Thyronectria* revisited and reinstated. Persoonia 33: 182–211. https://doi.org/10.3114/sim.2011.68.02

Katoh K, Standley DM (2016) A simple method to control over-alignment in the MAFFT multiple sequence alignment program. Bioinformatics 32(13): 1933–1942. https://doi.org/10.1093/bioinformatics/btw108

Lechat C, Gardiennet A, Fournier J (2018) *Thyronectria abieticola* (Hypocreales), a new species from France on *Abies alba*. Ascomycete.org 10: 55–61. https://doi.org/10.25664/ART-228

Lombard L, van der Merwe NA, Groenewald JZ, Crous PW (2015) Generic concepts in Nectriaceae. Studies in Mycology 80: 189–245. https://doi.org/10.1016/j.simyco.2014.12.002

Maharachchikumbura SSN, Hyde KD, Jones EBG, Mckenzie EHC, Huang SK, Abdel-Wahab M, Daranagama DA, Dayarathne M, D'Souza MJ, Goonasekara ID, Hongsanan S, Jayawardena RS, Kirk PM, Konta S, Liu JK, Liu ZY, Norphanphoun C, Pang KL, Perera RH, Senanayake IC, Shang QJ, Shenoy BD, Xiao YP, Bahkali AH, Kang JC, Somrothipol S, Suetrong S, Wen TC, Xu JC (2015) Towards a natural classification and backbone tree for Sordariomycetes. Fungal Diversity 72(1): 199–301. https://doi.org/10.1007/s13225-015-0331-z

Miller MA, Schwartz T, Pickett BE, He S, Klem EB, Scheuermann RH, Passarotti M, Kaufman S, O'Leary MA (2015) A RESTful API for Access to Phylogenetic Tools via the CIPRES Science Gateway. Evolutionary Bioinformatics 11: 43–48. https://doi.org/10.4137/EBO.S21501

Miller MA, Pfeiffer W, Schwartz T (2010) Creating the CIPRES science gateway for inference of large phylogenetic trees. Gateway Computing Environments Workshop (GCE), 14 Nov. 2010, New Orleans, LA, 1–8. https://doi.org/10.1109/GCE.2010.5676129

Nylander JAA, Wilgenbusch JC, Warren DL, Swofford DL (2008) AWTY (are we there yet?): a system for graphical exploration of MCMC convergence in Bayesian phylogenetics. Bioinformatics 24: 581–583. https://doi.org/10.1093/bioinformatics/btm388

O'Donnell K, Cigelnik E (1997) Two divergent intragenomic rDNA ITS2 types within a monophyletic lineage of the fungus *Fusarium* are nonorthologous. Molecular Phylogenetics and Evolution 7: 103–116. https://doi.org/10.1006/mpev.1996.0376

Rambaut A, Drummond A (2010) FigTree v.1.3.1. Institute of Evolutionary Biology, University of Edinburgh, Edinburgh, UK.

Rayner RW (1970) A mycological colour chart. Commonwealth Mycological Institute, Kew.

Rehner SA (2001) Primers for elongation factor 1-a (EF1-a). http://www.nacse.org/yfaaberg/aftol/EF1primer.pdf

Rehner SA, Samuels GJ (1994) Taxonomy and phylogeny of *Gliocladium* analysed from nuclear large subunit ribosomal DNA sequences. Mycological Research 98: 625–634. https://doi.org/10.1016/S0953-7562(09)80409-7

Ronquist F, Huelsenbeck JP (2003) MrBayes 3: Bayesian phylogenetic inference under mixed models. Bioinformatics 19: 1572–1574. https://doi.org/10.1093/bioinformatics/btg180

Rossman AY (2000) Towards monophyletic genera in the holomorphic Hypocreales. Studies in Mycology 45: 27–34.

Rossman AY, Samuels GJ, Rogerson CT, Lowen R (1999) Genera of Bionectriaceae, Hypocreaceae and Nectriaceae (Hypocreales, Ascomycetes). Studies in Mycology 42: 1–248.

Rossman AY, Seifert KA, Samuels GJ, Minnis AM, Schroers HJ, Lombard L, Crous PW, Põldmaa K, Cannon PF, Summerbell RC, Geiser DM, Zhuang WY, Hirooka Y, Herrera C, Salgado-Salazar C, Chaverri P (2013) Genera of Bionectriaceae, Hypocreaceae and Nectriaceae (Hypocreales) proposed for acceptance and rejection. IMA Fungus 4: 41–51. https://doi.org/10.5598/imafungus.2013.04.01.05

Samuels GJ, Lu BS, Chaverri P, Candoussau F, Fournier J, Rossman AY (2009) *Cyanonectria*, a new genus for *Nectria cyanostoma* and its *Fusarium* anamorph. Mycological Progress 8: 49–58. https://doi.org/10.1007/s11557-008-0577-x

Stamatakis A (2014) RAxML version 8: a tool for phylogenetic analysis and post-analysis of large phylogenies. Bioinformatics 30: 1312–1313. https://doi.org/10.1093/bioinformatics/btu033

Tulasne LR, Tulasne C (1865) Selecta Fungorum Carpologia: Nectriei-Phacidiei-Pezizei, 3.

Vilgalys R, Hester M (1990) Rapid genetic identification and mapping of enzymatically amplified ribosomal DNA from several Cryptococcus species. Journal of Bacteriology 172: 4238–4246. https://doi.org/10.1128/jb.172.8.4238-4246.1990

Voglmayr H, Akulov OY, Jaklitsch WM (2016) Reassessment of *Allantonectria*, phylogenetic position of *Thyronectroidea*, and *Thyronectria caraganae* sp. nov. Mycological Progress 15: 921–937. https://doi.org/10.1007/s11557-016-1218-4

Wijayawardene NN, Hyde KD, Rajeshkumar KC, Hawksworth DL, Madrid H, Kirk PM, Braun U, Singh RV, Crous PW, Kukwa M, Lücking R, Kurtzman CP, Yurkov A, Haelewaters D, Aptroot A, Lumbsch HT, Timdal E, Ertz D, Etayo J, Phillips AJL, Groenewald JZ, Papizadeh M, Selbmann L, Dayarathne MC, Jones EBG, Suetrong S, Tian Q, Castaneda-Ruiz RF, Bahkali AH, Pang KL, Tanaka K, Dai DQ, Sakayaroj J, Hujslova M, Lombard L, Shenoy BD, Suija A, Maharachchikumbura SSN, Thambugala KM, Wanasinghe DN, Sharma BO, Gaikwad S, Zucconi L, Onofri S, Egidi E, Raja HA, Kodsueb R, Caceres MES, Perez-Ortega S, Fluiza PO, Monteiro JS, Vasilyeva LN, Shivas RG, Prieto M, Wedin M, Olariaga I, Lateef AA, Agrawal Y, Fazeli SAS, Amoozegar MA, Zhao GZ, Pfliegler WP, Sharma G, Oset M, Abdel-Wahab MA, Takamatsu S, Bensch K, de Silva NI, Kesel AD, Karunarathna A, Boonmee S, Pfister DH, Lu YZ, Luo ZL, Boonyuen N, Daranagama DA, Senanayake IC, Jayasiri SC, Samarakoon MC, Zeng XY, Doilom M, Quijada L, Rampadarth S, Heredia G, Dissanayake AJ, Jawardana RS, Perera RH, Tang LZ, Phukhamsakda C, Hernandez-Restrepo M, Ma X, Tibpromma S, Gusmao LFP, Weerahewa D, Karunarathna SC (2017) Notes for genera: Ascomycota. Fungal Diversity 86(1): 1–594. https://doi.org/10.1007/s13225-017-0386-0

White TJ, Bruns T, Lee S, Taylor J (1990) Amplification and direct sequencing of fungal ribosomal RNA genes for phylogenetics. PCR Protocols: A Guide to Methods and Applications 18: 315–322. https://doi.org/10.1016/B978-0-12-372180-8.50042-1

Yang Q, Du Z, Liang YM, Tian CM (2018) Molecular phylogeny of *Nectria* species associated with dieback and canker diseases in China, with a new species described. Phytotaxa 356 (3): 199–214. https://doi.org/10.11646/phytotaxa.356.3.2

Zeng ZQ, Zhuang WY (2016) Revision of the genus *Thyronectria* (Hypocreales) from China. Mycologia 108: 1130–1140. https://doi.org/10.3852/16-004

Zhang YJ, Zhang S, Liu XZ, Wen HA, Wang M (2010) A simple method of genomic DNA extraction suitable for analysis of bulk fungal strains. Letters in applied microbiology 51: 114–118. https://doi.org/10.1111/j.1472-765X.2010.02867.x

MycoKeys 56: 67–80 (2019)
doi: 10.3897/mycokeys.56.35554
http://mycokeys.pensoft.net

RESEARCH ARTICLE

A peer-reviewed open-access journal
MycoKeys
Launched to accelerate biodiversity research

Morphology and phylogeny reveal two novel *Coryneum* species from China

Ning Jiang[1], Hermann Voglmayr[2,3], Cheng-Ming Tian[1]

1 *The Key Laboratory for Silviculture and Conservation of the Ministry of Education, Beijing Forestry University, Beijing 100083, China* **2** *Institute of Forest Entomology, Forest Pathology and Forest Protection, Department of Forest and Soil Sciences, BOKU-University of Natural Resources and Life Sciences, Franz Schwackhöfer Haus, Peter-Jordan-Straße 82/I, 1190 Vienna, Austria* **3** *Division of Systematic and Evolutionary Botany, Department of Botany and Biodiversity Research, University of Vienna, Rennweg 14, A-1030 Vienna, Austria*

Corresponding author: *Cheng-Ming Tian* (chengmt@bjfu.edu.cn)

Academic editor: *N. Wijayawardene* | Received 20 April 2019 | Accepted 31 May 2019 | Published 10 July 2019

Citation: Jiang N, Voglmayr H, Tian C-M (2019) Morphology and phylogeny reveal two novel *Coryneum* species from China. MycoKeys 56: 67–80. https://doi.org/10.3897/mycokeys.56.35554

Abstract

Coryneum is currently the sole genus of Coryneaceae in Diaporthales, distinguished from other diaporthalean genera by transversely distoseptate brown conidia. However, *Coryneum* species are presently difficult to identify because of variability and overlap of morphological characters and the lack of sequence data for most described species. During fungal collection trips in China, 13 *Coryneum* isolates were obtained from cankered branches of *Ilex* and *Quercus*. Morphological and phylogenetic analyses (ITS, LSU, *TEF1-a* and *RPB2*) revealed that these strains belong to two new species (*viz. Coryneum ilicis* **sp. nov.** and *C. songshanense* **sp. nov.**), and three known species, *C. gigasporum*, *C. sinense*, and *C. suttonii*. *Coryneum ilicis* has larger conidia and more distosepta than most *Coryneum* species. *Coryneum songshanense* was similar to *C. sinense* from the same host genus, *Quercus*, in conidial length, but distinct in conidial width and by molecular data.

Keywords

Coryneaceae, *Diaporthales*, systematics, taxonomy

Introduction

The genus *Coryneum* Nees is currently the only accepted genus in Coryneaceae and it forms a distinct phylogenetic lineage in Diaporthales (Senanayake et al. 2017, 2018, Voglmayr et al. 2017, Fan et al. 2018a, Jiang et al. 2018, Senwanna et al. 2018, Wijayawardene et al. 2017, 2018). The genus *Coryneum* was introduced based on the asexual

morph, with *C. umbonatum* Nees as the type species (Nees von Esenbeck 1816), and the sexual morph *Pseudovalsa* Ces. & De Not. was introduced later, based on *P. lanciformis* (Fr.) Ces. & De Not. (Cesati & De Notaris 1863). *Coryneum* was recommended to be adopted due to priority and the need of fewer new combinations (Rossman et al. 2015).

Most *Coryneum* species were considered as phytopathogens, which were discovered from cankers and dieback of shoots and twigs (Wijayawardene et al. 2016, Senanayake et al. 2017, Jiang et al. 2018). However, diseases are commonly mild and only rarely cause serious symptoms in the hosts. Additionally, pathogenicity tests have not yet been conducted.

Coryneum species are generally considered highly host-specific, and 28 species and a variety were accepted in this genus before this study (Sutton 1975, 1980, Wijayawardene et al. 2016, Jiang et al. 2018, Senwanna et al. 2018). *Coryneum terrophilum* was the only species isolated from soil, and the others were reported from dead branches (Table 1). Fagales species are the major hosts of *Coryneum* species, and host trees from other orders are also hardwoods with rough barks (Table 1).

Molecular phylogenies based on multi-gene loci including the internal transcribed spacer (ITS) and the large subunit (LSU) regions of the nuclear rDNA, translation elongation factor-1α (*TEF1-a*) and the second largest subunit of the RNA polymerase II (*RPB2*) have been widely used to infer species delimitation within many genera in Diaporthales (Voglmayr et al 2012, 2017, 2019, Voglmayr and Jaklitsch 2014, Fan et al. 2018b, Jiang et al. 2019), and are particularly important in speciose genera like *Coryneum*. Hence, DNA extraction from known species and fresh collections from the potential hosts will greatly improve the elucidation of species concept and circumscription in *Coryneum*. Thus, the main objectives of the present study were to identify *Coryneum* taxa based on morphology and phylogenetic evidence, and to analyse the relationships between *Coryneum* species and host genera.

Materials and methods

Sample collection and isolation

Sample collection trips were conducted in Beijing, Hebei and Shaanxi Provinces of China during June to October in 2017 and 2018, aiming to collect fresh specimens with *Coryneum*–like taxa. Fagales plants were the main hosts and other hardwoods with rough barks were also investigated. Healthy branches and twigs were covered by green leaves, hence the dying and dead materials were conspicuous during our investigations. Asexual fruiting bodies were easily discovered as black spots on the host barks. Tree tissues with fruiting bodies were cut into small pieces, packed in paper bags and taken to the laboratory for further studies. Isolations were obtained by removing the ascospores or conidial masses from the fruiting bodies on to clean potato dextrose agar (PDA) plates, which were incubated at 25 °C until spores germinated. Single germinating spores were transferred on to new PDA plates, which were kept at 25 °C in the dark. Specimens were deposited at the Museum of the Beijing Forestry University (BJFC) and axenic cultures are maintained at the China Forestry Culture Collection Centre (CFCC).

Table 1. Hosts, conidial sizes, and numbers of distosepta of currently accepted *Coryneum* species.

Species	Host genus	Host family	Host order	Conidial size (µm)	No. of distosepta	References
C. arausiacum	*Quercus*	Fagaceae	Fagales	42–56 × 13–16	4–5	Senanayake et al. (2017)
C. betulinum	*Betula*	Betulaceae	Fagales	31–36 × 14–17	4–5	Sutton (1975)
C. calophylli	*Calophyllum*	Guttiferae	Parietales	38–48 × 12.5–14.5	5–6	Sutton (1975)
C. carpinicola	*Carpinus*	Betulaceae	Fagales	50–68 × 8–11	7–11	Sutton (1975)
C. castaneicola	*Castanea*	Fagaceae	Fagales	56–80 × 9.5–13	5–8	Sutton (1975)
C. cesatii	*Aesculus*	Hippocastanaceae	Sapindales	80–90 × 13–15	6–7	Sutton (1975)
C. clusiae	*Clusia*	Clusiaceae	Malpighiales	30–40 × 20–30	3–5	Sutton (1975)
C. compactum	*Ulmus*	Ulmaceae	Urticales	40–58 × 15–21	4–6	Sutton (1975)
C. depressum	*Quercus*	Fagaceae	Fagales	44–53 × 19–23	4–6	Sutton (1975)
C. elevatum	*Quercus*	Fagaceae	Fagales	56–69 × 24–28	5–7	Sutton (1975)
C. gigasporum	*Castanea*	Fagaceae	Fagales	88–117 × 18–23	7–9	Jiang et al. (2018)
C. gregoryi	*Eucalyptus*	Myrtaceae	Myrtales	32.5–43 × 12–16	5–9	Sutton and Sharma (1983)
C. heveanum	*Hevea*	Euphorbiaceae	Malpighiales	40–68 × 14–20	4–6	Senwanna et al. (2018)
C. ilicis	*Ilex*	Aquifoliaceae	Sapindales	82–105 × 9.5–12.5	10–11	This study
C. japonicum	*Quercus*	Fagaceae	Fagales	45–60 × 11–12	5–7	Sutton (1975)
C. lanciforme	*Betula*	Betulaceae	Fagales	45–53 × 16–18	4–6	Sutton (1975)
C. megaspermum	*Quercus*	Fagaceae	Fagales	73–97 × 13–16	7–11	Sutton (1980)
C. megaspermum var. *cylindricum*	*Quercus*	Fagaceae	Fagales	100–125 × 10–13	7–8	Sutton (1975)
C. modonium	*Castanea*	Fagaceae	Fagales	50–71 × 14–19	5–8	Sutton (1975)
C. neesii	*Quercus*	Fagaceae	Fagales	68–82 × 18–22	6–8	Sutton (1975)
C. pruni	*Prunus*	Rosaceae	Rosales	14–23 × 5.5–9	4–5	Wijayawardene et al. (2016)
C. psidii	*Psidium*	Myrtaceae	Myrtales	25–40 × 14–17	5–6	Sutton (1975)
C. pyricola	*Pyrus*	Rosaceae	Rosales	61–70 × 24–32	5–7	Sutton (1975)
C. quercinum	*Quercus*	Fagaceae	Fagales	45–60 × 14–16	6–7	Muthumary and Sutton (1986)
C. sinense	*Quercus*	Fagaceae	Fagales	50–76 × 13–17	5–7	Jiang et al. (2018)
C. songshanense	*Quercus*	Fagaceae	Fagales	51–76 × 9–11.5	5–7	This study
C. stromatoideum	*Tsuga*	Pinaceae	Pinales	105–180 × 16–20	9–17	Sutton (1975)
C. suttonii	*Castanea*	Fagaceae	Fagales	60–76 × 10–14.5	4–5	Jiang et al. (2018)
C. sydowianum	*Alnus*	Betulaceae	Fagales	50–58 × 14–17	5–6	Sutton (1975)
C. terrophilum	NA	NA	NA	25–55 × 15–24	3–7	Sutton and Sharma (1983)
C. umbonatum	*Quercus*	Fagaceae	Fagales	57–72 × 13–16	5–7	Sutton (1975)

Morphological analysis

Species identification was based on the morphological characters of the sexual and asexual morphs produced on natural substrates. Cross-sections were prepared manually using a double-edged blade under a Leica stereomicroscope (M205 FA). Photomicrographs were captured with a Nikon Eclipse 80i microscope equipped with a Nikon digital sight DS-Ri2 high-definition colour camera, using differential interference contrast (DIC) illumination and the Nikon software, NIS-Elements D Package 3.00. Measurements of ascospores and conidia are reported as the maximum and minimum in parentheses and the range representing the mean ± standard deviation of the number of measurements is given in parentheses (Voglmayr et al. 2017). Cultural characteristics of isolates incubated on MEA in the dark at 25 °C were recorded.

Recognition and identification of *Coryneum* species were based on fruiting bodies formed on tree bark, supplied by conidiomata produced on PDA plates. Ascomata and conidiomata from tree bark were sectioned by hand using a double-edged blade,

and conidiomata from PDA plates were picked using a needle, which were observed under a dissecting microscope. At least 10 conidiomata/ascomata, 10 asci, and 50 conidia/ascospores were measured to calculate the mean sizes and standard deviation. Microscopy photographs were captured with a Nikon Eclipse 80i compound microscope equipped with a Nikon digital sight DS-Ri2 high definition colour camera, using differential interference contrast illumination.

DNA extraction, PCR amplification and sequencing

Genomic DNA was extracted from colonies grown on cellophane-covered PDA plates using a modified CTAB method (Doyle and Doyle 1990). PCR amplifications were performed in a DNA Engine Peltier Thermal Cycler (PTC-200; Bio-Rad Laboratories, Hercules, CA, USA). The primer sets ITS1/ITS4 (White et al. 1990) were used to amplify the ITS region. The primer pair LR0R/LR5 (Vilgalys and Hester 1990) was used to amplify the LSU region. The primer pairs EF1-688F/EF1-986R or EF1-728F/TEF1-LLErev (Carbone and Kohn 1999, Jaklitsch et al. 2006, Alves et al. 2008) were used to amplify *TEF1-a* gene. The primer pair dRPB2-5f/dRPB2-7r (Voglmayr et al. 2016) was used to amplify the *RPB2* gene. The polymerase chain reaction (PCR) assay was conducted as described by Fan et al. (2018a). PCR amplification products were assayed via electrophoresis in 2 % agarose gels. DNA sequencing was performed using an ABI PRISM® 3730XL DNA Analyzer with a BigDye Terminater Kit v.3.1 (Invitrogen, USA) at the Shanghai Invitrogen Biological Technology Company Limited (Beijing, China). Novel sequences generated in the current study were deposited in GenBank (Table 2).

Phylogenetic analyses

Sequences generated from the above primers of the different genomic regions (ITS, LSU, *TEF1-a* and *RPB2*) were analysed in comparison to known species, *Stilbospora macrosperma* (CBS 115073) and *Stegonsporium pyriforme* (CBS 120522) were used as the outgroup taxa (Jiang et al. 2018). All sequences were aligned using MAFFT v. 6 (Katoh and Toh 2010) and edited manually using MEGA v. 6 (Tamura et al. 2013). Phylogenetic analyses were performed using PAUP v. 4.0b10 for maximum parsimony (MP) analysis (Swofford 2003), and PhyML v. 3.0 for Maximum Likelihood (ML) analysis (Guindon et al. 2010).

A partition homogeneity test with heuristic search and 1000 replicates was performed using PAUP v. 4.0b10 to assess incongruence among the ITS, LSU, *TEF1-a*, and *RPB2* sequence datasets in reconstructing phylogenetic trees. MP analysis was run using a heuristic search option of 1000 search replicates with random-addition of sequences with a tree bisection and reconnection (TBR) algorithm; branches of zero length were collapsed (collapse = minbrlen), and all equally most parsimonious trees were saved. Other calculated parsimony scores were tree length (TL), consistency index (CI), retention index (RI), and rescaled consistency (RC). ML analysis was performed

Table 2. Strains used in the phylogenetic tree and their culture accession and GenBank numbers. Strains from this study are in bold.

Species	Strains	GenBank numbers			
		ITS	LSU	TEF1-*α*	RPB2
Coryneum castaneicola	CFCC 52315	MH683551	MH683559	MH685731	MH685723
Coryneum castaneicola	CFCC 52316	MH683552	MH683560	MH685732	MH685724
Coryneum depressum	D202	MH674330	MH674330	MH674338	MH674334
Coryneum heveanum	MFLUCC 17-0369	MH778707	MH778703	MH780881	NA
Coryneum heveanum	MFLUCC 17-0376	MH778708	MH778704	NA	NA
Coryneum gigasporum	CFCC 52319	MH683557	MH683565	MH685737	MH685729
Coryneum gigasporum	CFCC 52320	MH683558	MH683566	MH685738	MH685730
Coryneum gigasporum	**G14**	**MK799957**	**MK799944**	**MK799830**	**MK799820**
Coryneum gigasporum	**G15**	**MK799958**	**MK799945**	**MK799831**	**MK799821**
Coryneum ilicis	**CFCC 52994**	**MK799948**	**MK799935**	**NA**	**NA**
Coryneum ilicis	**CFCC 52995**	**MK799949**	**MK799936**	**NA**	**NA**
Coryneum ilicis	**CFCC 52996**	**MK799950**	**MK799937**	**NA**	**NA**
Coryneum lanciforme	D215	MH674332	MH674332	MH674340	MH674336
Coryneum modonium	D203	MH674331	MH674331	MH674339	MH674335
Coryneum modonium	CBS 130.25	MH854812	MH866313	NA	NA
Coryneum sinense	CFCC 52452	MH683553	MH683561	MH685733	MH685725
Coryneum sinense	CFCC 52453	MH683554	MH683562	MH685734	MH685726
Coryneum sinense	**X20**	**MK799952**	**MK799939**	**MK799825**	**MK799815**
Coryneum sinense	**X23**	**MK799953**	**MK799940**	**MK799826**	**MK799816**
Coryneum sinense	**X60**	**MK799951**	**MK799938**	**MK799824**	**MK799814**
Coryneum songshanense	**CFCC 52997**	**MK799946**	**MK799933**	**MK799822**	**MK799812**
Coryneum songshanense	**CFCC 52998**	**MK799947**	**MK799934**	**MK799823**	**MK799813**
Coryneum suttonii	CFCC 52317	MH683555	MH683563	MH685735	MH685727
Coryneum suttonii	CFCC 52318	MH683556	MH683564	MH685736	MH685728
Coryneum suttonii	**Z15-1**	**MK799954**	**MK799941**	**MK799827**	**MK799817**
Coryneum suttonii	**Z17**	**MK799955**	**MK799942**	**MK799828**	**MK799818**
Coryneum suttonii	**Z86**	**MK799956**	**MK799943**	**MK799829**	**MK799819**
Coryneum umbonatum	D201	MH674329	MH674329	MH674337	MH674333

using a GTR site substitution model, including a gamma-distributed rate heterogeneity and a proportion of invariant sites (Guindon et al. 2010). The branch support was evaluated using a bootstrapping method of 1000 bootstrap replicates (Hillis and Bull 1993). The MP bootstrap analyses were done with the same settings as for the heuristic search, but with 10 rounds of heuristic search during each bootstrap replicate. Phylograms were shown using FigTree v. 1.4.3 (Rambaut 2016).

Results

Phylogenetic analyses

The alignment based on the combined sequence dataset (ITS, LSU, *TEF1-a*, and *RPB2*) included 30 ingroup taxa and two outgroup taxa (*Stilbospora macrosperma* and *Stegonsporium pyriforme*), comprising 3544 characters in the aligned matrix. Of these, 2570 characters were constant, 267 variable characters were parsimony-uninformative and 706 characters were parsimony informative. The partition homogeneity test resulted in an insignificant value (level 95%), indicating that ITS, LSU, *TEF1-a* and

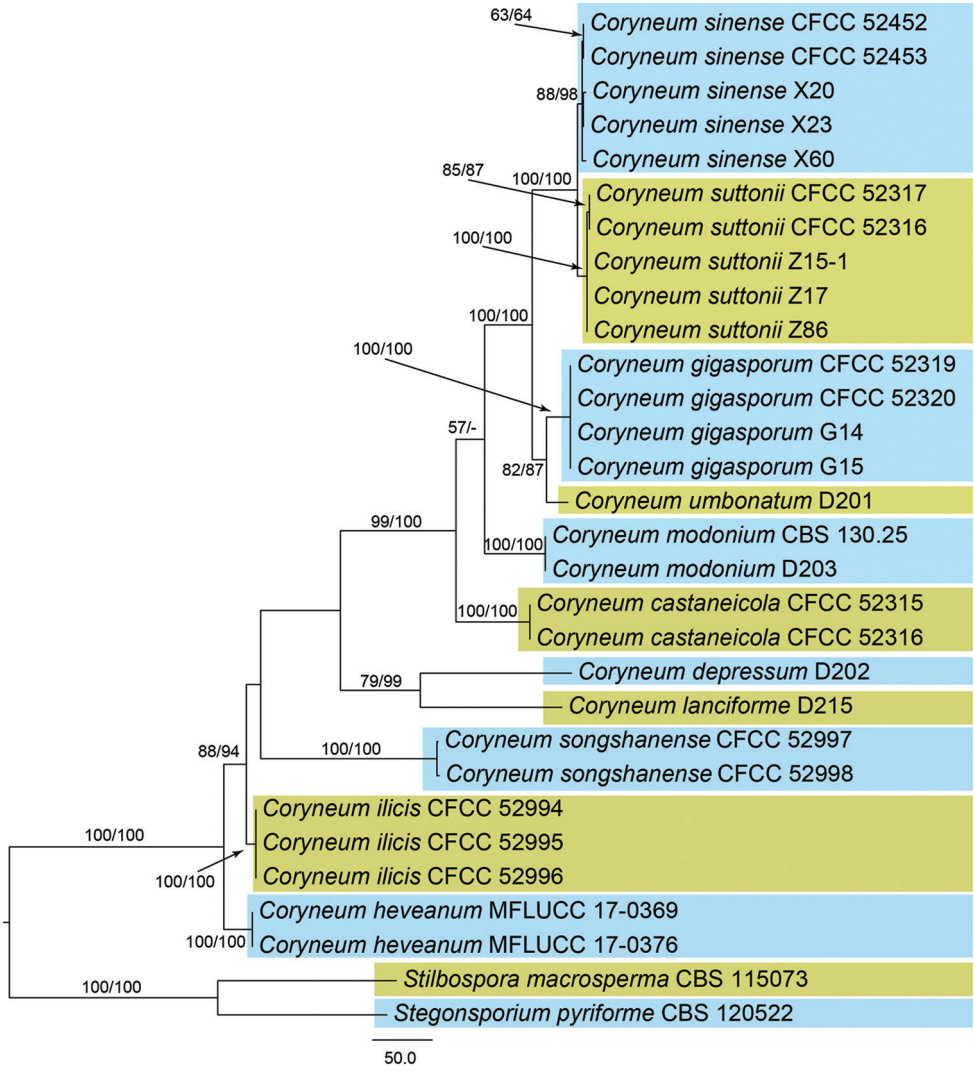

Figure 1. Phylogenetic tree based on an MP analysis of a combined DNA dataset of ITS, LSU, *TEF1-a* and *RPB2* gene sequences for the species of *Coryneum*. Bootstrap values ≥ 50 % for MP/ML analyses are presented at the branches. Scale bar = 50 nucleotide substitutions.

RPB2 sequence dataset could be combined. The MP analysis resulted in 2 equally most parsimonious trees; the first tree (TL = 1624, CI = 0.784, RI = 0.822, RC = 0.645) is shown in Fig. 1. The two MP trees were identical, except for an interchanged position of *C. ilicis* and *C. songshanense* (not shown). Tree topology of the best tree revealed by the ML analyses was identical to that of the MP tree shown. The phylogram based on the four gene sequences showed that the accessions here studied represented 2 new and 3 known species in *Coryneum* (Fig. 1).

Taxonomy

Coryneum ilicis **C.M. Tian & N. Jiang, sp. nov.**
MycoBank: MB830201
Figure 2

Diagnosis. *Coryneum ilicis* is characterised by its host, *Ilex pernyi*, and large conidia with 10–11 distosepta.

Holotype. CHINA. Shaanxi Province: Zhashui County, on branches of *Ilex pernyi*, 12 August 2017, N. Jiang (holotype: BJFC-S1720; ex-type culture from ascospore: CFCC 52994; living culture from conidium: CFCC 52996).

Etymology. Named after the host genus on which it was collected, *Ilex*.

Description. Associated with canker on branches of *Ilex pernyi*. ***Sexual morph:*** Pseudostromata 0.5–1.5 mm diam., typically distinct, circular, without perithecial bumps, containing 1 or 2 perithecia embedded in a well-developed entostroma. Central column and entostroma grey. Ostioles inconspicuous and often invisible at the surface of the ectostromatic disc. Perithecia (350–)500–700(–850) µm diam. (n = 20), globular, somewhat flattened at the base. Asci 110–155 × 13–20 µm, 8-spored, unitunicate, clavate, shortly pedicellate, apically rounded, with a conspicuous apical ring. Ascospores (26.2–)29.7–35.5(–36.2) × (11.0–)11.8–14.3(–15.2) µm, l/w = (1.9–)2.2–2.9(–3.2) (n = 50), 1-seriate, fusiform, ends pointed, uniseptate, constricted at the septa, hyaline, guttulate, smooth-walled. ***Asexual morph:*** Conidiomata acervular, 0.2–1 mm wide, 0.2–1.2 mm high, solitary, erumpent through the outer periderm layers of the host, scattered, surface tissues above slightly domed. Conidiophores 40–85 µm long, 3–7 µm wide, branched, cylindrical, septate, hyaline at the apex, pale brown at the base. Conidiogenous cells holoblastic, integrated, indeterminate, cylindrical, expanding towards the apices, pale brown, smooth, with 0–1 percurrent extensions. Conidia (82–)87–95(–105) × (9.5–)10.5–11.5(–12.5) µm, l/w = (7.4–)7.7–9.1(–9.3) (n = 50), variable in shape, curved, broadly fusiform to fusiform, cylindrical or clavate, dark brown, smooth-walled, 10–11-distoseptate, apical cell with a hyaline tip, truncate and black at the base.

Culture characters. On PDA at 25 °C, colonies growing slowly and unevenly, reaching 70 mm diam. within 25 d, gradually becoming brownish dark grey in colour with scant cottony aerial mycelium, asexual morphs developed after 35 d.

Additional specimen examined. CHINA. Shaanxi Province: Zhashui County, on branches of *Ilex pernyi*, 12 August 2017, N. Jiang (isotype: BJFC-S1721; living culture: CFCC 52995).

Notes. *Coryneum ilicis* is the sole species known from the host genus *Ilex*; it can be easily recognised by host association and phylogeny (Fig. 1). Morphologically, conidia of *Coryneum ilicis* are larger and have more distosepta than in most of the other species (Table 1).

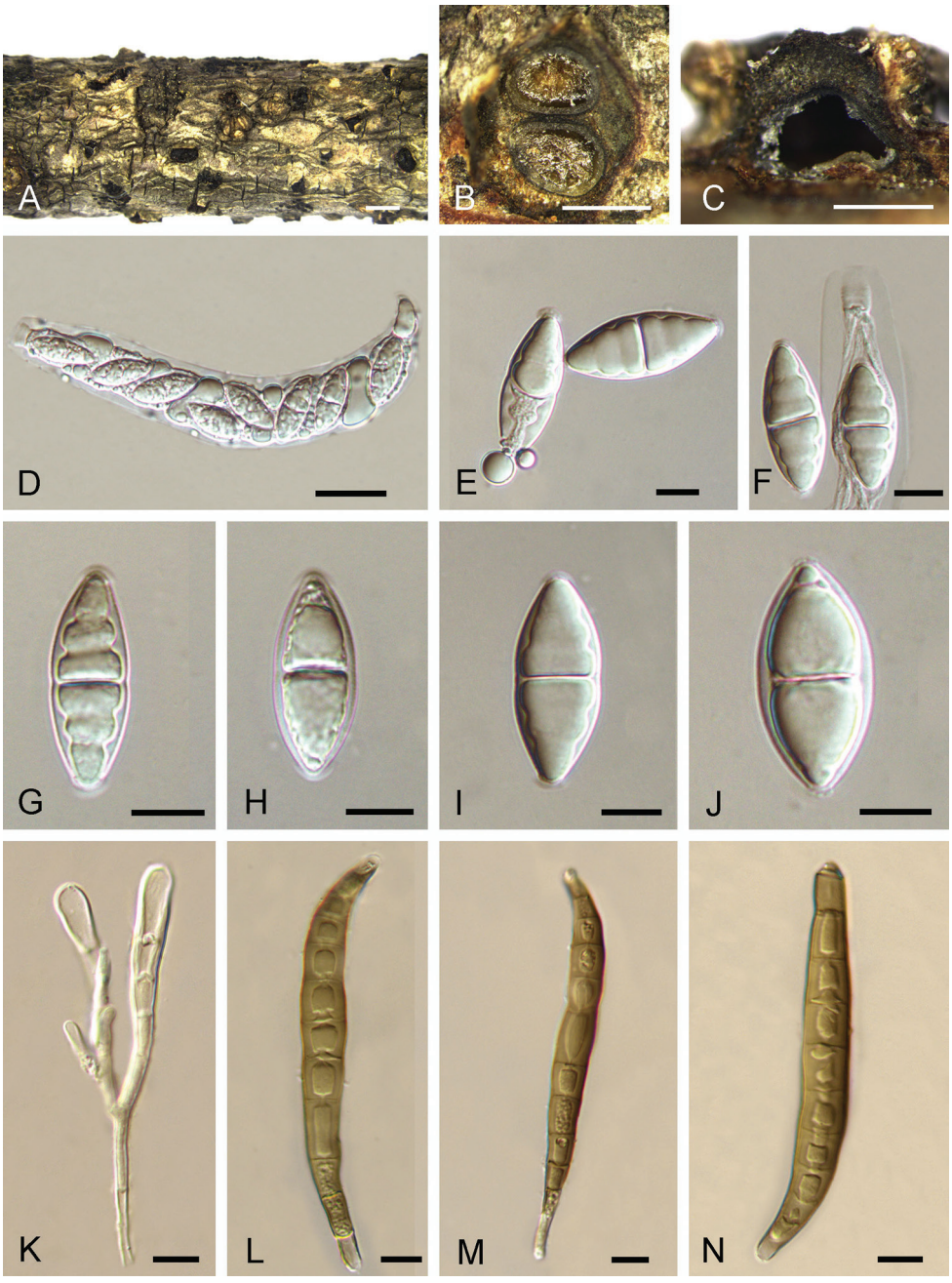

Figure 2. *Coryneum ilex* from *Ilex pernyi* (BJFC-S1720, holotype) **A** Fruiting bodies on natural substrate in surface view **B** pseudostroma in transverse section, showing perithecia and gray entostroma **C** longitudinal sections through pseudostromata **D** ascus **E–J** ascospores **K** conidiophores **L–N** conidia. Scale bars: 1 mm (**A**); 0.5 mm (**B, C**); 20 µm (**D**); 10 µm (**E–N**).

Coryneum songshanense **C.M. Tian & N. Jiang, sp. nov.**
MycoBank: MB830202
Figure 3

Diagnosis. *Coryneum songshanense* can be distinguished from the morphologically similar *C. sinense* by its narrower conidia.

Holotype. CHINA. Beijing City: Songshan Mountain, on dead twigs of *Quercus dentata*, 15 June 2018, N. Jiang & C.M. Tian (holotype: BJFC-S1722; ex-type culture from ascospore: CFCC 52997).

Etymology. Named after the mountain on which it was collected, Songshan Mountain.

Description. Associated with canker on twigs of *Quercus dentata*. ***Sexual morph:*** Pseudostromata 0.3–1 mm diam., typically distinct, circular, without perithecial bumps, containing up to 6 perithecia embedded in a well-developed entostroma. Ectostromatic disc distinct, circular, black, 0.3–0.5 mm diam. Central column and entostroma grey. Ostioles inconspicuous and often invisible at the surface of the ectostromatic disc. Perithecia (150–)200–450(–550) µm diam. (n = 20), globular, somewhat flattened at the base with black short neck. Asci 75–145 × 17–23 µm, 8-spored, unitunicate, clavate, shortly pedicellate, apically rounded, with an inconspicuous apical ring. Ascospores (24.1–)25.5–35.4(–38.2) × (7.5–)7.9–9.8(–10.6) µm, l/w = (3.0–)3.3–3.8(–4.2) (n = 50), 2-seriate, fusiform, ends pointed, uniseptate or aseptate, not constricted at the septa, hyaline, guttulate, smooth-walled. ***Asexual morph:*** Conidiomata acervular, 0.2–0.6 mm wide, 0.2–0.5 mm high, solitary, erumpent through the outer periderm layers of the host, scattered, surface tissues above slightly domed. Conidiophores 15–35 µm long, 4–7 µm wide, unbranched, cylindrical, septate, hyaline at the apex, pale brown at the base. Conidiogenous cells holoblastic, integrated, indeterminate, cylindrical, expanding towards the apices, pale brown, smooth, with 0–1 percurrent extensions. Conidia (51–)56–67(–76) × (9–)10–11(–11.5) µm, l/w = (5.2–)5.5–6.9(–8.1) (n = 50), variable in shape, curved, broadly fusiform to fusiform, cylindrical or clavate, dark brown, smooth-walled, 5–7-distoseptate, apical cell with a hyaline tip, truncate and black at the base.

Culture characters. On PDA at 25 °C, colonies growing slowly and unevenly, reaching 70 mm diam. within 30 d, gradually becoming brownish dark grey in colour with scant cottony aerial mycelium, asexual morphs developed after 40 d.

Additional specimen examined. CHINA. Beijing City: Songshan Mountain, on dead twigs of *Quercus dentata*, 15 June 2018, N. Jiang & C.M. Tian (isotype: BJFC-S1723; living culture from conidium: CFCC 52998).

Notes. So far, ten species and one variety have been described from *Quercus* branches, and they can be distinguished by conidial characteristics (Muthumary and Sutton 1986, Jiang et al. 2018, Table 1). *Coryneum songshanense* and *C. sinense* can be distinguished from *C. arausiacum*, *C. depressum*, *C. elevatum*, *C. japonicum*, *C. megaspermum*, *C. megaspermum* var. *cylindricum*, *C. neesii*, *C. umbonatum*, and *C. quercinum* by unbranched conidiophores (Sutton 1975, Muthumary and Sutton 1986, Jiang

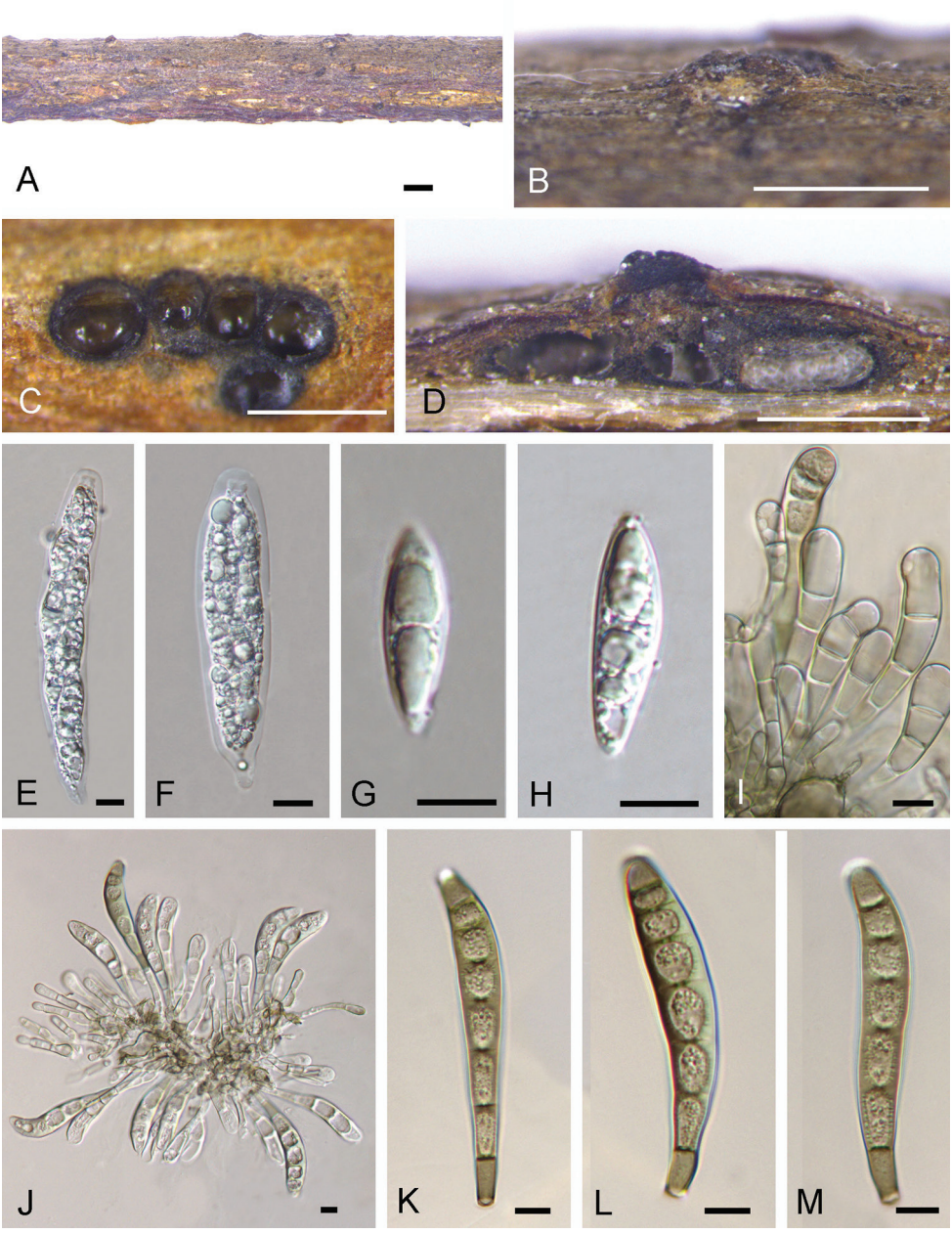

Figure 3. *Coryneum songshanense* from *Quercus dentata* (BJFC-S1722, holotype) **A, B** Fruiting bodies on natural substrate in surface view **C** pseudostroma in transverse section, showing perithecia and gray entostroma **D** longitudinal sections through pseudostromata **E, F** immature asci **G, H** immaure Ascospores **I, J** conidiophores **K–M** conidia. Scale bars: 1 mm (**A, B**); 0.5 mm (**C, D**); 10 μm (**E–M**).

et al. 2018). *Coryneum songshanense* is obviously distinguished from *C. sinense* in narrower conidia (9–11.5 µm in *Coryneum songshanense* vs. 13–17 µm in *C. sinense*) and phylogeny (Fig. 1).

Discussion

In this study, fresh *Coryneum* specimens were collected in China and identified based on combined morphological amd molecular data. Additional accessions of three recently described *Coryneum* species, *C. gigasporum*, *C. sinense*, and *C. suttonii* (Jiang et al. 2018), were identified, with matching conidial characteristics and sequences (Fig. 1). The new species *C. ilicis* was discovered on *Ilex pernyi* (Aquifoliaceae, Sapindales), which represents a new host family and genus for *Coryneum*. *Coryneum cesatii* was reported from the same host order, Sapindales, on branches of *Aesculus* (Hippocastanaceae) (Sutton 1975). The second new species, *Coryneum songshanense*, was discovered on dead twigs of *Quercus dentata* (Fagaceae, Fagales). Host species belonging to Fagales show higher diversity of *Coryneum* species (Table 1), and it is likely that additional taxa will be discovered by molecular data, considering that in many regions suitable hosts have not yet been adequately studied.

However, most of the *Coryneum* species are lacking DNA sequences, thus species identification based on DNA sequence analyses is presently difficult. Hence, polyphasic approach, i.e. incorporating morphological characters (such as conidial sizes and numbers of distosepta), as well as host associations are important for species identification (Sutton 1975, 1980, Jiang et al. 2018). However, host identifications may be incorrect and many geographical areas remain insufficiently studied. In addition, the morphological characters often significantly overlap between species, which makes identifications solely by morphology challenging. Hence, studies based on the types of already described species and new collections from potential hosts are important to achieve a reliable species classification and circumscription within *Coryneum*.

Acknowledgements

This study was financed by the National Natural Science Foundation of China (Project No.: 31670647) and the Short-term International Student Program for Postgraduates of Forestry First-Class Discipline (2019XKJS0501). Financial support from the Austrian Science Fund (FWF; project P27645-B16) to H. Voglmayr is gratefully acknowledged. We are grateful to Chungen Piao and Minwei Guo (China Forestry Culture Collection Center (CFCC), Chinese Academy of Forestry, Beijing) for support with strain preservation during this study.

References

Alves A, Crous PW, Correia A, Phillips AJL (2008) Morphological and molecular data reveal cryptic speciation in *Lasiodiplodia theobromae*. Fungal Diversity 28: 1–13.

Carbone I, Kohn LM (1999) A method for designing primer sets for speciation studies in filamentous ascomycetes. Mycologia 91: 553–556. https://doi.org/10.2307/3761358

Cesati V, De Notaris G (1863) Schema di classificazione degle sferiacei italici aschigeri piu' o meno appartenenti al genere *Sphaeria* nell'antico significato attribuitoglide Persono. Commentario della Società Crittogamologica Italiana 1: 177–420.

Doyle JJ, Doyle JL (1990) Isolation of plant DNA from fresh tissue. Focus 12: 13–15. https://doi.org/10.2307/2419362

Fan XL, Bezerra JD, Tian CM, Crous PW (2018a) Families and genera of diaporthalean fungi associated with canker and dieback of tree hosts. Persoonia 40: 119–134. https://doi.org/10.3767/persoonia.2018.40.05

Fan XL, Du Z, Bezerra JD, Tian CM (2018b) Taxonomic circumscription of melanconis-like fungi causing canker disease in China. Mycokeys 42: 89–124. https://doi.org/10.3897/mycokeys.42.29634

Guindon S, Dufayard JF, Lefort V, Anisimova M, Hordijk W, Gascuel O (2010) New algorithms and methods to estimate maximum-likelihood phylogenies: assessing the performance of PhyML 3.0. Systematic Biology 59: 307–321. https://doi.org/10.1093/sysbio/syq010

Hillis DM, Bull JJ (1993) An empirical test of bootstrapping as a method for assessing confidence in phylogenetic analysis. Systematic Biology 42: 182–192. https://doi.org/10.1093/sysbio/42.2.182

Jaklitsch WM, Komon M, Kubicek CP, Druzhinina IS (2006) *Hypocrea voglmayrii* sp. nov. from the Austrian Alps represents a new phylogenetic clade in *Hypocrea*/*Trichoderma*. Mycologia 97: 1365–1378. https://doi.org/10.1080/15572536.2006.11832743

Jiang N, Fan XL, Crous PW, Tian CM (2019) Species of *Dendrostoma* (Erythrogloeaceae, Diaporthales) associated with chestnut and oak canker diseases in China. Mycokeys 48: 67–96. https://doi.org/10.3897/mycokeys.48.31715

Jiang N, Voglmayr H, Tian CM (2018) New species and records of *Coryneum* from China. Mycologia 110: 1172–1188. https://doi.org/10.1080/00275514.2018.1516969

Katoh K, Toh H (2010) Parallelization of the MAFFT multiple sequence alignment program. Bioinformatics 26: 1899–1900. https://doi.org/10.1093/bioinformatics/btq224

Muthumary J, Sutton BC (1986) *Coryneum quercinum* sp. nov. on *Quercus alba* from India. Transactions of the British Mycological Society 86: 512–515. https://doi.org/10.1016/S0007-1536(86)80204-2

Nees von Esenbeck CG (1816) Das System der Pilze und Schwämme. Stahelsche Buchhandlung, Würzburg, 334 pp. https://doi.org/10.5962/bhl.title.110007

Rambaut A (2016) FigTree, version 1.4.3. University of Edinburgh, Edinburgh.

Rossman AY, Adams GC, Cannon PF, Castlebury LA, Crous PW, Gryzenhout M, Jaklitsch WM, Mejia LC, Stoykov D, Udayanga D, Voglmayr H, Walker DM (2015) Recommendations of generic names in Diaporthales competing for protection or use. IMA Fungus 6: 145–154. https://doi.org/10.5598/imafungus.2015.06.01.09

Senanayake IC, Crous PW, Groenewald JZ, Maharachchikumbura SSN, Jeewon R, Phillips AJL, Bhat JD, Perera RH, Li QR, Li WJ, Tangthirasunun N, Norphanphoun C, Karunarathna SC, Camporesi E, Manawasighe IS, Al-Sadi AM, Hyde KD (2017) Families of Diaporthales based on morphological and phylogenetic evidence. Studies in Mycology 86: 217–296. https://doi.org/10.1016/j.simyco.2017.07.003

Senanayake IC, Jeewon R, Chomnunti P, Wanasinghe DN, Norphanphoun C, Karunarathna A, Pem D, Perera RH, Camporesi E, McKenzie EHC, Hyde KD, Karunarathna SC (2018) Taxonomic circumscription of Diaporthales based on multigene phylogeny and morphology. Fungal Diversity 93: 241–443. https://doi.org/10.1007/s13225-018-0410-z

Senwanna C, Hyde KD, Phookamsak R, Jones EG, Cheewangkoon R (2018) *Coryneum heveanum* sp. nov. (Coryneaceae, Diaporthales) on twigs of Para rubber in Thailand. Mycokeys 43: 75–90. https://doi.org/10.3897/mycokeys.43.29365

Sutton BC (1975) Coelomycetes V. *Coryneum*. Mycological Papers 138: 1–224.

Sutton BC (1980) The Coelomycetes: Fungi Imperfect With Pycnidia, Acervuli and Stromata. Commonwealth Mycological Institute, Kew.

Swofford DL (2003) PAUP*: Phylogenetic Analyses Using Parsimony, * and Other Methods, Version 4.0b10. Sinauer Associates, Sunderland.

Tamura K, Stecher G, Peterson D, Filipski A, Kumar S (2013) MEGA6: Molecular Evolutionary Genetics Analysis version 6.0. Molecular Biology and Evolution 30: 2725–2729. https://doi.org/10.1093/molbev/mst197

Voglmayr H, Akulov OY, Jaklitsch WM (2016) Reassessment of *Allantonectria*, phylogenetic position of *Thyronectroidea*, and *Thyronectria caraganae* sp. nov. Mycological Progress 15: 921–937. https://doi.org/10.1007/s11557-016-1218-4

Voglmayr H, Castlebury LA, Jaklitsch WM (2017) *Juglanconis* gen. nov. on Juglandaceae, and the new family Juglanconidaceae (Diaporthales). Persoonia 38: 136–155. https://doi.org/10.3767/003158517X694768

Voglmayr H, Jaklitsch WM (2014) Stilbosporaceae resurrected: generic reclassification and speciation. Persoonia 33: 61–82. https://doi.org/10.3767/003158514X684212

Voglmayr H, Jaklitsch WM, Mohammadi H, Chakusary MK (2019) The genus *Juglanconis* (Diaporthales) on *Pterocarya*. Mycological Progress 18: 425–437. https://doi.org/10.1007/s11557-018-01464-0

Voglmayr H, Rossman AY, Castlebury LA, Jaklitsch W (2012) Multigene phylogeny and taxonomy of the genus *Melanconiella* (Diaporthales). Fungal Diversity 57: 1–44. https://doi.org/10.1007/s13225-012-0175-8

Vilgalys R, Hester M (1990) Rapid genetic identification and mapping of enzymatically amplified ribosomal DNA from several *Cryptococcus* species. Journal of Bacteriology 172: 4238–4246. https://doi.org/10.1128/jb.172.8.4238-4246.1990

White TJ, Bruns T, Lee S, Taylor JM (1990) Amplification and direct sequencing of fungal ribosomal RNA genes for phylogenetics. In: Innis MA, Gelfand DH, Sninsky JJ, White TJ (Eds) PCR protocols: A Guide to the Methods and Applications. Academic Press, New York, 315–322. https://doi.org/10.1016/B978-0-12-372180-8.50042-1

Wijayawardene NN, Hyde KD, Rajeshkumar KC, Hawksworth DL, Madrid H, Kirk PM, Braun U, Singh RV, Crous PW, Kukwa M, Lücking R, Kurtzman CP, Yurkov A, Haelewa-

ters D, Aptroot A, Lumbsch HT, Timdal E, Ertz D, Etayo J, Phillips AJL, Groenewald JZ, Papizadeh M, Selbmann L, Dayarathne MC, Weerakoon G, Gareth Jones EB, Suetrong S, Tian Q, Castañeda-Ruiz RF, Bahkali AH, Pang K, Tanaka K, Dai DQ, Sakayaroj J, Hujslová M, Lombard L, Shenoy BD, Suija A, Maharachchikumbura SSN, Thambugala KM, Wanasinghe DN, Sharma DO, Gaikwad S, Pandit G, Zucconi L, Onofri S, Egidi E, Raja HA, Kodsueb R, Cáceres MES, Pérez-Ortega S, Fiuza PO, Monteiro JS, Vasilyeva LN, Shivas RG, Prieto M, Wedin M, Olariaga I, Lateef AA, Agrawal Y, Fazeli SAS, Amoozegar MA, Zhao GZ, Pfliegler WP, Sharma G, Oset M, Abdel-Wahab MA, Takamatsu S, Bensch K, de Silva NI, De Kesel A, Karunarathna A, Boonmee S, Pfister DH, Lu Y, Luo Z, Boonyuen N, Daranagama DA, Senanayake IC, Jayasiri SC, Samarakoon MC, Zeng X, Doilom M, Quijada L, Rampadarath S, Heredia G, Dissanayake AJ, Jayawardana RS, Perera RH, Tang LZ, Phukhamsakda C, Hernández-Restrepo M, Ma X, Tibpromma S, Gusmao LFP, Weerahewa D, Karunarathna SC (2017) Notes for genera: Ascomycota. Fungal Diversity 86: 1–594. https://doi.org/10.1007/s13225-017-0386-0

Wijayawardene NN, Hyde KD, Lumbsch HT, Liu JK, Maharachchikumbura SSN, Ekanayaka AH, Tian Q, Phookamsak R (2018) Outline of Ascomycota: 2017. Fungal Diversity 88: 167–263. https://doi.org/10.1007/s13225-018-0394-8

Wijayawardene NN, Hyde KD, Wanasinghe DN, Papizadeh M, Goonasekara ID, Camporesi E, Bhat DJ, McKenzie EHC, Phillips AJL, Diederich P, Tanaka K, Li WJ, Tangthirasunun N, Phookamsak R, Dai DQ, Dissanayake AJ, Weerakoon G, Maharachchikumbura SSN, Hashimoto A, Matsumura M, Bahkali, Wang Y (2016) Taxonomy and phylogeny of dematiaceous coelomycetes. Fungal Diversity 77: 1–136. https://doi.org/10.1007/s13225-016-0360-2

MycoKeys 56: 81–99 (2019)
doi: 10.3897/mycokeys.56.31819
http://mycokeys.pensoft.net

RESEARCH ARTICLE

A peer-reviewed open-access journal
MycoKeys
Launched to accelerate biodiversity research

Amanita ahmadii, a new species of *Amanita* subgenus *Amanitina* section *Validae* from Pakistan

Sana Jabeen[1,2], Munazza Kiran[2], Junaid Khan[3], Ishtiaq Ahmad[1,4,5], Habib Ahmad[5], Hassan Sher[3], Abdul Nasir Khalid[2]

1 *Department of Botany, Division of Science and Technology, University of Education, Lahore, Punjab, Pakistan* **2** *Department of Botany, University of the Punjab, Quaid-e-Azam Campus-54590, Lahore, Punjab, Pakistan* **3** *Center for Plant Sciences and Biodiversity, University of Swat, Swat, Khyber Pakhtunkhwa, Pakistan* **4** *Centre of Plant Biodiversity and Conservation, University of Peshawar, Peshawar, Khyber Pakhtunkhwa, Pakistan* **5** *Islamia College University, Peshawar, Khyber Pakhtunkhwa, Pakistan*

Corresponding author: *Sana Jabeen* (sanajabeenue@gmail.com; sanajabeen@ue.edu.pk)

Academic editor: *M.-A. Neves* | Received 21 November 2018 | Accepted 26 December 2018 | Published 23 July 2019

Citation: Jabeen S, Kiran M, Khan J, Ahmad I, Ahmad H, Sher H, Khalid AN (2019) *Amanita ahmadii*, a new species of *Amanita* subgenus *Amanitina* section *Validae* from Pakistan. MycoKeys 56: 81–99. https://doi.org/10.3897/mycokeys.56.31819

Abstract

A new species from coniferous forests in Pakistan, *Amanita ahmadii*, is described on the basis of morpho-anatomy and molecular data set analyses. This species is characterized by its medium-sized to large basidiomata, grayish brown to brown pileal surface and rimose pileus margin with gray to dark brown verrucose veil remnants, a cream stipe with bulbous base having grayish brown or brown longitudinal striations above the annulus, a scaly surface towards the base, globose to broadly ellipsoid and amyloid basidiospores, and the absence of clamped septa in all tissues. Molecular phylogenetic analyses based on ITS and LSU sequences confirmed its identity as a new taxon nested within subgen. *Amanitina* sect. *Validae*.

Keywords

Amanitaceae, nrDNA, Swat

Introduction

Amanitaceae E. J. Gilbert is a large family of agaricoid fungi that has been classified by many mycologists and split into various genera subgenera and sections (Corner and Bas 1962; Bas 1969). During recent years, it has been split into two genera, *Amanita* Pers., a genus of putatively ectomycorrhizal fungi, and *Saproamanita* Redhead, Vizzini, Drehmel & Contu, a genus of putatively saprotrophic fungi (Redhead et al. 2016). This generic split has been rejected by Tulloss et al. (2016) based in part on the guidelines of Vellinga et al. (2015) for introducing new genera. Concise amended characterizations have been provided for the monophyletic family Amanitaceae and its two monophyletic genera, *Amanita* and *Limacella* Earle. This declaration is based on the current use of next-generation sequencing in studies of fungal ecology opposing the splitting of the genus. Recently Cui et al. (2018) and Yang et al. (2018) inferred the phylogeny of Amanitaceae based on multi-locus sequencing data. The results indicated that Amanitaceae is monophyletic and consists of five genera. The genus *Amanita* consists of 95% of the species which are characterized by agaricoid basidiomata, colorless and hyaline, ballistosporic and smooth basidiospores, free lamellae, presence of volval remnants (Persoon 1797). A total of 540 known species of *Amanita* are distributed worldwide (Yang 2000, Kirk et al. 2008, Menolli et al. 2009, Tulloss 2009, Wartchow et al. 2009, Justo et al. 2010, Wartchow and Gamboa-Trujillo 2012, Cho et al. 2015, Hosen et al. 2015, Tang et al. 2015, Wartchow and Cortez 2016, Jabeen et al. 2017, Cui et al. 2018, Kiran et al. 2018a, b). From Pakistan, 19 species of *Amanita* are known to date (Ahmad et al. 1997, Jabeen et al. 2017, Kiran et al. 2018a, b). Tulloss et al. (2001) described one new species, *A. pakistanica* Tulloss, S.H. Iqbal & Khalid, but refrained from describing two more due to lack of materials. The work on these species is in progress by several workers, and it is estimated that the total number of *Amanita* from Pakistan could be above 50. Many taxa of the genus have been reported as edibles (Tulloss and Bhandary 1992, Buyck 1994, Montoya-Esquivel 1997), though some others are deadly poisonous (Yang 2015, Cai et al. 2016). Most of the species are ecologically important forming mycorrhizal symbiosis (Yang 1997, 2000, Kiran et al. 2018a).

Members of *Amanita* subgen. *Amanitina* (E. J. Gilbert) E. J. Gilbert have non-striated pileus margins, attenuate lamellulae and amyloid basidiospores (Cui et al. 2018)). Six sections in this subgenus are recognized (Cui et al. 2018), based on the morphology of the remnants of the universal veil and the pileal margin. The sect. *Validae* is characterized by pilei that are usually distinctly colored, margins that are non-appendiculate and do not exceed the gill margin, non-fragile and membranous annuli and basal bulbs that are usually small (Tulloss and Yang 2018, Yang 1997, Cui et al. 2018).

During our ongoing studies of ectomycorrhizal fungi in Khyber Pakhtunkhwa province, we collected specimens of an unknown *Amanita* species belonging to *Amanita* subgen. *Amanitina* sect. *Validae*. The aim of the present study was to characterize

and identify the taxon based on molecular phylogeny using the sequence data of the internal transcribed spacer (ITS) and partial large subunit (LSU) of ribosomal RNA. Here, we describe this taxon as a new species.

Materials and methods

Sampling sites

Specimens were collected from three different areas in two districts of Khyber Pakhtunkhwa province of Pakistan. One of these, the Swat district, has a very rich biodiversity. The mountains are covered with snow throughout the winter and in summer temperature ranges between 16–33 °C. The average annual precipitation in Swat district ranges from 1000 mm to 1200 mm. The first area, Gabin Jabba, is a lush green valley in Swat district, which is characterized by a moist temperate vegetation with *Picea smithiana* (Wall.) Boiss. and *Abies pindrow* Royle as the dominant tree species. Mashkun, the second area in Swat district, is in the western part of the Himalayas. This collection site is a dry temperate forest with *A. pindrow*, *P. smithiana* and *Cedrus deodara* (Roxb. ex D. Don) G. Don as the dominant tree species along with *Pinus wallichiana* A. B. Jacks.

The third area is Kumrat valley, which lies at the extreme North of the Dir Upper district. It is located in the foothills of the Hindu Kush mountains with an elevation of about 950–2440 m (Siddiqui et al. 2013). Snowfall occurs frequently in winter, rainfall during monsoon season ranges from 100 mm to 255 mm. Forests are dominated by a mixture of *C. deodara*, *A. pindrow*, *Picea smithiana*, and *Pinus wallichiana*, and *Populus nigra* L. is the main broad-leaved tree.

Macroscopic and microscopic characterization

Specimens were collected during routine macrofungal surveys and photographed in their natural habitats using a Nikon D3200 camera. Morphological features of fresh specimens were recorded and colors were designated using Munsell Soil Color Charts (Munsell 1975) and then forced-air dried for long term preservation. For detailed anatomical descriptions, tissues from different parts of the basidiomata were mounted on glass slides in 5% Potassium Hydroxide solution (KOH; w/v). Phloxine (1% w/v aqueous solution) was used for a better contrast. Melzer's reagent was used to check the amyloidity of basidiospores. Anatomical features were noted under a compound microscope (MX4300H, Meiji Techno Co., Ltd, Japan). Measurements were recorded using a Carl Zeiss (Jena) ocular micrometer and line drawings were made using Leitz Wetzlar camera lucida. Size and shape of basidiospores are presented in a form following the description of ranges for biometric variables according to Tulloss (2016). Voucher specimens are deposited in the Herbarium at the University of the Punjab (LAH), Quaid-e-Azam Campus, Lahore, Pakistan and at the Swat University Herbarium (SWAT), Swat, Pakistan.

DNA extraction, PCR and sequencing

For genomic DNA extraction, a standard CTAB method (Bruns 1995) was followed. Internal transcribed spacer regions along with central 5.8S region of nuclear ribosomal DNA (nrDNA) were amplified (Gardes and Bruns 1993) using forward primer ITS1F and reverse primer ITS4 (White et al. 1990). For LSU amplification, LR0R as forward and LR5 as reverse primers were used (Ge et al. 2014). The PCR products were sent to Macrogen Inc. (Korea) for sequencing.

Sequence alignment and phylogenetic analyses

Consensus sequences were generated from the sequences obtained by both primers (forward and reverse) in BioEdit software v. 7.2.5 (Hall 1999). Sequences of *Amanita* subgen. *Amanitina* sect. *Validae* at NCBI (http://www.ncbi.nlm.nih.gov/) and from published literature (Kim et al. 2013, Cai et al. 2014, Cui et al. 2018) were added to the datasets. Taxa from the sect. *Phalloideae* were chosen as outgroup (Cui et al. 2018). Shorter ITS and LSU sequences were omitted from the final matrices. Species and specimens used for the molecular phylogenetic analyses are given in Table 1. Multiple sequences were aligned using online webPRANK by EMBL-EBI, Wellcome Trust Genome Campus, UK (https://www.ebi.ac.uk/goldman-srv/webprank/). The phylogeny was inferred by maximum likelihood (ML) analysis using model selection for best DNA analysis for each dataset in MEGA6 software (Tamura et al. 2013). Models with the lowest BIC scores (Bayesian Information Criterion) were considered to describe the substitution pattern the best. Non-uniformity of evolutionary rates among sites may be modeled by using a discrete gamma distribution (+G) with 5 rate categories and by assuming that a certain fraction of sites are evolutionarily invariable (+I). The phylogenetic analyses were performed at 1000 bootstrap replicates. Percentage identity and divergence in nrDNA-ITS of the taxa were analyzed using MegAlign (DNAStar, Inc.). Sequences generated in this study were submitted to GenBank under accession numbers KY996724, KY996755, MF116158 and MF070490 for ITS and KY996725 and MK166021 for LSU.

Results

Phylogeny

Consensus sequences of the ITS region were BLAST searched at NCBI. These sequences showed 98% identity to *A.* aff. *fritillaria* (KJ466372 and KJ466373) sequences from China (Cai et al. 2014) with 94–100% query cover. It also showed 95% identity with an *A. franchetii* (JX515561) sequence from Bulgaria with 100% query cover and 0.0 E value. The LSU consensus sequence BLAST at NCBI showed 99% identity to *A.* aff. *flavoconia* (HQ539663) and *Amanita* sp. (KT072738) sequences from the eastern USA and *A. fritillaria* (KF245897) sequences from South Korea with 99% query cover.

Table 1. Species and specimens of *Amanita* used for the molecular phylogenetic analyses.

Species	Voucher	Country	GenBank accession number		Reference
			ITS	LSU	
A. aff. *brunnescens*	BW_HF 10C	USA	–	HQ539661	–
A. aff. *citrina*	BW_PNC	USA	–	HQ539662	–
	HKAS 34170	China	AY436449	AY436489	Zhang et al. 2004, Thongbai et al. 2016
A. aff. *flavorubens*	PSMCC 121	USA	–	HQ539663	–
	BW_HF-FR	USA	–	HQ539664	–
A. aff. *fritillaria*	HKAS56832	China	KJ466372	KJ466479	Cai et al. 2014, Thongbai et al. 2016
	HKAS57649	China	KJ466373	KJ466480	Cai et al. 2014
A. aff. *spissacea*	2C5	Japan	AB973749	–	–
A. ahmadii	LAH35010	Pakistan	KY996724	KY996725	–
	SWAT0001351	Pakistan	MF070490	–	–
	LAH35241	Pakistan	KY996755	MK166021	–
	LAH35242	Pakistan	MF116158	–	–
A. augusta	DBB49390	USA	JQ937287		–
	DBB21873	USA	JX515564	–	–
A. augusta as "*A. franchetii*"	07040	USA	GQ250398	–	–
A. bisporigera	RET 377-9	USA	KJ466374	KJ466434	Thongbai et al. 2016
A. brunneolocularis	ANDES_F313 NVE57	Colombia	FJ890033	FJ890044	Vargas et al. 2011
A. brunnescens	RET 637-7	USA	KT006762	KT006766	Thongbai et al. 2016
	BW_HP12	USA	–	HQ539674	–
	RET 529-10	USA	KP284273	KP284284	–
	RET 554-1	USA	KP284275	KP284285	–
	RET 549-9	USA	–	KP284283	–
	JS94/2	–	–	AF097379	Drehmel et al. 1999
A. castanea	MFLU 15-1424	Thailand	KU904823	KU877539	Thongbai et al. 2016
A. cf. *flavorubescens*	JMP0098	USA	EU819454	–	Palmer et al. 2008
A. cf. *spissacea*	BZ2015-40	Thailand	KY747464	–	Cai et al. 2012
	OR1214	Thailand	KY747469	KY747478	Cai et al. 2012
A. citrina	LEM 960298	Japan	AB015679	–	Oda et al. 1999, Thongbai et al. 2016
	JM96/61	–	–	AF097378	–
	TM02_102	Canada	–	EU522722	Porter et al. 2008
	KA12-1226	South Korea	KF245908	KF245892	Kim et al. 2013
	JSH s.n.	–	–	AF041547	–
	JS94/1	–	–	AF097377	Drehmel et al. 1999
	ANDES_F405 IP25	Colombia	–	FJ890046	Vargas et al. 2011
	BW JLR 102106-1	USA	–	HQ539679	–
	KA12-1612	South Korea	KF245909	KF245893	Kim et al. 2013
A. citrinoindusiata	HKAS100522	China	MH508320	MH486468	Cui et al. 2018
	HKAS58884	China	MH508323	MH486471	Cui et al. 2018
	HKAS58886	China	MH508324	MH486472	Cui et al. 2018
	HKAS58796	China	MH508321	MH486469	Cui et al. 2018
	HKAS58888	China	MH508325	MH486473	Cui et al. 2018
	HKAS58874	China	MH508322	MH486470	Cui et al. 2018
A. excelsa	HKAS 31510	Germany	AY436453	AY436491	Thongbai et al. 2016
	Ge 816	China	–	HQ539691	–

Species	Voucher	Country	GenBank accession number		Reference
			ITS	LSU	
A. flavipes	KA12-0685	South Korea	KF245911	KF245895	Kim et al. 2013
	HKAS 36582	China	AY436455		Zhang et al. 2004
	KA12-1517	South Korea	KF245912	KF245896	Kim et al. 2013
A. flavoconia	TENN61564	USA	JF313655	–	–
	BW_PH22	–	–	HQ539693	–
	ANDESF408CV3	Colombia	FJ890029	FJ890041	Thongbai et al. 2016
	TM03_435 25S	Canada	–	EU522816	Porter et al. 2008
	NVE 351	Colombia	KF937301	–	Vasco-Palacios et al. 2014
	NVE 242	Colombia	KF937300	–	Vasco-Palacios et al. 2014
A. flavoconia	HKAS 34047	USA	AY436456		Zhang et al. 2004
	RV5Aug96	–	–	AF042609	Moncalvo et al. 2000
A. flavorubens	RET 295-9	USA	–	HQ539694	–
A. flavorubescens	TENN61660	USA	JF313650	–	–
	F:PRL6062	USA	GQ166902	–	Thongbai et al. 2016
	RV96/102	–	–	AF097380	Drehmel et al. 1999
A. franchetii	JM96/27	–	–	AF097381	Drehmel et al. 1999
A. franchetii f. *lactella* as "*A. franchetii*"	DBBJUS01	Spain	JX515563	–	–
	DBB52095	Bulgaria	JX515562	–	–
	DBB51482	Bulgaria	JX515561	–	–
A. franchetii f. *queletii* as "*A. aspera*"	IFO-8262	–	AF085485	–	Lim and Jung 1998
A. fritillaria	–	China	JF273505	–	Legendre et al. 2009
	HKAS 38331	China	AY436457	–	Zhang et al. 2004
	KA12-1231	South Korea	KF245913	KF245897	Kim et al. 2013
A. lavendula	RET 639-7	USA	KP866163	KR865979	Thongbai et al. 2016
A. luteofusca	PSC 1093b	Australia	–	HQ539705	–
A. luteolovelata	PSC 2187	Australia	–	HQ539706	–
A. morrisii	RET 672-6	USA	KR919762	KR919770	–
	RET 271-7	USA	KT213441	KT213442	Thongbai et al. 2016
	RET 445-10	USA	KR919760	KR919768	–
A. novinupta	GO-2009-234	Mexico	KC152066	–	–
	GO-2009-315	Mexico	KC152065	–	–
	GO-2009-301	Mexico	KC152067	–	–
	RET 060-2	USA	KF561974	KF561978	Thongbai et al. 2016
	RET 093-10	USA	–	HQ539716	–
	NY 00066710	USA	KJ535437	KJ535441	–
A. phalloides	GDGM:40312	Italy	KC755034	–	
A. porphyria	LEM960303	Japan	AB015677	–	Oda et al. 1999
	DAVFP:26784	USA	JF899548	–	
	RET 079-1	Switzerland	KP866181	KP866192	Thongbai et al. 2016
	HKAS 31531	China	AY436471	AY436500	Thongbai et al. 2016
	RET 309-8	Norway	KP866176	KP866189	–
	RET 404-2	Czech Republic	KP866171	KP866184	–
	RET 404-9	Czech Republic	–	KP866185	–

Species	Voucher	Country	GenBank accession number		Reference
			ITS	LSU	
A. rubescens	JMP0003	USA	EU819464	–	Palmer et al. 2008
	TRTC156957	Canada	JN020972	–	Dentinger et al. 2011
	LE241998	Russia	JF313652	–	–
	RK01-01	Denmark	AJ889923	–	–
	EMF4	China	JF273507	–	–
	LEM950063	Japan	AB015682	–	Oda et al. 1999
	ASIS23255	South Korea	KM052530	–	–
	ASIS23444	South Korea	KM052535	–	–
	KA 12-1221	Korea	KF245919	KF245903	Thongbai et al. 2016
	RET 122-8	Turkey	–	HQ539735	–
	ANDES_F416 NVE160	Colombia	FJ890031	FJ890043	Vargas et al. 2011
	RV5Aug96	–	–	AF042607	Moncalvo et al. 2000
	RV97/23	–	–	AF097383	Drehmel et al. 1999
	JM96/53	–	–	AF097382	Drehmel et al. 1999
	KA12-0936	South Korea	KF245918	KF245902	Kim et al. 2013
A. sp.	ANDES_F241 IP24	Colombia	FJ890032	FJ890047	Vargas et al. 2011
	RET 516-10	USA	KP711830	KP711838	–
	RET 516-5	USA	KP711836	KP711837	–
	RET 530-1	USA	KT072736	KT072737	–
	RET 539-8	USA	KT072735	KT072738	–
	HKAS 38419	China	AY436474	AY436502	Thongbai et al. 2016
A. spissa	UP541	–	EF493270	–	Nygren et al. 2008
	KF02-47	–	AJ889924	–	–
	UP542	–	EF493271	–	Nygren et al. 2008
	KA12-0884	South Korea	KF245910	KF245894	Kim et al. 2013
	NYBG 47779	Germany	–	HQ539743	–
A. spissacea	LEM960187	Japan	AB015683	–	Oda et al. 1999
	ASIS24872	South Korea	KM052552	KU139485	–
	ASIS26240	–	KT894841	KU139454	–
	ASIS24978	–	KM052550	KU139487	–
	ASIS24775	–	KM052543	KU139484	–
	ASIS24949	–	KM052546	KU139486	–
A. virosa	HKAS 56694	China	JX998030	JX998058	Cai et al. 2012
	HMJAU23304	China	KJ466431	KJ466498	Cai et al. 2012
	JM 97/42	–	–	AF159086	Moncalvo et al. 2000

Taxa from subgen. *Amanitina* sect. *Phalloideae* (Fr.) Quél. were chosen as the outgroup (Kim et al. 2013). The sequences generated during this study clustered with the similar taxa in sect. *Validae* (Figs 1–3). Our species clustered with *A.* aff. *fritillaria*, *A. citrinoindusiata*, *A. franchetii* f. *franchetii* , *A. franchetii* f. *lactella* (as *A. franchetii* in GenBank), *A. franchetii* f. *queletii* (as *A. aspera* in GenBank) and *A. spissa* in phylogenetic analysis. However, *A. ahmadii* separated from *A.* aff. *fritillaria* with a strong bootstrap value of 95%, 49% and 100% in ITS, LSU and ITS+LSU sequence dataset analyses, respectively (Figs 1–3).

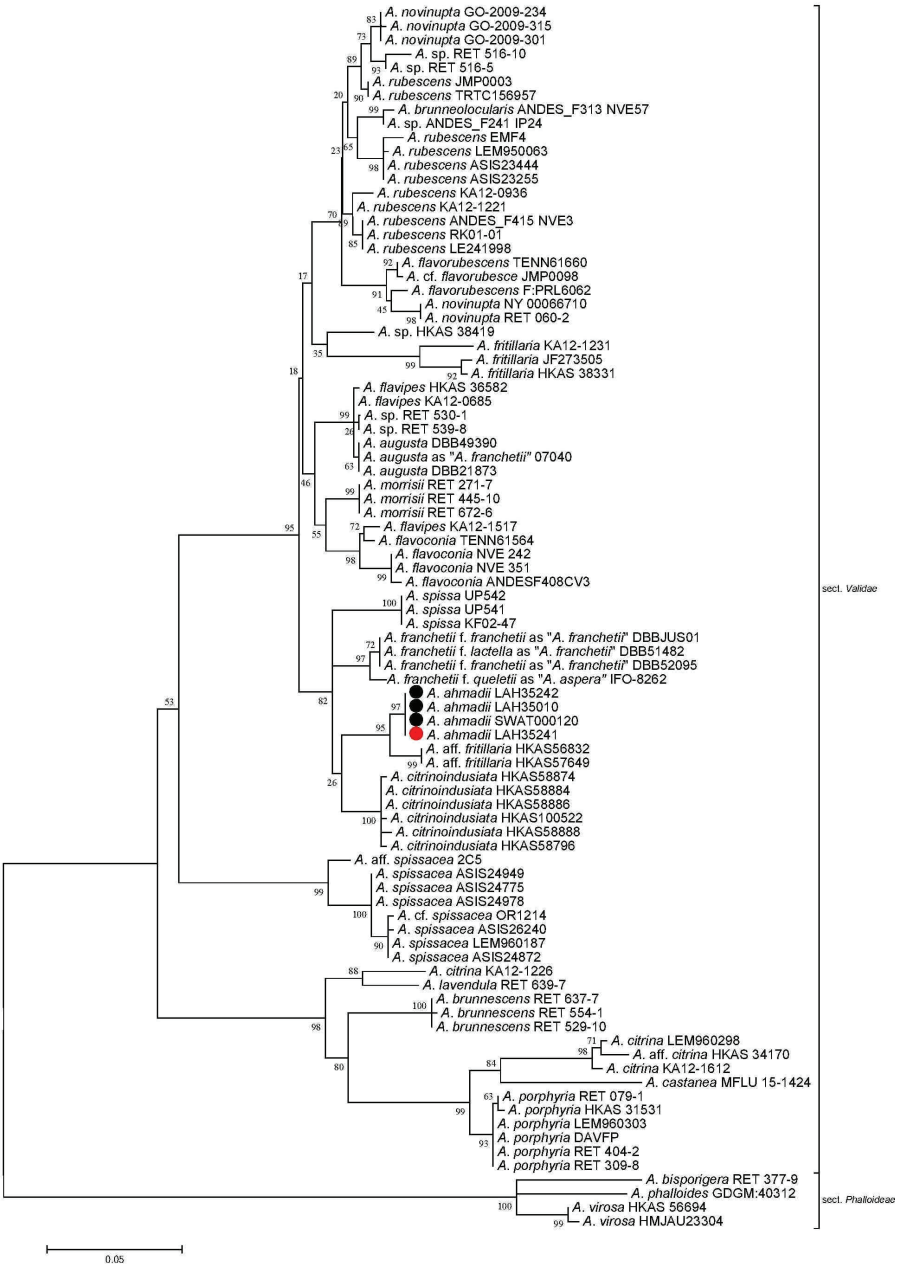

Figure 1. Molecular phylogenetic analysis of ITS sequences using the maximum likelihood method based on the Tamura 3-parameter model (Tamura 1992). The percentage of trees in which the associated taxa clustered together is shown next to the branches. A discrete gamma distribution was used to model evolutionary rate differences among sites (5 categories (+*G*, parameter = 0.4454)). The tree is drawn to scale, with branch lengths measured in the number of substitutions per site. The analysis involved 88 nucleotide sequences. There were a total of 1018 positions in the final dataset. Sequences generated during the present investigation are marked with bullets. Red represents the holotype.

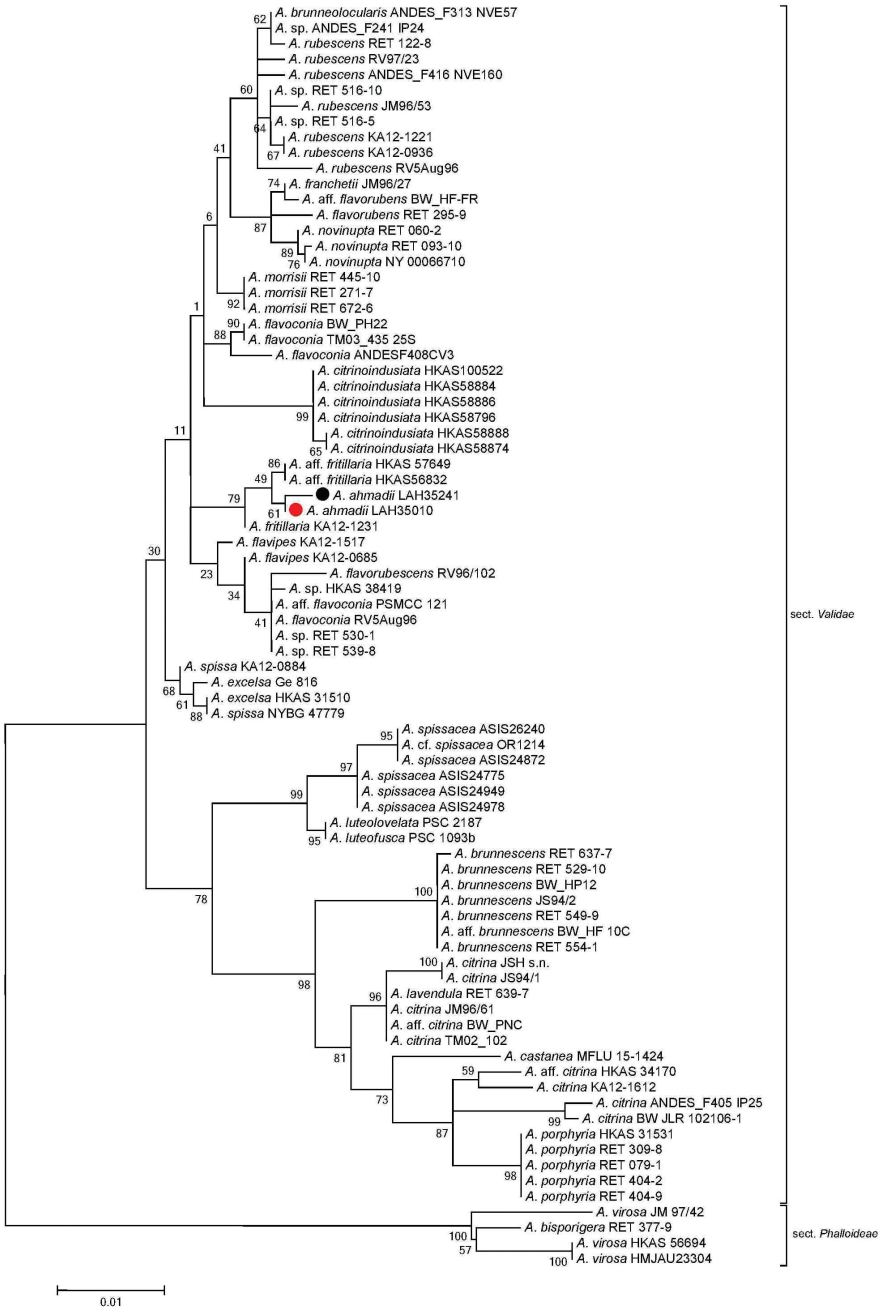

Figure 2. Molecular phylogenetic analysis of LSU sequences by using the maximum likelihood method based on the Kimura 2-parameter model (Kimura 1980). A discrete gamma distribution was used to model evolutionary rate differences among sites (5 categories (+*G*, parameter = 0.2164)). The tree is drawn to scale, with branch lengths measured in the number of substitutions per site. The analysis involved 81 nucleotide sequences. There were a total of 871 positions in the final dataset. Sequences generated during the present investigation are marked with bullets. Red represents the holotype.

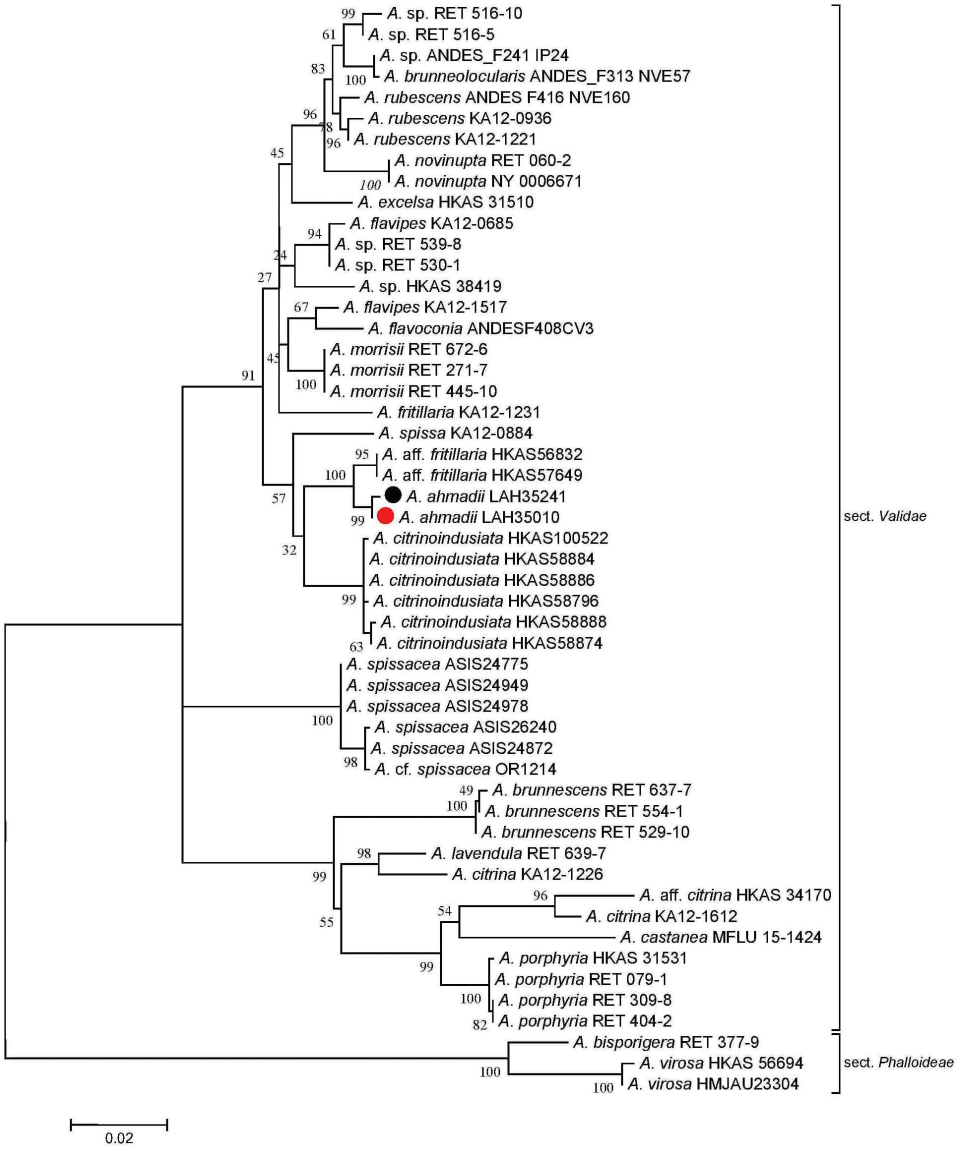

Figure 3. Molecular phylogenetic analysis of ITS+LSU sequences by using the maximum likelihood method based on the Tamura-Nei model (Tamura and Nei 1993). A discrete gamma distribution was used to model evolutionary rate differences among sites (5 categories (+*G*, parameter = 0.2250)). The rate variation model allowed for some sites to be evolutionarily invariable ([+*I*], 43.3848% sites). The tree is drawn to scale, with branch lengths measured in the number of substitutions per site. The analysis involved 52 nucleotide sequences. There were a total of 1760 positions in the final dataset. Sequences generated during the present investigation are marked with bullets. Red represents the holotype.

Taxonomy

***Amanita ahmadii* Jabeen, I. Ahmad, Kiran, J. Khan & Khalid, sp. nov.**
MycoBank number: MB821204
Figs 4, 5

Diagnosis. Small to medium-sized basidiomata, grayish brown to brown pileal surface having rimose and non-appendiculate pileal margins, verrucose, gray to dark bluish or brown veil remnants, dry and split stipe surface at the base forming scales, globose to subglobose, smooth, amyloid basidiospores.

Holotype. Pakistan, Khyber Pakhtunkhwa province, Malakand division, Swat district, Mashkun, 2500 m a.s.l., on soil under *Cedrus deodara*, 5 Sept. 2013, Sana Jabeen SJ35 (LAH35010; GenBank ITS: KY996724; LSU: KY996725).

Etymology. The species epithet *ahmadii* refers to Sultan Ahmad, the pioneer Pakistani mycologist.

Description. Pileus 4–7 cm in diameter, convex to flat at maturity; cuticle gray (2.5BG4/2) to grayish brown (10YR3/2) or brown (2.5Y4/4) with time; surface dry; universal veil remnants on pileus verrucose, aligned in one direction, scattered, gray (2.5Y4/2) to dark brown (2.5Y2/2); margins non-appendiculate, incurved when young, highly rimose by maturity. Lamellae off-white (2.5BG4/2) to cream (5Y9/4) becoming brownish when dry, adnexed, subdistant to close; edges entire. Lamellulae small (1/3 of the lamellae), attenuate, truncate. Stipe 6.7–9 × 0.6–1.5 cm, apex slightly wider and white, with up to 1.5 cm wide bulbous base, central, cylindrical; surface with grayish brown (5GY5/2) striations above the annulus, splitting towards the base forming scales on white (2.5BG4/2) to cream (5Y9/4) context. Annulus superior, membranous, skirt-like, with longitudinal striations on the upper surface, gray (2.5Y4/2) with a darker lower part. Universal veil absent. Ordorless and not changing color upon bruising.

Basidiospores [60/3/3] (6.5) 7–8.5 (9.5) × (6) 6.5–7.5 (8) µm, Q = (1) 1.03–1.22 (1.33), avg Q = 1.10, globose to broadly ellipsoid, amyloid in Melzer's reagent. Basidia (32) 34.5–59 (67) × 7–8 µm, clavate, frequently 4 sterigmate, 2 sterigmata also observed, thin-walled, hyaline in 5% KOH. Subhymenium pseudoparenchymatous, cells isodiameteric, intermixed and densely packed. Veil remnants made up of hyphae with terminal subglobose to elongated cells (42.5) 49.5–54 (57) × (13) 13–16 (19) µm on a branched filament 3–4 µm wide; septa frequent; clamp connections absent. Pileipellis filamentous, 4–5 µm in diameter, branched, septate; clamp connections absent, light brown with some hyaline tissue in 5% KOH. Universal veil remnants of globose to subglobose cells (6.8) 8–12.2 (12.7) × (4.4) 7.5–10.5 (11) µm with filaments (0.7) 0.9–2.6 (3.5) µm in diameter. Hyphae from stipe 3–24 µm wide, filamentous, branched, hyaline in 5% KOH, septate; clamp connections absent in all tissues.

Habitat and distribution. In coniferous forests of Pakistan with a moist temperate to dry temperate climate.

Figure 4. *Amanita ahmadii* basidiomata. **A, B** LAH35010 (holotype) **C** SWAT0001351. Photos by Abdul Nasir Khalid and Junaid Khan. Scale bars: 1 cm (**A**); 1.2 cm (**B**); 0.5 cm (**C**).

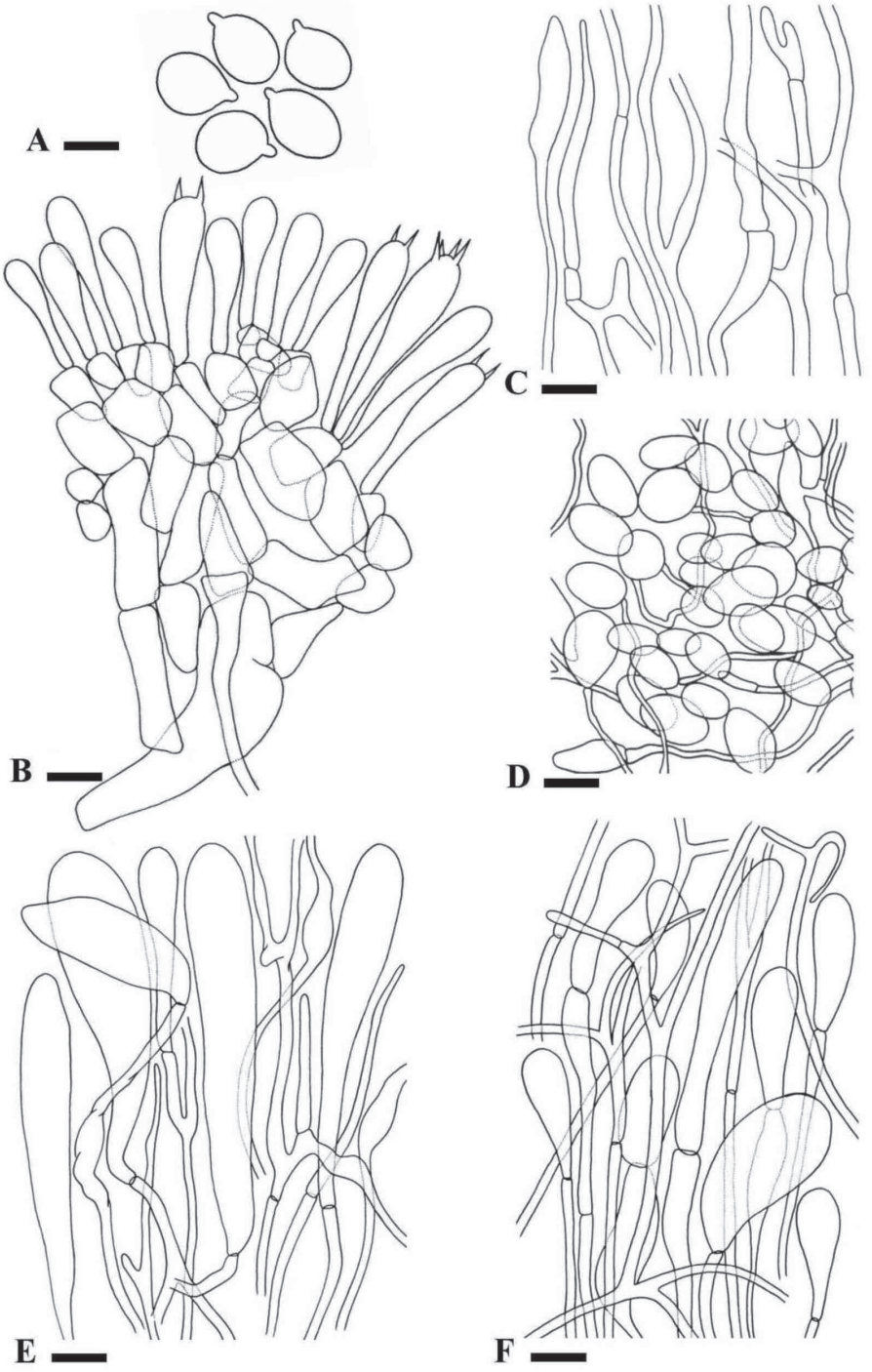

Figure 5. *Amanita ahmadii* LAH35010 (holotype). **A** Basidiospores **B** Basidia, basidioles and subhymenium **C** Pileipellis **D** Universal veil remnants on pileus surface **E** Hyphae from stipe **F** Partial veil. Drawings by Sana Jabeen. Scale bars: 5.5 μm (**A**); 8 μm (**B–D**); 22 μm (**E, F**).

Additional specimens examined. Pakistan, Khyber Pakhtunkhwa province, Malakand division, Dir Upper district, Kumrat, 2232 m a.s.l., on soil under conifers, 2 Sept. 2015, Abdul Nasir Khalid FS82 (LAH35241; GenBank ITS: KY996755; LSU: MK166021); Swat district, Mashkun, 2500 m a.s.l., on soil under *Cedrus deodara*, 4 Aug. 2013, Ishtiaq Ahmad IS213P65 (LAH35242; GenBank ITS: MF116158); Gabin Jabba valley, 2450 m a.s.l., on soil under *Picea smithiana*, 30 Aug. 2015, Junaid Khan GJ-1508 (SWAT001351; GenBank ITS: MF070490).

Discussion

Amanita ahmadii is characterized by its grayish brown to brown pileus surface with abundant gray to dark brown verrucose veil remnants and by its rimose margins. Anatomically it is characterized by its globose to broadly ellipsoid basidiospores. The species is morphologically similar to *A. fritillaria* Sacc. by its grayish to brownish gray pileus surface, and verrucose volval remnants. *Amanita fritillaria* differs by bearing ellipsoid basidiospores (Corner and Bas 1962, Yang 1997, 2005, 2015). In phylogenetic trees based on ITS, LSU and combined sequence datasets of both regions, *A. fritillaria* was inferred as a distinct lineage from *A. ahmadii*.

Amanita aff. *fritillaria* (HKAS56832 and HKAS57649, Cai et al. 2014) forms a sister clade to *A. ahmadii* (Figs 1–3), but it is morphologically distinct. The former taxon possesses a brownish and purplish pileus surface (Zhu L. Yang pers. comm.) while the latter has a grayish brown or brown pileus surface with highly rimose margins (Cai et al. 2014). *Amanita fritillaria* f. *malayensis* Corner & Bas was described from Singapore (Corner and Bas 1962), but more recently was also found in subtropical, evergreen, broad-leaved forests in China; it differs from *A. ahmadii* in having a dark umber to rather pale grayish umber pileus (Yang 2005, 2015).

The European sequences labeled as "*A. franchetii*" and "*A. aspera*" in GenBank are close relatives of *A. ahmadii* in the ITS phylogenetic analysis. *Amanita franchetii* (Boud.) Fayod is somewhat variable in appearance and there are three morphological infraspecific taxa, including *A. franchetii* f. *franchetii* (Boud.) Fayod (JX515562 and JX515563), *A. franchetii* f. *lactella* Neville & Poumarat (JX515561) and *A. franchetii* f. *queletii* (Bon & Dennis) Neville & Poumarat (AF085485) (Neville and Poumarat 2004). The last taxon most closely resembles *A. ahmadii* but differs in having more yellow hues on the stipe and pronounced reddening on the bulb with age. *Amanita augusta* Bojantchev & R. M. Davis, as "*A. franchetii*" in GenBank (GQ250398), another species from western North America looks similar to *A. ahmadii* but its yellowish brown pileus with yellow universal veil remnants and ellipsoid spores (Bojantchev and Davis 2013) distinguishes it from *A. ahmadii*. During phylogenetic analyses, all these taxa were inferred as distinct species.

The novel species also showed differences from *A. castanea* Thongbai, Tulloss, Raspé & K. D. Hyde from Thailand. *Amanita castanea* bears a viscid, shiny and sericeous pileal surface, which is dark brown at center and light brown to brownish orange towards

margin, with universal veil mostly towards the margin, rarely over disc, as scattered gray to brownish gray, reddish brown to grayish brown warts or small floccose patches and globose basidiospores (Thongbai et al. 2016). All these characters distinguish *A. castanea* from *A. ahmadii*. In molecular phylogenetic analyses, *A. castanea* is clustered with the species in a distant clade within sect. *Validae* (Figs 1–3). *Amanita ahmadii* also showed morphological distinctions from *A. citrinoindusiata* Zhu L. Yang, Y. Y. Cui & Q. Cai, a newly reported species in the same section from China. This species is characterized by its robust, brownish gray, gray to dark gray pileus and a stipe bearing a citrine to yellowish annulus. This suggests it is a separate species from *A. ahmadii* (Cui et al. 2018). Molecular data also supports the separation of these two taxa in phylogenetic trees (Figs 1–3).

The European *A. excelsa* Gonn. & Rabenh is also morphologically close to *A. ahmadii* in having a gray-brown pileus. However, *A. excelsa* differs from *A. ahmadii* in having mealy, gray irregular and non-persistent patches of volval remnants on the pileus. The volva in *A. excelsa* has 2–5 pale ochre brown zones of friable material above the bulb, and lastly, the broadly ellipsoid to ellipsoid, occasionally elongate basidiospores also distinguish *A. excelsa* from *A. ahmadii* (Neville & Poumarat, 2004). The phylogenetic position of these taxa also indicates that they are separate. Based on morphological characters and molecular phylogenic analysis, our new species belongs to *Amanita* subgen. *Amanitina* sect. *Validae*.

Acknowledgements

This work was financially supported by the Higher Education Commission (HEC)-Pakistan to Dr Sana Jabeen under Indigenous PhD Fellowships for 5000 Scholars (Phase-II), Dr Sana Jabeen, Dr Ishtiaq Ahmad and Munazza Kiran under International Research Support Initiative Program (IRSIP) and Dr Hassan Sher under Pak-US science and technology promotion program. We sincerely thank Prof. Donald H. Pfister for providing the opportunity to Dr Sana Jabeen, Dr Ishtiaq Ahmad and Munazza Kiran to work in his laboratory at Department of Organismic and Evolutionary Biology, Harvard University, MA, USA. Thanks are also due to Prof. Dr Zhu-Liang Yang (Key Laboratory for Plant Diversity and Biogeography of East Asia, Kunming Institute of Botany, Chinese Academy of Sciences, Kunming, China) for providing pictures to compare the morphology of the specimens and review of the manuscript. Special thanks are due to Dr Else C. Vellinga, (Department of Plant and Microbial Biology, University of California, Berkeley, CA, USA) for editing the text. Her useful comments and suggestions greatly improved this article. Authors are grateful to Dr Rosanne Healy (Assistant Scientist, Department of Plant Pathology, University of Florida. Gainesville, FL 32611) for linguistic suggestions and helpful comments resulting in the removal of technical errors. We are also thankful to Dr Abdul Rehman Khan Niazi (Department of Botany, University of the Punjab, Lahore, Pakistan) and all laboratory fellows for accompanying the tours to different areas of Pakistan.

References

Ahmad S, Iqbal SH, Khalid AN (1997) Fungi of Pakistan. Sultan Ahmad Mycological Society Pakistan, 248 pp.

Bas C (1969) Morphology and subdivision of *Amanita* and a monograph of its section *Lepidella*. Persoonia 5: 285–579.

Bojantchev D, Davis RM (2013) *Amanita augusta*, a new species from California and the Pacific Northwest. North American Fungi 8: 1–11. https://doi.org/10.2509/naf2013.008.005

Bruns TD (1995) Thoughts on the processes that maintain local species diversity of ectomycorrhizal fungi. In: Collins HP, Robertson GP, Klug MJ (Eds) The Significance and Regulation of Soil Biodiversity. Developments in Plant and Soil Sciences 63. Springer, Dordrecht, 63–73. https://doi.org/10.1007/978-94-011-0479-1_5

Buyck B (1994) Ubwoba: Les champignons comestibles de l'ouest du Burundi. Administration generale de la cooperation au developpement, Publication Agricole 34, Bruxelles, 123 pp.

Cai Q, Tang LP, Yang ZL (2012) DNA Barcoding of economically important mushrooms: A case study on lethal amanitas from China. Plant Diversity and Resources 34(6): 614–622. https://doi.org/10.3724/SP.J.1143.2012.12140

Cai Q, Tulloss RE, Tang LP, Tolgor B, Zhang P, Chen ZH, Yang ZL (2014) Multi-locus phylogeny of lethal amanitas: implications for species diversity and historical biogeography. BMC Evolutionary Biology 14: 143–158. https://doi.org/10.1186/1471-2148-14-143

Cai Q, Cui YY, Yang ZL (2016) Lethal *Amanita* species in China. Mycologia 108: 993–1009. https://doi.org/10.3852/16-008

Cho H, Park MS, Lee H, Oh SY, Jang Y, Fong JJ, Lim YW (2015) Four new species of *Amanita* in Inje County, Korea. Mycobiology 43: 408–414. https://doi.org/10.5941/MYCO.2015.43.4.408

Corner EJH, Bas C (1962) The genus *Amanita* in Singapore and Malaya. Persoonia 2: 241–304.

Cui YY, Cai Q, Tang LP, Liu JW, Yang ZL (2018) The family Amanitaceae: molecular phylogeny, higher-rank taxonomy and the species in China. Fungal Diversity 91(1): 5–230. https://doi.org/10.1007/s13225-018-0405-9

Dentinger BT, Didukh MY, Moncalvo JM (2011) Comparing COI and ITS as DNA barcode markers for mushrooms and allies (Agaricomycotina). PLoS ONE 6(9): e25081. https://doi.org/10.1371/journal.pone.0025081

Drehmel D, Moncalvo JM, Vilgalys R (1999) Molecular phylogeny of *Amanita* based on large-subunit ribosomal DNA sequences: implications for taxonomy and character evolution. Mycologia 91(4): 610–618. https://doi.org/10.2307/3761246

Gardes M, Bruns TD (1993) ITS primers with enhanced specificity for basidiomycetes application to the identification of mycorrhizae and rusts. Molecular Ecology 2: 113–118. https://doi.org/10.1111/j.1365-294X.1993.tb00005.x

Ge C, Cui YN, Jing PY, Hong XY (2014) An alternative suite of universal primers for genotyping in multiplex PCR. PloS ONE 9: e92826. https://doi.org/10.1371/journal.pone.0092826

Hall TA (1999) BioEdit: a user-friendly biological sequence alignment editor and analysis program for Windows 95/98/NT. Nucleic Acids Symposium Series 41: 95–98.

Hosen MI, Li TH, Deng WQ (2015) *Amanita cinereovelata*, a new species of *Amanita* section *Lepidella* from Bangladesh. Mycological Progress 14: 35. https://doi.org/10.1007/s11557-015-1058-7

Jabeen S, Kiran M, Ullah S, Wilson A, Mueller GM, Fiaz M, Khalid AN (2017) *Amanita glarea*, a new species in section *Vaginatae* from Pakistan. Phytotaxa 306: 135–145. https://doi.org/10.11646/phytotaxa.306.2.3

Jukes TH, Cantor CR (1969) Evolution of protein molecules. In: Munro HN (Ed.) Mammalian Protein Metabolism. Academic Press, New York, 21–132. https://doi.org/10.1016/B978-1-4832-3211-9.50009-7

Justo A, Morgenstern I, Hallen-Adams HE, Hibbett DS (2010) Convergent evolution of sequestrate forms in *Amanita* under Mediterranean climate conditions. Mycologia 102: 675–688. https://doi.org/10.3852/09-191

Kim CS, Jo JW, Kwag YN, Oh J, Shrestha B, Sung GH, Han SK (2013) Four newly recorded *Amanita* species in Korea: *Amanita* sect. *Amanita* and sect. *Vaginatae*. Mycobiology 41: 131–138. https://doi.org/10.5941/myco.2013.41.3.131

Kiran M, Khan J, Naseer A, Sher H, Khalid AN (2018a) *Amanita pallidorosea* in Pakistan and its ectomycorrhizal association with *Quercus oblongata*. Mycotaxon 132(4): 799–811. https://doi.org/10.5248/132.799

Kiran M, Khan J, Sher H, Pfister DH, Khalid AN (2018b) *Amanita griseofusca*: a new species of *Amanita* in section *Vaginatae* from Malam Jabba, Swat, Pakistan. Phytotaxa 364(2): 181–192. https://doi.org/10.11646/phytotaxa.364.2.5

Kirk PM, Cannon PF, Minter DW, Stalpers JA (Eds) (2008) Dictionary of the Fungi (10th edn). CABI International, Wallingford, 784 pp.

Legendre P, Mi X, Ren H, Ma K, Yu M, Sun IF, He F (2009) Partitioning beta diversity in a subtropical broad-leaved forest of China. Ecology 90(3): 663–674. https://doi.org/10.1890/07-1880.1

Lim YW, Jung HS (1998) Phylogenetic relationships of *Amanita* species based on ITS1-5.8 S rDNA-ITS2 region sequences. The Journal of Microbiology 36(3): 203–207.

Menolli N Jr, Capelari M, Baseia IG (2009) *Amanita viscidolutea*, a new species from Brazil with a key to Central and South American species of *Amanita* section *Amanita*. Mycologia 101: 395–400. https://doi.org/10.3852/07-079

Moncalvo JM, Lutzoni FM, Rehner SA, Johnson J, Vilgalys R (2000) Phylogenetic relationships of agaric fungi based on nuclear large subunit ribosomal DNA sequences. Systematic Biology 49(2): 278–305. https://doi.org/10.1093/sysbio/49.2.278

Montoya-Esquivel A (1997) Estudio etnomicológico en San Francisco Temezontla, estado de. Tlaxcala. Tesis de Maestría, Universidad Nacional Autonoma de Mexico, 133 pp. [In Spanish]

Munsell (1975) Munsell Color Co – Munsell Soil Color Charts. Baltimore, MD, 20 pp.

Nei M, Kumar S (2000) Molecular Evolution and Phylogenetics. Oxford University Press, New York, 333 pp.

Neville P, Poumarat S (2004) *Amaniteae*. Vol. 1. Fungi Europaei 9: 1–1119.

Nygren CM, Eberhardt U, Karlsson M, Parrent JL, Lindahl BD, Taylor AF (2008) Growth on nitrate and occurrence of nitrate reductase-encoding genes in a phylogenetically di-

verse range of ectomycorrhizal fungi. New Phytologist 180(4): 875–889. https://doi.org/10.1111/j.1469-8137.2008.02618.x

Oda T, Tanaka C, Tsuda M (1999) Molecular phylogeny of Japanese *Amanita* species based on nucleotide sequences of the internal transcribed spacer region of nuclear ribosomal DNA. Mycoscience 40(1): 57–64. https://doi.org/10.1007/BF02465674

Palmer JM, Lindner DL, Volk TJ (2008) Ectomycorrhizal characterization of an American chestnut (*Castanea dentata*) – dominated community in western Wisconsin. Mycorrhiza 19(1): 27. https://doi.org/10.1007/s00572-008-0200-7

Persoon CH (1797) Tentamen dispositionis methodicae fungorum. Petrum Philippum Wolf, Leipzig, Vol. 8, 1–76. http://bibdigital.rjb.csic.es/ing/Libro.php?Libro=3125

Porter TM, Skillman JE, Moncalvo J (2008) Fruiting body and soil rDNA sampling detects complementary assemblage of Agaricomycotina (Basidiomycota, Fungi) in a hemlock-dominated forest plot in southern Ontario. Molecular Ecology 17(13): 3037–3050. https://doi.org/10.1111/j.1365-294X.2008.03813.x

Redhead SA, Vizzini A, Drehmel DC, Contu M (2016) *Saproamanita*, a new name for both *Lepidella* E.-J. Gilbert and *Aspidella* E.-J. Gilbert (Amanitae, Amanitaceae). IMA Fungus 7: 119–29. https://doi.org/10.5598/imafungus.2016.07.01.07

Tamura K (1992) Estimation of the number of nucleotide substitutions when there are strong transition-transversion and G+C-content biases. Molecular Biology and Evolution 9: 678–687.

Tamura K, Nei M (1993) Estimation of the number of nucleotide substitutions in the control region of mitochondrial DNA in humans and chimpanzees. Molecular Biology and Evolution 10: 512–526.

Tamura K, Stecher G, Peterson D, Filipski A, Kumar S (2013) MEGA6: Molecular Evolutionary Genetics Analysis version 6.0. Molecular Biology and Evolution 30: 2725–2729. https://doi.org/10.1093/molbev/mst197

Tang LP, Cai Q, Lee SS, Buyck B, Zhang P, Yang ZL (2015) Taxonomy and phylogenetic position of species of *Amanita* sect. *Vaginatae* s.l. from tropical Africa. Mycological Progress 14: 1–15. https://doi.org/10.1007/s11557-015-1061-z

Thongbai B, Tulloss RE, Miller SL, Hyde KD, Chen J, Zhao RL, Raspé O (2016) A new species and four new records of *Amanita* (Amanitaceae; Basidiomycota) from northern Thailand. Phytotaxa 286(4): 211–231. https://doi.org/10.11646/phytotaxa.286.4.1

Tulloss RE (2009) *Amanita magniverrucata* – revision of an interesting species of *Amanita* section *Lepidella*. Mycotaxon 108: 93–104. https://doi.org/10.5248/108.93

Tulloss RE (2016) (mutable text) Biometric Variables: Meanings and How to Define a Range. Studies in the Amanitaceae. http://www.amanitaceae.org/?How%20To%E2%80%99s&howto=8 [Accessed on 2018-11-21]

Tulloss RE, Bhandary HR (1992) *Amanita chepangiana* – a new species from Nepal. Mycotaxon 43: 25–31.

Tulloss RE, Iqbal SH, Khalid AN, Bhatt RP, Bhat VK (2001) Studies in *Amanita* (Amanitaceae) from southern Asia. I. Some species of Pakistan's Northwest Frontier Province. Mycotaxon 77: 455–490.

Tulloss RE, Yang ZL [Eds] (2018) Amanitaceae studies. http://www.amanitaceae.org [Accessed on: 2018-11-20]

Vargas N, Bernal A, Sarria V, Franco-Molano A, Restrepo S (2011) Amatoxin and phallotoxin composition in species of the genus *Amanita* in Colombia: a taxonomic perspective. Toxicon 58(6–7): 583–590. https://doi.org/10.1016/j.toxicon.2011.09.005

Vasco-Palacios AM, López-Quintero C, Franco-Molano AE, Boekhout T (2014) *Austroboletus amazonicus* sp. nov. and *Fistulinella campinaranae* var. *scrobiculata*, two commonly occurring boletes from a forest dominated by *Pseudomonotes tropenbosii* (Dipterocarpaceae) in Colombian Amazonia. Mycologia 106(5): 1004–1014. https://doi.org/10.3852/13-324

Wartchow F, Cortez VG (2016) A new species of *Amanita* growing under *Eucalyptus* is discovered in south Brazil. Mycosphere 7: 262–267. https://doi.org/10.5943/mycosphere/7/3/2

Wartchow F, Gamboa-Trujillo JP (2012) *Amanita chocoana* – a new species from Ecuador. Mycotaxon 121: 405–412. https://doi.org/10.5248/121.405

Wartchow F, Tulloss RE, Cavalcanti MA (2009) *Amanita lippiae*: a new species from the semi-arid caatinga region of Brazil. Mycologia 101: 864–870. https://doi.org/10.3852/08-106

Yang ZL (1997) Die *Amanita*-Arten von Südwestchina. Bibliotheca Mycologica 170: 1–240.

Yang ZL (2000) Species diversity of the genus *Amanita* (Basidiomycetes) in China. Acta Botanica Yunnanica 22: 135–142.

Yang ZL (2005) Flora fungorum sinicorum. Vol. 27. Amanitaceae. Science Press, Beijing, 1–258 [In Chinese]

Yang ZL (2015) Atlas of the Chinese species of Amanitaceae. Science Press, Beijing, 1–213 [In Chinese]

Yang ZL, Cai Q, Cui YY (2018) Phylogeny, diversity and morphological evolution of Amanitaceae. Biochemical Systematics and Ecology 34: 359–380.

Zhang LF, Yang JB, Yang ZL (2004) Molecular phylogeny of eastern Asian species of *Amanita* (Agaricales, Basidiomycota): taxonomic and biogeographic implications. Fungal Diversity 17: 219–238.

MycoKeys 56: 101–129 (2019)
doi: 10.3897/mycokeys.56.37636
http://mycokeys.pensoft.net

RESEARCH ARTICLE

A peer-reviewed open-access journal
MycoKeys
Launched to accelerate biodiversity research

Phylogenetic and morphological classification of *Ophiocordyceps* species on termites from Thailand

Kanoksri Tasanathai[1], Wasana Noisripoom[1], Thanyarat Chaitika[1], Artit Khonsanit[1], Sasitorn Hasin[2], Jennifer Luangsa-ard[1]

1 *Plant Microbe Interaction Research Team, Bioscience and Biotechnology for Agriculture, BIOTEC, NSTDA, 113 Thailand Science Park, Phahonyothin Rd., Khlong Nueng, Khlong Luang, Pathum Thani 12120, Thailand* **2** *Innovation of Environmental Management, College of Innovative Management, Valaya Alongkorn Rajabhat University under the Royal Patronage, Khlong Luang, Pathum Thani 12120, Thailand*

Corresponding author: *Jennifer Luangsa-ard* (jajen@biotec.or.th)

Academic editor: *Marc Stadler* | Received 24 June 2019 | Accepted 22 July 2019 | Published 29 July 2019

Citation: Tasanathai K, Noisripoom W, Chaitika T, Khonsanit A, Hasin S, Luangsa-ard J (2019) Phylogenetic and morphological classification of *Ophiocordyceps* species on termites from Thailand. MycoKeys 56: 101–129. https://doi.org/10.3897/mycokeys.56.37636

Abstract

Seven new species occurring on termites are added to *Ophiocordyceps* – *O. asiatica*, *O. brunneirubra*, *O. khokpasiensis*, *O. mosingtoensis*, *O. pseudocommunis*, *O. pseudorhizoidea* and *O. termiticola*, based on morphological and molecular phylogenetic evidence. *O. brunneirubra* possesses orange to reddish-brown immersed perithecia on cylindrical to clavate stromata. *O. khokpasiensis*, *O. mosingtoensis* and *O. termiticola* have pseudo-immersed perithecia while *O. asiatica*, *O. pseudocommunis* and *O. pseudorhizoidea* all possess superficial perithecia, reminiscent of *O. communis* and *O. rhizoidea*. Phylogenetic analyses based on a combined dataset comprising the internal transcribed spacer regions (ITS) and the largest subunit (LSU) of the ribosomal DNA, partial regions of the elongation factor 1-α (*TEF*) and the largest and second largest subunits for the RNA polymerase genes (*RPB1*, *RPB2*) strongly support the placement of these seven new species in *Ophiocordyceps*.

Keywords

Entomopathogenic fungi, Hypocreales, Isoptera, Ophiocordycipitaceae, Taxonomy

Introduction

The entomopathogenic genus *Ophiocordyceps* was established by Petch in 1931. His description was based on four specimens including *O. blattae* Petch, the type species, occurring on a cockroach collected from Sri Lanka, *O. unilateralis* (Tul. & C. Tul.) Petch on ants, *O. peltata* (Wakef.) Petch on Coleoptera larva (*Cryptorhynchus* sp.) and *O. rhizoidea* (Höhn.) Petch on Coleoptera larva. The distinction of the genus from *Cordyceps* Fr. was made due the presence of clavate asci that gradually narrowed to a thickened apex, as opposed to the cylindrical asci in many *Cordyceps* species. The ascospores in *Ophiocordyceps sensu* Petch are elongated fusoid, multi-septate that remain whole after discharge. Sung et al. (2007) emended the definition of *Ophiocordyceps* to contain the anamorphic genera *Hirsutella* Pat., *Hymenostilbe* Petch, *Paraisaria* Samson & Brady and *Synglíocladium* Petch, with the stromata or subiculum of the teleomorphs mostly darkly pigmented [e.g. *O. acicularis* (Ravenel) Petch, *O. heteropoda* (Kobayasi) G.H. Sung, J.M. Sung, Hywel-Jones & Spatafora, *O. entomorrhiza* (Dicks.) G.H. Sung, J.M. Sung, Hywel-Jones & Spatafora, *O. unilateralis* species complex] and sometimes brightly coloured [e.g. *O. irangiensis* (Moureau) G.H. Sung, J.M. Sung, Hywel-Jones & Spatafora, *O. nutans* (Pat.) G.H. Sung, J.M. Sung, Hywel-Jones & Spatafora, *O. sphecocephala* (Klotzsch ex Berk.) G.H. Sung, J.M. Sung, Hywel-Jones & Spatafora]. The ascospores are usually cylindrical, multi-septate that could either dissociate into part-spores (*O. sphecocephala*, *O. nutans*) or remain whole ascospores (*O. unilateralis*). To date, *Ophiocordyceps* is the most speciose genus in Ophiocordycipitaceae with 235 names of accepted species (Spatafora et al. 2015; Khonsanit et al. 2018; Luangsa-ard et al. 2018). Most Asian species of *Ophiocordyceps* have fibrous, hard and pliant to wiry, dark coloured stromata with superficial to immersed perithecia (Kobayasi 1941; Kobmoo et al. 2012, 2015; Luangsa-ard et al. 2018).

Only a few species of entomopathogenic fungi have been reported from termites. Currently accepted species include *Ophiocordyceps bispora* (Stifler) G.H. Sung, J.M. Sung, Hywel-Jones & Spatafora on *Macrotermes* from Tanzania, *O. koningsbergeri* (Penz. & Sacc.) G.H. Sung, J.M. Sung, Hywel-Jones & Spatafora, known only from the type locality (Java, Indonesia) (Kobayasi 1941), *C. termitophila* Kobayasi & Shimizu known from Japan and Taiwan (Kobayasi and Shimizu 1978) and *O. octospora* (M. Blackw. & Gilb.) G.H. Sung, J.M. Sung, Hywel-Jones & Spatafora on *Tenuirostritermes* from Mexico (Blackwell and Gilbertson 1981). Penzig and Saccardo (1904) found *O. koningsbergeri* to be similar to *O. myrmecophila* (Ces., in Rabenshorst 1858) G.H. Sung, J.M. Sung, Hywel-Jones & Spatafora in that it had a terminal, globose head with immersed perithecia.

Termites (Isoptera) are one of the eusocial and soil insects that have successfully evolved since the Cretaceous Period and are classified into 7 families, 14 subfamilies, 280 genera and 2,500 species (Pearce 1999). They occur throughout tropic and subtropic regions and can also be found in many temperate areas and semi-arid environments of the world (Eggleton et al. 2000). Termites are abundant in Thailand and are found in natural forests as well as urban areas, mostly considered as serious pests of

wooden constructions. Current records of termite species from Thailand have been 199 species, 39 genera, 10 subfamilies and 4 families (Sornnuwat et al. 2004). Relationships between termites and fungi are classified into two categories. Firstly, termites cultivate fungi (*Termitomyces* spp.) in their fungus gardens within the subterranean nest or mound of fungus-growing termites (subfamily Macrotermitinae). Secondly, a parasitic interaction, in which fungi infect and consume termites as food for its nutrient value (Abe et al. 2000). Some species of fungi are known as pathogens of termites and they can be used as potential agents of biological control for each of the host's (i.e. termites) specificities (Rath 2000).

In surveys of entomopathogenic fungi in national parks and community forests collections of termite pathogens, most with superficial perithecia and rarely with immersed perithecia were found. The phenotypic characters of the collections in having wiry and pliant, darkly pigmented stromata identifies them primarily to be members of the Ophiocordycipitaceae, mostly as *Ophiocordyceps communis*. The aims of this study are (1) to clarify the relationships of these collections to known members of the Ophiocordycipitaceae, (2) to uncover hidden species in *O. communis* species complex and (3) to describe new taxa to accommodate species diversity in *Ophiocordyceps*.

Material and methods

Collection and isolation

Species occurring on termites (Isoptera) were found in the ground. The specimens were excavated carefully so as not to lose the host, which could be buried as deep as 15 cm under the ground and were placed in small plastics boxes before returning to the laboratory for isolation. The materials were examined under a stereomicroscope (OLYMPUS SZ61, Olympus Corporation, Japan). The fertile heads of the specimens containing mature perithecia were carefully placed over the Potato Dextrose Agar plate (PDA; fresh diced potato 200 g, dextrose 20 g, agar 15 g, in 1 litre distilled water). These were placed in a plastic box with moist tissue paper overnight to create a humid chamber. The following morning plates were examined with a stereomicroscope to check the discharged ascospores. Discharged ascospores were examined daily for germination and also for fungal contaminants.

Morphological study

The newly collected specimens were noted and photographed in the field using a digital Nikon D5100 camera and were taken to the laboratory and photographed using an Olympus SZX12 before they were placed in a moist chamber to facilitate ascospore discharge. The colour of the freshly collected specimens and cultures were characterised with the colour standard of the Online Auction Colour Chart. One to two perithecia

were removed from the stroma and mounted on a glass slide using lactophenol cotton blue to measure their sizes and shapes, as well as the sizes and shapes of the asci and ascospores. Cultures on PDA, Potato Sucrose Agar plate (PSA: potato 200 g/l, sucrose 20 g/l, calcium carbonate 5g/l, agar 20g/l) and quarter strength Sabouraud Dextrose Yeast Agar (SDYA/4; Difco) were observed using light microscopy (Olympus SZ60, CX 30) daily to check for germination and contamination for 2–3 wks. Colony growth rates and characteristics (colour, texture, pigmentation) under dark/light condition (L:D = 14:10) were recorded and photos were taken using the Nikon D5100 camera.

For micro-morphological description, microscope slide cultures were prepared from a block of media (PDA, PSA and SDYA/4, ca. 5 × 5 mm^2) inoculated with the fungus and overlaid by a glass coverslip. The cultures were incubated at 25 °C. Observations, measurements of the conidiogenous cells and conidia of the asexual morphs and photographs were taken with an Olympus DP11 microscope.

Host identification

Dead termite hosts were identified, based on morphological characteristics, such as mandibulate mouthparts, antennae, shape of head and thoraxes. The identification of dead insects was conducted after pure cultures were acquired. Termites were identified by using the extant families of Isoptera after Sornnuwat et al. (2004) and Krishna et al. (2013).

DNA extraction, PCR amplification and sequencing

Cultivation of fungi for molecular work. – Pure cultures were grown on PDA. After approximately 2 wks, the plates were checked for contaminants and small agar blocks were inoculated into sterile Erlenmeyer flasks containing 50 ml Sabouraud Dextrose Broth (Difco) and incubated for 1–2 wks at 25 °C without shaking. Mycelium was then harvested by filtration and washed several times with sterile distilled water. Filtered mycelium was lyophilised. The material was extracted from mycelium by a modified CTAB method as previously described (Luangsa-ard et al. 2004, 2005).

PCR amplification. – Five nuclear loci including the nuc rDNA region encompassing the internal transcribed spacers 1 and 2, along with the 5.8S rDNA (ITS), nuc 28S rDNA (*LSU*), the translation elongation factor 1-α gene (*TEF*) and the genes for RNA polymerase II largest (*RPB*1) and second largest (*RPB*2) subunits were sequenced. PCR primers used to amplify the gene regions for this study were: ITS5, ITS4 for ITS, LROR and LR7 for *LSU* (White et al. 1990), 983F and 2218R for *TEF*, CRPB1 and RPB1Cr for *RPB*1, RPB2-5F2 and RPB2-7Cr for *RPB*2 (Castlebury et al. 2004). The PCR reaction mixture consisted of 1× PCR buffer, 200 μM of each of the four dNTPs, 2.5 mM $MgCl_2$, 0.4 M Betaine, 1 U Taq DNA Polymerase, recombinant (Thermo Scientific, US) and 0.2 μM of each primer in a

total volume of 50 µl. PCR cycle conditions were as previously described in Sung et al. (2007). PCR amplicons were visualised by ethidium bromide staining after gel electrophoresis of 4 µl of the product in 0.8% agarose gel. Quantification of the PCR products was performed using a standard DNA marker of known size and weight. PCR products were purified using Qiagen columns (QIAquick PCR Purification Kit). Purified PCR products were sequenced with the PCR amplification primers.

Sequencing alignment and phylogenetic analyses

The DNA sequences, generated in this study, were examined for ambiguous bases using BioEdit 7.2.5 (Hall 2004) and then submitted to GenBank (Table 1). The dataset of taxa in Cordycipitaceae was assembled from previously published studies (Sung et al. 2007; Kepler et al. 2017) and were downloaded from GenBank for the construction of the phylogenetic tree (Table 1). Alignments were performed using MUSCLE 3.6 software with default settings (Edgar 2004). Sequences of *Cordyceps kyusyuensis* and *Cordyceps militaris* in the *Cordycipitaceae* were used as the outgroup.

Maximum Likelihood (ML) analyses was performed with RAxML-HPC2 on XSEDE v8.2.10 (Stamatakis 2014) with the use of GAMMA Model parameters. The reliability of ML internal branches was assessed using a non-parametric bootstrap method with 1000 replicates. Bayesian (BI) phylogenetic inference was performed with MrBayes on XSEDE v3.2.6 (Ronquist and Huelsenbeck 2003) using the GTR+I+G model as selected by MrModeltest v2.2 (Nylander 2004). The chain length of the Bayesian analyses was 5,000,000 generations, sampled every 1000 generations and a burn-in of 10% of the total run. Maximum parsimony analysis was conducted on the combined dataset using PAUP 4.0b10 (Swofford 2002).

Results

Phylogenetic analysis

We obtained 96 new sequences from 20 specimens (Table 1). The combined dataset of five genes consisted of 4013 bp (ITS 527 bp, *LSU* 824 bp, *TEF* 901 bp, *RPB1* 874 bp, *RPB2* 854 bp) and 99 taxa were analysed.

The ML and BI analyses displayed similar topologies resolving seven new species in *Ophiocordyceps* (Fig 1). The final ML optimisation likelihood = -51972.210615 and tree length = 5.567057. The parameters included base frequencies—A = 0.227576, C = 0.299408, G = 0.284488, T = 0.188528 and the rate matrix for the substitution model: [AC] = 1.240734, [A-G] = 2.882814, [A-T] = 0.983408, [C-G] = 1.338444, [C-T] = 5.445401, [G-T] = 1. 000000. In the BI analyses, the model selected was GTR+I+G, -lnL = 52578.1641. The parameters used included base frequencies—freqA = 0.1918,

Table 1. List of species and GenBank accession numbers of sequences used in this study.

Species	Strain nr.	Host/Substratum	GenBank accession no.				
			ITS rDNA	LSU	*TEF*	*RPB1*	*RPB2*
Cordyceps kyusyuensis	EFCC 5886	Lepidoptera	–	EF468813[1]	EF468754[1]	EF468863[1]	EF468917[1]
Cordyceps militaris	OSC 93623	Lepidoptera	JN049825[1]	AY184966[1]	DQ522332[1]	DQ522377[1]	AY545732[1]
Drechmeria gunnii	OSC 76404	Lepidoptera (pupa)	–	AF339522[2]	AY489616[2]	AY489650[2]	DQ522426[2]
Drechmeria sinensis	CBS 567.95	Nematoda	AJ292417[2]	AF339545[2]	DQ522343[2]	DQ522389[2]	DQ522443[2]
Hirsutella cf. *haptospora*	ARSEF 2228	Diptera: Itonididae	KM652166[3]	KM652118[3]	KM652001[3]	KM652041[3]	–
Hirsutella citriformis	ARSEF 1446	Hemiptera; Cixiidae	KM652154[3]	KM652106[3]	KM651990[3]	KM652031[3]	–
	ARSEF 1035	Hemiptera; Cixiidae	KM652153[3]	KM652105[3]	KM651989[3]	KM652030[3]	–
Hirsutella cryptosclerotium	ARSEF 4517	Hemiptera; Pseudococcidae	KM652157[3]	KM652109[3]	KM651992[3]	KM652032[3]	–
Hirsutella fusiformis	ARSEF 5474	Coleoptera: Curculionidae	–	KM652110[3]	KM651993[3]	KM652033[3]	–
Hirsutella gigantea	ARSEF 30	Hymenoptera: Pamphiliidae	–	–	JX566980[3]	KM652034[3]	–
Hirsutella haptospora	ARSEF 2226	Acari: Uropodina	KM652159[3]	–	KM651995[3]	KM652036[3]	–
Hirsutella illustris	ARSEF 5539	Hemiptera: Aphididae	KM652160[3]	KM652112[3]	KM651996[3]	KM652037[3]	–
Hirsutella lecaniicola	ARSEF 8888	Hemiptera: Coccidae	KM652162[3]	KM652114[3]	KM651998[3]	KM652038[3]	–
Hirsutella liboensis	ARSEF 9603	Lepidoptera: Cossidae	KM652163[3]	KM652115[3]	–	–	–
Hirsutella necatrix	ARSEF 5549	Acari	KM652164[3]	KM652116[3]	KM651999[3]	KM652039[3]	–
Hirsutella nodulosa	ARSEF 5473	Lepidoptera; Pyralidae	KM652165[3]	KM652117[3]	KM652000[3]	KM652040[3]	–
Hirsutella radiata	ARSEF 1369	Diptera	–	KM652119[3]	KM652002[3]	KM652042[3]	–
Hirsutella repens nom. inval.	ARSEF 2348	Hemiptera: Delphacidae	KM652167[3]	KM652120[3]	KM652003[3]	–	–
Hirsutella rhossiliensis	ARSEF 2931	Tylenchida: Heteroderidae	KM652168[3]	KM652121[3]	KM652004[3]	KM652043[3]	–
Hirsutella satumaensis	ARSEF 996	Lepidoptera: Pyralidae	KM652172[3]	KM652125[3]	KM652008[3]	KM652047[3]	–
Hirsutella sp.	ARSEF 8378	Hemiptera: Cixiidae	–	KM652127[3]	KM652010[3]	KM652049[3]	–
Hirsutella strigosa	ARSEF 2197	Hemiptera: Cicadellidae	KM652175[3]	KM652129[3]	KM652012[3]	KM652050[3]	–
	ARSEF 2044	Hemiptera: Delphacidae	KM652174[3]	KM652128[3]	KM652011[3]	–	–
Hirsutella subulata	ARSEF 2227	Lepidoptera: Microlepidoptea	KM652176[3]	KM652130[3]	KM652013[3]	KM652051[3]	–
Hirsutella thompsonii	ARSEF 257	Acari; Eriophyidae	KM652182[3]	KM652136[3]	KM652019[3]	KM652054[3]	–
	ARSEF 414	Acari; Eriophyidae	KM652184[3]	KM652139[3]	KM652021[3]	KM652056[3]	–
	ARSEF 3323	Acari: Tenuipalpidae	KM652188[3]	KM652143[3]	KM652024[3]	KM652059[3]	–
	ARSEF 3482		KM652189[3]	KM652144[3]	KM652025[3]	KM652060[3]	–
	ARSEF 253	Acari: Eriophyidae	KM652179[3]	KM652133[3]	KM652016[3]	–	–
	ARSEF 256	Acari: Eriophyidae	KM652181[3]	KM652135[3]	KM652018[3]	KM652053[3]	–
	ARSEF 258	Acari: Eriophyidae	–	KM652137[3]	KM652020[3]	KM652055[3]	–
	ARSEF 2800	Acari	KM652187[3]	KM652142[3]	KM652023[3]	KM652058[3]	–
Hirsutella thompsonii "var. *synnematosa*"	ARSEF 1947	Acari: Tarsonemidae	KM652191[3]	KM652146[3]	KM652026[3]	–	–
	ARSEF 5412	Acari: Tetranychidae	KM652193[3]	KM652148[3]	–	–	–
Hirsutella thompsonii var. *vinacea*	ARSEF 254	Acari: Eriophyidae	KM652194[3]	KM652149[3]	KM652028[3]	KM652062[3]	–
Hirsutella versicolor	ARSEF 1037	Hemiptera: Membracidae	–	KM652150[3]	KM652029[3]	KM652063[3]	–
Ophiocordyceps acicularis	OSC 110988	Coleoptera (larva)	–	EF468804[2]	EF468745[2]	EF468853[2]	–
	OSC 110987	Coleoptera (larva)	–	EF468805[2]	EF468744[2]	EF468852[2]	–
Ophiocordyceps agriotidis	ARSEF 5692	Coleoptera (larva)	JN049819[2]	DQ518754[2]	DQ522322[2]	DQ522368[2]	DQ522418[2]

Species	Strain nr.	Host/Substratum	GenBank accession no.				
			ITS rDNA	LSU	*TEF*	*RPB1*	*RPB2*
Ophiocordyceps aphodii	ARSEF 5498	Coleoptera	–	DQ518755[2]	DQ522323[2]	–	DQ522419[2]
Ophiocordyceps appendiculata	NBRC 106960	Coleoptera (larva)	JN943326[2]	JN941413[2]	–	JN992462[2]	–
Ophiocordyceps asiatica	**BCC 30516**	**Termitidae (adult termite)**	**MH754722**	**MH753675**	**MK284263**	**MK214105**	**MK214091**
	BCC 86435	**Termitidae (adult termite)**	**MH754723**	**MH753676**	**–**	**MK214106**	**MK214092**
Ophiocordyceps communis	**BCC 1842**	**Termitidae (adult termite)**	**MH754726**	**MH753680**	**MK284266**	**MK214110**	**MK214096**
	BCC 1874	**Termitidae (adult termite)**	**MH754725**	**MH753679**	**MK284267**	**MK214109**	**MK214095**
	BCC 2754	**Termitidae (adult termite)**	**MH754727**	**MH753681**	**MK284268**	**MK214111**	**MK214097**
Ophiocordyceps brunneipunctata	OSC 128576	Coleoptera (Elateridae larva)	–	DQ518756[2]	DQ522324[2]	DQ522369[2]	DQ522420[2]
Ophiocordyceps brunneirubra	**BCC 14384**	**Termitidae (adult termite)**	**MH754736**	**MH753690**	**GU797121**	**MK751465**	**MK751468**
	BCC 14478	**Termitidae (adult termite)**	**MH754734**	**MH753688**	**GU797122**	**MK751466**	**MK214102**
	BCC 14477	**Termitidae (adult termite)**	**MH754735**	**MH753689**	**GU797123**	**MK751467**	**MK214103**
Ophiocordyceps dipterigena	OSC 151911	Diptera (adult fly)	–	KJ878886[4]	KJ878966[4]	KJ879000[4]	–
Ophiocordyceps elongata	OSC 110989	Lepidoptera (larva)	–	EF468808[2]	EF468748[2]	EF468856[2]	–
Ophiocordyceps gracilioides	HUA 186095	Coleoptera (Elateridae larva)	–	–	KM411994[2]	KP212914[2]	–
	HUA 186092	Coleoptera (Elateridae larva)	–	KJ130992[2]	–	KP212915[2]	–
Ophiocordyceps gracilis	EFCC 8572	Lepidoptera (larva)	JN049851[2]	EF468811[2]	EF468751[2]	EF468859[2]	EF468912[2]
	EFCC 3101	Lepidoptera (larva)	–	EF468810[2]	EF468750[2]	EF468858[2]	EF468913[2]
Ophiocordyceps granospora	BCC 82255	Hymenoptera (*Polyrhachis* sp.)	MH028143[4]	MH028156[4]	MH028183[4]	MH02816[4]	MH02817[4]
Ophiocordyceps heteropoda	EFCC 10125	Hemiptera (cicada nymph)	JN049852[2]	EF468812[2]	EF468752[2]	EF468860[2]	EF468914[2]
Ophiocordyceps irangiensis	BCC 82793	Hymenoptera (*Polyrhachis illaudata*)	MH028141[4]	–	MH028185[4]	MH028163[4]	MH02817[4]
	BCC 82795	Hymenoptera (*Polyrhachis* sp.)	MH028142[4]	–	MH028186[4]	MH028164[4]	MH02817[4]
Ophiocordyceps khaoyaiensis	BCC 82796	Hymenoptera (*Polyrhachis armata*)	MH028150[4]	MH028153[4]	MH028187[4]	MH028165[4]	MH02817[4]
	BCC 82797	Hymenoptera (*Polyrhachis armata*)	MH028151[4]	MH028154[4]	MH028188[4]	MH028166[4]	MH02817[4]
Ophiocordyceps khokpasiensis	**BCC 48071**	**Termitidae (adult termite)**	**MH754728**	**MH753682**	**MK284269**	**MK214112**	**–**
	BCC 48072	**Termitidae (adult termite)**	**MH754729**	**MH753683**	**MK284270**	**MK214113**	**–**
	BCC 1764	**Termitidae (adult termite)**	**MH754730**	**MH753684**	**MK284271**	**MK214114**	**MK214098**
Ophiocordyceps konnoana	EFCC 7315	Coleoptera (larva)	–	–	EF468753[2]	EF468861[2]	EF468916[2]
Ophiocordyceps longissima	NBRC 108989	Hemiptera (cicada nymph)	AB968407[1]	AB968421[1]	AB968585[1]	–	–
	EFCC 6814	Hemiptera (cicada nymph)	–	EF468817[2]	EF468757[2]	EF468865[2]	–

Species	Strain nr.	Host/Substratum	GenBank accession no.				
			ITS rDNA	LSU	*TEF*	*RPB1*	*RPB2*
Ophiocordyceps mosingtoensis	**BCC 30904**	**Termitidae (adult termite)**	**MH754732**	**MH753686**	**MK284273**	**MK214115**	**MK214100**
	BCC 36921	**Termitidae (adult termite)**	**MH754731**	**MH753685**	**MK284272**	**MK214116**	**MK214099**
Ophiocordyceps myrmecophila	CEM **1710**	Hymenoptera (Adult ant)	–	KJ878894[4]	KJ878974[4]	KJ879008[4]	–
Ophiocordyceps myrmicarum	ARSEF 11864	Hymenoptera: Formicidae	–	–	JX566973[3]	KJ680151[3]	–
Ophiocordyceps nigrella	EFCC 9247	Lepidoptera (larva)	JN049853[2]	EF468818[2]	EF468758[2]	EF468866[2]	EF468920[2]
Ophiocordyceps pseudocommunis	**BCC 16757**	**Termitidae (adult termite)**	**MH754733**	**MH753687**	**MK284274**	**MK214117**	**MK214101**
Ophiocordyceps pseudocommunis	NHJ 12581	Termitidae (adult termite)	–	EF468831[3]	EF468775[3]	–	EF468930[3]
	NHJ 12582	Termitidae (adult termite)	–	EF468830[3]	EF468771[3]	–	EF468926[3]
Ophiocordyceps pseudorhizoidea	**BCC 48879**	**Termitidae (adult termite)**	**MH754720**	**MH753673**	**MK284261**	**MK214104**	**MK214089**
	BCC 86431	**Termitidae (adult termite)**	**MH754721**	**MH753674**	**MK284262**	**MK751469**	**MK214090**
	NHJ 12522	**Termitidae (adult termite)**	**JN0498572**	**EF4688252**	**EF4687642**	**EF4688732**	**EF4689232**
	NHJ 12529	**Termitidae (adult termite)**	**–**	**EF4688242**	**EF4687652**	**EF4688722**	**EF4689222**
Ophiocordyceps pulvinata	TNS-F-30044	Hymenoptera	**–**	–	GU904209[5]	GU904210[5]	**–**
Ophiocordyceps ravenelii	OSC 110995	Coleoptera (larva)	–	DQ518764[2]	DQ522334[2]	DQ522379[2]	–
Ophiocordyceps robertsii	KEW 27083	Lepidoptera (Hepialidae larva)	–	EF468826[2]	EF468766[2]	–	–
Ophiocordyceps satoi	J7	Hymenoptera (*Polyrhachis lamellidens*)	**–**	KX713599[5]	KX713683[5]	KX713711[5]	**–**
	J19	Hymenoptera (*Polyrhachis lamellidens*)	**–**	KX713601[5]	KX713684[5]	KX713710[5]	**–**
Ophiocordyceps sinensis	ARSEF 6282	Lepidoptera; Hepialidae	KM652173[3]	KM652126[3]	KM652009[3]	KM652048[3]	–
	EFCC 7287	Lepidoptera; Hepialidae (larva)	JN049854[2]	EF468827[2]	EF468767[2]	EF468874[2]	EF468925[2]
Ophiocordyceps sobolifera	KEW 78842	Hemiptera (cicada nymph)	JN049855[2]	EF468828[2]	–	EF468875[2]	DQ522432[2]
Ophiocordyceps spataforae	NHJ 12525	Hemiptera	–	EF469078[6]	EF469063[6]	EF469092[6]	EF469111[6]
	OSC 128575	Hemiptera	–	EF469079[6]	EF469064[6]	EF469093[6]	EF469110[6]
Ophiocordyceps sphecocephala	NBRC 101416	Hymenoptera (adult wasp)	–	JN941443[4]	–	JN992432[4]	–
Ophiocordyceps stylophora	OSC 111000	Coleoptera; Elateridae (larva)	JN049828[2]	DQ518766[2]	DQ522337[2]	DQ522382[2]	–
Ophiocordyceps termiticola	**BCC 1920**	**Termitidae (adult termite)**	**MH754724**	**MH753678**	**MK284265**	**MK214108**	**MK214094**
	BCC 1770	**Termitidae (adult termite)**	**GU723780**	**MH753677**	**MK284264**	**MK214107**	**MK214093**
Ophiocordyceps unilateralis	OSC 128574	Hymenoptera	–	DQ518768[2]	DQ522339[2]	DQ522385[2]	DQ522436[2]
Ophiocordyceps xuefengensis	GZUHHN 13	Lepidoptera; Phassus nodus (larva)	KC631804[2]	–	KC631790[2]	KC631795[2]	–
Ophiocordyceps yakusimensis	HMAS 199604	Hemiptera; (cicada nymph)	–	KJ878902[2]	–	KJ879018[2]	KJ878953[2]
Purpureocillium lilacinum	CBS 284.36	Soil	AY624189[2]	–	EF468792[2]	EF468898[2]	EF468941[2]
	CBS 431.87	Nematoda	AY624188[2]	EF468844[2]	EF468791[2]	EF468897[2]	EF468940[2]

Note. The accession numbers marked in bold font refer to sequences new in this study or have been generated by our group in Thailand. [1]Ban et al. (2015),[2]Sanjuan et al. (2015), [3]Simmons et al. (2015), [4]Khonsanit et al. (2018), [5]Araújo et al. (2018), [6]Luangsa-ard et al. (2018)

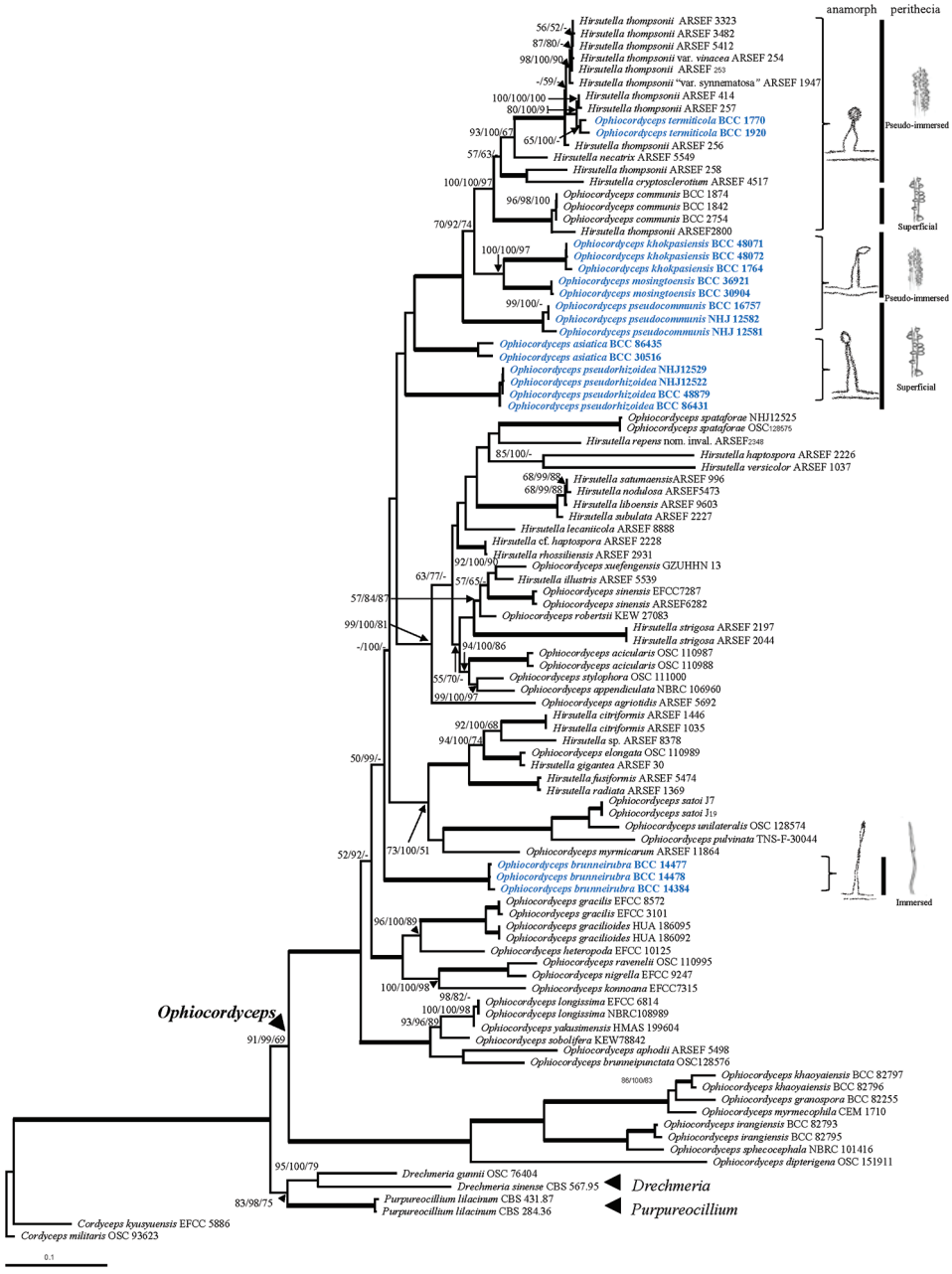

Figure 1. Phylogenetic tree based on combined data set of ITS, LSU, *TEF*, *RPB1* and *RPB2* sequences showing the relationship of seven new species on termites from Thailand with other species of *Ophiocordyceps*. Numbers above lines at significant nodes represent Maximum Likelihood bootstrap values, Bayesian posterior probabilities and MP bootstrap values. Bold lines mean support for the tree analyses were 100%.

freqC = 0.3427, freqG = 0.2769, freqT = 0.1886 and the rate matrix for the substitution model: [AC] = 1.2356, [A-G] = 3.1814, [A-T] = 1.1029, [C-G] = 1.1220, [C-T] = 4.7720, [G-T] = 1.0000. The MP analyses resulted in 32 equally most parsimonious trees with 4013 characters, 1912 of which are constant, 355 are variable and parsimony-uninformative, while 1746 are parsimony-informative and tree length has 10669 steps (CI, 0.348; RI, 0.689; RC, 0.240; HI, 0.652).

Taxonomy

Ophiocordyceps asiatica **Tasanathai, Noisripoom & Luangsa-ard, sp. nov.**
MycoBank MB 831297
Figure 2

Typification. THAILAND. Nakhon Ratchasima Province, Khao Yai National Park; 14°711'N, 101°421'E; on termite; 21 May 2008; K. Tasanathai, S. Mongkolsamrit, B. Thongnuch, P. Srikitikulchai, R. Ridkaew, A. Khonsanit (holotype BBH 38718 dried culture; ex-type living culture, BCC 30516). GenBank: ITS = MH754722, LSU = MH753675, *TEF* = MK284263, *RPB1* = MK214105, *RPB2* = MK214091

Etymology. '*asiatica*' referring to Asia.

Description. Stroma solitary, simple, filiform, up to 15 cm long, 1 mm wide, orange-brown (oac48-50), ca. 10 cm emerging above leaf litter, 5 cm buried in the soil. Asexual state (*Hirsutella*) produced at the terminal part of the stroma, ca. 2 cm long, light brown to grey. *Perithecia* superficial covering middle part of stroma, globose to subglobose, (240–)261.5–302(–320) × (180–)205–240.5(–260) µm. *Asci* 8-spored, filiform, (92.5–)104–143.5(–175) × 5–6.5 µm with cap, 2 × 2 µm. *Ascospores* whole, filiform, (80–)100–122.5(–132.5) × 1–2 µm, with septate. Asexual state *Hirsutella*, phialides arising singly or laterally from the hyphae along the terminal part of the stroma, (9–)9.5–13(–15) × (3–)3.5–4.8(–5) µm, *conidia* hyaline, fusiform, 4–5×2–3 µm.

Culture characteristics. Colonies on PDA, attaining a diam. of 27 mm after 20 d at 25 °C, mycelium sparse to abundant, grey in the middle to pale brown. *Conidiogenous cells* developing directly on the aerial mycelium, swollen towards the base, hyaline, smooth, tapering gradually towards the apex, which often forms a thin warty neck (1 µm), monophialidic or rarely polyphialidic 15–18.5(–20) × 2–3 µm µm. *Conidia* aseptate, hyaline, smooth, arising from phialides at the apex of each neck, fusiform, (7–)7.6–9 × 2–3 µm, with a mucous sheath.

Colonies on PSA, attaining a diam. of 25 mm after 20 d at 25 °C, *Conidiogenous cells* swollen towards the base, hyaline, smooth, tapering gradually towards the apex, which often forms a thin neck, monophialidic, (15–)17–21(–23) × 3–4 µm. *Conidia* aseptate, hyaline, smooth, arising from phialides at the apex of each neck, fusiform, (6–)6.5–8.5(–10) × 2–3 µm, with a mucous sheath.

Colonies on SDYA/4, slow-growing, attaining a diam. of 30 mm after 20 d at 25 °C. *Conidiogenous cells* swollen towards the base, hyaline, smooth, tapering gradu-

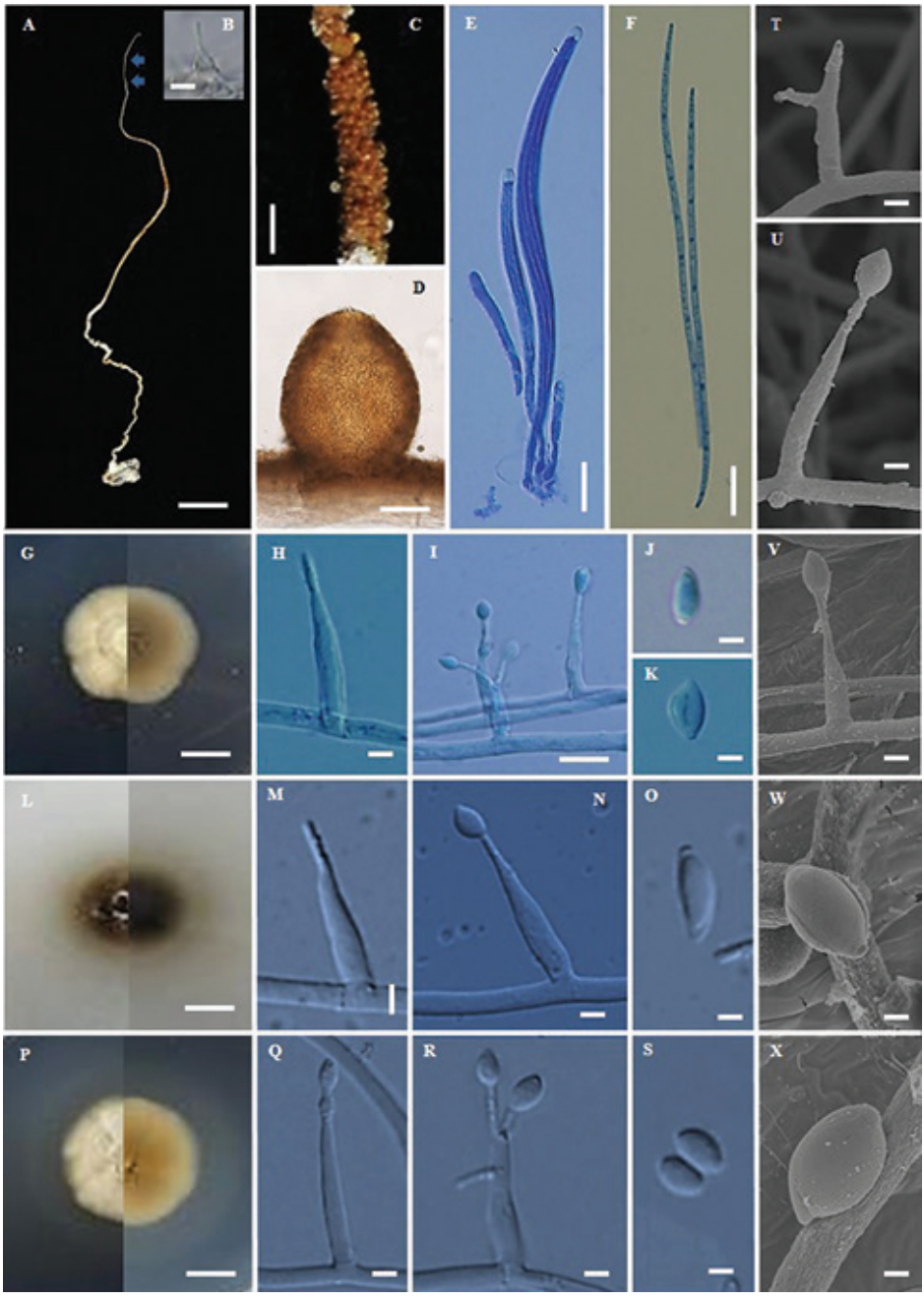

Figure 2. *Ophiocordyceps asiatica* (BBH38718, BCC30516) **A** stroma of fungus emerging from termite **B** phialide on specimen **C** part of stroma showing perithecia **D** perithecium **E** asci **F** ascospores **G** colony on PDA at 20 d obverse and reverse **H, I** phialides with conidia on PDA **J, K** conidium **L** colony on PSA at 20 d obverse and reverse **M, N** phialides with conidia on PSA **O** conidium **P** colony on SDYA/4 at 20 d obverse and reverse **Q, R** phialides with conidia **S** conidia **T–X** scanning electron micrographs of phialides with conidia on PDA. Scale bars: 10 mm (**A, G, L, P**); 5 µm (**B**); 1 mm (**C**); 8 µm (**D**); 15 µm (**E**); 10 µm (**F, I**); 3 µm (**H, J, K, M, N, S,T,V**); 2 µm (**O, Q, R, U,W, X**).

ally towards the apex, which often forms a thin neck, monophialidic or polyphialidic, (10–)12–15(–17) × (2–)2.5–3 µm. *Conidia* aseptate, hyaline, smooth, arising from phialides at the apex of each neck, fusiform, (7–)8.5–11.5(–13) × 2–3 µm, with a mucous sheath.

Distribution. Thailand, only known from Khao Yai National Park.

Ecology. Parasitic on a pair of termites from a reproductive caste (Order Isoptera: Family Termitidae, Subfamily Macrotermitinae) and these specimens were buried in the soil. The fungus emerged from the segment between the prothorax and mesothorax of one of the termite pairs.

Additional specimens examined. THAILAND. Saraburi Province, Khao Yai National Park; 14°586'N, 100°998'E; on termite; 4 June 2017; S. Mongkolsamrit, U. Pinruan, P. Srikitikulchai, R. Promharn, S. Sommai (BBH45363, BBC86435).

Notes. Four species, *O. asiatica*, *O. communis*, *O. pseudocommunis* and *O. pseudorhizoidea* look morphologically similar in having superficial perithecia and long wiry, pliant stroma emerging from the ground. In *O. asiatica* and *O. communis*, the stroma is dark brown, while in *O. pseudocommunis* and *O. pseudorhizoidea* it is cream to light brown. The perithecia in *O. communis*, *O. pseudocommunis* and *O. pseudorhizoidea* are larger than *O. asiatica*, but its ascospores are larger than in *O. pseudorhizoidea*.

Ophiocordyceps brunneirubra **Tasanathai, Noisripoom, Luangsa-ard & Hywel Jones, sp. nov.**

MycoBank MB 831289

Figure 3

Typification. THAILAND. Uthai Thani Province, Huai Kha Khaeng Wildlife Sanctuary; 15°605'N, 99°330'E; on termite; 28 August 2003; N.L. Hywel-Jones (holotype BBH 9008 dried culture; ex-type living culture: BCC14478). GenBank: ITS = MH754734, LSU = MH753688, *TEF* = GU797122, *RPB1* = MK751466, *RPB2* = MK214102

Etymology. '*brunneirubra*' referring to the reddish-brown appearance of the fertile head.

Description. Stroma solitary, simple or branched, narrowly clavate, slender and wiry, up to 9.5 cm long, 0.5 mm wide. Fertile head cylindric, orange brown (oac642) to red brown (oac635), up to 8 mm long, 1 mm wide. *Perithecia* immersed, ovoid, ordinal in arrangement, (300–)334.5–400(–403) × (130–)138.5–178(–200) µm. *Asci* 8-spored, cylindrical, (155–)176–214.5(–225) × 4.5–7(–8) µm. *Ascospores* whole, filiform, 156.5–197.5 × 2–3 µm, with septa.

Culture characteristics. Colonies on PDA, attaining a diam. of 25 mm within 20 d at 25 °C, orange (oac651) to orange brown (oac639). *Conidiogenous cells* monophialidic, arising from hyphae laterally or terminally, hyaline, tapering gradually or abruptly into a long slender neck, (32–)35.5–43.5(–50) µm long, (2–)2.5–3µm wide at the base, 1–1.5 µm wide at tip with warty surface. *Conidia* hyaline, one-celled, with

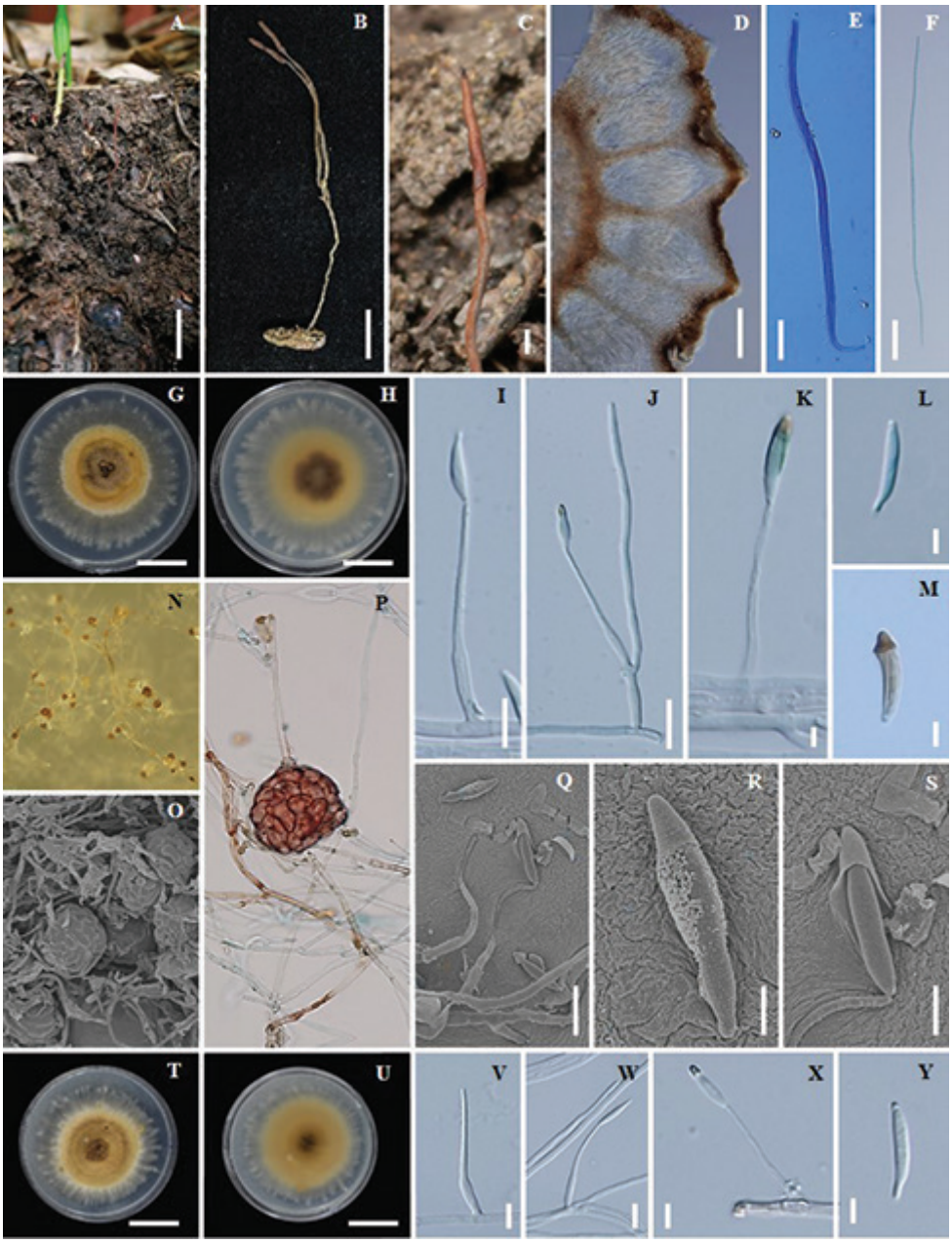

Figure 3. *Ophiocordyceps brunneirubra* (BBH 9008, BCC14478) **A, B** fungus on termite **C** part of stroma showing perithecia **D** immersed perithecia **E** asci **F** ascospore **G, H** colony on PDA at 20 d (**G**) colony obverse (**H**) colony reverse **I, J, K** phialides with conidia on PDA **L, M** conidia on PDA **N, P, O** sclerotia formed in culture **Q, R, S** scanning electron micrographs of phialides with conidia **T, U** colony on PSA at 20 d (**T**) colony obverse (**U**) colony reverse **V, W, X** phialides with conidia on PSA **Y** conidia on PSA. Scale bars: 25 mm (**A**); 15 mm (**B, G, H, T, U**); 1 mm (**C**); 130 µm (**D**); 10 µm (**I, Q, W**); 15 µm (**J**); 3 µm (**K, R**); 5 µm (**L**); 4 µm (**M, S, Y**); 6 µm (**V**); 7 µm (**X**).

a distinct gold cap covering the tip of the conidia, fusiform, (12–)13.5–15.5(–17) × 2–3 (–4) µm. Sclerotia formed in culture after 1 month, dark brown (oac635).

Colonies on PSA, attaining a diam. of 25 mm within 20 d at 25 °C, orange brown (oac716) to brown (oac721), reverse orange brown (oac721). *Conidiogenous cells* monophialidic, arising from hyphae laterally or terminally, hyaline, tapering gradually or abruptly into a long slender neck, (30–)32.5–39.5(–41) µm long, (2–)2.5–3.5(–4) µm wide at the base, 1–1.5 µm wide at tip with warty surface. *Conidia* hyaline, one-celled, arising from phialides, with a distinct gold cap covering the tip of the conidia, fusiform, (13–)14–16(–17) × 2–3 µm.

Colonies on SDYA/4, attaining a diam. of 25 mm within 20 d at 25 °C, dark brown (oac733), reverse orange brown (oac728). *Conidiogenous cells* monophialidic, arising from hyphae laterally or terminally, hyaline, tapering gradually or abruptly into a long slender neck, 25–40 µm long, 2–4 µm wide at the base, 1 µm wide at tip with warty surface. *Conidia* hyaline, one-celled, arising from phialides, with a distinct gold cap covering the tip of the conidia, fusiform, 12–15 × 2–3 µm.

Distribution. Thailand, only known from Huai Kha Kaeng Wildlife Sanctuary.

Ecology. Parasitic on a subterranean termite (Order Isoptera: Family Termitidae, Subfamily Macrotermitinae), collected from the soil. These termites belong to the reproductive caste (king or queen alates). The fungus emerged from between head and thoraxes of termite alates.

Additional specimens examined. THAILAND. Uthai Thani Province, Huai Kha Khaeng Wildlife Sanctuary; at 15°605'N, 99°330'E; on termites; 28 Aug 2003; N.L. Hywel-Jones (BBH9009, BCC14477), (BBH9005, BCC14384).

Notes. This species differs from other species on termites collected in Thailand in being singly infected by fungus instead of termite pairs and having immersed perithecia and red brown fertile terminal stroma. The species is not commonly found since it could easily be mistaken as a plant material sprouting from the ground. It is reminiscent of *O. brunneipunctata* but only on a different host. The shape of the conidia, like a banana with a hat or a cap, has never been seen in any kind of fungal spore morphology before.

Ophiocordyceps khokpasiensis **Tasanathai, Noisripoom & Luangsa-ard, sp. nov.**
MycoBank MB 831290
Figure 4

Typification. THAILAND. Kalasin Province, Phu Si Than Wildlife Sanctuary, Khok Pa Si Community Forest; 16°562'N, 104°103'E; on termite; 14 June 2011; K. Tasanathai, P. Srikitikulchai, A. Khonsanit, K. Sansatchanon, W. Noisripoom (holotype BBH32173 dried culture; ex-type living culture: BCC48071). GenBank: ITS = MH754728, LSU = MH753682, *TEF* = MK284269, *RPB1* = MK214112

Etymology. *'khokpasiensis'* referring to Khok Pa Si community forest, site of collection of type species.

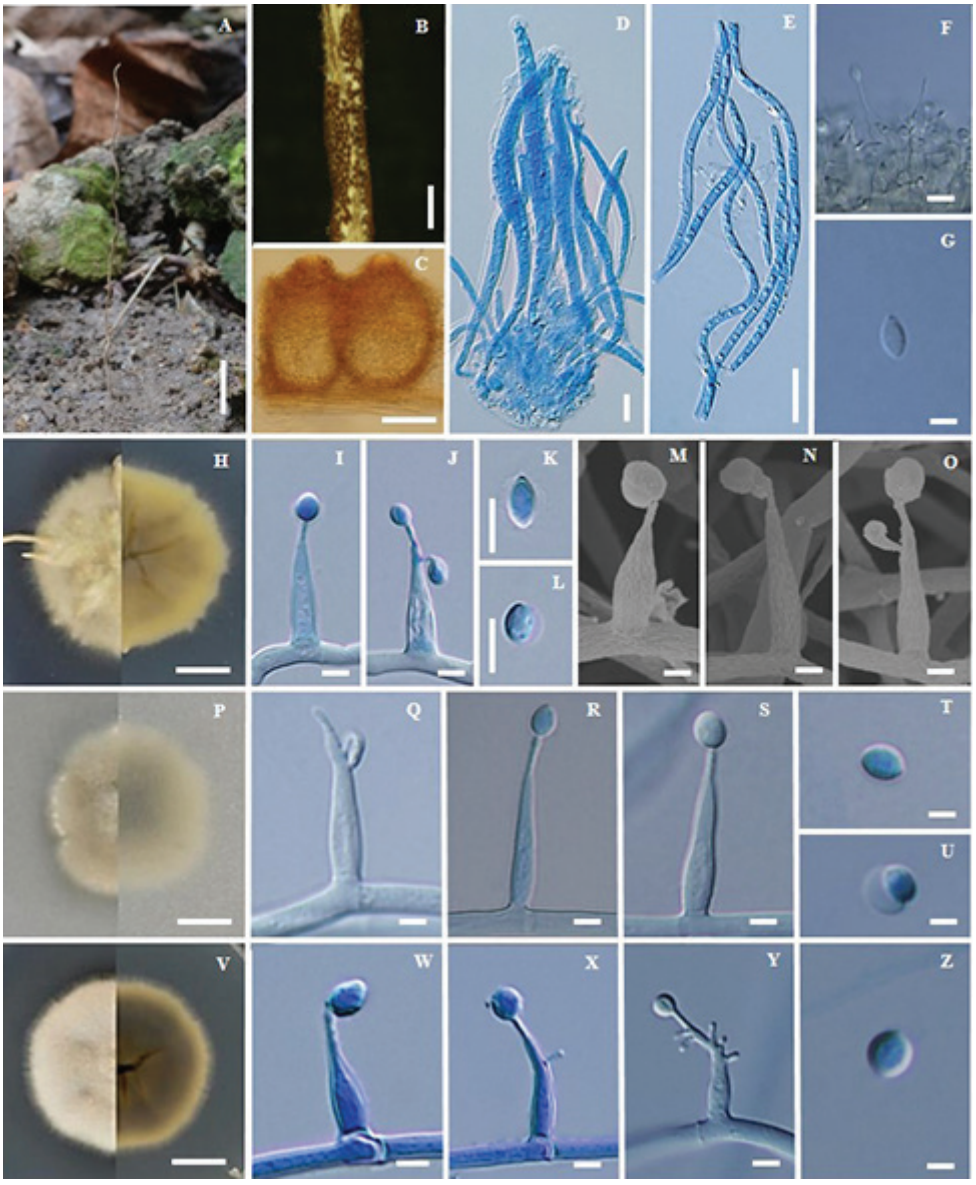

Figure 4. *Ophiocordyceps khokpasiensis* (BBH32173, BCC48071) **A** fungus on termite **B** part of stroma showing perithecia **C** pseudo-immersed perithecia **D** asci **E** ascospore **F** phialides with conidia from synnema **G** conidia from synnema **H** colony on PDA at 20 d colony obverse and reverse **I, J** phialides with conidia on PDA **K, L** conidium **M, N, O** scanning electron micrographs of phialides with conidia on PDA **P** colony on PSA at 20 d obverse and reverse **Q, R, S** phialides with conidia on PDA **T, U** conidium **V** colony on SDYA/4 at 20 d obverse and reverse **W, X, Y** phialides with conidia **Z** conidium. Scale bars: 2.5 cm (**A**); 1 mm (**B**); 100 µm (**C**); 5 µm (**D, G, I, J, K, L**); 20 µm (**E**); 6 µm (**F**); 7 mm (**H, P,V**); 3 µm (**M, N, O, Q, R, S,T, U**); 4 µm (**W, X,Y**); 2 µm (**Z**).

Description. Stroma solitary, simple, cylindrical, 16 cm long, 1 mm wide, brown (oac48-50), ca. 5.5 cm emerging above the leaf litter, ca. 10.5 cm buried in the soil. Asexual state (*Hirsutella*) produced ca. 1.5 cm at the terminal part of the stroma, light brown to grey. *Perithecia* pseudo-immersed, subglobose to broadly ellipsoidal, covering middle part of stroma, (200–)214–248.5(–250) × (120–)140–186(–200) µm. *Asci* 8-spored, filiform, (62.5–)86–115(–125) × 4–5 µm. *Ascospores* whole, filiform, (46–)51–74(–90) × 2–3 µm. Asexual state *Hirsutella*, phialides arising singly or laterally from the hyphae along the terminal part of the stroma, (8–)9–11(–12) × 3–4 µm. Conidia, hyaline, oval, 5–6.5(–7) × 2–3 µm.

Culture characteristics. Colonies on PDA, attaining a diam. of 25.5 mm within 20 d at 25 °C, cream (oac900) to grey (oac893). *Conidiogenous cells* swollen towards the base, hyaline, smooth, tapering gradually towards the apex, which often forms a thin neck, monophialidic or polyphialidic, (15–)16.5–23(–28) × 3–4.5(–5) µm. *Conidia* arising from phialides at the apex of each neck, globose to oval, one-celled (4–)4.5–5.5(–6) × 2.5–4 µm, embedded in a mucous sheath.

Colonies on PSA, attaining a diam. of 24 mm within 20 d at 25 °C, white to grey (oac843). *Conidiogenous cells* swollen towards the base, hyaline, smooth, tapering gradually towards the apex, which often forms a thin neck, monophialidic or polyphialidic, (14–)15.5–22.5(–28) × 3–4.5(–5) µm. *Conidia* arising from phialides at the apex of each neck, globose to oval, one-celled 4–5(–6) × (2–)2.5–3.5(–5) µm, embedded in a mucous sheath.

Colonies on SDYA/4, attaining a diam. of 25 mm within 20 d at 25 °C, grey to brown (oac473). *Conidiogenous cells* swollen towards the base, hyaline, smooth, tapering gradually towards the apex, which often forms a thin neck, monophialidic or polyphialidic, (9–)11.5–15.5(–19) × (2–)3–3.5(–4) µm. *Conidia* arising from phialides at the apex of each neck, globose to oval, one celled 3.5–4.5(–5) × 2.5–3 (–3.5) µm, embedded in a mucous sheath.

Distribution. North-eastern Thailand.

Ecology. Parasitic on a pair of termites from a reproductive caste (Order Isoptera: Family Termitidae, Subfamily Macrotermitinae) and these specimens were buried in the soil. The fungus emerged from the segment between the prothorax and mesothorax of one of the termite pairs.

Additional specimens examined. THAILAND. Saraburi Province, Namtok Samlan National Park (Phra Buddha Chai); 14°526'N, 100°9'E; on termite; 15 June 1996; Hywel-Jones, NL (BBH5116, BCC1764). Kalasin Province: Phu Si Than Wildlife Sanctuary, Khok Pa Si Community Forest; 16°562'N, 104°103'E; on termite; 14 June 2011; K. Tasanathai, P. Srikitikulchai, A. Khonsanit, K. Sansatchanon, W. Noisripoom (BBH32173, BCC48072).

Notes. Other *Ophiocordyceps* species reported on termites with pseudo-immersed perithecia are *O. mosingtoensis* and *O. termiticola*. *O. khokpasiensis* and *O. termiticola* shares similarity in the colour of the perithecia but in *O. termiticola*, the perithecia are denser while it is loosely arranged in *O. khokpasiensis*. *O. mosingtoensis* produces a more

robust stroma compared to *O. khokpasiensis* and *O. termiticola*. The gross morphology of *O. khokpasiensis* is similar to *O. asiatica*, *O. communis*, *O. pseudocommunis* and *O. pseudorhizoidea.* However, all these other species produce superficial perithecia.

Ophiocordyceps mosingtoensis **Tasanathai, Noisripoom & Luangsa-ard, sp. nov.**
MycoBank MB 831291
Figure 5

Typification. THAILAND. Nakhon Ratchasima Province, Khao Yai National Park; 14°711'N, 101°421'E; on termite; 17 June 2009; K. Tasanathai, P. Srikitikulchai, S. Mongkolsamrit, T. Chohmee, R. Ridkaew, N.L. Hywel-Jones (holotype BBH26809 dried culture; ex-type living culture, BCC36921). GenBank: ITS = MH754731, LSU = MH753685, *TEF* = MK284272, *RPB1* = MK214116, *RPB2* = MK214099

Etymology. '*mosingtoensis*' referring to name after the type locality.

Description. Stroma solitary, simple, cylindrical, up to 11 cm long, 1 mm wide, brown (oac 48-50), ca. 8.5 cm emerging above the leaf litter, ca. 2.5 cm buried in the soil. Asexual state (*Hirsutella*) produced ca. 1 cm at the terminal part of the stroma, light brown to grey. *Perithecia* pseudo-immersed, broadly ovoid covering middle part of stroma, (400–)414–469 (–500) × (200–)208–263(–300) µm. *Asci* 8-spored, filiform, (187.5–) 217–265(–287.5) × 4.5–6.5(–7.5) µm with cap, 2 µm. *Ascospores* whole, filiform, (230–)240–291(–315) × 1.5–3 µm, with septa.

Culture characteristics. Colonies on PDA, attaining a diam. of 16 mm within 20 d at 25 °C, cream (oac872) to grey (oac909). *Conidiogenous cells* swollen towards the base, hyaline, smooth, tapering gradually towards the apex, which often forms a thin neck, monophialidic, (10–)12.5–16 (–17) × (2–) 2.5–3 µm. *Conidia* arising from phialides at the apex of each neck, oval, 3–4.5(–5) × 2–2.5(–3) µm.

Colonies on PSA, attaining a diam. of 17 mm within 20 d at 25 °C, white to grey (oac872). *Conidiogenous cells* swollen towards the base, hyaline, smooth, tapering gradually towards the apex, which often forms a thin neck, monophialidic, (10–)11.5–15(–17) × (2–)2.5–3.5(–4) µm. *Conidia* arising from phialides at the apex of each neck, oval, (3–)3.5–5(–5.5) × 2–3 µm.

Colonies on SDYA/4, attaining a diam. of 17 mm within 20 d at 25 °C, white to grey (oac802). *Conidiogenous cells* swollen towards the base, hyaline, smooth, tapering gradually towards the apex, which often forms a thin neck, monophialidic or polyphialidic, (9–)10.5–14.5(–17) × (2–)2.5–3 µm. *Conidia* arising from phialides at the apex of each neck, oval, (3–)3.5–4.5(–5) × 2–3 µm.

Distribution. Thailand, only known from Khao Yai National Park.

Ecology. Parasitic on a pair of termites from a reproductive caste (Order Isoptera: Family Termitidae, Subfamily Macrotermitinae) and these specimens were buried in the soil. The fungus emerged from the segment between the prothorax and mesothorax of one of the termite pairs.

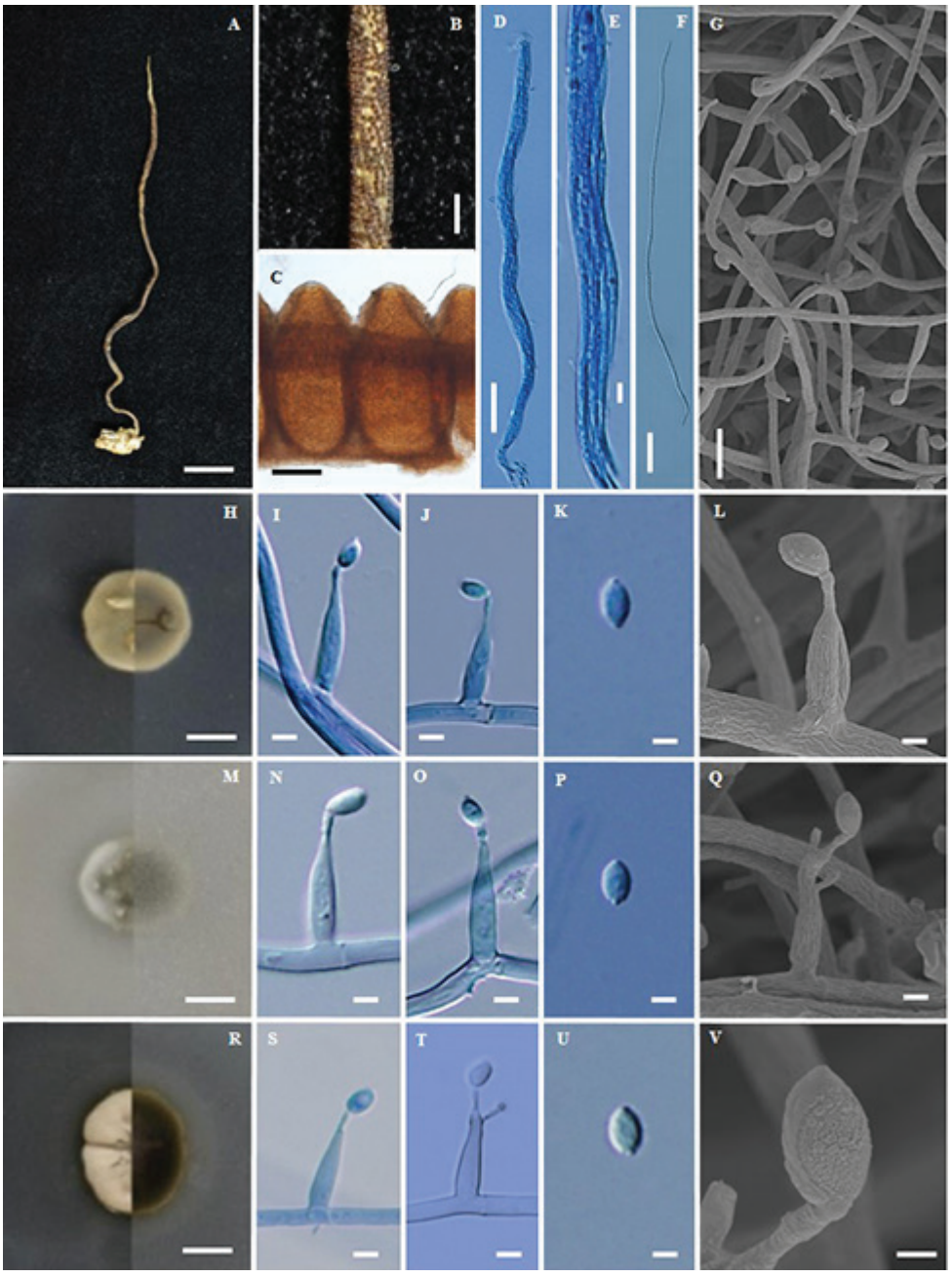

Figure 5. *Ophiocordyceps mosingtoensis* (BBH26809, BCC36921) **A** stroma of fungus emerging from termite **B** part of stroma showing perithecia **C** pseudo-immersed perithecia **D, E** ascus **F** ascospore **G, L, Q,V** scanning electron micrographs of phialides with conidia on PDA **H** colony on PDA at 20 d obverse and reverse **I, J** phialides with conidia **K** conidium **M** colony on PSA at 20 d obverse and reverse **N, O** phialides with conidia **P** conidium **R** colony on SDYA/4 at 20 d obverse and reverse **S, T** phialides with conidia **U** conidium. Scale bars: 10 mm (**A**); 1 mm (**B**); 150 µm (**C**); 25 µm (**D**); 4 µm (**E**); 30 µm (**F**); 10 µm (**G**); 8 mm (**H, M, R**); 3 µm (**I, J, N, O, S, T**); 2 µm (**K, L, P, Q, U**); 1 µm (**V**).

Additional specimens examined. THAILAND. Nakhon Ratchasima Province, Khao Yai National Park; 14°711'N, 101°421'E; on termite; 18 June 2008; J.J. Luangsa-ard, K. Tasanathai, S. Mongkolsamrit, B. Thongnuch, P. Srikitikulchai, R. Ridkaew (BBH 23860, BCC 30904).

Note. *O. mosingtoensis* has a sturdier, robust stroma compared with *O. termiticola* and *O. khokpasiensis* which also produce pseudo-immersed perithecia.

Ophiocordyceps pseudocommunis **Tasanathai, Noisripoom & Luangsa-ard, sp. nov.**
MycoBank MB 831351
Figure 6

Typification. THAILAND. Nakhon Nayok Province, Khao Yai National Park; 14°163'N, 101°268'E; on termite; 13 July 2004; S. Sivichai, K. Tasanathai, N. Boonyuen, P. Puyngain (holotype BBH10001 dried culture; ex-type living culture, BCC16757). GenBank: ITS = MH754733, LSU = MH753687, *TEF* = MK284274, *RPB1* = MK214117, *RPB2* = MK214101

Etymology. '*pseudocommunis*' referring to close affinity to *Ophiocordyceps communis*.

Description. Stroma solitary, simple, cylindrical, 21.5 cm long, 0.5 mm wide, brown (oac48-50), ca. 12 cm emerging above the leaf litter, ca. 9 cm buried in the soil. Asexual state (Hymenostilbe-like) produced ca. 5 cm at the terminal part of the stroma, light brown to brown. *Perithecia* superficial, subglobose, covering middle part of the stroma, (520–)536.5–596.5(–600) × (360–)373.5–425 (–440) µm. *Asci*, 8-spored, filiform, 160–164.5(–165) × 14–17 µm. *Ascospores* whole, filiform, (107.5–)120.5–138 (–147.5) × (6–)6.5–7 (7.5) µm, with 7–8 septa. Asexual state Hymenostilbe-like, conidiogenous cells forming a compact hymenium-like layer and had two to four denticles at their apices, cylindrical to clavate, (17–)18.5–21(–22) × (2–)2.5–7.5(–8) µm. Conidia, hyaline, fusiform, (6–)6.5–7.5(–8) × 2–3 µm.

Culture characteristics. Colonies on PDA, attaining a diam. of 26.5 mm within 20 d at 25 °C, white (oac909) to grey (oac851). *Conidiogenous cells* arising from hyphae laterally or terminally, hyaline, tapering gradually or abruptly into a long slender neck. *Conidia* hyaline, septate (2–3), arising from phialides at the apex of each neck, fusiform, (13–)14.5–20.5(–27) × (3–)3.5–5 µm.

Colonies on PSA, attaining a diam. of 15 mm within 20 d at 25 °C, white (oac909) to grey (oac851). *Conidiogenous cells* arising from hyphae laterally or terminally, hyaline, tapering gradually or abruptly into a long slender neck. *Conidia* hyaline, septate (1–4), arising from phialides at the apex of each neck, fusiform, (7–)9–15.5(–20) × (2–)2.5–4 µm.

Colonies on SDYA/4, attaining a diam. of 19 mm within 20 d at 25 °C, cream (oac816) to brown (oac781). *Conidiogenous cells* arising from hyphae laterally or terminally, hyaline, tapering gradually or abruptly into a long slender neck. *Conidia* hyaline, septate, arising from phialides at the apex of each neck, fusiform, (7–)9–18.5(–27) × (3–)3.5–6(–8) µm.

Distribution. Only reported from Khao Yai National Park.

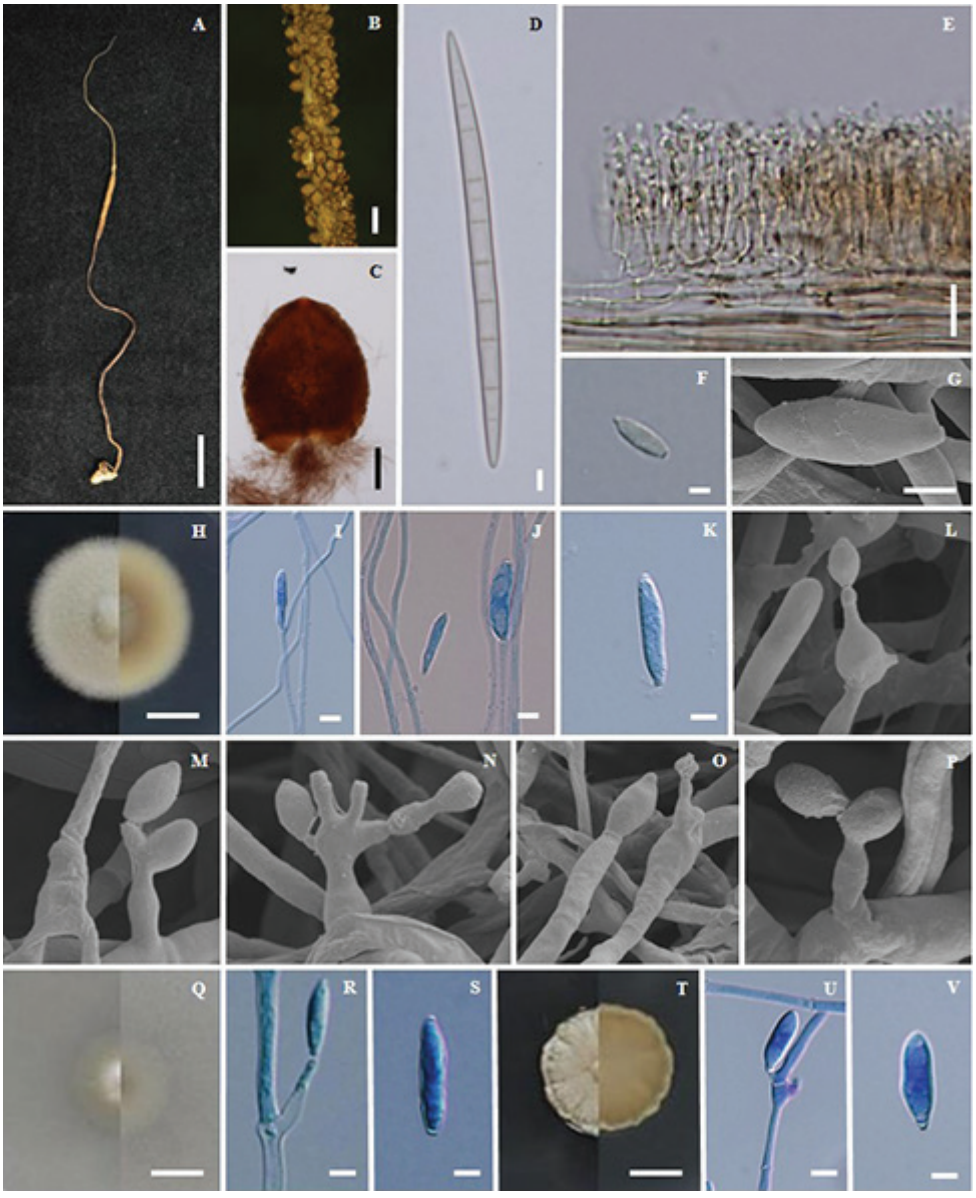

Figure 6. *Ophiocordyceps pseudocommunis* (BBH10001, BCC16757) **A** stroma of fungus emerging from termite **B** part of stroma showing superficial perithecia **C** perithecium **D** ascospore **E** phialides with conidia from synnema **F** conidia from synnema **G, L, M, N, O, P** scanning electron micrographs of phialides with conidia on PDA **H** colony on PDA at 20 d obverse and reverse **I, J** phialides with conidia on PDA **K** conidium **Q** colony on PDA at 20 d obverse and reverse **R** phialides with conidia on PSA **S** conidium **T** colony on SDYA/4 at 20 d obverse and reverse **U** phialides with conidia **V** conidium. Scale bars: 10 mm (**A**); 0.5 mm (**B**); 150 µm(**C**); 6 µm (**D**); 7 µm (**E**); 2 µm (**F**); 4 µm (**G**); 8 mm (**H, Q, T**); 8 µm (**I**); 5 µm (**J, K, U, V**); 3 µm (**R, S**).

Ecology. Parasitic on a pair of termites from a reproductive caste (Order Isoptera: Family Termitidae, Subfamily Macrotermitinae) and these specimens were buried in the soil. The fungus emerged from the segment between the prothorax and mesothorax of one of the termite pairs.

Additional specimens examined. THAILAND. Nakhon Ratchasima Province, Khao Yai National Park; 14°711'N, 101°421'E; on termite; 22 July 2003; R. Nasit, N.L. Hywel-Jones, J.W. Spatafora (NHJ12581, NHJ12582).

Ophiocordyceps pseudorhizoidea **Tasanathai, Noisripoom & Luangsa-ard, sp. nov.**
MycoBank MB 830982
Figure 7

Typification. THAILAND. Khonkaen Province, Phu Wiang National Park; 16°799'N, 102°279'E; on termite; 17 July 2017; K. Tasanathai, S. Mongkolsamrit, W. Noisripoom (holotype BBH45361 dried culture; ex-type living culture, BCC86431). GenBank: ITS = MH754721, LSU = MH753674, *TEF* = MK284262, *RPB1* = MK751469, *RPB2* = MK214090

Etymology. *'pseudorhizoidea*' referring to close affinity to what was called *Ophiocordyceps rhizoidea* on termites by NHJ.

Description. Stroma solitary, simple, filiform, up to 21 cm long, 1 mm wide, light-brown (oac675), ca. 15 cm emerging above leaf litter, 5.5 cm buried in the soil. Asexual state (*Hirsutella*) produced at the terminal part of the stroma, ca. 6 cm long, light brown to grey. *Perithecia* superficial, ovoid, covering the middle part of stroma, (280–) 287.5–315.5 (–390) × (160–) 177–209.5 (–220) µm. *Asci* 8-spored, cylindrical, 120–150 × 5–7 µm with cap, 3–4 × 4–5 µm. *Ascospores* whole, filiform, (65–) 69.5–78.5 (–82.5) × 2–2.8 (–3) µm, with septate. Asexual state *Hirsutella.* Phialides (10–)15.5–23.5(–26) × 3–4(–5) µm, conidia hyaline, fusiform, (5–)5.5–6.5(–7) × 3–4 µm.

Culture characteristics. Colonies on PDA, attaining a diam. of 10 mm within 20 d at 25 °C, cream to grey (oac844), reverse oac772 to oac815. *Conidiogenous cells* monophialidic, arising from hyphae laterally or terminally, hyaline, tapering gradually or abruptly into a long slender neck, (9–)10.5–17.5(–21) µm long, 2–3.2(–4) µm wide at the base, 1–1.5 µm wide at tip with warty surface. *Conidia* hyaline, one-celled, fusiform, (5–)6.5–8.5(–10) × 1–2 µm. with mucous sheath.

Colonies on PSA, attaining a diam. of 10 mm within 20 d at 25 °C, (oac841) to (oac843), reverse (oac868). *Conidiogenous cells* monophialidic cells arising from hyphae laterally or terminally, hyaline, tapering gradually or abruptly into a long slender neck, (10–)12–16.5(–19) µm long, 2–3 µm wide at the base, 1–1.5 µm wide at tip with warty surface. *Conidia* hyaline, one-celled, arising from phialides, fusiform, (6–)6.5–8(–8.5) × 1.5–2.5(–3) µm with mucous sheath.

Colonies on SDYA/4, attaining a diam. of 10 mm within 20 d at 25 °C, oac844, reverse oac722 in middle to oac815. *Conidiogenous cells* monophialidic cells arising from hyphae laterally or terminally, hyaline, tapering gradually or abruptly into a long

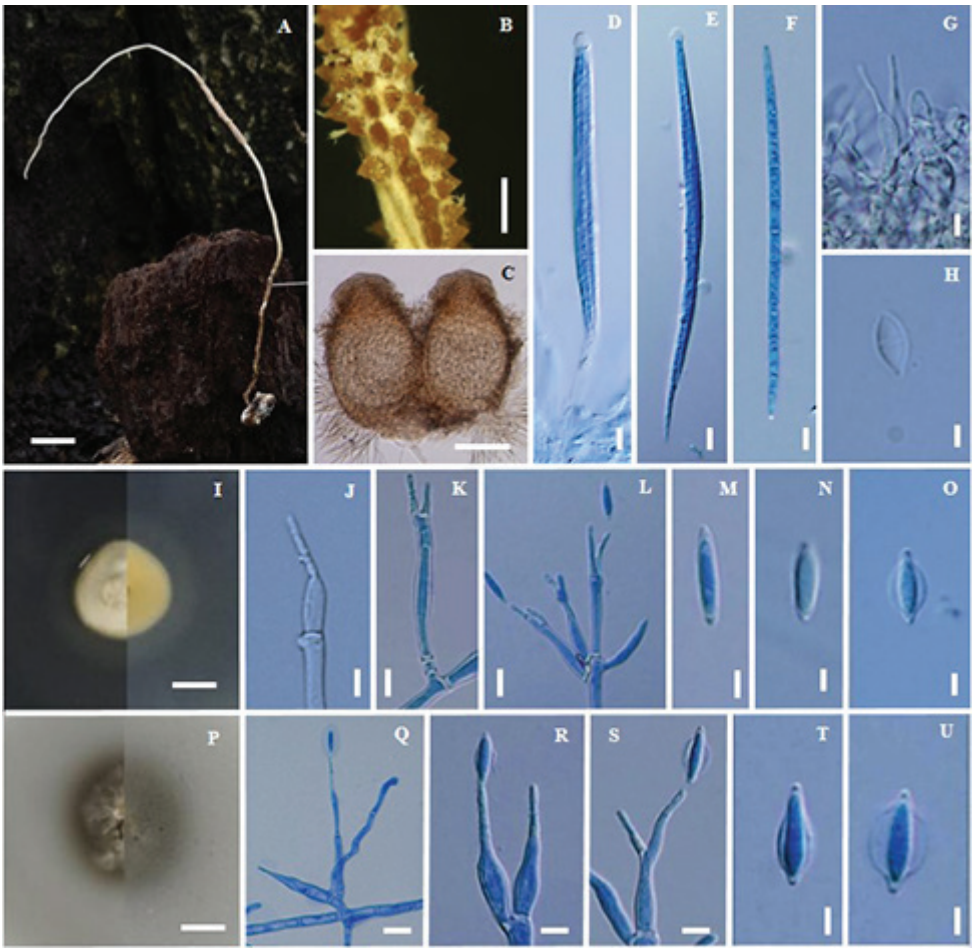

Figure 7. *Ophiocordyceps pseudorhizoidea* (BBH45361, BCC86431) **A** stroma of fungus emerging from termite **B** part of stroma showing perithecia **C** perithecia **D, E** ascus **F** ascospore **G, H** phialides with conidia from synnema **I** colony on PDA at 20 d obverse and reverse **J, K, L** phialides with conidia on PDA **M, N, O** conidium **P** colony on PSA at 20 d obverse and reverse **Q, R, S** phialides with conidia on PSA **T, U** conidia with mucous sheath. Scale bars: 15 mm (**A**); 1 mm (**B**); 120 µm (**C**); 8 µm (**D, E**); 10 µm (**F, G**); 3 µm (**H, R**); 6 mm (**I, P**); 5 µm (**J, K, L, Q**); 2 µm (**M, N, O, T, U**); 4 µm (**S**).

slender neck, (13–)17–25.5(–30) µm long, (3–)3.5–4 µm wide at the base, 1 µm wide at tip with warty surface. *Conidia* hyaline, one-celled, arising from phialides, fusiform, (6–)7.5–9(–10) × 1–2 µm with mucous sheath.

Distribution. Thailand.

Ecology. Parasitic on a pair of termites from a reproductive caste (Order Isoptera: Family Termitidae, Subfamily Macrotermitinae) and these specimens were buried in the soil. The fungus emerged from the segment between the prothorax and mesothorax of one of the termite pairs.

Table 2. Morphological comparisons of closely related *Ophiocordyceps* species used in this study

Species	Host	Stromata (cm)	Perithecia (µm)	Asci (µm)	Ascospores (µm)	Reference
Ophiocordyceps asiatica	Termites	solitary, simple, filiform, up to 15 long orange brown	superficial, globose to subglobose 240–320 × 180–260	filiform 92.5–175 × 5–6.3	whole with septate 90–132.5 × 1–2	This study
Ophiocordyceps brunneirubra	Termites	solitary, simple or branched, narrowly clavate, slender and wiry, 9.5 cm long, orange brown to red brown	Immersed, ovoid, 300–400 × 130–200	cylindrical, 155–225 × 4.5–8	filiform, whole with septate, 156.5–197.5 × 2–3	This study
Ophiocordyceps khokpasiensis	Termites	solitary, simple cylindrical, 16 cm long, brown	pseudo-immersed, subglobose 200–250 × 120–200	filiform, 62.5–125 × 4–5	filiform, whole, 46–90 × 2–3	This study
Ophiocordyceps mosingtoensis	Termites	solitary simple cylindrical, 11 cm long, brown to grey	pseudo-immersed, ovoid 400–500 × 200–300	filiform, 187.5–287.5 × 4.5–7.5	whole with septate, 230–315 × 1.5–3	This study
Ophiocordyceps pseudocommunis	Termites	solitary simple cylindrical , 21 cm long, brown	superficial, subglobose 520–600 × 360–440	filiform, 160–165 × 14–17	whole with 7–8 septa, 107.5–147.5 × 6–7.5	This study
Ophiocordyceps communis	Termites	solitary simple filiform, 5-13 cm long, yellow brown	superficial 285-675 × 195-390	filiform, 215-250 × 15	filiform, whole, 100–180 × 5–6	Sung et al. 2007
Ophiocordyceps pseudorhizoidea	Termites	solitary, simple, filiform, up to 21 cm long, light brown	superficial, ovoid 280–390 × 160–220	cylindrical, 120–150 × 5–7	whole with septate 65–82.5 × 2–3	This study
Ophiocordyceps rhizoidea	Coleoptera larva	simple, solitary, 7–8 cm long, 0.5-1 mm	superficial 360 × 300	160-210 × 13-16	ca 80 × 5-7	von Höhnel, 1909
Ophiocordyceps termiticola	Termites	solitary, simple, filiform, up to 14 cm long yellow brown	pseudo-immersed, globose to subglobose 200–280 × 150–250	filiform 62.5–110 × 4–6	filiform, whole, 85 × 2	This study

Additional specimens examined. THAILAND. Chanthaburi Province, Khao Soi Dao Wildlife Sanctuary; 13°136'N, 102°218'E; on termite; 8 June 2011; K. Tasanathai, P. Srikitikulchai, S. Mongkolsamrit, A. Khonsanit, K. Sansatchanon (BBH31259, BCC 48879).

Notes. Like *O. communis* and *O. pseudocommunis*, this species shows similarity to *O. rhizoidea*. However, von Hohnel's description of the host in *O. rhizoidea* was a Coleoptera larva. *O. rhizoidea* has longer and wider asci and ascospores than *O. pseudorhizoidea*, while in *O. communis* and *O. pseudocommunis*, they are distinctly longer (Table 2).

Ophiocordyceps termiticola **Tasanathai, Noisripoom & Luangsa-ard, sp. nov.**
MycoBank MB 831296
Figure 8

Typification. THAILAND. Kanchanaburi Province, Khao Laem National Park; 14°746'N, 98°625'E; on termite; 20 June 1995; N.L. Hywel-Jones, R. Nasit, S. Sivichai (holotype BBH5634 dried culture; ex-type living culture, BCC 1920). GenBank: ITS = MH754724, LSU = MH753678, *TEF* = MK284265, *RPB1* = MK214108, *RPB2* = MK214094

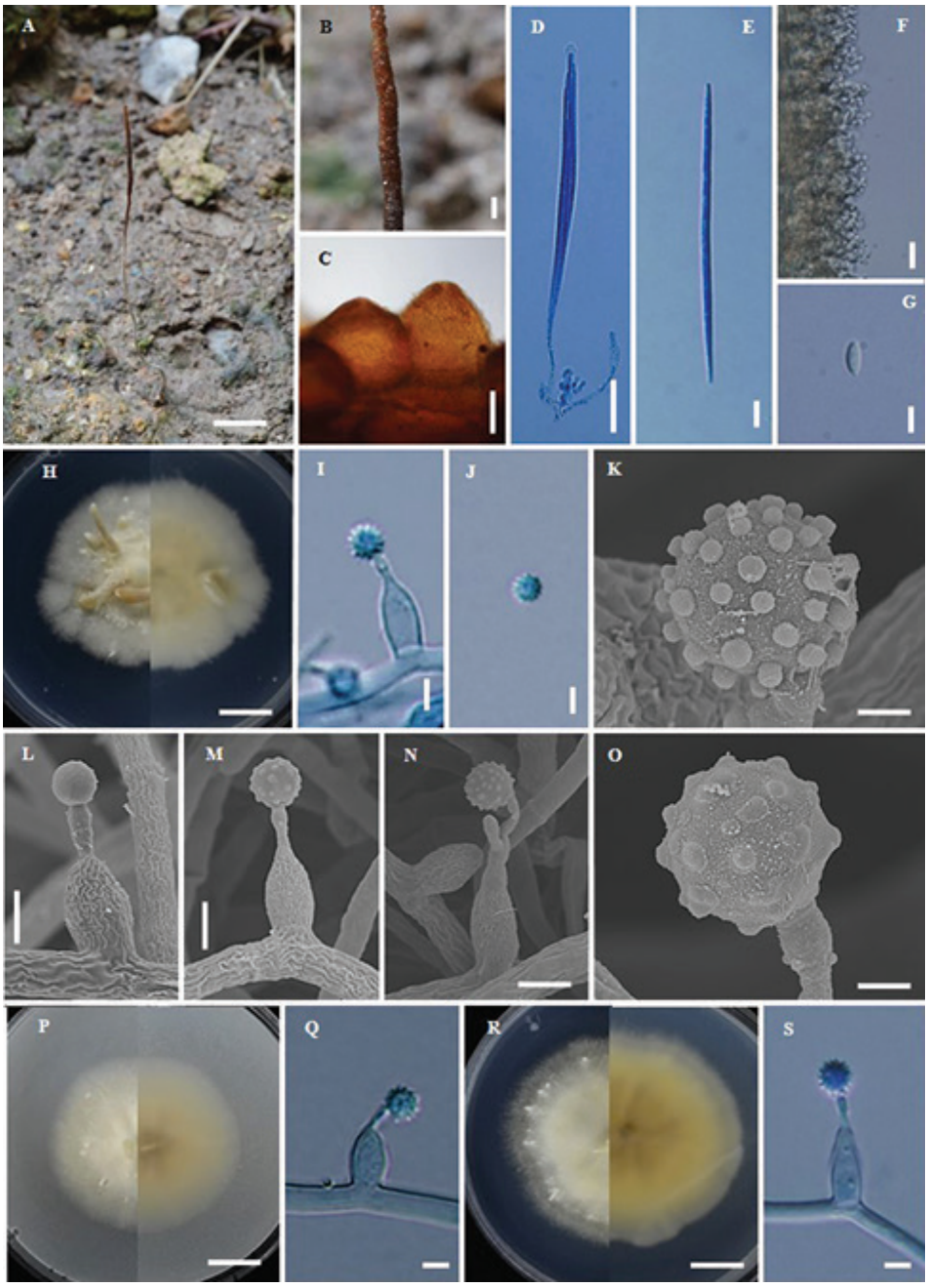

Figure 8. *Ophiocordyceps termiticola* (BBH5634, BCC 1920) **A** stroma of fungus emerging from termite **B** part of stroma showing perithecia **C** perithecia **D** ascus **E** ascospore **F** phialides with conidia on synnema **G** conidium **H** colony on PDA at 20 d obverse and reverse **I** phialides with conidia on PDA **J** conidium **K–O** scanning electron micrographs of phialides with conidia on PDA **P** colony on PSA at 20 d obverse and reverse **Q** phialides with conidia on PSA **R** colony on SDYA/4 at 20 d obverse and reverse **S** phialides with conidia. Scale bars: 2 cm (**A**); 1 µm (**B, K, O**); 100 µm (**C**); 15 µm (**D**); 8 µm (**E**); 5 µm (**F, G**); 7 mm (**H, P, R**); 3 µm (**I, J, L, M, N, Q, S**).

Etymology. '*termiticola*' referring to the host family, Termitidae.

Description. Stroma solitary, simple, filiform, up to 14 cm long, 1 mm wide, yellow-brown, ca. 6 cm emerging above the leaf litter, ca. 8 cm buried in the soil. Asexual state (Hymenostilbe-like) produced ca. 1 cm at the terminal part of the stroma, grey. *Perithecia* pseudo-immersed, globose to subglobose, produced on one-third of the terminal part of the stroma ending near the apex, (200–)225–261(–280) × (150–)178–229(–250) µm. *Asci* 8-spored, filiform, (62.5–)76.5–100.5(–110) × (4–)4.5–5.5(–6) µm. *Ascospores* whole, filiform, 85 × 2 µm, Asexual state Hymenostilbe-like, conidiogenous cells formed a compact hymenium-like layer and had from two to four denticles at their apices, cylindrical to clavate, (10–)11.5–16(–17) × 3–5(–6) µm. Conidia, hyaline, fusiform 7 × 3 µm.

Culture characteristics. Colonies on PDA, attaining a diam. of 28 mm within 20 d at 25 °C, grey (oac781) to pale grey (oac851). *Conidiogenous cells* monophialidic to polyphialidic, arising from hyphae laterally, with an inflated base (7–)7.5–10(–11) × (2.5–) 3–3.5(–4) µm. *Conidia* hyaline, globose, 2.5–3 (–3.5) µm, one-celled with warty surface.

Colonies on PSA, attaining a diam. of 22 mm within 20 d at 25 °C, white to pale grey, cotton-like. *Conidiogenous cells* monophialidic to polyphialidic, hyaline, smooth, with an inflated base (7–)8–10.5(–13) × 3–4 (–5) µm. *Conidia* hyaline, globose, (2–)2.7–3.4(–4) µm, one celled with warty surface.

Colonies on SDYA/4, attaining a diam. of 29 mm within 20 d at 25 °C, grey to pale grey (oac851). *Conidiogenous cells* monophialidic to polyphialidic, hyaline, smooth, with an inflated base (7–)8–10.5(–13) × 3–4 µm. *Conidia* hyaline, globose, 3–3.5(–4) µm, one-celled with warty surface.

Distribution. Thailand.

Ecology. Parasitic on a pair of termites from a reproductive caste (Order Isoptera: Family Termitidae, Subfamily Macrotermitinae) and these specimens were buried in the soil. The fungus emerged from the segment between the prothorax and mesothorax of one of the termite pairs.

Additional specimens examined. THAILAND. Chanthaburi Province, Khao Soi Dao Wildlife Reserve; 13°136'N, 102°218'E; on termite; 20 June 1996; R. Nasit, S. Sivichai, K. Tasanathai (BBH5179, BCC1770).

Notes. Both *O. termiticola* and *O. khokpasiensis* produce pseudo-immersed reddish perithecia on a stroma. In *O. termiticola*, the perithecia are tightly packed, while in *O. khokpasiensis*, they are loosely aggregated and the length of the anamorphic layer at the end of the fertile part is longer in the latter.

Discussion

Out of the 230+ species of *Ophiocordyceps* worldwide, less than 10 species occur on termites. The majority of these species produce cylindrical, wiry to pliant, mostly simple, seldom multiple, stromata. Species found in Africa and Mexico, *O. bispora* (*Cordycepioideus bisporus*) and *O. octospora* (*Cordycepioideus octosporus*), produce thick-walled,

multiseptate ascospores, suggesting an adaptation to the harsh environmental conditions in these countries (Ochiel et al. 1997; Blackwell and Gilbertson 1981, 1984). All termite pathogenic species in Thailand including *O. asiatica*, *O. brunneirubra*, *O. communis*, *O. khokpasiensis*, *O. mosingtoensis*, *O. pseudocommunis*, *O. pseudorhizoidea* and *O. termiticola* produce filiform, multiseptate, whole ascospores on predominantly superficial and pseudo-immersed perithecia. The dark to pallidly coloured stroma of these species are cylindrical, wiry and pliant and the anamorph is produced at the terminal part of the stroma, after the fertile part.

Interestingly, our results clearly present *Ophiocordyceps* species occurring on reproductive castes of termites, especially subterranean termite species in the Family Termitidae, Subfamily Macrotermitinae. All species of subterranean termites construct their nests below ground or build mounds above ground and excavate their foraging tunnel in several ways (Eggleton 2010; Ahmad et al. 2018). Usually, the reproductive caste of termites, i.e. flying termites, includes male and female swarms during mating season at the start of the rainy season. The winged queen emerges from the colony for her nuptial flight or the mating flight, releasing pheromones to attract the males to mate. When the male finds the queen, they do a tandem run that lasts for as long as the pair finds a suitable place to start a new colony, during which they shed their wings. In termites, both male and female are the same size (Howard and Thorne 2010; Ahmad et al. 2018). Specimens of termites might have been infected by *Ophiocordyceps* species after their nuptial flight, when they bury themselves in the ground to establish a nesting area for starting a new colony.

Fungi represent a silent threat to the termite community. Termites have many predators, such as other amphibians (toads), birds, reptiles (lizards, gecko, snakes), small mammals, rodents and even humans. The percentage of the infection to these reproductive castes may be low in comparison to the individuals in a termite swarm, however, only few survive or evade the imminent threat of arthropods and other animals. Eventually, the number of infections caused by *Ophiocordyceps* becomes significant when only a few can actually survive to start a new colony.

The number of available morphological characters needed to delimit species in fungi are so limited and this may be an important reason why cryptic species are abundant in Kingdom Fungi, i.e. morphologically indistinguishable biological/phylogenetic units present within taxonomic species (Balasundaram et al. 2015) or, as Bickford et al. (2007) put it: 'two or more distinct species that are erroneously classified (and hidden) under one species name'. Many species of entomopathogenic fungi in Ophiocordycipitceae belong to species complexes or are cryptic species. Zombie ant pathogens in *Ophiocordyceps* have all been classified as *Ophiocordyceps unilateralis sensu lato* until morphological and molecular studies, including host identification, were completed (Araujo et al. 2015, 2018; Luangsa-ard et al. 2010; Kobmoo et al. 2012, 2015). The use of DNA-based molecular analyses has subsequently uncovered several new species in the genus (Khonsanit et al. 2018; Luangsa-ard et al. 2018). In culture, the conidiogenous cells of these termite pathogens produce phialides that are either monophialidic or have several lateral necks. The anamorphs of these species do not always form *Hirsutella* asexual states but more of an intermediate between *Hirsutella*

and *Hymenostilbe*. This could either be a transition into a different genus or forming a diverging lineage in *Ophiocordyceps* – in the process of a speciation event or that the production of these anamorphs are so plastic that they cannot be used in taxonomy.

The knowledge that *Ophiocordyceps* species infect reproductive castes of termites can be used as basic information to study the biological control of subterranean termite pests and to better implement them. All specimens of termites collected are subterranean termites and produce relatively fast growing synnemata with numerous infectious propagules (ascopores) which can be developed further for biological control strategies.

Acknowledgements

The authors are grateful to Platform Technology Management Section, National Center for Genetic Engineering and Biotechnology (BIOTEC), Grant No. P19-50231 and CPMO Grant No. P15-51452 for their support of the biodiversity studies of invertebrate-pathogenic fungi in Thailand. We thank the Department of National Parks for their kind support and permission to collect fungi in the national parks. We also thank Suchada Mongkolsamrit for her help in collecting fungi. This study was supported by National Science and Technology Development Agency (NSTDA). We are grateful to the reviewers whose comments and suggestions helped improve our manuscript.

References

Abe T, Bignell DE, Higashi M (2000) Termites: Evolution, Sociality, Symbioses, Ecology. Kluwer academic publishers, London, United Kingdom, 247p. https://doi.org/10.1007/978-94-017-3223-9

Ahmad SK, Dawah HA, Khan A (2018) Ecology of Termites, 47–68. In: Khan MdA, Ahmad W (Eds) Termites and Sustainable Management Volume 1 – Biology, Social Behaviour and Economic Importance. https://doi.org/10.1007/978-3-319-72110-1_3

Araújo JPM, Evans HC, Geiser DM, Mackay WP, Hughes DP (2015) Unravelling the diversity behind the *Ophiocordyceps unilateralis* (Ophiocordycipitaceae) complex: three new species of zombie-ant fungi from the Brazilian Amazon. Phytotaxa 220(3): 224–238. https://doi.org/10.11646/phytotaxa.220.3.2

Araújo JPM, Evans HC, Kepler RM, Hughes DP (2018) Zombie-ant fungi across continents: 15 new species and new combinations within *Ophiocordyceps*. I. *Myrmecophilous* hirsutelloid species. Studies in Mycology 90: 119–160. https://doi.org/10.1016/j.simyco.2017.12.002

Balasundaram SV, Engh IB, Skrede I, Kauserud H (2015) How many DNA markers are needed to reveal cryptic fungal species? Fungal Biology 119: 940–945. https://doi.org/10.1016/j.funbio.2015.07.006

Bickford D, Lohman DJ, Sodhi NS, Ng PKL, Meier R, Winker K, Ingram KK, Das I (2007) Cryptic species as a window on diversity and conservation. Trends Ecol. Evol. 22, 148–155. https://doi.org/10.1016/j.tree.2006.11.004

Blackwell M, Gilbertson RL (1981) *Cordycepioideus octosporus*, a termite suspected pathogen from Jalisco, Mexico. Mycologia 73: 358–362. https://doi.org/10.2307/3761220

Blackwell M, Gilbertson RL (1984) New information on *Cordycepioideus bisporus* and *Cordycepioideus octosporus*. Mycologia 76: 763–765. https://doi.org/10.1080/00275514.1984.12023912

Castlebury LA, Rossman AY, Sung GH, Hyten AS, Spatafora JW (2004) Multigene phylogeny reveals new lineage for Stachybotrys chartarum, the indoor air fungus. Mycological Research 108(8): 864–872. https://doi.org/10.1017/S0953756204000607

Edgar RC (2004) MUSCLE: multiple sequence alignment with high accuracy and high throughput. Nucleic Acids Research 32(5): 1792–1797. https://doi.org/10.1093/nar/gkh340

Eggleton P (2000) Termites: Evolutions, Sociality Symbioses, Ecology. Kluwer Academic Publishers, Dordrecht, 25–51. In: Abe T, Bignell DE, Higashi M (Eds)

Eggleton P (2010) An Introduction to Termites: Biology, Taxonomy and Functional Morphology. In: Bignell DE, Roisin Y, Lo N (Eds) Biology of Termites: a Modern Synthesis. Springer, Dordrecht, 1–26. https://doi.org/10.1007/978-90-481-3977-4_1

Hall T (2004) BioEdit, version 6.0.7. Department of Microbiology, North Carolina State University.

Howard KJ, Thorne BL (2010) Eusocial Evolution in Termites and Hymenoptera: 97–132. In: Bignell DE, Roisin Y, Lo N (Eds) Biology of Termites: a Modern Synthesis. Springer Science & Business Media, London, New York. https://doi.org/10.1007/978-90-481-3977-4_5

Khonsanit A, Luangsa-ard JJ, Thanakitpipattana D, Kobmoo N, Piasai1 O (2018) Cryptic species within *Ophiocordyceps myrmecophila* complex on formicine ants from Thailand. Mycological Progress 18: 147–161. https://doi.org/10.1007/s11557-018-1412-7

Kobayasi Y (1941) The genus *Cordyceps* and its allies. Science reports of the Tokyo Bunrika Daigaku 84: 53–260.

Kobayasi Y, Shimizu (1978) *Cordyceps* species from Japan. Bull. Natn. Sci. Mus. Tokyo, 4: 43–63.

Kobmoo N, Mongkolsamrit S, Tasanathai K, Thanakitpipattana D, Luangsa-ard JJ (2012) Molecular phylogenies reveal host-specific divergence of *Ophiocordyceps unilateralis sensu lato* following its host ants. Molecular Ecology 21: 3022–3031. https://doi.org/10.1111/j.1365-294X.2012.05574.x

Kobmoo N, Mongkolsamrit S, Wutikhun T, Tasanathai K, Khonsanit A, Thanakitpipattana D, Luangsa-ard JJ (2015) *Ophiocordyceps unilateralis*, an ubiquitous pathogen of ants from Thailand. Fungal Biol 119: 44–52. https://doi.org/10.1016/j.funbio.2014.10.008

Krishna K, Grimaldi DA, Krishna V, Engel MS (2013) Treatise on the Isoptera of the world: Introduction. Bulletin of the American Museum of Natural History, 2704 pp. https://doi.org/10.1206/377.6

Luangsa-ard JJ, Hywel-Jones NL, Samson RA (2004) The polyphyletic nature of *Paecilomyces* sensu lato based on 18S-generated rDNA phylogeny. Mycologia 96: 773–780. https://doi.org/10.1080/15572536.2005.11832925

Luangsa-ard JJ, Hywel-Jones NL, Manoch L (2005) On the relationships of *Paecilomyces* sect. Isarioidea species. Mycological Research 109: 581–589. https://doi.org/10.1017/S0953756205002741

Luangsa-ard JJ, Ridkaew R, Tasanathai K, Thanakitpipattana D, Hywel-Jones NL (2011) *Ophiocordyceps halabalaensis*: a new species of *Ophiocordyceps* pathogenic to *Camponotus gigas* in Hala Bala Wildlife Sanctuary, Southern Thailand. Fungal Biology 115: 608–614. https://doi.org/10.1016/j.funbio.2011.03.002

Luangsa-ard JJ, Tasanathai K, Thanakitpipattana D, Khonsanit A, Stadler M (2018) Novel and interesting *Ophiocordyceps* spp. (Ophiocordycipitaceae, Hypocreales) with superficial perithecia from Thailand. Studies in Mycology 89: 125–142. https://doi.org/10.1016/j.simyco.2018.02.001

Nylander JAA (2004) MrModeltest v.2. Program distributed by the author. Evolutionary Biology Centre, Uppsala University, Uppsala.

Ochiel GRS, Evans HC, Eilenberg J (1997) Cordycepioideus, a pathogen of termites in Kenya. Mycologist 11: 7–9. https://doi.org/10.1016/S0269-915X(97)80059-6

Pearce MJ (1999) Termites: Biology and Pest Management. CAB International, London.

Penzig O, Saccardo PA (1904) Icones Fungorum Javanicum: 55–57. https://doi.org/10.5962/bhl.title.17234

Petch T (1931) Notes on entomogenous fungi. Transactions of the British Mycological Society 16(1): 55–75. https://doi.org/10.1016/S0007-1536(31)80006-3

Rath AC (2000) The Use of Entomopathogenic Fungi for Control of Termites, Biocontrol Science and Technology 10: 5, 563–581. https://doi.org/10.1080/095831500750016370

Ronquist F, Huelsenbeck JP (2003) MrBayes 3: Bayesian phylogenetic inference under mixed models. Bioinformatics 19(12): 1572–1574. https://doi.org/10.1093/bioinformatics/btg180

Stamatakis A (2014) RAxML version 8: a tool for phylogenetic analysis and post-analysis of large phylogenies. Bioinformatics 30(9): 1312–1313. https://doi.org/10.1093/bioinformatics/btu033

Spatafora JW, Quandt CA, Kepler RM, Sung GH, Shrestha B, Hywel-Jones NL, Luangsa-ard JJ (2015) New 1F1N species combinations in Ophiocordycipitaceae (Hypocreales). IMA Fungus 6(2): 357–362. https://doi.org/10.5598/imafungus.2015.06.02.07

Sornnuwat Y, Vongkaluang C, Takematsu Y (2004) A systematic key to termites of Thailand. Kasetsart J. (Nat. Sci.) 38: 349–368.

Sung GH, Hywel-Jones NL, Sung JM, Luangsa-ard JJ, Shrestha B, Spatafora JW (2007) Phylogenetic classification of *Cordyceps* and the clavicipitaceous fungi. Studies in Mycology 57: 5–59. https://doi.org/10.3114/sim.2007.57.01

Swofford DL (2002) PAUP*: phylogenetic analysis using parsimony (*and other methods), version 4.0b10. Sinauer Associates, Sunderland.

White TJ, Bruns T, Lee S, Taylor JW (1990) Amplification and direct sequencing of fungal ribosomal RNA genes for phylogenetics. PCR Protocols: a guide to methods and applications. Academic Rress, San Diego, California 18(1): 315–322. https://doi.org/10.1016/B978-0-12-372180-8.50042-1